TRW No. 08710-6012-R000

STUDY OF A NAVIGATION AND TRAFFIC CONTROL TECHNIQUE EMPLOYING SATELLITES

(Interim Report)

VOLUME II

SYSTEM ANALYSIS

By David A. Conrad

DECEMBER 1967

Prepared under Contract No. NAS 12-539 by

TRW SYSTEMS GROUP

One Space Park • Redondo Beach, California 90278

Electronics Research Center

NATIONAL AERONAUTICS AND SPACE ADMINISTRATION

Mr. Peter Engels
Technical Monitor
NAS 12-539
Electronics Research Center
575 Technology Square
Cambridge, Massachusetts 02139

Requests for copies of this report should be referred to:

NASA Scientific and Technical Information Facility
P. O. Box 33, College Park, Maryland 20740

TRW No. 08710-6012-R000

STUDY OF A NAVIGATION AND TRAFFIC CONTROL TECHNIQUE EMPLOYING SATELLITES

(Interim Report)

VOLUME II

SYSTEM ANALYSIS

By David A. Conrad

DECEMBER 1967

Prepared under Contract No. NAS 12-539 by

TRW
SYSTEMS GROUP
One Space Park • Redondo Beach, California 90278

Electronics Research Center
NATIONAL AERONAUTICS AND SPACE ADMINISTRATION

CONTENTS

CONTENTS (Continued)

CONTENTS (Continued)

ILLUSTRATIONS

ILLUSTRATIONS (Continued)

TABLES

TABLES (Continued)

LIST OF SYMBOLS

SECTION		
2.1:	None	
2.2:	E	elevation angle of line of sight from horizontal
	E_{ground}	elevation angle at ground
	$E_{ionosphere}$	elevation angle at ionosphere
	RSS	root-sum-square
	σ	standard deviation of measurement error
2.3.1 and 2.3.2:	C95	radius of circle containing the user with probability 0.95
	RSS	root-sum-square
	σ	standard deviation
	T	time after T_0
	T_0	epoch at which system constellation is defined
	T_{45}, T_{90}, etc	times 45 min, 90 min, etc after T_0
	u	radial position of satellite
	v	in-track position of satellite
	w	cross-track position of satellite
2.3.3:	δx_1	$\hat{x}_1 - x_1$
	δx_2	$\hat{x}_2 - x_2$
	E ( )	expectation operator
	RSS	root-sum-square
	σ	standard deviation
	Σ_{ij}	$E\left[\delta x_i \delta x_j^T\right]$ $\quad i = 1, 2$
	Σ_{in}	portion of Σ_{ii} due to random errors
	Σ_{is}	portion of Σ_{ii} due to satellite errors

	Σ_R	$E\left[(\delta x_1 - \delta x_2)(\delta x_1 - \delta x_2)^T\right]$
	T	time after T_0
	x_1	deviation of position of user 1 from nominal
	x_2	deviation of position of user 2 from nominal
	$\hat{x}_1$	estimate of x_1
	$\hat{x}_2$	estimate of x_2
2.4:	J_2, J_{22} etc	coefficients of earth gravitational potential harmonics
	μ	earth gravitational coefficient
	σ_u, σ_v, σ_w	standard deviations of u, v, w
	u	radial satellite position error
	v	in-track satellite position error
	w	cross-track satellite position error
2.5.1:	A_i	sensitivity matrix $\partial y_i / \partial x_i$
	B_i	sensitivity matrix $\partial y_i / \partial z$
	C95	radius of circle containing user with probability 0.95
	Q	giant normal matrix defined in Eq (8)
	Q_i	normal matrix defined in Eq. (16)
	W_i	weighting matrix defined in Eq (17)
	x	giant state vector defined in Eq (9)
	x_i	deviation of i^{th} satellite position vector from nominal
	y_i	vector of measurement deviations to i^{th} satellite
	z	vector of deviations of satellite-independent parameters

2.5.2:	σ_v	standard deviation of velocity error
	ψ (psi)	standard deviation of heading error
2.5.3:	A	sensitivity matrix $\partial y/\partial x$
	b	vector of measurement bias deviations
	$\hat{b}$	minimum variance estimate of b
	C	column vector with all elements unity
	C_m	m-dimensional column vector with unity elements
	ϵ	vector of random measurement errors
	E	expectation operator
	I_m	m-dimensional identity matrix
	m	dimension of z
	n	dimension of y, C and ϵ
	p	dimension of x
	P	$A^T T^T T T^T T A$ Eq (34)
	Q	$A^T T^T T A$ Eq (33)
	σ_ϵ	standard deviation of components of ϵ
	T	transformation matrix from range to range-difference measurements Eq. (12)
	T(superscript)	matrix transpose
	T_k	k^{th} row of T
	W	equivalent weighting matrix defined in Eq (21)
	$\bar{W}$	equivalent weighting matrix defined in Eq (18)
	x	user position vector (deviation from nominal)
	$\hat{x}$	minimum variance estimate of x

	$\hat{x}_2$	suboptimal estimate of x according to Eq. (28)
	y	pseudorange measurement vector (deviation from nominal)
	z	range-difference measurement deviation vector
	z_k	k^{th} element of z
	Λ_δ	covariance matrix of range-difference measurement errors.
	Λ_{x_2}	covariance matrix of $\hat{x}_2$
3:	See page 89	
4.1:	ΔV	characteristic velocity
	e	orbital eccentricity
	λ_N	longitude of ascending node
	λ_{N_o}	initial longitude of ascending node
	i	orbital inclination to equator
	J_2, J_{22} etc	coefficients of earth gravitational potential harmonics
	Ω	right ascension of ascending node
	Ω_M	heliocentric longitude of ascending node of moon.
	T_0	epoch at which system constellation is defined.
	T_{45}, T_{90}, etc	T_0+45 min, T_0+90 min. etc

STUDY OF A NAVIGATION AND TRAFFIC CONTROL TECHNIQUE EMPLOYING SATELLITES

Volume II. System Analysis
By David A. Conrad

1. INTRODUCTION

This volume documents the analyses made of the satellite constellation and ground-station network and presents the results of tracking accuracy and error analysis studies. User equations are also derived and presented.

Sec. 2 contains the satellite constellation analysis. The navigation accuracy obtained is discussed in subsec. 2.1; measurement errors and orbit determination errors are discussed in subsecs. 2.2 and 2.3, respectively.

Sec. 3 presents the navigation equations used by four classes of user.

Sec. 4 describes certain supporting studies, including orbital perturbations and stationkeeping requirements, eclipse histories, and the selection of injection nodes. The appendixes contain descriptions of the computer programs used in the analysis and derivations of some of the equations used in these studies.

The findings being submitted to NASA-ERC were the result of a strong team effort. While numerous technical personnel made contributions to the study results contained in the various volumes of this interim report, the following TRW Systems people made significant contributions to the analyses presented in this volume:

Coverage:	H. T. Ekstrand, E. B. Mielak, P. D. Burgess
Error Sources:	A. J. Mallinckrodt, A. Garabedian
Navigation Accuracy:	S. Y. Itoga, D. J. Johnson, J. E. Land, D. A. Conrad

Orbit Determination:	D. J. Johnson
Navigation Equations:	D. M. Layton, D. A. Conrad, A. N. Drucker
Orbit Perturbations:	G. S. Gedeon
Eclipse Periods and Injection Nodes:	H. T. Ekstrand, A. J. Mallinckrodt
SPIT Program and Applications:	A. J. Mallinckrodt, T. P. Nosek, C. L. Whitman
NAVSAP Program:	S. Y. Itoga, D. Kuhn, D. J. Johnson
System Analysis Study Direction:	D. A. Conrad, D. D. Otten

2. ANALYSIS OF SELECTED CONSTELLATION

2.1 SYSTEM DEFINITION

The analysis of various possible satellite system configurations was based on the following criteria:

- The selected system must be compatible with an interim system that provides near-continuous coverage for the North Atlantic; that is, the interim system must be a portion of the final system. This requirement is most easily satisfied by satellites with 24-hr orbital periods.
- The final system must provide global coverage, with the possible exception of the polar regions.
- There should be sufficient redundancy so that at least three satellites are visible in the $\pm 60^{\circ}$ latitude band after one satellite has failed.
- The four satellites covering a given area should be positioned in such a way that there is minimum geometric degradation of accuracy.
- The number of orbit planes should be as small as possible to minimize establishment and maintenance costs.

The constellation selected on the basis of these criteria consists of two orbit planes with eight satellites in each plane. Both planes are inclined 18.5° to the equatorial plane with their ascending nodes spaced 157.5° apart. The satellites are positioned within their orbit planes to yield the configuration shown in Figure 1.

This constellation was selected from a variety of possible constellations on the basis of coverage and accuracy considerations.* The portion of the earth between 60° north and south latitudes was to be emphasized. One of the assumptions made for the comparative analysis was that the minimum elevation angle for user antennas would be 5° above the horizon. During the study (see Vol. III) it developed that a more suitable compromise

*Constellations evaluated and discarded are described in Ref. 1 and include 1 x 12, (1 orbit plane x 12 satellites per orbit plane) 2 x 12, and 4 x 3 configurations, all at 30° inclination. Ascending node spacing was 180° for the 2 x 12 system and both 90° and 75° were considered for the 4 x 3 system. Orbital period was 24 hr in all cases.

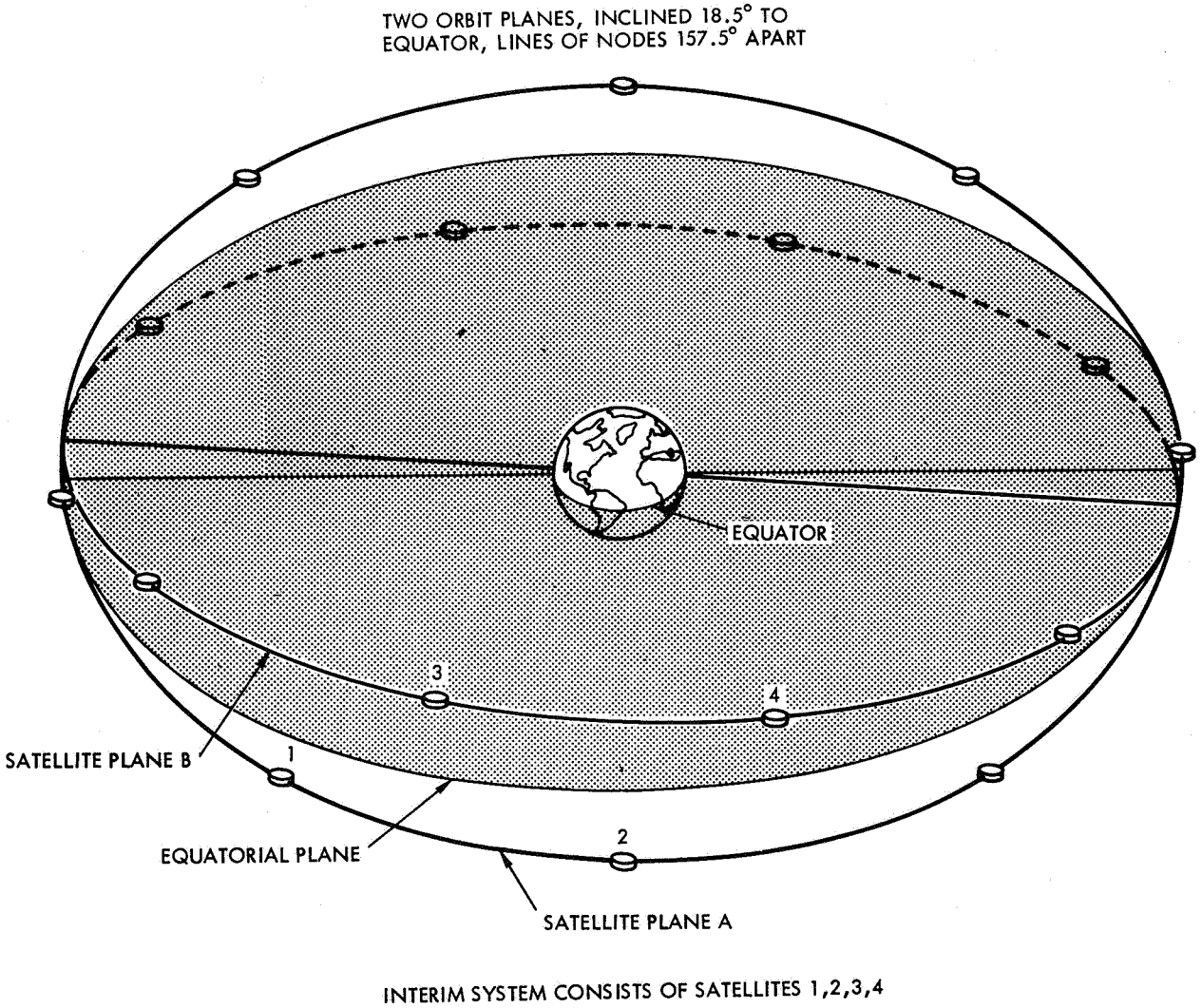

Figure 1. Satellite Geometry

for aircraft-mounted antennas would be to limit the elevation angle to a minimum of 10^{o}.

It is clear that selection of an optimum constellation requires exact definition of the coverage requirements for each region of the earth under consideration. Following this, detailed accuracy, coverage, and booster analyses can be performed. Such a study was beyond the scope of this contract,* nevertheless, the results presented for the selected constellation are indicative of the performance that may be expected from the proposed NAVSTAR system. Performance would, of course, be slightly improved for an optimized constellation.

2.2 MEASUREMENT ERROR SOURCES

Although it is a relatively straightforward matter to identify the error sources associated with user measurements and to assign a number to each source, a difficulty arises in properly qualifying these numbers with respect to their important correlation properties. In general, each measurement may be associated with a particular time, a particular location, and a particular satellite by either a ground station or a user. The related types of measurement correlation are:

- Time Serial Correlation, affecting error sources which are neither pure (constant) bias nor independent for each measurement sample. This intermediate class of error sources may be highly correlated over many measurements but not over all available data; proper treatment of this case requires an estimate of the effective correlation time so that the effect of serial smoothing can be suitably represented. An example is ionospheric error, which is a slowly varying quantity.

- Inter-station Correlation, where a phenomenon is physically common to some or all measurements associated with the same satellite. An example is the error due to satellite oscillator drift.

- Intersatellite Correlation, where a phenomenon is physically common to some or all measurements associated with the same station, such as ground survey error.

In general, information is not available on which to base a detailed functional correlation model for partial correlations when they exist. In

*Some of this work has been subsequently performed by TRW for the Navy (Ref. 4).

many cases, it would not be possible to incorporate such partial correlations within the framework of present programs even if they were known. As a feasible approximation, we have chosen to represent such correlations as an "on-off" phenomenon. That is, the related measurements are represented as either fully correlated or completely independent, as a function of the estimated time constant, distance separation, etc. Present programs will generally permit such gross representations in terms of appropriately constrained biases or measurement errors in the appropriate domain.

The sources of measurement error are as follows:

Tropospheric retardation
Ionospheric refraction
Receiver noise
Receiver drift
Quantization
Multipath effects
Oscillator error
Speed of light

The characteristics of these error sources are discussed separately in the following paragraphs and are summarized in Table I.

2.2.1 Tropospheric Error (Refs. 2, 3, 9, 10, and 11)

The total tropospheric retardation is rather accurately estimated by

$$\sigma = 8 \text{ ft Csc E (class b user)}$$

where E is the elevation angle of the line of sight from the horizontal.

This will be taken as the total error σ_r for a low-accuracy user who does not make a refraction correction (class b user). For a high-accuracy (class a) user or ground station the residual from a standard correction of this type is about 5 percent of the correction itself or

$$\sigma = 0.4 \text{ ft Csc E (class a user or ground station)}$$

This error is considered correlated for time differences less than 1 hr, for ground position differences less than 20 mi, and for all satellites viewed by a given station.

TABLE I

ERROR SUMMARY

Source	σ (ft)		Correlation
Ground Station Range			
Troposphere	$0.4 \csc E \sqrt{10^{o^2} + E^2}$		All ranges for which $\tau < 1$ hr, $\Delta < 20$ mi
Ionosphere	$6.9 \csc \sqrt{10^{o^2} + E^2}$		All ranges for which $\tau < 1$ hr, $\Delta < 600$ mi
Receiver Noise	7.8		none
Receiver Quantization	5.1		none
Multipath	0		
Receiver Drift	12		All ranges from a given ground station for $\tau < 1$ hr
User Range Measurement	Class a	Class b	
Troposphere	$0.4 \csc E$	$8 \csc E$	All ranges for which $\tau < 1$ hr, $\Delta < 20$ mi
Ionosphere	$6.9 \csc \sqrt{(10^o)^2 + E^2}$	$13.8 \csc \sqrt{(10^o)^2 + E^2}$	All ranges for which $\tau < 1$ hr, $\Delta < 20$ mi
Receiver Noise	14	32	none
Receiver Quantization	10.2	21	none
Multipath	45	45	none
Receiver Drift	17	17	All user range measurement for $\tau < 1$ hr
Osc Error	9.2	9.2	All user range measurements to a given satellite for which $\tau < 2$ hr
Speed of Light	<4	<4	

2.2.2 Ionospheric Error (Refs. 2 and 3)

Accounting for the elevation angle effect in ionospheric error is a little more complicated because the significant variable is the elevation angle at the ionosphere. Approximating this reasonably well by

$$E_{\text{ionosphere}} = \sqrt{(10^{\circ})^2 + (E_{\text{ground}})^2}$$

we can write for the average daytime (worst-case) ionospheric retardation at 1500 MHz

$$\sigma = 13.8 \text{ ft Csc } \sqrt{(10^{\circ})^2 + E^2} \text{ (class b user)}$$

this will be taken as the total error for the low-accuracy (class b) user. For the high-accuracy user or ground station who makes a correction based on a precomputed table as a function of local apparent time, geomagnetic latitude, and elevation angle, the anticipated residual is reduced as much as 50 percent:

$$\sigma = 6.9 \text{ ft Csc } \sqrt{(10^{\circ})^2 + E^2} \quad \text{(class a user and ground station)}$$

This error is considered correlated for distances less than 600 mi, for time less than 1 hr and for all satellites seen from a given ground station.

2.2.3 Thermal Noise

The error due to thermal noise is a function of the received SNR. For the user and ground station this error will be 32 and 18 ft, respectively, in a 26-Hz bandwidth. It is now further planned that after acquisition, the class a user and the ground station will provide a further bandwidth narrowing by averaging over 8 frames of the 78-Hz component or $T = 8/78 = 0.102$ sec. The effective bandwidth of this averaging process is $1/2T = 4.9$ Hz resulting in a further improvement factor of $\sqrt{4.9/26} = 1/2.3$. This leads to net errors of

$$\sigma = \begin{cases} 32 & \text{ft (class b user)} \\ 14 & \text{ft (class a user)} \\ 7.8 & \text{ft (ground station)} \end{cases}$$

These errors are fully correlated during any one observation, uncorrelated between successive (16 sec) frames, and uncorrelated between all independent ranges (not range differences).

2.2.4 Quantizing Noise

The user has a 10-MHz clock for range count, whereas a ground station will have a 20-MHz clock. These result in 29 and 14.5 ft 1-σ quantization errors, respectively, for the user and ground station. These are independent at 1/78 sec basic sample intervals and it is presently planned that for a class a user or ground station a complete measurement will consist of an accumulation or average of 8 such measurements for a further advantage of $\sqrt{8}$ resulting in:

$$\sigma = \begin{cases} 29 \text{ ft} & \text{(class b user)} \\ 10.2 \text{ ft} & \text{(class a user)} \\ 5.1 \text{ ft} & \text{(ground station)} \end{cases}$$

This error is completely uncorrelated betweel all range measurements and serially between frames.

2.2.5 Oscillator Error (Ref. 5)

From Ref. 5 (Fig. 4), for a quartz oscillator and a 2-hr typical extrapolation period

$$\sigma = 9.2 \text{ ft}$$

This is linearly proportional to T for times other than 2 hr. As such, the error is to be considered correlated for all times less than 2 hr and for all ranges from all stations to a given satellite.

2.2.6 Multipath

This factor is assumed negligible for the ground station or for a surface ship due to ground antenna directivity and short multipath lengths (Ref. 6). For the aircraft, present planning is to utilize modulation characteristics to ensure worst-case (elevation angle 10°, worst altitude) multipath error less than 45 ft. This error may be considered essentially uncorrelated from frame to frame (10 sec) and between all range measurements from all stations to all satellites.

2.2.7 Receiver Drift Errors

The drifts in the IF, carrier phase-locked loop, and the range signal phase-locked loop have been estimated to RSS to

$$\sigma = \begin{cases} 17 \text{ ft} & \text{(class a or b user)} \\ 12 \text{ ft} & \text{(ground station)} \end{cases}$$

This should be considered correlated for times less than about 1 hr and for all ranges measured by a given ground station.

2.2.8 Speed of Light

The present fractional uncertainty in the velocity of light is estimated at 0.3×10^{-6}. However, it is of course completely correlated between all range measurements. Ideally, it should be modelled as an unrecovered systematic error source common to all ground and user measurements. Short of this, it is suggested that the error can be bounded by a representation as an additional user position error (not range-measurement error) of 0.3×10^{-6} of the distance to the "average," (or in the case of relative navigation, to the reference) ground station. Taking that distance conservatively as 2000 mi the effective position error is 4 ft or less, which can safely be ignored.

2.2.9 Summary

It is difficult to RSS these diverse error sources since they are, in many cases, not directly comparable because of different correlation effects and have to be treated as separate error sources. Nevertheless, to give an idea of the resulting orders of magnitude, ignoring all correlations and RSSing all measurement errors for an assumed elevation angle of 10°, the tabulation below yields the following results.

	Ground Station	Class a User	Class b User
Troposphere	2.3	2.3	46
Ionosphere	28	28	56
Receiver Noise	7.8	14	32
Quantization	5.1	10.2	29
Multipath	0	45	45
Drift	12	17	17
Oscillator Error	0	9.2	9.2
RSS	32	59	98

It is to be re-emphasized, however, that these RSS numbers are not for direct program input. For such purposes, these numbers must be appropriately modified taking into account the restrictions of the program in which the data are to be used and the serial and intermeasurement correlations.

2.3 NAVIGATION ACCURACY AND COVERAGE

The overall navigation accuracy provided by the proposed system was analyzed for the complete worldwide system and for an interim system covering the North Atlantic. (The interim system consists of the four satellites labeled numerically in Figure 1.) Special analyses were made of the accuracy of velocity estimates from doppler measurements and of the accuracy of relative navigation. These analyses are discussed separately in this section.

2.3.1 Worldwide System Accuracy and Coverage

The navigation accuracies obtained by a user of the system depend on three elements:

- Measurement noise and bias (discussed in detail in Subsection 2.2)
- Satellite position uncertainties (discussed in subsec. 2.4)
- Relative geometry between user and satellites, which varies with user location and time of day.

For purposes of analysis, the (range) measurement noise standard deviation is taken as 50 ft for either the interim or worldwide system. This value is derived by taking the RSS of the receiver noise, quantization error, multipath error, satellite oscillator error, and a portion of the tropospheric and ionospheric errors.*

*Tropospheric and ionospheric errors are correlated among all satellites, but have different values depending on elevation angle. Half of the 28-ft ionospheric error (see subsec. 2.2) is treated as a bias and the other half as random; the 14-ft random half is included in the RSS calculation. The remaining errors behave like biases in the user equipment and are dominated by the uncertainty in user oscillator calibration.

Since no attempt is made to calibrate the user oscillator, a large a priori bias is assumed in the user equipment. This parameter is then solved for along with the user position, as indicated in the discussion of the navigation equations (subsec. 3.2). The equivalence of this procedure to range difference is discussed in par. 2.5.3.

Navigation accuracies were determined first in the absence of orbit determination uncertainties (i.e., assuming perfect knowledge of satellite positions). This analysis illustrates the effect of measurement errors alone and thus serves to establish an upper bound on usable accuracies of an ideal satellite tracking network. It will be seen later that the effect of tracking (i.e., satellite position) errors is to cause only a 5 to 10 percent decrease in accuracy.

The results of the navigation accuracy analysis assuming no satellite position errors are shown in Figure 2 for the worldwide system and for an assumed uncertainty of 75 ft (1σ) in a priori knowledge of user altitude. The accuracy figures and those of the following subsection were obtained from the MSAT computer program described in app. B. The coverage boundaries were computed using the program described in apps. C and D. The following information is presented in the figure:

- The subsatellite points for those satellites in the northern hemisphere
- The absolute navigation accuracy obtainable within each contour, defined as the C95 value, or the uncertainty corresponding to 95 percent confidence that the actual location is within a circle of the given radius. It will be noted that near the equator the accuracy contours do not always coincide with the coverage regions.

In interpreting these results, it should be kept in mind that the figures are absolute accuracies, that is, accuracies of position determination relative to an earth-centered coordinate system. If the user accuracy is desired relative to another point on the earth, then it is necessary to add (RSS) the uncertainty in the location of that point. As will be seen later, in par. 2.3.4 on relative navigation, some of the errors may cancel when the two points are in the same vicinity and both estimate position using navigation satellites.

Figure 2 and the succeeding polar plots through Figure 14 are to be used with the clear polar overlay found in the pocket inside the back cover of this report. At time T_0* the Greenwich meridian of the overlay (found in pocket inside back cover) aligned with the indexing axis on the map.

Some of the characteristics to be seen from the figure irrespective of the overlay orientation are: 1) for latitudes up to 55°, navigation accuracy is within 250 ft (C95) at all longitudes; 2) the highest accuracies are associated with large numbers of visible satellites, but the number required for a given accuracy decreases toward the poles because of more favorable geometry; 3) there are two small regions of indeterminacy near the pole.

Navigation accuracies for particular regions of the northern hemisphere can be determined for 3-hr intervals after time T_0 by rotating the overlay 45° counterclockwise for each 3 hr. The system configuration is such that at the end of 3 hr each satellite is at the position occupied 3 hr earlier by the one leading it. The system is thus identical, but the earth has rotated 45° eastward during this period.

Accuracy contours for times within this 3-hr interval are given in Figure 3, 4, and 5 for 45, 90, and 135 min after time T_0, respectively. These maps show that the accuracy contours change in size and shape through the interval, with a general movement to the west. Navigation accuracy remains high up to 55° latitude and is generally equivalent to that obtainable at T_0.

These plots provide a good general idea of the coverage and accuracy provided by the system and of the variations of coverage with time. More detailed data on overall navigation accuracy as a function of geographical location are presented in the computer-generated tables, Tables II through VI.** Table II presents results for the system at time T_0, with zero satellite position uncertainties. Table III presents the same data computed with satellite position uncertainties of the expected magnitudes (see subsec. 2.4 for a discussion of these uncertainties). Although the altitude

*T_0 denotes an arbitrary epoch at which the system is defined. T_{45}, T_{90}, etc. denote times 45 min, 90 min, etc. after T_0.

**A one (1) in these and the following tables denotes that insufficient satellites are visible to provide a fix.

uncertainty for Table III is 150 ft rather than the 75 ft of Table II, the prime contributor to the C95 increase is the satellite error.* Comparison of the two tables shows that the increase in C95 due to the inclusion of satellite errors ranges from less than 10 to 50 ft, occasionally reaching values between 50 and 100 ft. The effect tends to increase at higher latitudes.

Tables IV and V present the same data for the system at T_{45}, indicating that the change in geometry over this period results in very minor changes in C95 position uncertainty of a few feet either more or less. Some large changes can be seen at high latitudes because of the rotation of the regions of indeterminacy near the poles.

Table VI shows the same information for T_{90}, with the satellite position errors included. Again the changes from the comparable T_0 values are small, on the order of 20 ft or less, except in certain high-latitude regions.

It will be recalled that these results are based on an a priori user altitude uncertainty (except as noted) of 75 ft. This assumption will be valid for surface vessels and may hold for aircraft with recently calibrated altimeters. In general, however, altimeter readings using pressure equivalents may not have this accuracy after long flight intervals. The sensitivity of navigation uncertainty to a priori altitude accuracy is indicated in Figure 6, which is based on an a priori altitude sigma of 2500 ft. This is equivalent to essentially no a priori information. In the regions where only three satellites are visible, there is a loss of accuracy. In regions with more redundancy, however, the variation is much less.

*Figure 4-24 of Reference 4 shows the variation of C95 with altitude for a 4-satellite interim system. In that case, with 75 ft altitude error, the C95 is 240 ft, and with 150 ft altitude error, the C95 is 320 ft. With more satellites visible, this variation will be sharply reduced.

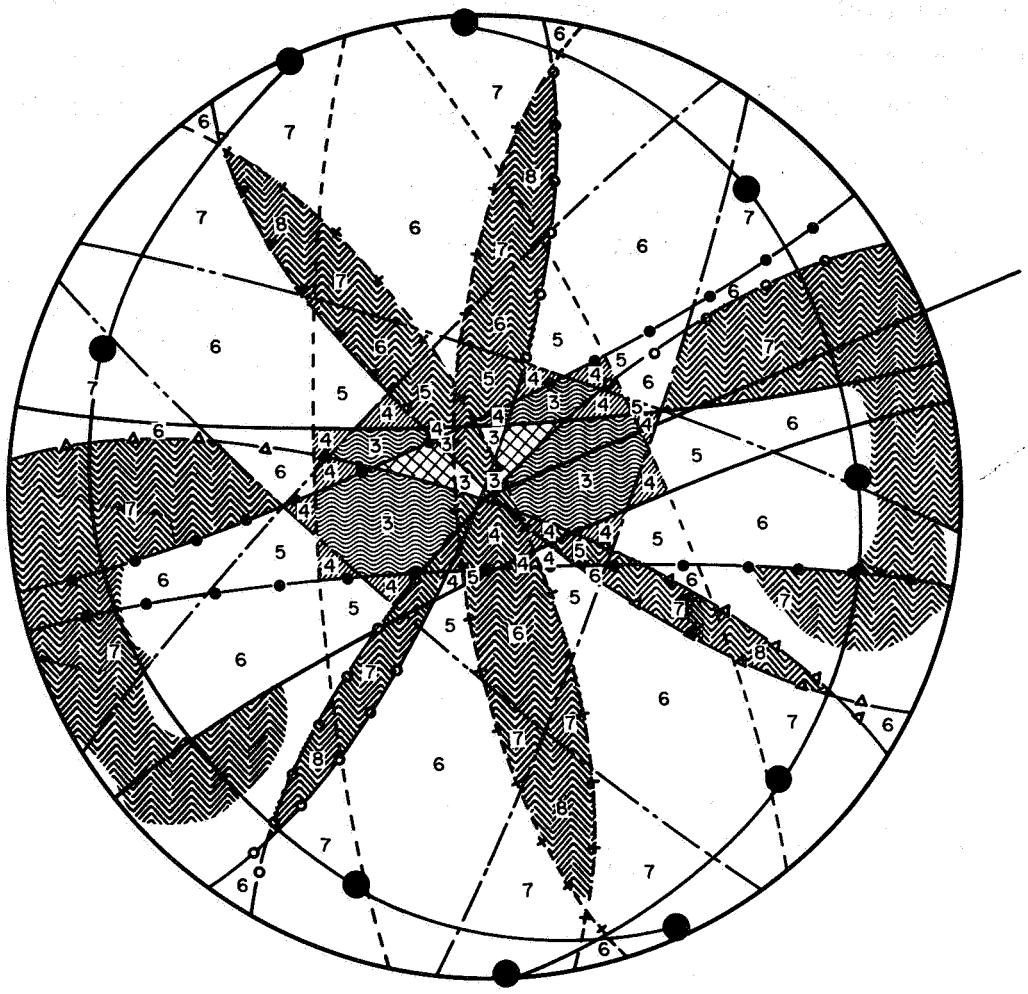

KEY

C95

< 150 FT

150 - 250 FT

250 - 400 FT

400 - 600 FT

> 600 - 5000 FT

INDETERMINATE

A PRIORI ALTITUDE SIGMA = 75 FEET

NOTE:

● INDICATES SUBSATELLITE POINT (ABOVE EQUATOR)

Figure 2. Worldwide Accuracy at T_0

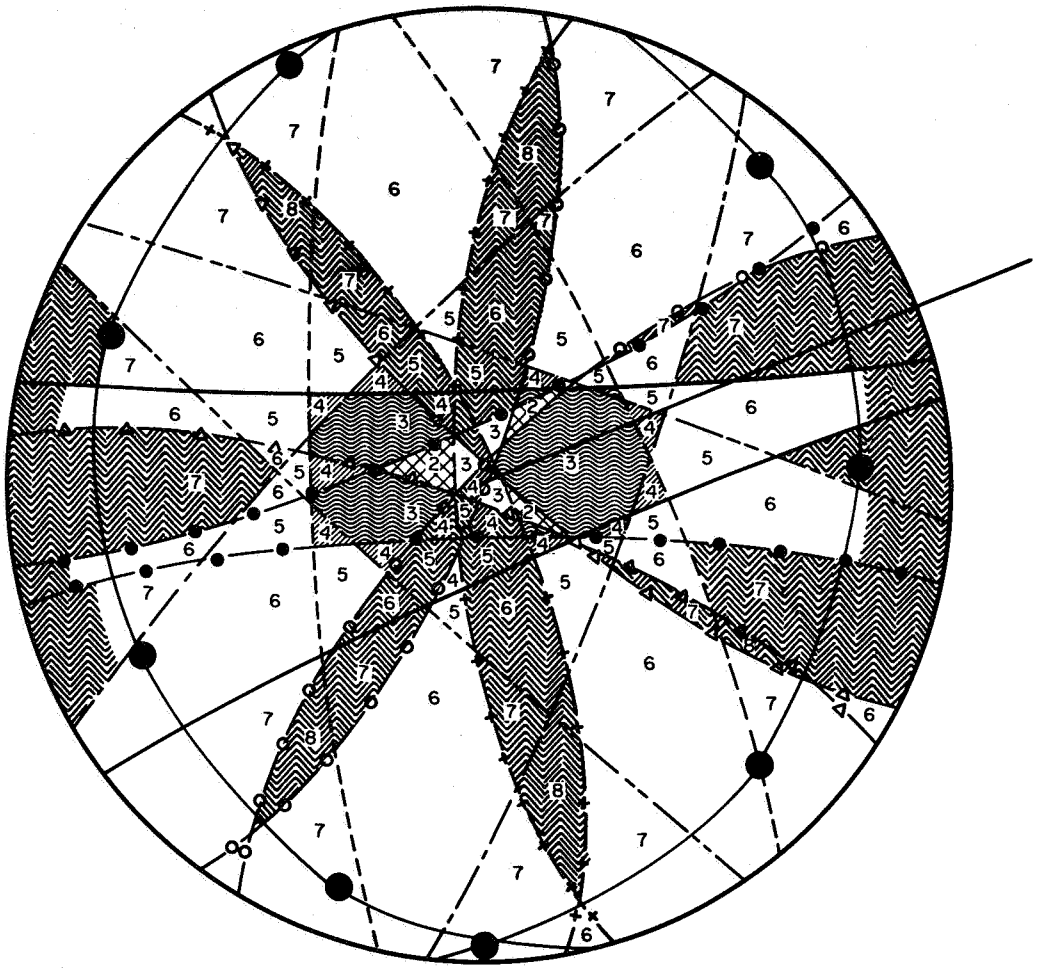

KEY

C95
< 150 FT

150 - 250 FT

250 - 400 FT

400 - 600 FT

> 600 - 5000 FT

INDETERMINATE

A PRIORI ALTITUDE SIGMA = 75 FEET

NOTE:

● INDICATES SUBSATELLITE POINT (ABOVE EQUATOR)

Figure 3. Worldwide Accuracy at T_{45}

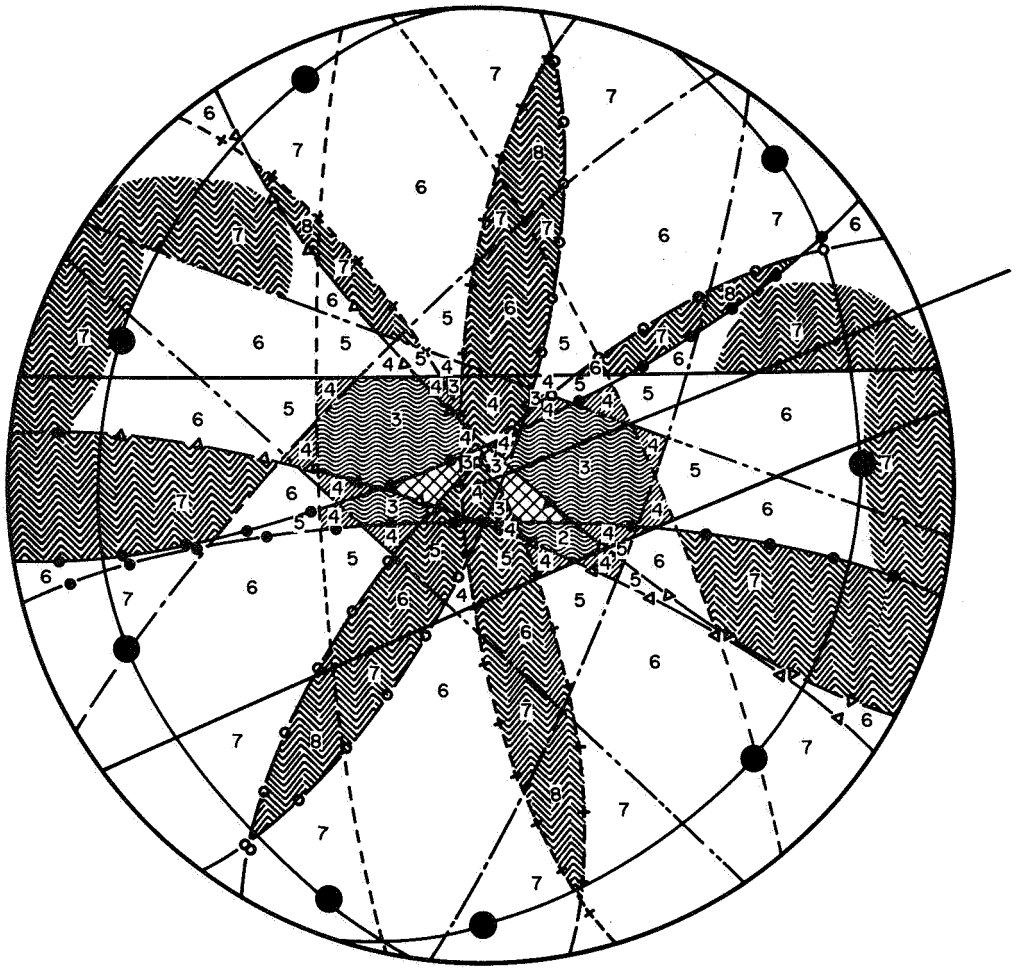

KEY

C95

< 150 FT

150 - 250 FT

250 - 400 FT

400 - 600 FT

>600 - 5000 FT

INDETERMINATE

A PRIORI ALTITUDE SIGMA = 75 FEET

NOTE:

● INDICATES SUBSATELLITE POINT (ABOVE EQUATOR)

Figure 4. Worldwide Accuracy at T_{90}

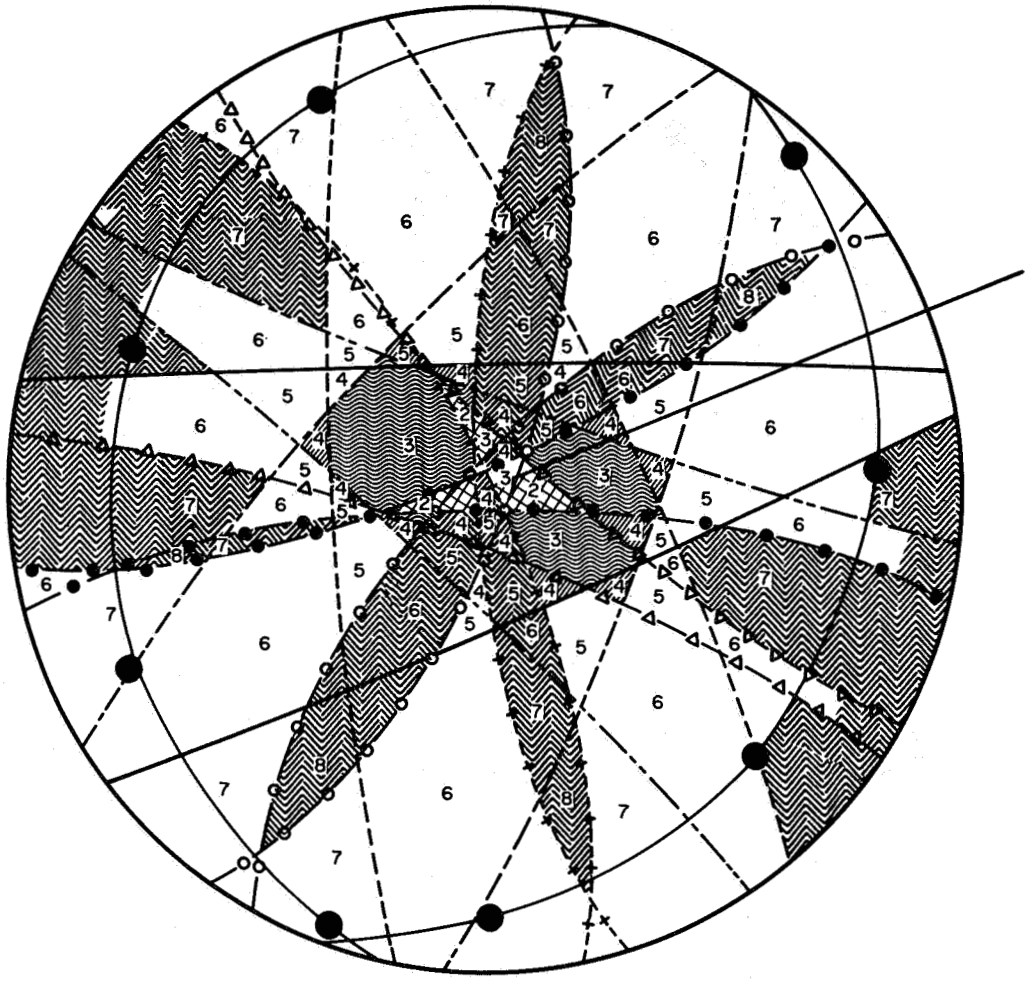

KEY

C95
< 150 FT

150 - 250 FT

250 - 400 FT

400 - 600 FT

>600 - 5000 FT

INDETERMINATE

A PRIORI ALTITUDE SIGMA = 75 FEET

NOTE:

● INDICATES SUBSATELLITE POINT (ABOVE EQUATOR)

Figure 5. Worldwide Accuracy at T_{135}

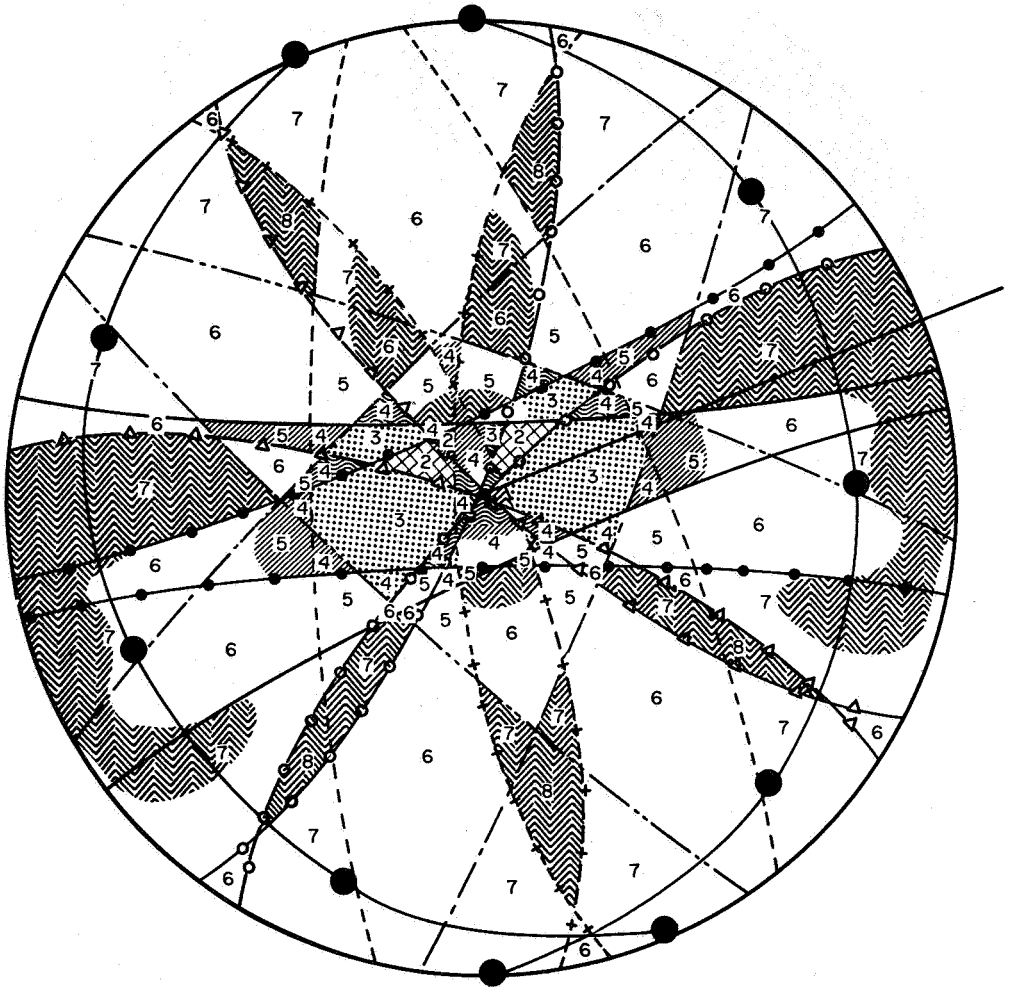

KEY

C95

< 150 FT

150 - 250 FT

250 - 400 FT

400 - 600 FT

>600 - 5000 FT

INDETERMINATE

A PRIORI ALTITUDE SIGMA = 2500 FEET

NOTE:

● INDICATES SUBSATELLITE POINT (ABOVE EQUATOR)

Figure 6. Worldwide Accuracy at T_0 With Poor Altitude Data

TABLE II

WORLDWIDE NAVIGATION ACCURACY (C95) AS A FUNCTION OF USER LONGITUDE AND LATITUDE AT T = 0 WITHOUT SATELLITE ERRORS

NORTH LATITUDE

LONGITUDE	0	10	20	30	40	50	60	70	80	90	
-180	143	146	151	161	172	220	306	462	424	1	
-170	151	149	153	160	172	186	226	461	424	1	
-160	150	149	149	150	173	220	225	458	423	1	
-150	152	151	151	151	152	127	120	142	146	1	
-140	164	165	167	167	170	126	119	141	146	1	
-130	165	167	177	171	169	173	183	206	150	1	
-120	208	191	178	171	169	173	200	112	149	1	
-110	127	127	125	123	121	117	114	112	149	1	
-100	215	179	141	130	120	126	114	111	149	1	Symmetric About -98.75
-90	177	177	175	172	171	118	114	111	149	1	
-80	176	191	179	172	170	173	200	112	149	1	
-70	166	190	178	171	169	173	183	206	149	1	
-60	164	166	167	171	170	174	184	210	150	1	
-50	169	151	151	130	124	126	119	142	146	1	
-40	151	149	149	150	151	220	225	457	423	1	
-30	151	150	153	160	172	186	226	461	424	1	
-20	143	146	151	161	172	187	306	462	424	1	
-10	145	148	155	166	180	223	529	461	424	1	
0	143	142	142	144	147	198	520	457	423	1	
10	151	142	143	145	148	160	278	451	421	1	
20	150	153	156	160	210	239	499	1	1	1	
30	152	162	160	162	168	178	363	441	1	1	
40	164	163	161	163	169	178	211	437	1	1	
50	165	163	161	158	171	209	210	270	1	1	
60	208	175	133	123	126	117	111	126	194	1	
70	177	175	178	169	167	114	111	125	129	1	
80	215	193	177	168	166	171	198	125	129	1	Symmetric About 81.25
90	177	175	178	169	167	172	111	125	129	1	
100	176	175	171	123	125	117	111	126	194	1	
110	166	164	161	158	172	118	112	126	194	1	
120	164	162	161	163	169	211	211	436	1	1	
130	169	162	160	162	168	178	212	440	1	1	
140	151	153	156	162	168	239	364	1	1	1	
150	151	158	143	145	148	160	276	450	421	1	
160	143	142	142	144	147	151	523	456	423	1	
170	145	148	155	166	180	224	527	460	424	1	

SYSTEM: 2x8

ORBITAL PERIOD: 24 hours
TIME FROM EPOCH: 0 hours

ORBITAL INCLINATION: 18.5°
SPACING OF ASCENDING NODES: 157.5°
ARGUMENT OF LATITUDE OF THE FIRST SATELLITE IN EACH PLANE AT EPOCH: 0°
SATELLITE SPACING WITHIN EACH PLANE: 45°

MEASUREMENT NOISE (1σ): 50 feet
USER ALTITUDE UNCERTAINTY (1σ): 75 feet
SATELLITE POSITION UNCERTAINTY (1σ)
RADIAL (u): 0
IN-TRACK (v): 0
CROSS-TRACK (w): 0
MINIMUM USER ELEVATION ANGLE: 5°

(1) Denotes indeterminate point

TABLE III

WORLDWIDE NAVIGATION ACCURACY (C95) AS A FUNCTION OF USER LONGITUDE AND LATITUDE AT T = 0 WITH SATELLITE ERRORS

NORTH LATITUDE

LONGITUDE	0	10	20	30	40	50	60	70	80	90
0	151	149	150	152	156	210	607	515	462	1
10	160	150	151	153	156	171	393	506	459	1
20	159	162	165	169	232	264	585	1	1	1
30	162	172	169	171	178	189	390	497	1	1
40	174	174	170	172	178	189	223	490	1	1
50	177	174	171	168	181	223	221	300	1	1
60	229	188	147	135	146	132	116	134	204	1
70	191	189	199	184	178	125	118	133	136	1
80	244	219	197	183	177	181	209	132	136	1
90	191	189	198	183	177	182	119	132	136	1
100	190	188	184	136	145	132	119	133	204	1
110	179	177	175	172	185	134	120	135	203	1
120	175	174	173	175	181	227	225	482	1	1
130	181	174	171	172	179	190	226	489	1	1
140	160	162	165	172	179	267	382	1	1	1
150	160	169	153	155	158	170	389	509	461	1
160	151	150	151	153	156	160	609	517	463	1
170	153	157	165	178	194	257	620	521	465	1
180	151	155	160	172	185	252	331	523	465	1
190	160	158	161	170	183	199	238	521	464	1
200	159	158	157	158	185	231	237	516	462	1
210	162	160	159	160	161	140	129	162	163	1
220	175	176	177	178	181	139	127	160	163	1
230	177	178	192	183	179	183	194	218	157	1
240	229	210	194	184	180	182	212	120	157	1
250	191	190	188	187	182	131	129	118	156	1
260	244	193	157	145	133	156	128	117	156	1
270	191	192	190	187	185	132	128	118	156	1
280	190	213	197	187	182	185	213	119	156	1
290	178	209	194	185	181	184	195	219	157	1
300	175	177	178	184	181	185	196	223	158	1
310	181	162	162	142	135	141	129	162	163	1
320	160	159	159	161	162	233	240	518	464	1
330	161	159	163	172	185	201	239	522	465	1
340	151	155	160	171	185	201	328	523	465	1
350	153	156	165	178	193	255	619	520	464	1

SYSTEM: 2x8

ORBITAL PERIOD: 24 hours
TIME FROM EPOCH: 0 hours

ORBITAL INCLINATION: 18.5°
SPACING OF ASCENDING NODES: 157.5°
ARGUMENT OF LATITUDE OF THE FIRST SATELLITE IN EACH PLANE AT EPOCH: 0°
SATELLITE SPACING WITHIN EACH PLANE: 45°

MEASUREMENT NOISE (1σ): 50 feet
USER ALTITUDE UNCERTAINTY (1σ): 150 feet
SATELLITE POSITION UNCERTAINTY (1σ)
RADIAL (u): 15 feet
IN-TRACK (v): 117 feet
CROSS-TRACK (w): 38 feet
MINIMUM USER ELEVATION ANGLE: 5°

(1) Denotes indeterminate point

TABLE IV

WORLDWIDE NAVIGATION ACCURACY (C95) AS A FUNCTION OF USER LONGITUDE AND LATITUDE AT T = 45 MIN. WITHOUT SATELLITE ERRORS

NORTH LATITUDE

LONG	0	10	20	30	40	50	60	70	80	90
-180	145	148	152	160	169	181	320	460	423	129
-170	159	155	155	160	168	180	220	458	422	129
-160	156	155	154	154	169	217	219	322	139	129
-150	158	157	156	155	121	125	117	135	139	129
-140	170	172	171	170	136	123	115	134	139	129
-130	172	173	184	174	170	172	180	205	98	129
-120	223	201	185	174	170	172	180	205	149	129
-110	178	179	177	175	171	172	114	111	149	129
-100	209	179	140	129	120	120	114	111	149	129
-90	172	171	169	166	126	125	114	111	149	129
-80	170	169	170	166	168	174	206	112	149	129
-70	158	175	168	165	167	174	207	211	149	129
-60	156	158	161	165	168	175	209	212	1	129
-50	158	145	145	147	149	163	161	452	1	129
-40	145	144	144	145	148	164	230	456	422	129
-30	146	146	152	162	176	192	298	459	423	129
-20	141	145	150	162	176	221	529	460	423	129
-10	146	147	152	162	174	223	523	458	422	129
0	145	144	144	145	176	191	513	453	421	129
10	159	145	145	146	148	164	499	447	419	129
20	156	158	159	164	167	123	244	440	417	129
30	158	171	164	163	166	174	204	1	415	129
40	170	172	165	164	167	175	203	253	192	129
50	172	169	165	162	169	116	110	123	192	129
60	223	176	132	121	122	115	109	122	193	129
70	178	176	171	168	167	111	109	122	129	129
80	209	189	175	167	166	171	192	123	129	129
90	172	170	175	167	166	171	135	128	129	129
100	170	169	168	123	127	117	113	138	1	129
110	158	156	154	153	153	214	216	437	1	129
120	156	154	153	161	170	216	217	443	1	129
130	158	154	155	160	169	180	504	447	1	129
140	145	148	152	157	199	230	511	450	1	129
150	146	150	141	143	146	155	282	451	1	129
160	141	140	140	143	146	154	286	455	1	129
170	146	150	159	171	187	224	323	459	423	129

LONGITUDE

MEASUREMENT NOISE (1σ): 50 feet
USER ALTITUDE UNCERTAINTY (1σ): 75 feet
SATELLITE POSITION UNCERTAINTY (1σ)
RADIAL (u): 0
IN-TRACK (v): 0
CROSS-TRACK (w): 0
MINIMUM USER ELEVATION ANGLE: 5°

SYSTEM: 2x8

ORBITAL PERIOD: 24 hours
TIME FROM EPOCH: .75 hours

ORBITAL INCLINATION: 18.5°
SPACING OF ASCENDING NODES: 157.5°
ARGUMENT OF LATITUDE OF THE FIRST SATELLITE IN EACH PLANE AT EPOCH: 0°
SATELLITE SPACING WITHIN EACH PLANE: 45°

(1) Denotes indeterminate point

TABLE V

WORLDWIDE NAVIGATION ACCURACY (C95) AS A FUNCTION OF USER LONGITUDE AND LATITUDE AT T = 45 MIN. WITH SATELLITE ERRORS

NORTH LATITUDE

LONGITUDE	0°	10	20	30	40	50	60	70	80	90
0	154	153	153	155	189	203	598	510	461	136
10	170	154	154	156	158	177	578	501	458	136
20	167	168	169	175	178	134	306	490	454	136
30	169	184	176	173	176	185	217	1	450	136
40	183	186	177	174	176	185	214	270	203	136
50	185	182	178	173	178	135	118	131	203	136
60	249	191	148	135	143	132	117	129	203	136
70	193	191	186	184	179	122	117	129	137	136
80	237	214	195	182	177	181	202	130	137	136
90	185	184	195	182	177	182	156	138	137	136
100	183	182	180	137	147	130	121	154	1	136
110	170	169	168	167	166	229	230	486	1	136
120	167	166	165	174	183	230	230	495	1	136
130	169	165	166	171	181	193	585	501	1	136
140	154	158	162	167	225	262	595	505	1	136
150	155	161	151	153	157	166	402	507	1	136
160	150	149	150	152	156	165	408	519	1	136
170	155	160	170	185	201	256	348	522	465	136
180	154	157	162	170	180	193	343	522	465	136
190	170	164	164	169	179	192	232	519	464	136
200	166	165	164	163	180	230	230	386	150	136
210	169	166	167	166	132	141	127	153	150	136
220	183	184	184	182	158	139	125	151	150	136
230	186	186	205	190	182	182	191	216	106	136
240	249	226	206	190	182	182	190	215	157	136
250	193	193	191	192	183	183	123	118	157	136
260	237	194	157	145	133	136	127	118	157	136
270	185	186	184	182	144	154	123	118	157	136
280	183	183	185	180	181	187	220	119	157	136
290	169	191	182	178	179	186	221	223	158	136
300	166	169	171	173	179	187	224	225	1	136
310	168	156	156	158	161	176	173	515	1	136
320	155	154	154	156	159	177	244	520	464	136
330	155	156	163	175	190	208	324	523	465	136
340	150	154	159	175	191	254	621	522	465	136
350	155	156	162	173	187	257	612	518	463	136

SYSTEM: 2x8

ORBITAL PERIOD: 24 hours
TIME FROM EPOCH; .75 hours

ORBITAL INCLINATION: 18.5°
SPACING OF ASCENDING NODES: 157.5°
ARGUMENT OF LATITUDE OF THE FIRST SATELLITE IN EACH PLANE AT EPOCH: 0
SATELLITE SPACING WITHIN EACH PLANE: 45°

MEASUREMENT NOISE (1σ): 50 feet
USER ALTITUDE UNCERTAINTY (1σ): 150 feet
SATELLITE POSITION UNCERTAINTY (1σ)
RADIAL (u): 15 feet
IN-TRACK (v): 117 feet
CROSS-TRACK (w): 38 feet
MINIMUM USER ELEVATION ANGLE: 5°

(1) Denotes indeterminate point

TABLE VI

WORLDWIDE NAVIGATION ACCURACY (C95) AS A FUNCTION OF USER LONGITUDE AND LATITUDE AT T = 90 MIN. WITH SATELLITE ERRORS

NORTH LATITUDE

LONGITUDE	0	10	20	30	40	50	60	70	80	90
0	159	158	157	158	184	231	583	503	458	136
10	185	160	159	159	160	230	483	493	455	136
20	175	175	175	179	145	131	172	482	451	136
30	178	199	185	177	176	183	210	171	111	136
40	190	201	186	177	176	182	207	157	111	136
50	191	188	183	180	178	135	117	156	160	136
60	257	191	149	135	138	135	116	155	160	136
70	191	189	185	182	179	135	117	156	160	136
80	220	202	188	179	177	183	208	279	111	136
90	177	178	187	179	177	184	210	172	448	136
100	174	175	175	138	147	133	173	488	452	136
110	162	161	161	161	162	233	492	498	455	136
120	160	158	158	174	186	200	589	506	457	136
130	153	159	163	171	184	260	603	511	459	136
140	151	155	160	181	220	257	611	514	1	136
150	153	156	166	180	197	214	612	514	1	136
160	151	150	150	153	156	169	283	317	1	136
170	160	167	179	194	224	257	371	519	1	136
180	160	162	166	172	178	188	229	518	1	136
190	185	175	171	171	177	187	226	333	145	136
200	175	174	172	174	179	188	224	146	144	136
210	178	177	175	172	132	148	127	144	135	136
220	190	191	189	144	160	139	126	142	134	136
230	192	192	212	194	184	183	191	141	134	136
240	257	233	211	194	183	182	190	214	91	136
250	191	192	190	194	184	182	183	141	134	136
260	219	191	155	145	160	139	127	142	134	136
270	177	177	177	175	173	149	128	143	135	136
280	174	174	175	175	181	190	227	145	143	136
290	161	176	172	173	179	189	228	333	144	136
300	159	162	166	173	179	190	230	515	1	136
310	153	152	152	155	158	169	366	514	1	136
320	151	150	151	153	157	169	411	519	1	136
330	153	156	166	180	198	216	618	519	1	136
340	151	155	160	166	220	257	612	517	463	136
350	160	158	162	171	183	197	600	512	461	136

SYSTEM: 2x8

ORBITAL PERIOD: 24 hours
TIME FROM EPOCH: 1.5 hours

ORBITAL INCLINATION: 18.5°
SPACING OF ASCENDING NODES: 157.5°
ARGUMENT OF LATITUDE OF THE FIRST SATELLITE IN EACH PLANE AT EPOCH: 0°
SATELLITE SPACING WITHIN EACH PLANE: 45°

MEASUREMENT NOISE (1σ): 50 feet
USER ALTITUDE UNCERTAINTY (1σ): 150 feet
SATELLITE POSITION UNCERTAINTY (1σ)
RADIAL (u): 15 feet
IN-TRACK (v): 117 feet
CROSS-TRACK (w): 38 feet
MINIMUM USER ELEVATION ANGLE: 5°

(1) Denotes indeterminate point

2.3.2 Interim System Accuracy and Coverage

The interim system analyzed consists of two satellites in each of the same two orbit planes used for the worldwide system. The satellites are positioned to provide the best coverage over the North Atlantic.

With only two satellites in each plane, the system configuration at time T_0 does not repeat every 3 hr as in the 2 x 8 worldwide system, but only after 24 hr. Figures 7 through 14 show coverage and accuracy contours for this system every 3 hr of the 24-hr cycle. Detailed numerical data for the same time periods are presented in Tables VII through XIV for the case of no satellite errors and in Tables XV through XXII for the case of the assumed nominal satellite position uncertainties. It can be seen that for the interim system also the effect of including satellite errors is relatively minor.

In general, the above data indicate that the four satellite system yields C95 uncertainties of less than 400 ft at latitudes below 50^{o} An aircraft flying from New York to London would have a navigation uncertainty varying from about 400 ft at the beginning of the trip to about 600 ft at the end. This is two orders of magnitude better than the navigation accuracy available today.

As shown by the maps for the various times of day, the accuracy contours change during the day because of changing user-to-satellite geometry, but the average C95 accuracies are comparable to the T_0 values except for T = 18 and T = 21 hr, when the geometry is unfavorable for users in the northern hemisphere.

The variation in C95 navigation accuracy with time of day is summarized in Figure 15, where it is shown for three typical user locations. The locations selected are near New York, near the midpoint of the flight corridor, and a point south of the latter location. It can be seen that the accuracy is approximately constant except for the period between T = 16 and T = 22 hr when the uncertainty rises rapidly. For a short period, the user's position cannot be determined because only three satellites are visible and the measurements from the three are redundant due to adverse geometry. At one point, the three sateillites and the user are in the same plane.

The position would still be determinable at this time except for the large bias in the user measurement. The coplanarity of the user and three satellites causes the spherical surfaces of constraint from satellite to user to be tangent, so that the user's location on a line in the northwest/ southeast direction cannot be determined.

In general, it is clear that the interim system provides high accuracy during most of the day, but is degraded for a period of about an hour. This difficulty can be alleviated by increasing the orbit plane inclination at the cost of decreased average accuracy, or by adding one or two satellites to the interim system.

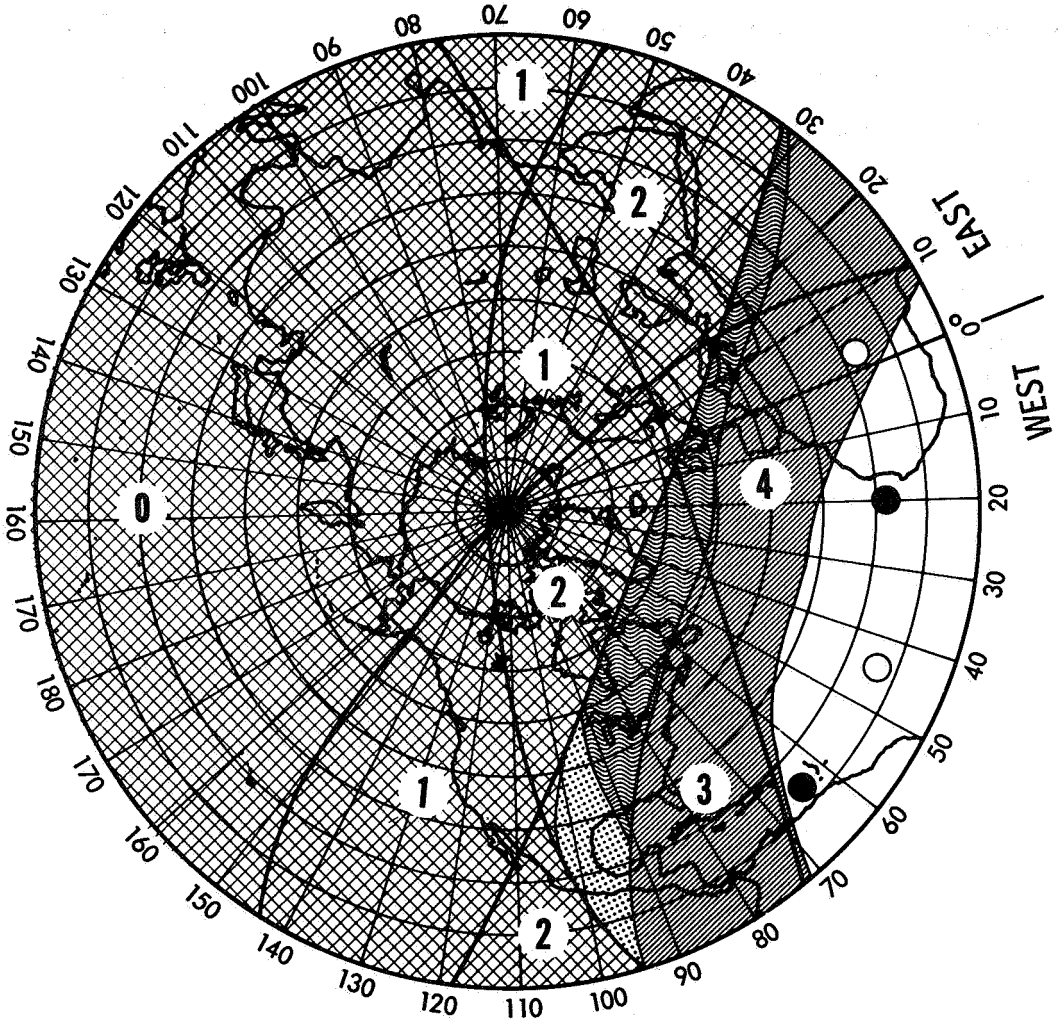

KEY

C95
< 150 FT

150 - 250 FT

250 - 400 FT

400 - 600 FT

>600 - 5000 FT

INDETERMINATE

NOTE:

1) NUMBERS IN CIRCLES INDICATE NUMBER OF SATELLITES VISIBLE

2) ● INDICATES SUB-SATELLITE POINT VISIBLE ON MAP (ABOVE EQUATOR)

○ SUB-SATELLITE POINTS BELOW EQUATOR

3) A PRIORI ALTITUDE SIGMA = 75 FEET

Figure 7. Interim System Accuracy at T_0

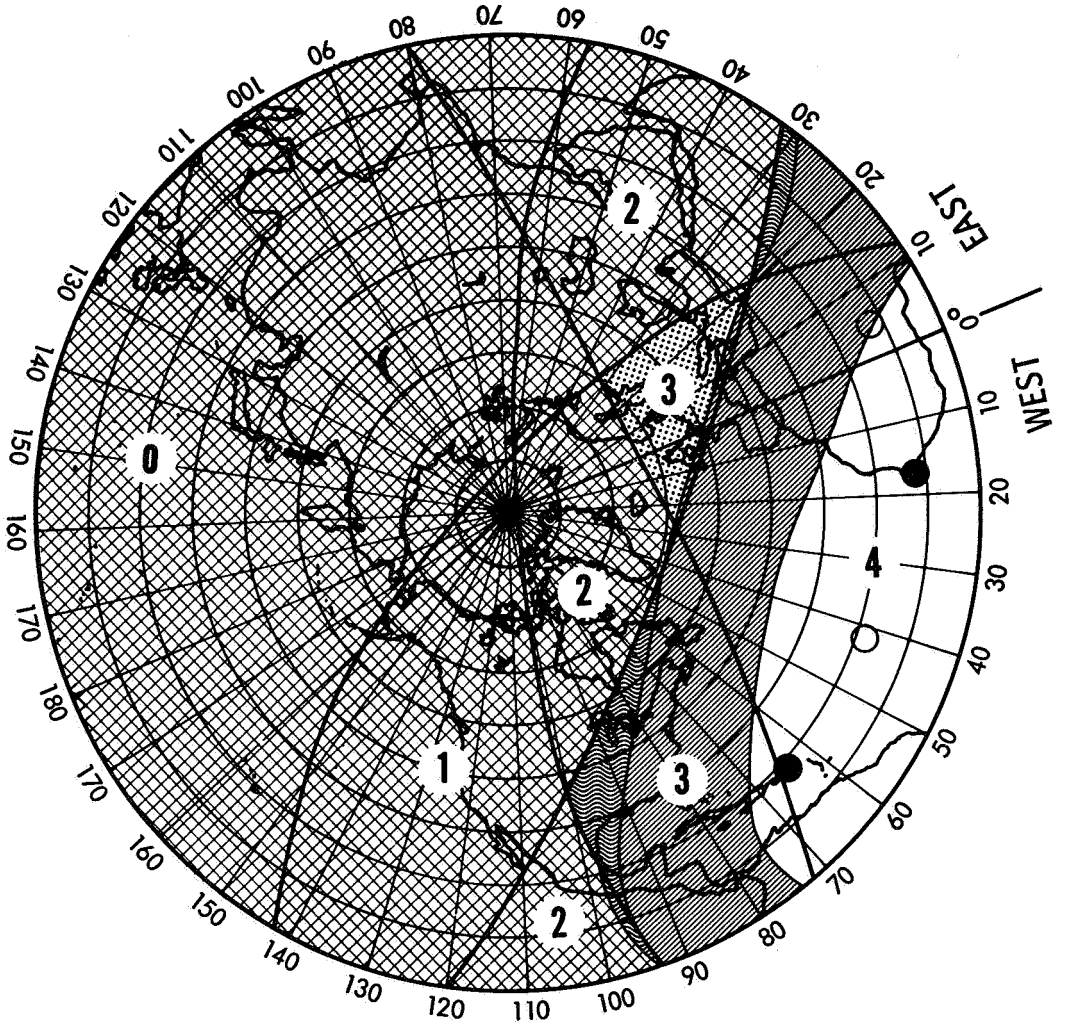

KEY

C95

< 150 FT

150 - 250 FT

250 - 400 FT

400 - 600 FT

>600 - 5000 FT

INDETERMINATE

NOTE:

1) NUMBERS IN CIRCLES INDICATE NUMBER OF SATELLITES VISIBLE

2) ● INDICATES SUB-SATELLITE POINT VISIBLE ON MAP (ABOVE EQUATOR)

○ SUB-SATELLITE POINTS BELOW EQUATOR

3) A PRIORI ALTITUDE SIGMA = 75 FEET

Figure 8. Interim System Accuracy at T_0 + 3 Hours

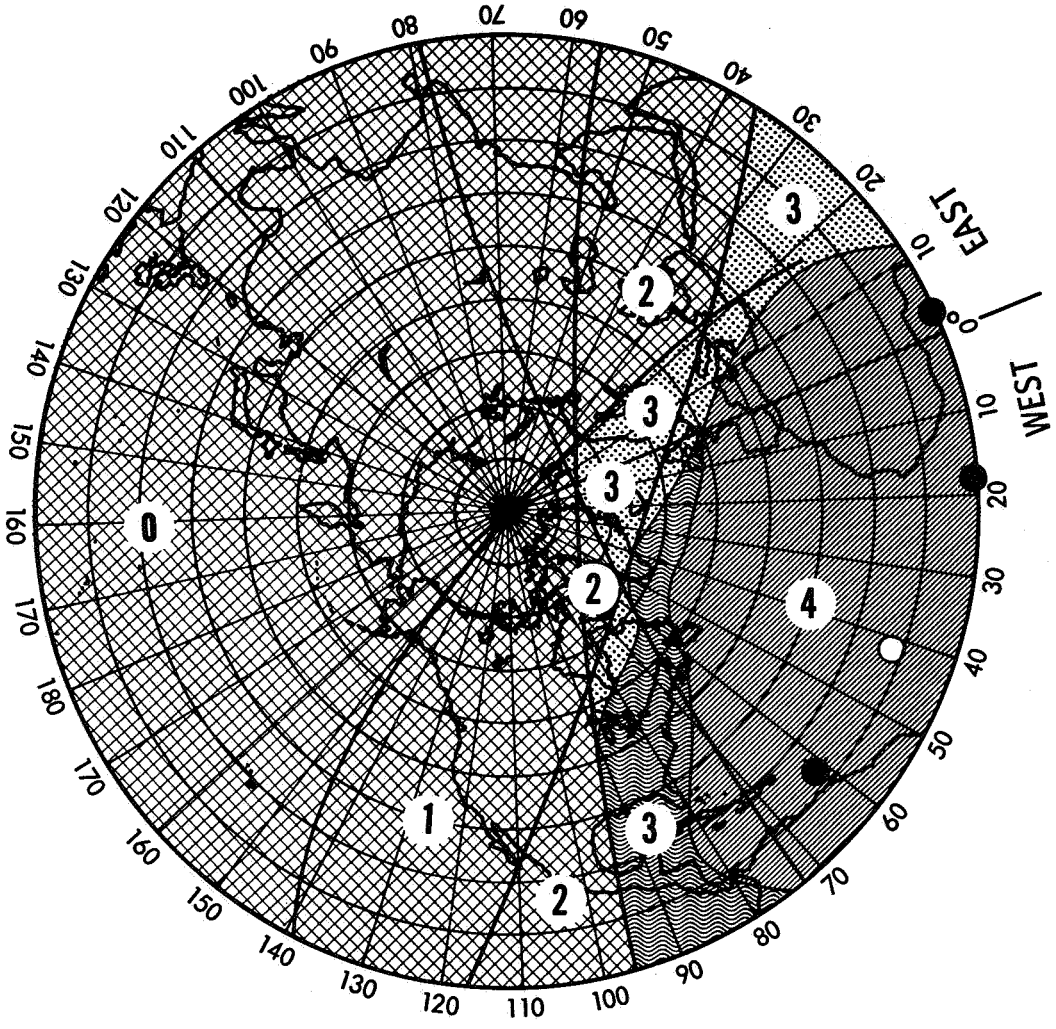

KEY

- C95 < 150 FT
- 150 - 250 FT
- 250 - 400 FT
- 400 - 600 FT
- > 600 - 5000 FT
- INDETERMINATE

NOTE:

1) NUMBERS IN CIRCLES INDICATE NUMBER OF SATELLITES VISIBLE
2) ● INDICATES SUB-SATELLITE POINT VISIBLE ON MAP (ABOVE EQUATOR)

   ○ SUB-SATELLITE POINTS BELOW EQUATOR
3) A PRIORI ALTITUDE SIGMA = 75 FEET

Figure 9. Interim System Accuracy at T_0 + 6 Hours

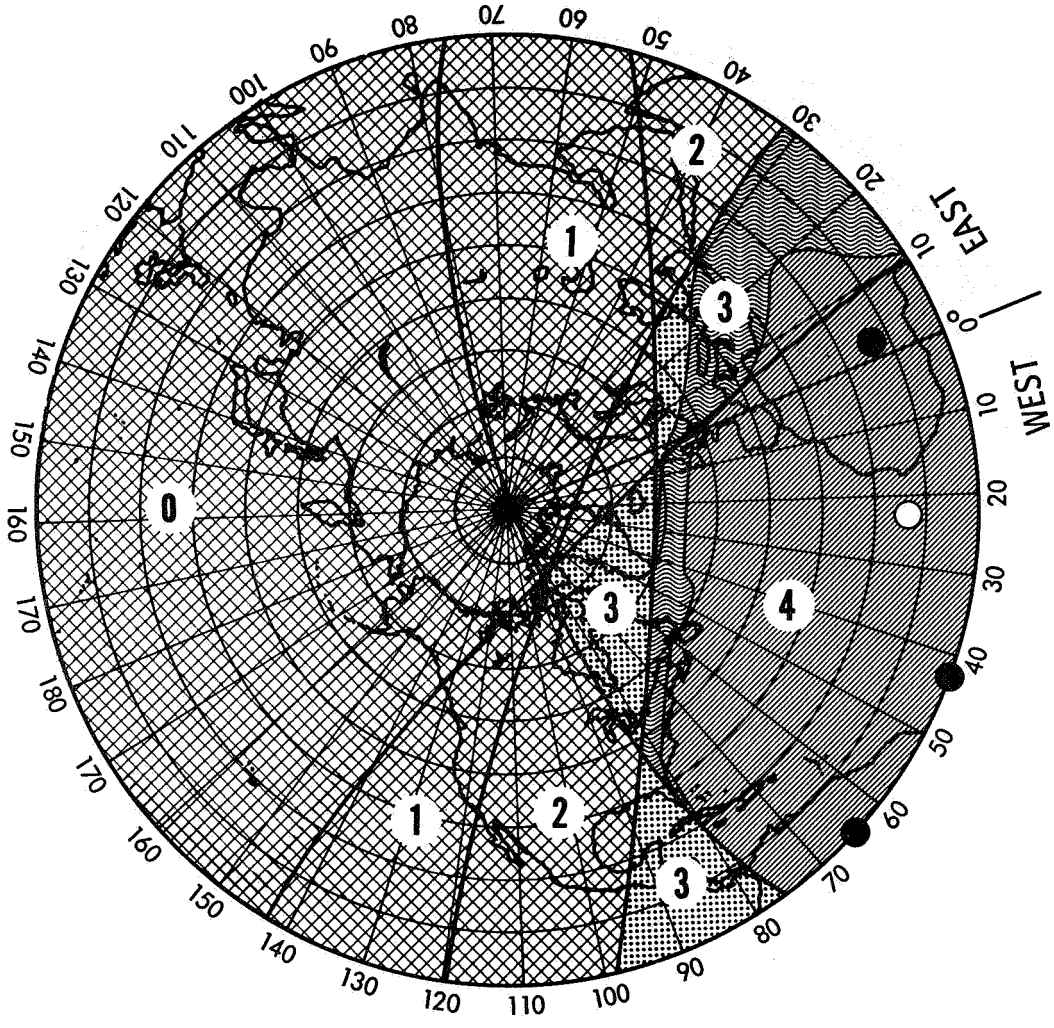

KEY

- C95 < 150 FT
- 150 - 250 FT
- 250 - 400 FT
- 400 - 600 FT
- > 600 - 5000 FT
- INDETERMINATE

NOTE:

1) NUMBERS IN CIRCLES INDICATE NUMBER OF SATELLITES VISIBLE
2) ● INDICATES SUB-SATELLITE POINT VISIBLE ON MAP (ABOVE EQUATOR)
   ○ SUB-SATELLITE POINTS BELOW EQUATOR
3) A PRIORI ALTITUDE SIGMA = 75 FEET

Figure 10. Interim System Accuracy at T_0 + 9 Hours

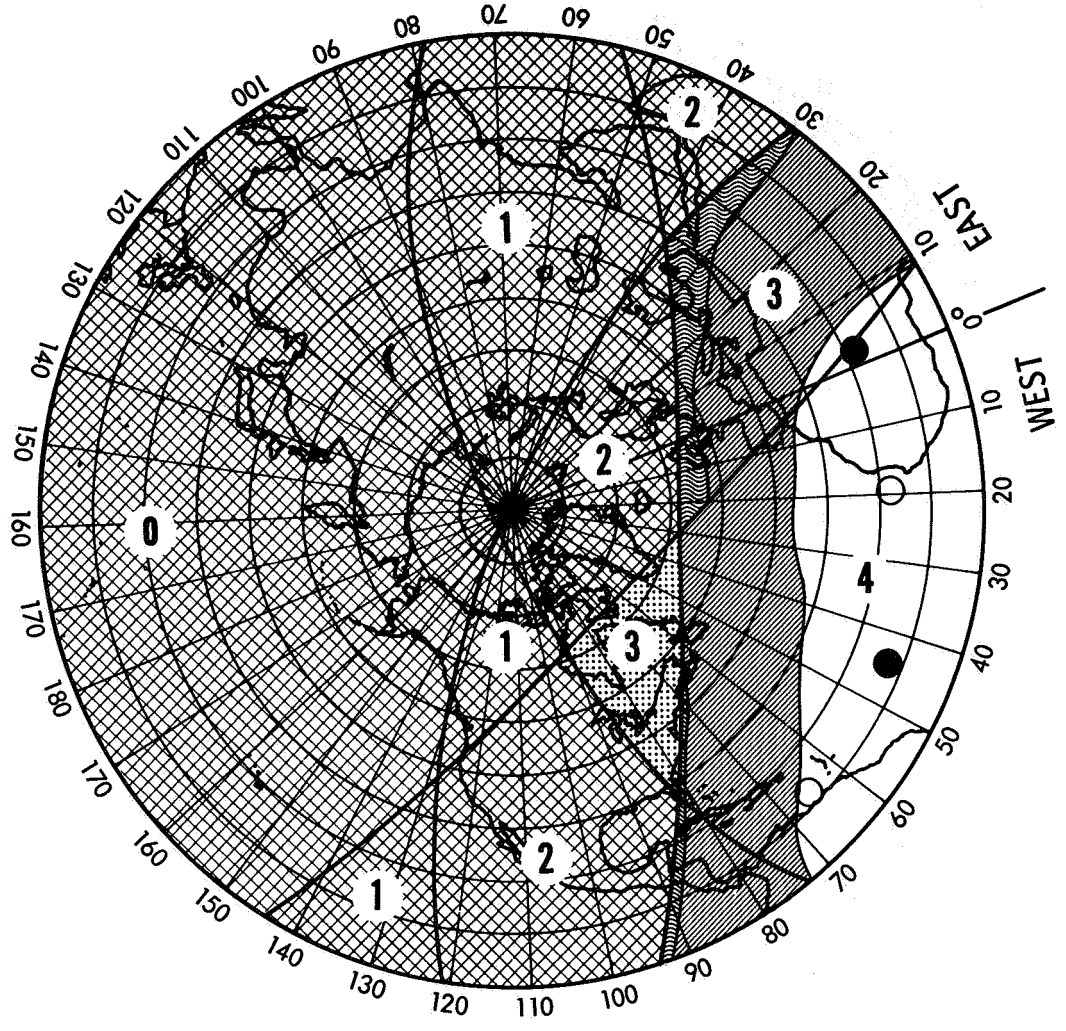

KEY

C95
< 150 FT

150 - 250 FT

250 - 400 FT

400 - 600 FT

>600 - 5000 FT

INDETERMINATE

NOTE:

1) NUMBERS IN CIRCLES INDICATE NUMBER OF SATELLITES VISIBLE

2) ● INDICATES SUB-SATELLITE POINT VISIBLE ON MAP (ABOVE EQUATOR)

○ SUB-SATELLITE POINTS BELOW EQUATOR

3) A PRIORI ALTITUDE SIGMA = 75 FEET

Figure 11. Interim System Accuracy at T_0 + 12 Hours

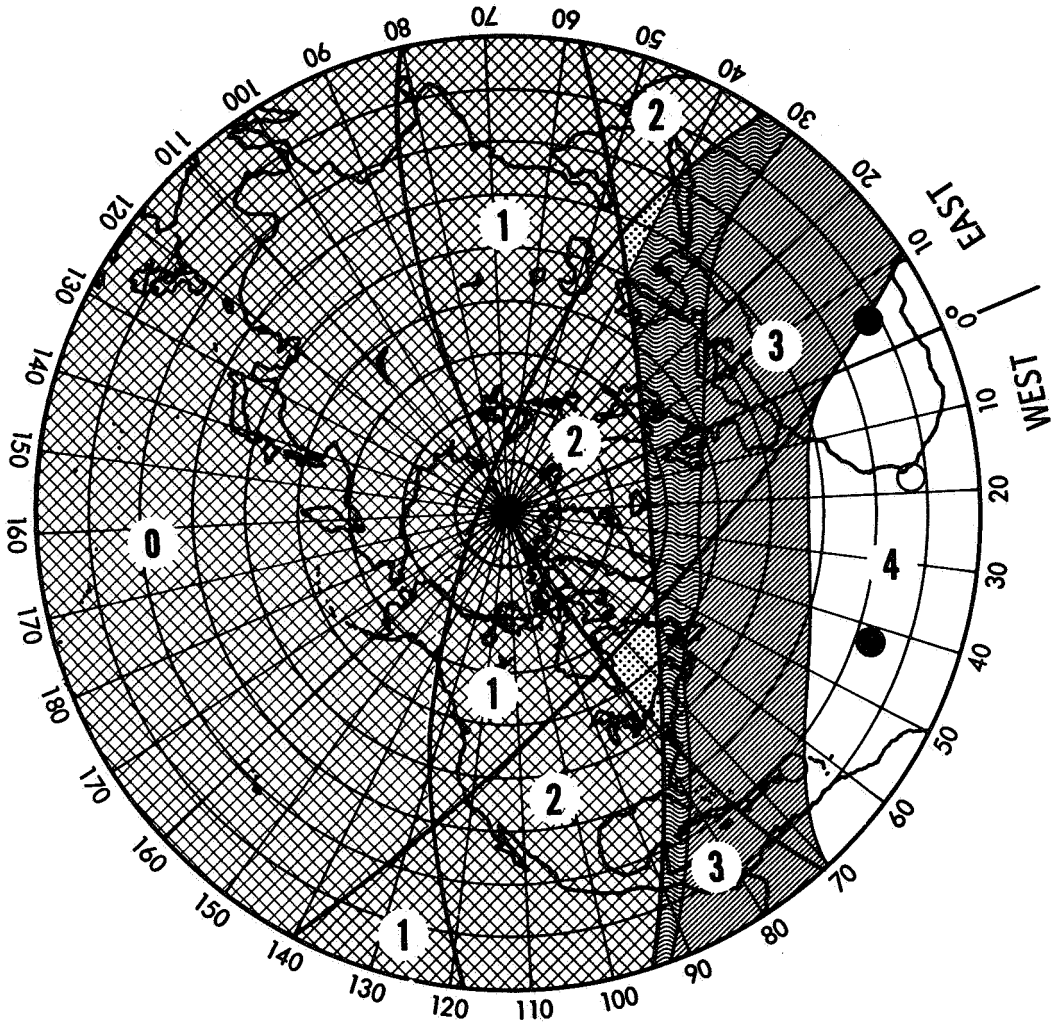

KEY

C95
< 150 FT

150 - 250 FT

250 - 400 FT

400 - 600 FT

> 600 - 5000 FT

INDETERMINATE

NOTE:

1) NUMBERS IN CIRCLES INDICATE NUMBER OF SATELLITES VISIBLE

2) ● INDICATES SUB-SATELLITE POINT VISIBLE ON MAP (ABOVE EQUATOR)

○ SUB-SATELLITE POINTS BELOW EQUATOR

3) A PRIORI ALTITUDE SIGMA = 75 FEET

Figure 12. Interim System Accuracy at T_0 + 15 Hours

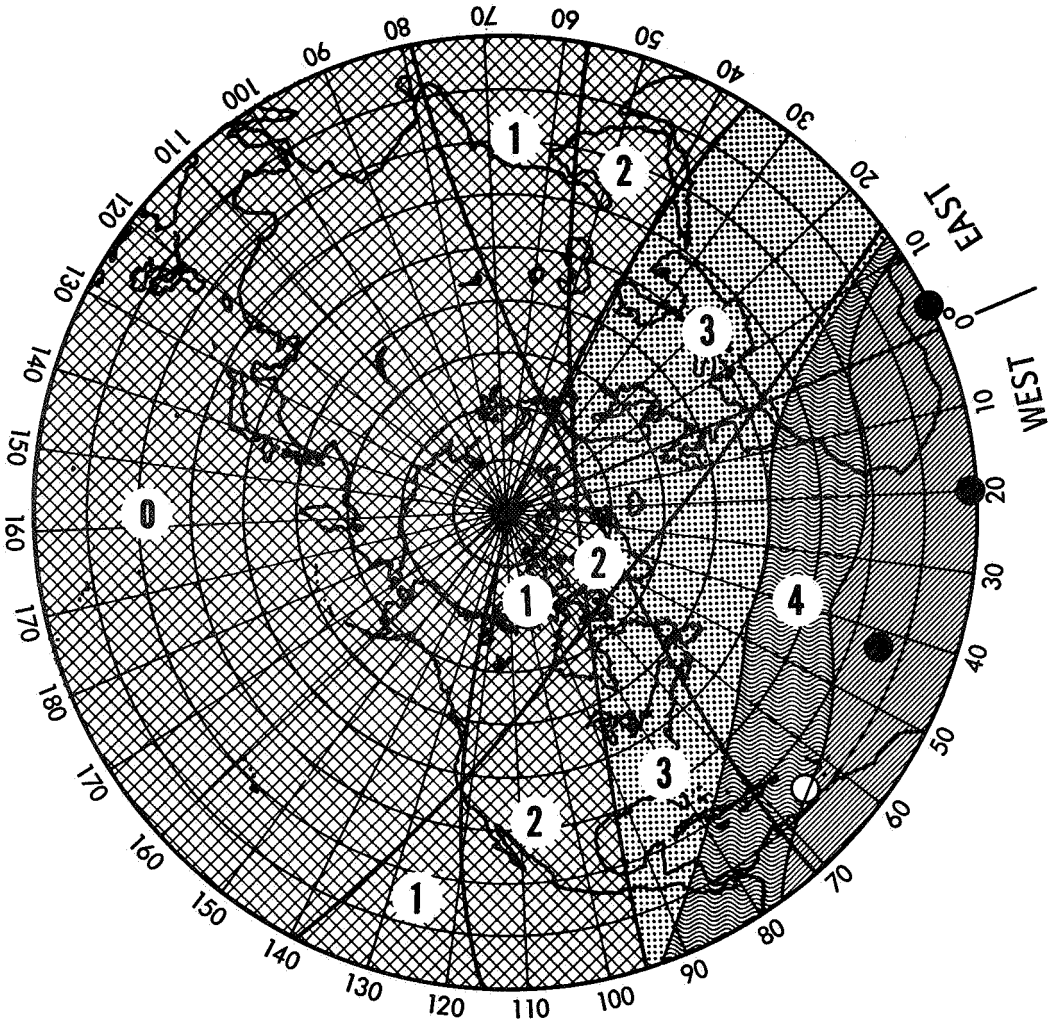

KEY

C95 < 150 FT	
150 - 250 FT	
250 - 400 FT	
400 - 600 FT	
> 600 - 5000 FT	
INDETERMINATE	

NOTE:

1) NUMBERS IN CIRCLES INDICATE NUMBER OF SATELLITES VISIBLE
2) ● INDICATES SUB-SATELLITE POINT VISIBLE ON MAP (ABOVE EQUATOR)
   ○ SUB-SATELLITE POINTS BELOW EQUATOR
3) A PRIORI ALTITUDE SIGMA = 75 FEET

Figure 13. Interim System Accuracy at T_0 + 18 Hours

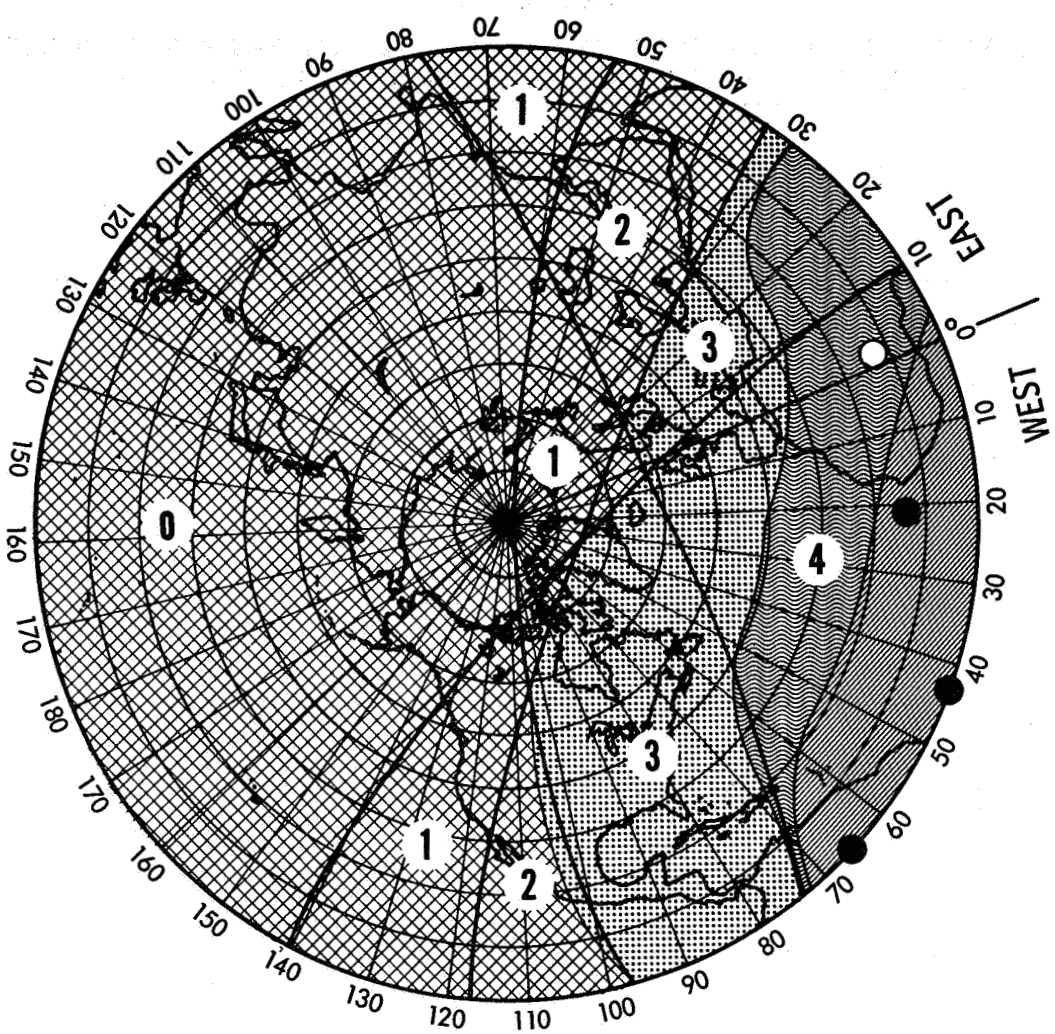

KEY

C95 < 150 FT	
150 - 250 FT	
250 - 400 FT	
400 - 600 FT	
> 600 - 5000 FT	
INDETERMINATE	

NOTE:

1) NUMBERS IN CIRCLES INDICATE NUMBER OF SATELLITES VISIBLE

2) ● INDICATES SUB-SATELLITE POINT VISIBLE ON MAP (ABOVE EQUATOR)

○ SUB-SATELLITE POINTS BELOW EQUATOR

3) A PRIORI ALTITUDE SIGMA = 75 FEET

Figure 14. Interim System Accuracy at T_0 + 21 Hours

TABLE VII

INTERIM SYSTEM NAVIGATION ACCURACY (C95) AS A FUNCTION OF USER LONGITUDE AND LATITUDE AT T = 0 HR WITHOUT SATELLITE ERRORS

LONGITUDE	NORTH LATITUDE									
	0	10	20	30	40	50	60	70	80	90
-110	1	1	1	1	1	1	1	1	1	1
-100	1	1	511	550	621	1	1	1	1	1
-90	375	365	379	414	475	571	1	1	1	1
-80	302	297	309	341	393	477	1	1	1	1
-70	237	261	272	299	345	421	547	1	1	1
-60	211	210	223	275	317	386	504	1	1	1
-50	195	197	211	241	289	367	481	1	1	1
-40	189	193	207	237	283	360	473	1	1	1
-30	187	193	210	240	287	357	480	1	1	1
-20	190	194	219	251	299	371	504	1	1	1
-10	199	211	235	270	321	395	1	1	1	1
0	217	233	261	301	356	431	1	1	1	1
10	257	270	303	347	406	4533	1	1	1	1
20	308	335	381	458	1	1	1	1	1	1
30	400	1	1	1	1	1	1	1	1	1
40	1	1	1	1	1	1	1	1	1	1
50	1	1	1	1	1	1	1	1	1	1

SYSTEM: 2x8 Interim (2x2)

ORBITAL PERIOD: 24 hours
TIME FROM EPOCH: 0 hours

ORBITAL INCLINATION: 18.5°
SPACING OF ASCENDING NODES: 157.5°
ARGUMENT OF LATITUDE OF THE FIRST SATELLITE IN EACH PLANE AT EPOCH: 45°, 225°
SATELLITE SPACING WITHIN EACH PLANE: 45°

MEASUREMENT NOISE (1σ): 50 feet
USER ALTITUDE UNCERTAINTY (1σ): 75 feet
SATELLITE POSITION UNCERTAINTY (1σ)
RADIAL (u): 0
IN-TRACK (v) 0
CROSS-TRACK (w) 0
MINIMUM USER ELEVATION ANGLE: 5°

(1) Denotes indeterminate point

TABLE VIII

INTERIM SYSTEM NAVIGATION ACCURACY (C95) AS A FUNCTION OF USER LONGITUDE AND LATITUDE AT T = 3 HR WITHOUT SATELLITE ERRORS

NORTH LATITUDE

LONGITUDE	0	10	20	30	40	50	60	70	80	90
-100	1	1	1	528	1	1	1	1	1	1
-90	371	356	360	387	446	1	1	1	1	1
-80	293	283	289	313	363	454	1	1	1	1
-70	239	243	249	272	317	397	1	1	1	1
-60	211	207	217	241	292	367	1	1	1	1
-50	196	195	205	230	271	351	1	1	1	1
-40	189	191	203	227	268	329	1	1	1	1
-30	182	191	205	231	273	333	1	1	1	1
-20	190	197	214	242	285	345	2845	1	1	1
-10	199	209	229	261	305	367	2191	1	1	1
0	216	229	253	289	337	4081	1707	1	1	1
10	247	264	292	331	381	2223	1361	1	1	1
20	316	345	403	1	2349	1485	1115	1	1	1
30	403	1	1	1	1	1	1	1	1	1
40	1	1	1	1	1	1	1	1	1	1
50	1	1	1	1	1	1	1	1	1	1

SYSTEM: 2x8 Interim (2x2)

ORBITAL PERIOD: 24 hours
TIME FROM EPOCH: 3 hours

ORBITAL INCLINATION: 18.5°
SPACING OF ASCENDING NODES: 157.5°
ARGUMENT OF LATITUDE OF THE FIRST SATELLITE IN EACH PLANE AT EPOCH: 45°, 225°
SATELLITE SPACING WITHIN EACH PLANE: 45°

MEASUREMENT NOISE (1σ): 50 feet
USER ALTITUDE UNCERTAINTY (1σ): 75 feet
SATELLITE POSITION UNCERTAINTY (1σ)
RADIAL (u): 0
IN-TRACK (v) 0
CROSS-TRACK (w) 0
MINIMUM USER ELEVATION ANGLE: 5°

(1) Denotes indeterminate point

TABLE IX

INTERIM SYSTEM NAVIGATION ACCURACY (C95) AS A FUNCTION OF USER LONGITUDE AND LATITUDE AT T = 6 HR WITHOUT SATELLITE ERRORS

LONGITUDE	NORTH LATITUDE									
	0	10	20	30	40	50	60	70	80	90
-100	1	1	1	1	1	1	1	1	1	1
-90	525	465	441	463	539	1	1	1	1	1
-80	436	399	389	410	473	593	1	1	1	1
-70	346	313	303	317	442	545	1	1	1	1
-60	319	294	288	300	330	379	693	1	1	1
-50	303	285	281	293	319	365	433	1	1	1
-40	296	280	278	289	315	359	425	716	1	1
-30	293	279	279	291	317	359	424	714	1	1
-20	295	281	282	295	323	366	431	714	1	1
-10	300	287	289	305	335	379	681	718	1	1
0	310	296	301	320	353	401	687	726	1	1
10	329	313	321	345	383	672	697	737	1	1
20	837	989	1357	2387	1	687	715	754	1	1
30	833	986	1	1	1	1	1	1	1	1
40	1	1	1	1	1	1	1	1	1	1
50	1	1	1	1	1	1	1	1	1	1

SYSTEM: 2x8 Interim (2x2)

ORBITAL PERIOD: 24 hours
TIME FROM EPOCH: 6 hours

ORBITAL INCLINATION: 18.5°
SPACING OF ASCENDING NODES: 157.5°
ARGUMENT OF LATITUDE OF THE FIRST SATELLITE IN EACH PLANE AT EPOCH: 45°, 225°
SATELLITE SPACING WITHIN EACH PLANE: 45°

MEASUREMENT NOISE (1σ): 50 feet
USER ALTITUDE UNCERTAINTY (1σ): 75 feet
SATELLITE POSITION UNCERTAINTY (1σ)
RADIAL (u): 0
IN-TRACK (v) 0
CROSS-TRACK (w) 0
MINIMUM USER ELEVATION ANGLE: 5°

(1) Denotes indeterminate point

TABLE X

INTERIM SYSTEM NAVIGATION ACCURACY (C95) AS A FUNCTION OF USER LONGITUDE AND LATITUDE AT T = 9 HR WITHOUT SATELLITE ERRORS

LONGITUDE	NORTH LATITUDE 0	10	20	30	40	50	60	70	80	90
-100	1	1	1	1	1	1	1	1	1	1
-90	833	985	1413	1	1	1	1	1	1	1
-80	841	993	1347	375	415	682	709	749	1	1
-70	323	308	315	387	374	423	694	734	1	1
-60	307	293	297	365	397	395	685	723	1	1
-50	298	285	287	302	331	375	680	717	1	1
-40	294	281	281	294	321	364	429	714	1	1
-30	293	279	278	290	316	359	423	714	1	1
-20	297	281	279	290	316	360	426	717	1	1
-10	307	286	282	293	321	368	436	1	1	1
0	324	297	291	303	334	384	700	1	1	1
10	351	319	309	391	448	555	1	1	1	1
20	453	411	398	419	485	610	1	1	1	1
30	559	491	463	483	1	1	1	1	1	1
40	1	1	1	1	1	1	1	1	1	1
50	1	1	1	1	1	1	1	1	1	1

SYSTEM: 2x8 Interim (2x2)

ORBITAL PERIOD: 24 hours
TIME FROM EPOCH; 9 hours

ORBITAL INCLINATION: 18.5°
SPACING OF ASCENDING NODES: 157.5°
ARGUMENT OF LATITUDE OF THE FIRST SATELLITE IN EACH PLANE AT EPOCH: 45°, 225°
SATELLITE SPACING WITHIN EACH PLANE: 45°

MEASUREMENT NOISE (1σ): 50 feet
USER ALTITUDE UNCERTAINTY (1σ): 75 feet
SATELLITE POSITION UNCERTAINTY (1σ)
RADIAL (u): 0
IN-TRACK (v) 0
CROSS-TRACK (w) 0
MINIMUM USER ELEVATION ANGLE: 5°

(1) Denotes indeterminate point

TABLE XI

INTERIM SYSTEM NAVIGATION ACCURACY (C95) AS A FUNCTION OF USER LONGITUDE AND LATITUDE AT T = 12 HR WITHOUT SATELLITE ERRORS

LONGITUDE	NORTH LATITUDE 0	10	20	30	40	50	60	70	80	90
-100	1	1	1	1	1	1	1	1	1	1
-90	375	413	1	1	1	1	976	1	1	1
-80	302	328	382	375	2835	1623	1169	1	1	1
-70	237	253	281	319	369	2522	1437	1	1	1
-60	211	223	246	281	327	5061	1813	1	1	1
-50	195	205	225	255	299	361	2337	1	1	1
-40	189	195	211	239	281	341	3033	1	1	1
-30	187	191	205	230	271	331	1	1	1	1
-20	190	191	203	227	268	330	1	1	1	1
-10	199	197	207	232	274	355	1	1	1	1
0	217	213	221	255	297	373	1	1	1	1
10	257	251	257	281	327	414	1	1	1	1
20	308	297	303	328	380	1	1	1	1	1
30	400	383	386	415	476	1	1	1	1	1
40	1	1	1	1	1	1	1	1	1	1
50	1	1	1	1	1	1	1	1	1	1

SYSTEM: 2x8 Interim (2x2)

ORBITAL PERIOD: 24 hours
TIME FROM EPOCH: 12 hours

ORBITAL INCLINATION: 18.5°
SPACING OF ASCENDING NODES: 157.5°
ARGUMENT OF LATITUDE OF THE FIRST SATELLITE IN EACH PLANE AT EPOCH: 45°, 225°
SATELLITE SPACING WITHIN EACH PLANE: 45°

MEASUREMENT NOISE (1σ): 50 feet
USER ALTITUDE UNCERTAINTY (1σ): 75 feet
SATELLITE POSITION UNCERTAINTY (1σ)
RADIAL (u): 0
IN-TRACK (v) 0
CROSS-TRACK (w) 0
MINIMUM USER ELEVATION ANGLE: 5°

(1) Denotes indeterminate point

TABLE XII

INTERIM SYSTEM NAVIGATION ACCURACY (C95) AS A FUNCTION OF USER LONGITUDE AND LATITUDE AT T = 15 HR WITHOUT SATELLITE ERRORS

LONGITUDE	NORTH LATITUDE									
	0	10	20	30	40	50	60	70	80	90
-100	1	1	1	1	1	1	1	1	1	1
-90	371	406	1	1	1	1	1	1	1	1
-80	292	317	360	432	1	1	1	1	1	1
-70	239	259	290	334	392	3388	1	1	1	1
-60	212	227	253	292	346	420	1	1	1	1
-50	196	208	230	264	230	387	1	1	1	1
-40	189	197	216	247	295	366	496	1	1	1
-30	187	193	209	238	285	356	477	1	1	1
-20	190	193	207	237	284	361	473	1	1	1
-10	199	200	214	243	304	370	485	1	1	1
0	216	215	228	280	322	393	513	1	1	1
10	247	268	279	307	355	432	1	1	1	1
20	316	310	323	355	410	497	1	1	1	1
30	403	391	404	440	503	604	1	1	1	1
40	1	1	602	675	1	1	1	1	1	1
50	1	1	1	1	1	1	1	1	1	1

SYSTEM: 2x8 Interim (2x2)

ORBITAL PERIOD: 24 hours
TIME FROM EPOCH: 15 hours

ORBITAL INCLINATION: 18.5°
SPACING OF ASCENDING NODES: 157.5°
ARGUMENT OF LATITUDE OF THE FIRST SATELLITE IN EACH PLANE AT EPOCH: 45°, 225°
SATELLITE SPACING WITHIN EACH PLANE: 45°

MEASUREMENT NOISE (1σ): 50 feet
USER ALTITUDE UNCERTAINTY (1): 75 feet
SATELLITE POSITION UNCERTAINTY (1σ)
RADIAL (u): 0
IN-TRACK (v): 0
CROSS-TRACK (w): 0
MINIMUM USER ELEVATION ANGLE: 5°

(1) Denotes indeterminate point

TABLE XIII

INTERIM SYSTEM NAVIGATION ACCURACY (C95) AS A FUNCTION OF USER LONGITUDE AND LATITUDE AT T = 18 HR WITHOUT SATELLITE ERRORS

LONGITUDE	NORTH LATITUDE 0	10	20	30	40	50	60	70	80	90
-100	1	1	1	1	1	1	1	1	1	1
-90	525	621	767	1004	1450	1	1	1	1	1
-80	436	499	597	753	1031	1642	4042	1	1	1
-70	346	405	494	620	826	1248	2585	1	1	1
-60	319	364	436	542	693	865	2016	1	1	1
-50	304	341	402	495	634	812	939	1	1	1
-40	296	328	384	469	599	777	927	1158	1	1
-30	293	324	376	459	585	762	926	1090	1	1
-20	295	325	378	461	590	767	927	1088	1	1
-10	300	332	389	478	614	839	938	1098	1	1
0	310	347	411	513	795	859	961	1121	1	1
10	329	783	764	779	821	892	998	1158	1	1
20	838	785	782	811	864	943	1053	1209	1	1
30	833	801	821	867	932	1017	1129	1	1	1
40	1	1	1	967	1041	1127	1234	1	1	1
50	1	1	1	1	1	1	1	1	1	1

SYSTEM: 2x8 Interim (2x2)

ORBITAL PERIOD: 24 hours
TIME FROM EPOCH: 18 hours

ORBITAL INCLINATION: 18.5°
SPACING OF ASCENDING NODES: 157.5°
ARGUMENT OF LATITUDE OF THE FIRST SATELLITE IN EACH PLANE AT EPOCH: 45°, 225°
SATELLITE SPACING WITHIN EACH PLANE: 45°

MEASUREMENT NOISE (1σ): 50 feet
USER ALTITUDE UNCERTAINTY (1): 75 feet
SATELLITE POSITION UNCERTAINTY (1σ)
RADIAL (u): 0
IN-TRACK (v): 0
CROSS-TRACK (w): 0
MINIMUM USER ELEVATION ANGLE: 5°

(1) Denotes indeterminate point

TABLE XIV

INTERIM SYSTEM NAVIGATION ACCURACY (C95) AS A FUNCTION OF USER LONGITUDE AND LATITUDE AT T = 21 HR WITHOUT SATELLITE ERRORS

LONGITUDE	NORTH LATITUDE 0	10	20	30	40	50	60	70	80	90
-110	1	1	1	1	1	1	1	1	1	1
-100	1	1	877	936	1008	1096	1204	1	1	1
-90	833	795	808	849	912	996	1107	1	1	1
-80	841	783	776	801	851	928	1037	1195	1	1
-70	323	365	762	774	813	882	988	1147	1	1
-60	307	342	404	502	791	853	954	1114	1	1
-50	298	329	385	472	605	835	934	1095	1	1
-40	294	324	376	459	587	764	925	1088	1	1
-30	294	325	377	459	587	764	928	1093	1	1
-20	297	331	387	473	605	784	929	1112	1	1
-10	302	346	409	505	646	824	941	1	1	1
0	324	372	447	558	712	879	1219	1	1	1
10	356	419	514	648	866	1322	2820	1	1	1
20	453	523	630	801	1107	1799	1	1	1	1
30	559	668	832	1103	1	1	1	1	1	1
40	1	1	1	1	1	1	1	1	1	1

SYSTEM: 2x8 Interim (2x2)

ORBITAL PERIOD: 24 hours
TIME FROM EPOCH: 21 hours

ORBITAL INCLINATION: 18.5°
SPACING OF ASCENDING NODES: 157.5°
ARGUMENT OF LATITUDE OF THE FIRST SATELLITE IN EACH PLANE AT EPOCH: 45°, 225°
SATELLITE SPACING WITHIN EACH PLANE: 45°

MEASUREMENT NOISE (1σ): 50 feet
USER ALTITUDE UNCERTAINTY (1): 75 feet
SATELLITE POSITION UNCERTAINTY (1σ)
RADIAL (u): 0
IN-TRACK (v): 0
CROSS-TRACK (w): 0
MINIMUM USER ELEVATION ANGLE: 5°

(1) Denotes indeterminate point

TABLE XV

INTERIM SYSTEM NAVIGATION ACCURACY (C95) AS A FUNCTION OF USER LONGITUDE AND LATITUDE AT T = 0 HR WITH SATELLITE ERRORS

LONGITUDE	NORTH LATITUDE									
	0	10	20	30	40	50	60	70	80	90
-100	1	1	734	776	864	1	1	1	1	1
-90	530	507	518	563	644	775	1	1	1	1
-80	395	381	396	440	515	634	1	1	1	1
-70	296	307	323	365	436	547	728	1	1	1
-60	246	249	274	321	388	493	665	1	1	1
-50	215	220	246	292	357	463	631	1	1	1
-40	200	208	234	280	345	454	621	1	1	1
-30	196	207	235	281	345	429	634	1	1	1
-20	202	217	248	295	359	441	673	1	1	1
-10	221	240	273	321	385	464	1	1	1	1
0	253	279	314	362	425	500	1	1	1	1
10	319	337	373	420	479	6235	1	1	1	1
20	413	453	523	639	1	1	1	1	1	1
30	568	1	1	1	1	1	1	1	1	1
40	1	1	1	1	1	1	1	1	1	1
50	1	1	1	1	1	1	1	1	1	1

SYSTEM: 2x8 Interim (2x2)

ORBITAL PERIOD; 24 hours
TIME FROM EPOCH: 0 hours

ORBITAL INCLINATION: 18.5°
SPACING OF ASCENDING NODES: 157.5°
ARGUMENT OF LATITUDE OF THE FIRST SATELLITE IN EACH PLANE AT EPOCH: 45°, 225°
SATELLITE SPACING WITHIN EACH PLANE: 45°

MEASUREMENT NOISE (1σ): 50 feet
USER ALTITUDE UNCERTAINTY (1σ): 150 feet
SATELLITE POSITION UNCERTAINTY (1σ)
RADIAL (u): 15 feet
IN-TRACK (v): 117 feet
CROSS-TRACK (w): 38 feet
MINIMUM USER ELEVATION ANGLE: 5°

(1) Denotes indeterminate point

TABLE XVI

INTERIM SYSTEM NAVIGATION ACCURACY (C95) AS A FUNCTION OF USER LONGITUDE AND LATITUDE AT T = 3 HR WITH SATELLITE ERRORS

LONGITUDE	NORTH LATITUDE									
	0	10	20	30	40	50	60	70	80	90
-100	1	1	1	793	1	1	1	1	1	1
-90	522	503	515	561	652	1	1	1	1	1
-80	385	373	386	430	512	651	1	1	1	1
-70	299	294	309	351	429	556	1	1	1	1
-60	247	244	261	298	380	501	1	1	1	1
-50	215	215	234	273	331	474	1	1	1	1
-40	200	203	223	263	320	396	1	1	1	1
-30	196	202	226	265	322	396	1	1	1	1
-20	202	213	239	279	335	408	3552	1	1	1
-10	221	234	263	305	360	430	2714	1	1	1
0	256	272	302	344	398	5062	2099	1	1	1
10	312	328	357	398	448	2744	1661	1	1	1
20	402	471	563	1	2933	1822	1349	1	1	1
30	577	1	1	1	1	1	1	1	1	1
40	1	1	1	1	1	1	1	1	1	1
50	1	1	1	1	1	1	1	1	1	1

SYSTEM: 2x8 Interim (2x2)

ORBITAL PERIOD; 24 hours
TIME FROM EPOCH: 3 hours

ORBITAL INCLINATION: 18.5°
SPACING OF ASCENDING NODES: 157.5°
ARGUMENT OF LATITUDE OF THE FIRST SATELLITE IN EACH PLANE AT EPOCH: 45°, 225°
SATELLITE SPACING WITHIN EACH PLANE: 45°

MEASUREMENT NOISE (1σ). 50 feet
USER ALTITUDE UNCERTAINTY (1σ): 150 feet
SATELLITE POSITION UNCERTAINTY (1σ)
RADIAL (u): 15 feet
IN-TRACK (v): 117 feet
CROSS-TRACK (w): 38 feet
MINIMUM USER ELEVATION ANGLE: 5°

(1) Denotes indeterminate point

TABLE XVII

INTERIM SYSTEM NAVIGATION ACCURACY (C95) AS A FUNCTION OF USER LONGITUDE AND LATITUDE AT T = 6 HR WITH SATELLITE ERRORS

NORTH LATITUDE

LONGITUDE	0	10	20	30	40	50	60	70	80	90
-100	1	1	1	1	1	1	1	1	1	1
-90	673	603	580	611	709	1	1	1	1	1
-80	526	479	468	501	587	742	1	1	1	1
-70	426	380	362	374	523	661	1	1	1	1
-60	370	333	321	335	373	435	838	1	1	1
-50	339	309	300	314	351	410	494	1	1	1
-40	324	298	292	307	341	398	480	764	1	1
-30	320	296	292	307	341	396	477	758	1	1
-20	324	300	297	313	348	403	483	757	1	1
-10	336	311	309	328	364	420	717	759	1	1
0	361	333	332	352	392	448	721	765	1	1
10	406	373	371	393	433	703	731	777	1	1
20	921	1110	1548	2739	1	719	749	794	1	1
30	933	1142	1	1	1	1	1	1	1	1
40	1	1	1	1	1	1	1	1	1	1
50	1	1	1	1	1	1	1	1	1	1

SYSTEM: 2x8 Interim (2x2)

ORBITAL PERIOD: 24 hours
TIME FROM EPOCH: 6 hours

ORBITAL INCLINATION: 18.5°
SPACING OF ASCENDING NODES: 157.5°
ARGUMENT OF LATITUDE OF THE FIRST SATELLITE IN EACH PLANE AT EPOCH: 45°, 225°
SATELLITE SPACING WITHIN EACH PLANE: 45°

MEASUREMENT NOISE (1σ): 50 feet
USER ALTITUDE UNCERTAINTY (1σ): 150 feet
SATELLITE POSITION UNCERTAINTY (1σ)
RADIAL (u): 15 feet
IN-TRACK (v): 117 feet
CROSS-TRACK (w): 38 feet
MINIMUM USER ELEVATION ANGLE: 5°

(1) Denotes indeterminate point

TABLE XVIII

INTERIM SYSTEM NAVIGATION ACCURACY (C95) AS A FUNCTION OF USER LONGITUDE AND LATITUDE AT T = 9 HR WITH SATELLITE ERRORS

NORTH LATITUDE

LONGITUDE	0	10	20	30	40	50	60	70	80	90
-100	1	1	1	1	1	1	1	1	1	1
-90	935	1145	1687	1	1	1	1	1	1	1
-80	927	1121	1552	447	488	725	752	792	1	1
-70	393	365	365	389	431	487	732	774	1	1
-60	355	331	331	352	392	448	719	761	1	1
-50	334	312	311	330	367	422	713	753	1	1
-40	323	302	300	316	351	406	484	749	1	1
-30	321	298	294	309	343	398	478	749	1	1
-20	327	300	294	309	344	401	482	752	1	1
-10	344	312	302	317	354	413	496	1	1	1
0	380	339	326	339	378	439	846	1	1	1
10	443	393	372	449	529	671	1	1	1	1
20	554	500	484	516	603	762	1	1	1	1
30	729	648	618	647	1	1	1	1	1	1
40	1	1	1	1	1	1	1	1	1	1
50	1	1	1	1	1	1	1	1	1	1

SYSTEM: 2x8 Interim (2x2)

ORBITAL PERIOD; 24 hours
TIME FROM EPOCH: 9 hours

ORBITAL INCLINATION: 18.5°
SPACING OF ASCENDING NODES: 157.5°
ARGUMENT OF LATITUDE OF THE FIRST SATELLITE IN EACH PLANE AT EPOCH: 45°, 225°
SATELLITE SPACING WITHIN EACH PLANE: 45°

MEASUREMENT NOISE (1σ): 50 feet
USER ALTITUDE UNCERTAINTY (1σ): 150 feet
SATELLITE POSITION UNCERTAINTY (1σ)
RADIAL (u): 15 feet
IN-TRACK (v): 117 feet
CROSS-TRACK (w): 38 feet
MINIMUM USER ELEVATION ANGLE: 5°

(1) Denotes indeterminate point

TABLE XIX

INTERIM SYSTEM NAVIGATION ACCURACY (C95) AS A FUNCTION OF USER LONGITUDE AND LATITUDE AT T = 12 HR WITH SATELLITE ERRORS

LONGITUDE \ NORTH LATITUDE	0	10	20	30	40	50	60	70	80	90
-100	1	1	1	1	1	1	1	1	1	1
-90	531	596	1	1	1	1	1188	1	1	1
-80	397	445	533	460	3590	2020	1431	1	1	1
-70	298	316	348	392	445	3144	1768	1	1	1
-60	247	264	296	340	396	6314	2240	1	1	1
-50	216	230	260	303	359	431	2899	1	1	1
-40	200	211	237	278	335	409	3779	1	1	1
-30	196	202	225	265	322	398	1	1	1	1
-20	203	204	225	264	322	398	1	1	1	1
-10	222	220	238	276	334	477	1	1	1	1
0	259	254	269	312	387	509	1	1	1	1
10	321	310	323	365	442	571	1	1	1	1
20	415	400	411	454	537	1	1	1	1	1
30	571	548	557	603	695	1	1	1	1	1
40	1	1	1	1	1	1	1	1	1	1
50	1	1	1	1	1	1	1	1	1	1

SYSTEM: 2x8 Interim (2x2)

ORBITAL PERIOD; 24 hours
TIME FROM EPOCH: 12 hours

ORBITAL INCLINATION: 18.5°
SPACING OF ASCENDING NODES: 157.5°
ARGUMENT OF LATITUDE OF THE FIRST SATELLITE IN EACH PLANE AT EPOCH: 45°, 225°
SATELLITE SPACING WITHIN EACH PLANE: 45°

MEASUREMENT NOISE (1σ) 50 feet
USER ALTITUDE UNCERTAINTY (1σ): 150 feet
SATELLITE POSITION UNCERTAINTY (1σ)
RADIAL (u): 15 feet
IN-TRACK (v): 117 feet
CROSS-TRACK (w): 38 feet
MINIMUM USER ELEVATION ANGLE: 5°

(1) Denotes indeterminate point

TABLE XX

INTERIM SYSTEM NAVIGATION ACCURACY (C95) AS A FUNCTION OF USER LONGITUDE AND LATITUDE AT T = 15 HR WITH SATELLITE ERRORS

NORTH LATITUDE

LONGITUDE	0	10	20	30	40	50	60	70	80	90
-100	1	1	1	1	1	1	1	1	1	1
-90	524	575	1	1	1	1	1	1	1	1
-80	338	427	495	606	1	95023	1	1	1	1
-70	301	325	363	413	474	4694	1	1	1	1
-60	248	270	307	357	420	497	1	1	1	1
-50	216	235	269	317	381	462	1	1	1	1
-40	200	214	245	292	356	439	661	1	1	1
-30	196	206	234	280	344	423	627	1	1	1
-20	203	209	235	280	345	453	619	1	1	1
-10	222	225	250	295	363	466	633	1	1	1
0	258	259	282	327	394	499	672	1	1	1
10	313	321	336	377	448	559	1	1	1	1
20	423	406	418	461	536	656	1	1	1	1
30	578	549	557	599	680	813	1	1	1	1
40	1	1	1	847	934	1	1	1	1	1
50	1	1	1	1	1	1	1	1	1	1

SYSTEM: 2x8 Interim (2x2)

ORBITAL PERIOD; 24 hours
TIME FROM EPOCH: 15 hours

ORBITAL INCLINATION: 18.5°
SPACING OF ASCENDING NODES: 157.5°
ARGUMENT OF LATITUDE OF THE FIRST SATELLITE IN EACH PLANE AT EPOCH: 45°, 225°
SATELLITE SPACING WITHIN EACH PLANE: 45°

MEASUREMENT NOISE (1σ): 50 feet
USER ALTITUDE UNCERTAINTY (1σ): 150 feet
SATELLITE POSITION UNCERTAINTY (1σ)
RADIAL (u): 15 feet
IN-TRACK (v): 117 feet
CROSS-TRACK (w): 38 feet
MINIMUM USER ELEVATION ANGLE: 5°

(1) Denotes indeterminate point

TABLE XXI

INTERIM SYSTEM NAVIGATION ACCURACY (C95) AS A FUNCTION OF USER LONGITUDE AND LATITUDE AT T = 18 HR WITH SATELLITE ERRORS

NORTH LATITUDE

LONGITUDE	0	10	20	30	40	50	60	70	80	90
-100	1	1	1	1	1	1	1	1	1	1
-90	675	794	976	1273	1833	1	1	1	1	1
-80	526	610	736	936	1287	2057	5064	1	1	1
-70	425	500	603	734	1018	1555	3236	1	1	1
-60	369	432	521	641	790	938	2525	1	1	1
-50	338	392	470	580	725	887	993	1	1	1
-40	324	371	443	545	685	852	979	1184	1	1
-30	320	364	432	531	668	835	983	1164	1	1
-20	325	368	437	537	673	838	981	1160	1	1
-10	337	384	457	561	700	882	992	1169	1	1
0	362	415	496	607	836	905	1017	1193	1	1
10	406	840	812	823	867	943	1058	1232	1	1
20	926	850	833	864	918	1001	1119	1289	1	1
30	938	879	890	934	999	1087	1204	1	1	1
40	1	1	1	1055	1126	1212	1321	1	1	1
50	1	1	1	1	1	1	1	1	1	1

SYSTEM: 2x8 Interim (2x2)

ORBITAL PERIOD; 24 hours
TIME FROM EPOCH: 18 hours

ORBITAL INCLINATION: 18.5°
SPACING OF ASCENDING NODES: 157.5°
ARGUMENT OF LATITUDE OF THE FIRST SATELLITE IN EACH PLANE AT EPOCH: 45°, 225°
SATELLITE SPACING WITHIN EACH PLANE: 45°

MEASUREMENT NOISE (1σ): 50 feet
USER ALTITUDE UNCERTAINTY (1σ): 150 feet
SATELLITE POSITION UNCERTAINTY (1σ)
RADIAL (u): 15 feet.
IN-TRACK (v): 117 feet
CROSS-TRACK (w): 38 feet
MINIMUM USER ELEVATION ANGLE: 5°

(1) Denotes indeterminate point

TABLE XXII

INTERIM SYSTEM NAVIGATION ACCURACY (C95) AS A FUNCTION OF USER LONGITUDE AND LATITUDE AT T = 21 HR WITH SATELLITE ERRORS

NORTH LATITUDE

LONGITUDE	0	10	20	30	40	50	60	70	80	90
-100	1	1	975	1039	1117	1209	1323	1	1	1
-90	930	873	885	931	1000	1090	1210	1	1	1
-80	923	850	840	867	924	1008	1127	1298	1	1
-70	393	455	817	830	874	951	1067	1242	1	1
-60	354	403	489	602	642	912	1025	1202	1	1
-50	333	381	455	559	699	888	999	1178	1	1
-40	322	368	437	538	674	841	987	1168	1	1
-30	320	365	435	535	671	838	987	1173	1	1
-20	327	375	448	550	689	854	979	1193	1	1
-10	345	399	479	588	731	888	989	1	1	1
0	381	445	534	652	797	936	2632	1	1	1
10	444	520	622	782	1057	1629	3492	1	1	1
20	554	641	774	986	1366	2224	1	1	1	1
30	727	855	1053	1384	1	1	1	1	1	1
40	1	1	1	1	1	1	1	1	1	1
50	1	1	1	1	1	1	1	1	1	1

SYSTEM: 2x8 Interim (2x2)

ORBITAL PERIOD: 24 hours
TIME FROM EPOCH: 21 hours

ORBITAL INCLINATION: 18.5°
SPACING OF ASCENDING NODES: 157.5°
ARGUMENT OF LATITUDE OF THE FIRST SATELLITE IN EACH PLANE AT EPOCH: 45°, 225°
SATELLITE SPACING WITHIN EACH PLANE: 45°

MEASUREMENT NOISE (1σ): 50 feet
USER ALTITUDE UNCERTAINTY (1σ): 150 feet
SATELLITE POSITION UNCERTAINTY (1σ)
RADIAL (u): 15 feet
IN-TRACK (v): 117 feet
CROSS-TRACK (w): 38 feet
MINIMUM USER ELEVATION ANGLE: 5°

(1) Denotes indeterminate point

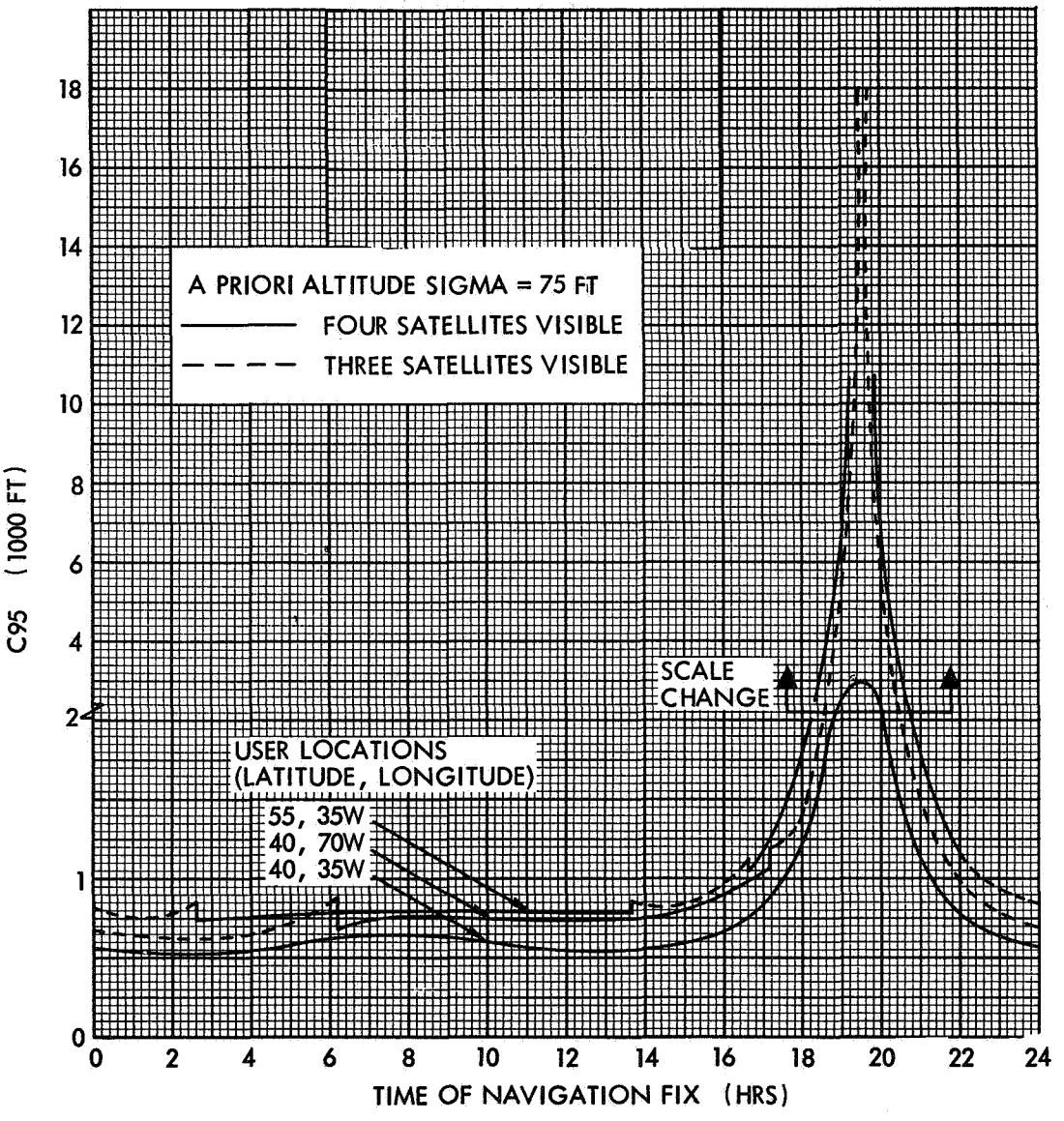

Figure 15. Variation of Interim System Navigation Accuracy with Time of Day

2.3.3 Velocity Estimation from Doppler Data

By using the Navigation Satellite Accuracy Program (NAVSAP), it was determined that a user can accurately estimate his velocity from doppler measurements at one instant of time.

Required modifications to the usual mode of program operation are described in app. E. Six user locations in the North Atlantic were chosen for the analysis, and a 5^{o} (min) elevation angle was assumed for visibility. Two runs were made with two different a priori error covariance matrices for satellite velocity, as determined from orbit determination runs, but the difference between the two cases proved insignificant (0.1 ft/sec).

The measurement noise was pessimistically assumed to be 0.707 ft/sec (1σ), and the user velocity error covariance matrix was diagonal with a standard deviation of 100 ft/sec in each direction. Results are given in Table XXIII, which shows the RSS user velocity error in ft/sec at each of the six locations. The range is from 1.22 to 1.92 ft/sec. This error can easily be reduced, and will be determined by the cost of the user hardware.

TABLE XXIII

USER VELOCITY ESTIMATION ERRORS (FT/SEC)

	North Latitude	
West Longitude	30^{o}	60^{o}
60^{o}	1.92	1.81
30^{o}	1.80	1.25
0^{o}	1.40	1.22

2.3.4 Relative Navigation Accuracy Analysis

Relative navigation accuracy is the accuracy with which a user can determine his position relative to (1) another user, (2) a ground station, or (3) his own home base. All three modes have the characteristic that certain common error sources can be expected to cancel, providing the possibility of increased accuracy over the absolute navigation case.

In mode 1, each user estimates his position independently with common error sources, especially satellite errors, causing common position estimation errors. The users then communicate their estimates to each other and compute their relative positions. It can be expected that the common errors will tend to cancel in the subtraction, leaving only the effects of the independent random errors made by the two users. However, the random effects add (RSS).

In mode 2, a ground station replaces the second user. The station takes measurements like those of the user, but its advantage is in being stationary and capable of taking many measurements, thereby reducing the effect of noise. Hence, not only do the common error sources cancel, but the doubling of the noise effect occurring in mode 1 is eliminated in mode 2. Furthermore, if the absolute position of the ground station is known, the computed position can be used for calibration purposes, enabling the user to obtain a more accurate absolute position determination.

In mode 3, the user is assumed to make a preliminary fix while at his home base and then, during his subsequent flight, to navigate with respect to this base. This is similar to mode 2, except that user receiver bias is calibrated at the home base. Also, due to the elapsed time between calibration and navigation fix, there may be drifts in some of the calibrated errors, such as receiver drift and tropospheric and ionospheric errors. In the case of the last two errors, distance, as well as time, determines the degree of correlation and, hence, cancellation (see subsec. 2.2 on Measurement Error Source).

The ideas expressed in the preceding paragraphs can be investigated in terms of the covariance matrices of the two participants, whether they are two users, mode 1; a user and a ground station, mode 2; or the same

user at two different locations, mode 3. The covariance matrix of relative position error is

$$E\left[(\delta x_1 - \delta x_2)(\delta x_1 - \delta x_2)^T\right] = E\left(\delta x_1\ \delta x_1^T\right) + E\left(\delta x_2\ \delta x_2^T\right) - E\left(\delta x_1\ \delta x_2^T\right) - E\left(\delta x_2\ \delta x_1^T\right) \quad (1)$$

where δx_1 and δx_2 are the estimation errors $\hat{x}_1 - x_1$ and $\hat{x}_2 - x_2$, and E denotes the expected value. The difference $\delta x_1 - \delta x_2$ is the error in estimating the position of user 1 relative to user 2. x_1, x_2 are the actual position vectors and $\hat{x}_1$, $\hat{x}_2$ are their estimates.

This equation contains the essential elements of the relative navigation problem. The first two terms are the individual estimation errors of the two users, including the effects of common error sources (in this case, satellite position and satellite clock errors). The last two terms are the correlations between the errors of the two users. These correlations are due to the common satellite errors and can be expected to reduce the portions of the first two terms that are attributable to satellite errors. The effect is brought out by rewriting Eq. (1) in the form

$$\Sigma_R = \underbrace{\Sigma_{1n} + \Sigma_{1s}}_{\Sigma_{11}} + \underbrace{\Sigma_{2n} + \Sigma_{2s}}_{\Sigma_{22}} - \Sigma_{12} - \Sigma_{21} \quad (2)$$

Here the Σ's denote the covariance matrices $\left(\text{e.g., } \Sigma_{12} = E\left(\delta x_1 \delta x_2^T\right)\right)$, and Σ_{11} and Σ_{22} have been divided into two parts, the first part due to random errors (e.g., Σ_{1n}) and the second due to satellite errors (e.g., Σ_{1s}).

Equation (2) assumes its minimum value either when the satellite errors are zero (in which case $\Sigma_{12} = \Sigma_{21} = \Sigma_{1s} = \Sigma_{2s} = 0$) or when the correlations directly cancel the satellite errors of the two users. This minimum is given by

$$\Sigma_{R_{min}} = \Sigma_{1n} + \Sigma_{2n} \quad (3)$$

These equations apply to all three modes of relative navigation. In modes 2 and 3, however, the component Σ_{11} will be significantly smaller than in mode 1, where it is of the same order of magnitude as Σ_{22}.

The individual terms in Eq. (2) were evaluated for the interim system at T = 0 by using the NAVSAP program (details of the analysis are included in app. F). Some typical results are shown in Table XXIV, where user 2 moves to several positions north of a base station (user 1), who is at latitude 0° and longitude -30°. The eight columns of the table are headed by the appropriate covariance matrices in Eq. (2); the numerical values given are the C95 values corresponding to these covariance matrices.

The first two columns show the uncertainties in the positions of user 1 and user 2 as determined in earth-centered coordinates. User 1's uncertainty is, of course, independent of user 2's position; therefore all figures in the first column are the same. User 2's uncertainty changes with his latitude as shown.

Columns 3 and 4 are the same as columns 1 and 2, except that no satellite errors are included (Σ_{1s} and Σ_{2s} are zero)*. Since mode 2 assumes that the effect of noise in user 1's measurement (Σ_{1n}) is zero, column 4 can be interpreted as mode 2 relative navigation without satellite errors.

Columns 5 and 6 are the RSS of columns 1 and 2, and 3 and 4, respectively (covariance matrices add; C95's RSS). They can be interpreted to represent the uncertainty in user 2's position in relation to someone like user 1 (who sees similar satellite configurations), but located far from user 1 and, therefore, seeing different satellites. Column 5 includes satellite errors, while column 6 excludes them (or assumes that they are correlated and therefore produce a negligible effect). In this case, the user correlation terms Σ_{12} and Σ_{21} do not

*Par. 2.5.1 on satellite error correlations shows that correlation effects may reduce the effect of satellite errors to negligible values. Thus, cases excluding satellite errors may alternatively be considered as cases in which intersatellite correlation is taken into account.

TABLE XXIV

RELATIVE NAVIGATION ACCURACY (C95 IN FT)

	1	2	3	4	5	6	7	8
Latitude of User 2	$\Sigma_{11} = \Sigma_{1n} + \Sigma_{1s}$	$\Sigma_{22} = \Sigma_{2n} + \Sigma_{2s}$	Σ_{1n}	Σ_{2n}	$\Sigma_{11} + \Sigma_{22}$	$\Sigma_{1n} + \Sigma_{2n}$	Σ_R	$\Sigma_R - \Sigma_{1n} = \Sigma_{22} - \Sigma_{12} - \Sigma_{21}$
0°	269	269	187	187	380	265	265	187
5°	269	271	187	189	381	266	266	189
10°	269	277	187	193	386	269	269	193
15°	269	285	187	200	392	274	275	202
20°	269	298	187	210	402	281	283	212
		Absolute-rel. to ECR system		Mode (2) w.o. sat. errors or w. inter-sat. correl.	Worldwide rel. or Mode (1) w.o. user correl.	Worldwide rel. w. no. sat. errors or w. inter-sat. correl.	Local rel. w. sat. errors. Mode (1)	Mode (2) with sat. error. (Base station noise smoothed)

Notes: measurement noise = 50 ft (1σ)
altitude uncertainty = 75 ft (1σ)
satellite errors (1σ)
radial = 49 ft
intrack = 360 ft
crosstrack = 99 ft

subtract as they do in local (using the same satellites) relative navigation. This situation will be designated worldwide relative navigation. It is representative of the intuitive notion of navigation as being relative to some distant point of the earth's surface rather than relative to an arbitrary earth-centered coordinate system.

Colum 7 is the C95 corresponding to local relative navigation in mode 1, including all the terms of Eq. (2). The significant point to be noted is that the values are nearly identical to those of column 6. That is, local relative navigation causes cancellation of nearly all the effects of satellite errors*. The difference between columns 7 and 5 should also be noted; it is due to the effects of user correlation (Σ_{12} and Σ_{21}) and illustrates the intuitive idea of error reduction in relative navigation.

Column 8 is column 7 less the effect of noise in determining the base station (user 1) position. Thus, column 8 gives the uncertainties for mode 2, local relative navigation, where the base station can take many measurements and reduce the effects of noise to a negligible value. Since the relative navigation effect causes the nearly complete cancellation of satellite errors, column 8 is nearly equal to column 4.

This brief analysis of relative navigation accuracy leads to the following conclusions:

- Local relative navigation results in cancellation of satellite errors
- Satellite errors are not the major source of navigation uncertainties, so that the improvement of local relative navigation accuracy (column 7) with respect to worldwide relative navigation (column 5) is not as pronounced as might be expected.
- If intersatellite correlations are taken into account, it is expected (although not yet proved) that column 6 is a better representation of worldwide relative navigation than is column 5. In that case, worldwide and local relative navigation uncertainties are nearly identical and both approach the minimum value of Eq. (3).

*In this case, both users see identical satellites. If only some of the satellites were common, the cancellation would be less complete.

2.4 ORBIT DETERMINATION ERRORS

The accuracy with which a user can determine his position depends, in part, on the accuracy of his knowledge of the satellite ephemerides. The effect of tracking errors on satellite position determination accuracy was analyzed. A series of preliminary analyses were made to obtain answers to the following subsidiary questions:

- Which uncertainties make the largest contributions to the total position uncertainty?
- Which parameters should be solved for in processing the tracking data?
- Are range measurements alone sufficient, or will angle and range-rate measurements increase tracking accuracy?
- Which geopotential harmonics should be estimated?
- Should measurement biases be assumed constant or changing?
- How many tracking stations are required for satisfactory position determination?
- How long a tracking period is required?

In order to find answers to these questions, several tracking configurations were analyzed in addition to the finally selected configuration. Details of these preliminary analyses and results are given in app. K, and the minimum-variance estimation methods of the TRW System's ESPOD computer program used to derive the results are briefly described in app. G.

The conclusions reached can be summarized as follows:

- The predominant error source is the uncertainty in the earth's gravitational constant μ. This uncertainty leads to large period errors, which appear as large v (in-track) errors.
- Solving for the parameters (measurement bias errors, survey errors, and uncertainties in μ and J_2) results in a considerable improvement in accuracy, particularly in the v (downrange) direction.

- Adding the angle (AE) and range-rate ($\dot{R}$) measurements to the range (R) measurements does not affect the system accuracy; therefore, only range measurements are required.

- The J_{22} geopotential harmonic should be solved for. With this coefficient solved for, the position uncertainties are unaffected, but if it is not solved for, it leads to large increases in total error, especially in the along-track and cross-track directions. A run was also made to determine the effects of J_{33}; this term had no effect on the position uncertainties.

- The use of three stations rather than two substantially reduces the in-track error, an effect that can be expected to be even more pronounced for shorter (less than 72 hr) tracking intervals, in which case it would also affect cross-track errors significantly.

- Reducing the tracking period from 72 to 36 hr has little significant effect on the results. Hence, 36 hr is sufficient.

With this background, it was possible to analyze a realistic tracking configuration, corresponding to the proposed system, which uses essentially the same equipment as a user, taking measurements from a particular satellite at a rate of one every 16 sec. Three stations were chosen, collocated with present tracking facilities. The station locations and the satellite ground track used in this analysis are shown in Figure 16. The error sources considered and their values are shown in Table XXV.

The results of the proposed tracking configuration analysis for the single satellite and set of ground stations selected are shown in Figure 17, where the epoch is at the end of a 36-hr tracking interval.

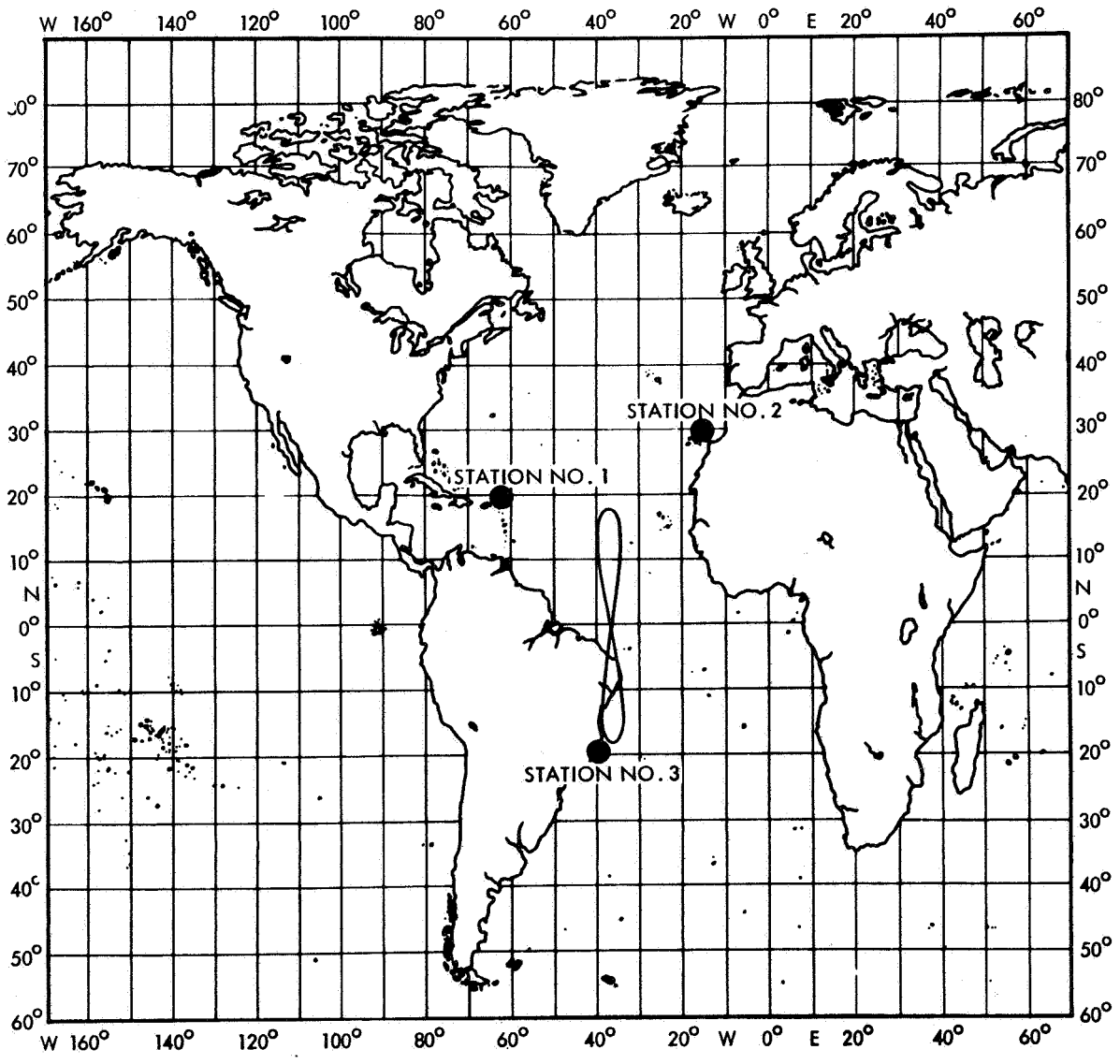

Figure 16. Recommended Tracking Configuration

TABLE XXV

ERROR SOURCES FOR ORBIT DETERMINATION ANALYSIS

Measurement errors	
Noise	30 ft
Bias	50 ft
Station location errors	
Latitude	100 ft
Longitude	100 ft
Altitude	100 ft
Gravitational potential uncertainties	
μ	1.06×10^{-11} ft^3/sec^2
J_2	2.0×10^{-7}
J_{22}	2.0×10^{-7}
J_{33}	2.6×10^{-7}

At the end of 36-hr tracking, the figure shows the following tracking errors:

σ_u (radial)	10.8 ft
σ_v (in-track)	140.0 ft
σ_w (cross-track)	5.0 ft

These results assume a constant bias in the measurements. In a real tracking situation, however, the biases are slowly varying. To represent this condition in the program approximately, piecewide constant biases (all uncorrelated) were assumed over 3-hr tracking intervals. The first 15 hr of the tracking period were then re-run, which produced the results shown in Figure 18. The results shown in Figure 17 are included for easier comparison.

It can be seen that the effect is a significant degradation in accuracy over extended tracking intervals.

Additional study of the tracking of several satellites simultaneously is indicated. Measurements from additional satellites provide more information for determining geopotential terms and biases, and the satellite position errors become correlated because of common error sources, particularly the uncertainties in the geopotential model. Covariance matrices containing these correlations result in smaller

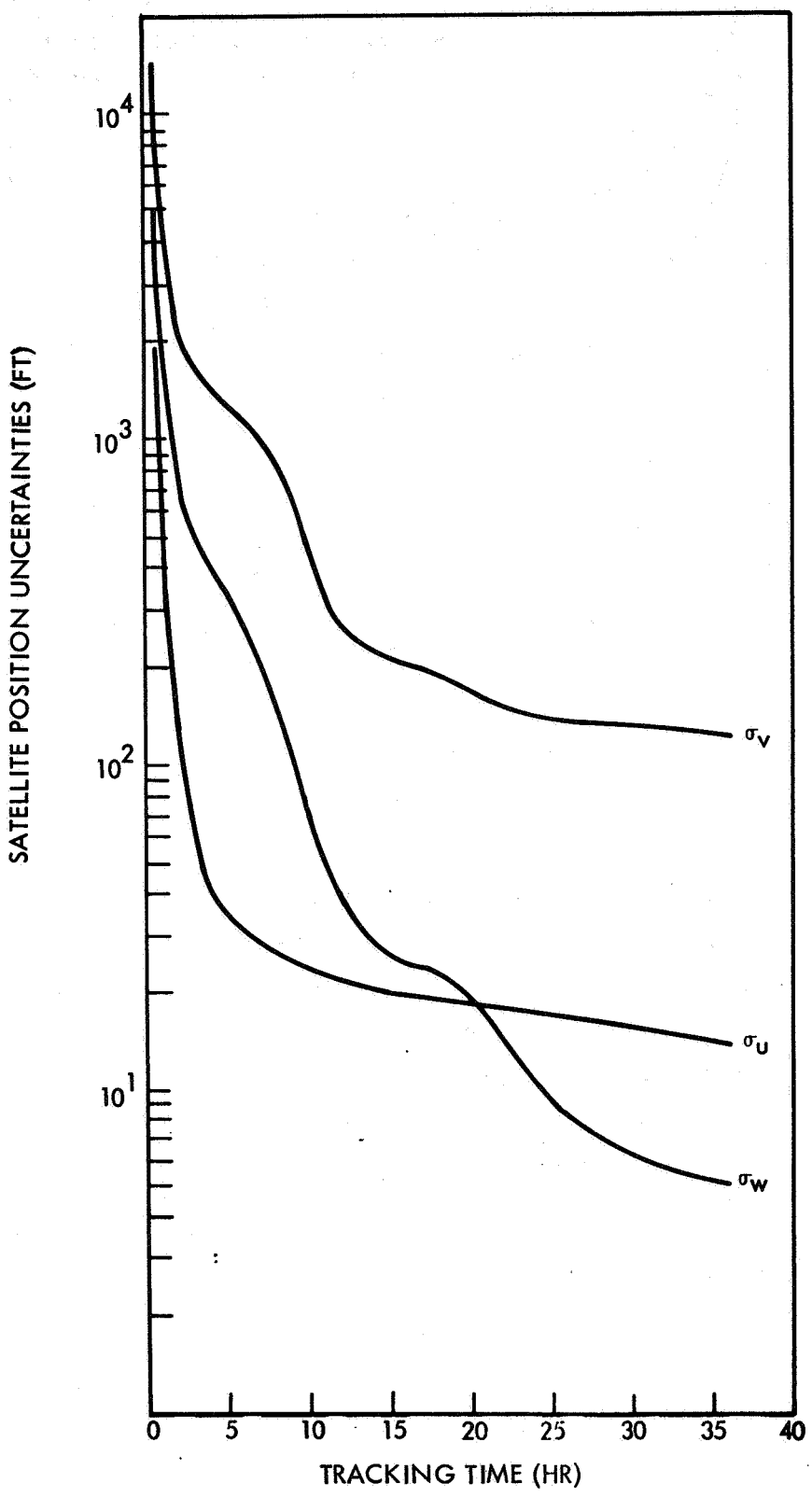

Figure 17. Results of Tracking for 36 Hr at 16-sec Data Interval

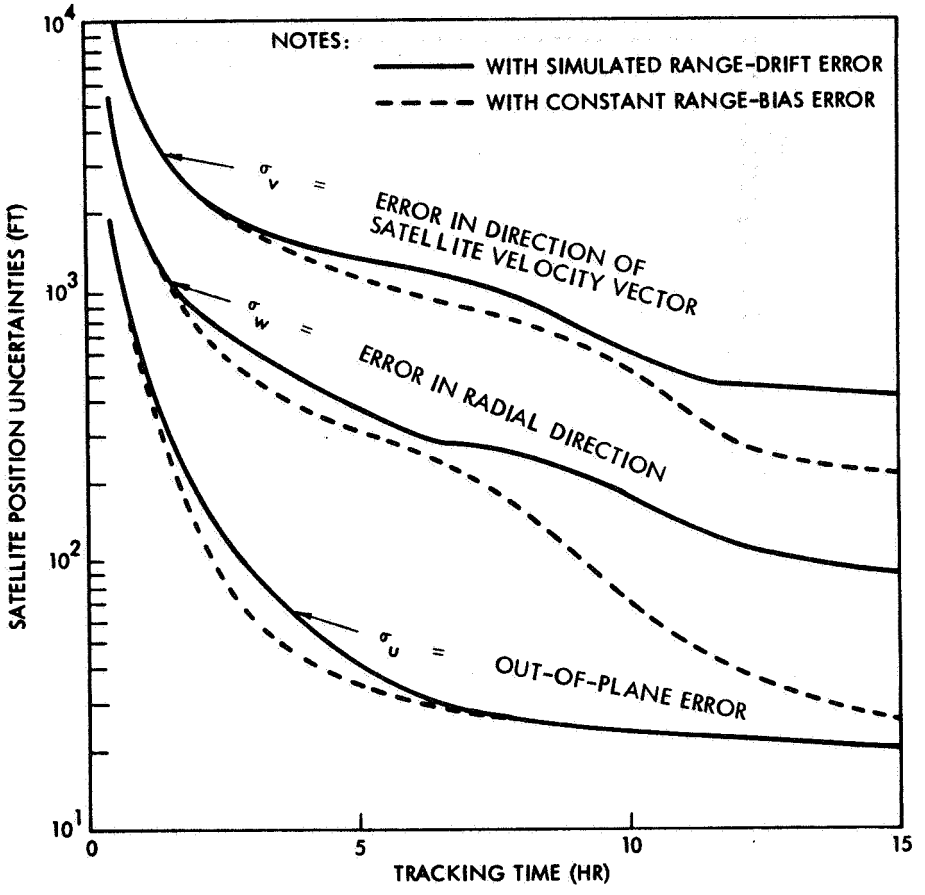

Figure 18. Comparison of Effects of Constant Range-Bias Error with Simulated Range-Drift Error

user position errors, as discussed in par. 2.5.1. The magnitude of the correlations should be determined for the tracking procedures used in the actual system.

Another important source of error that must be investigated in detail is the effect of satellite oscillator drift on range measurements and, consequently, on navigation accuracy. Present error models assume that the satellite clocks can be calibrated so that the drift error after 3 hr is less than 10 ft. Actually, the oscillator drift characteristics must be estimated from the tracking data along with the orbital parameters.

To determine the error in the estimate of satellite oscillator drift and the consequent effect on orbit determination accuracy and navigation accuracy will require 1) a suitable mathematical model of the oscillator drift mechanism and 2) the incorporation of this model into the present series of error analysis programs (NAVSAP and ESPOD).

2.5 ANALYSIS OF OTHER FACTORS AFFECTING NAVIGATION ACCURACY AND COVERAGE

Results of analyses of a number of factors affecting the overall navigation accuracy provided by the system are presented in this subsection. Par. 2.5.1 discusses the effects of satellite error correlations and illustrates these effects. The remaining paragraphs discuss the effects of : 1) user motion, 2) using range-difference measurements and 3) increasing the minimum elevation angle of the antennas.

2.5.1 Effect of Correlated Satellite Position Errors

The majority of navigation-satellite user position accuracy studies assumed that position errors of the several satellites are uncorrelated, with equal covariance matrices resulting from tracking studies using the TRW orbit-determination program. It is apparent, however, that correlations do exist, arising from numerous common error sources. In particular, station measurement biases and location errors will equally influence all satellites seen from that station, and earth potential model uncertainties cause correlations between errors in all satellites.

It has been postulated that the correlations arising from these common errors may have a significant effect on the resulting user position determination errors. This claim has been corroborated by the results of the Single Point in Time (SPIT) accuracy program presented in app. H. In that analysis, tracking stations and users make simultaneous observations of a group of satellites. Correlations in satellite position errors arise from common ground-station bias errors, and these correlated satellite errors are used directly to compute user position errors. Appendix I contains a more complete description of the SPIT program and its assumptions. The results show a high degree of correlation and a significant reduction in position errors over the uncorrelated case. In fact, the position errors closely approach those obtained with the assumption of perfectly known satellite positions.

To confirm the effect, using more realistic satellite errors, additional runs have been made using the Navigation Satellite Accuracy

Program (NAVSAP), in which perfectly correlated satellite errors were assumed; that is

$$E\left(x_1 x_2^T\right) = E\left(x_1 x_1^T\right) = E\left(x_2 x_2^T\right) \tag{4}$$

where x_1 and x_2 are satellite position vectors. This implies $x_1 = x_2$ with probability one. These results are shown in Table XXVI, along with comparable results for no satellite errors and uncorrelated errors. Again, the position errors are reduced to values near to those obtained with zero satellite errors.

A more complete analysis of this effect is proposed for future work. In particular, the correlations that arise in a realistic tracking situation must be determined. Since the present TRW orbit determination program is limited to a single satellite, multiple runs must be made and the resulting normal matrices assembled to determine a joint normal matrix, which can then be inverted to yield the overall satellite error

TABLE XXVI

NAVIGATION ACCURACY WITH CORRELATED SATELLITE ERRORS

	C95 (ft)		
Latitude	0^o	30^o	60^o
No Satellite Errors	327	341	364
Correlated Errors	337	349	369
Uncorrelated Errors	442	455	474

NOTES:

1. Range measurements from all visible satellites - User oscillator uncalibrated
2. Measurement Noise = 100 ft. (1σ)
3. User a priori altitude error = 150 ft. (1σ)
4. Satellite a priori position error covariance matrix from app. K (450 ft downrange error)
5. User longitude = 60^o west

covariance matrix. More specifically, consider a linearized tracking model associated with tracking the i^{th} satellite

$$y_i = A_i x_i + B_i z + \epsilon_i \tag{5}$$

x_i is the satellite state vector, consisting of positions, velocities, and possibly satellite oscillator bias. z is a vector of satellite-independent parameters, including station locations, biases, and earth potential parameters. y_i is the measurement vector, A_i and B_i are the appropriate partial-derivative matrices, and ϵ_i is the measurement error. x_i, y_i, and z are to be interpreted as small deviations from reference values.

For each satellite, the tracking program will generate a normal matrix of the form

$$Q_i = \begin{bmatrix} A_i^T W_i A_i & A_i^T W_i B_i \\ B_i^T W_i A_i & B_i^T W_i B_i \end{bmatrix} \tag{6}$$

where

$$W_i = \left[E(\epsilon_i \epsilon_i^T) \right]^{-1} \tag{7}$$

These individual matrices are then assembled into the giant normal matrix Q as follows:

$$Q = \begin{bmatrix} A_1^T W_1 A_1 & 0 & 0 & \cdots & A_1^T W_1 B_1 \\ 0 & A_2^T W_2 A_2 & 0 & \cdots & A_2^T W_2 B_2 \\ \cdot & & & & \cdot \\ \cdot & & & & \cdot \\ \cdot & & & & \cdot \\ 0 & & & A_n^T W_n A_n & A_n^T W_n B_n \\ B_1^T W_1 A_1 & B_2^T W_2 A_2 & \cdots & B_n^T W_n A_n & \sum_{i=1}^{n} B_i^T W_i B_i \end{bmatrix} \tag{8}$$

The inverse of this matrix is the covariance matrix of the giant state vector

$$x = \begin{bmatrix} x_1 \\ x_2 \\ \cdot \\ \cdot \\ \cdot \\ x_n \\ z \end{bmatrix} \tag{9}$$

assuming all of the components of z are estimated. If some are not, their errors can be taken into account, using a well known formula involving submatrices of Eq. (8). These computations are readily performed by the TRW Matrix Abstraction Program (MAP).

2.5.2 Sequential Estimation of Position of a Rapidly Moving User (SST)

The navigation equations presented in Section 3 provide for continual updating of user position as measurements are processed. Every 16 sec, the system recycles through the visible satellites, and the new measurements are processed to refine the previous estimate. If the user were stationary, this recursive estimation procedure would result in a continual reduction of the errors due to measurement noise. The same is true if the user were flying along a perfectly predictable flight path. In that case, the estimate is propagated to the new measurement time, and the new fix is used to refine the propagated estimate. Unfortunately, the flight path of an SST is not perfectly predictable; hence, errors are introduced in propagating the previous estimate forward. If large enough, these errors can effectively nullify the previous estimate and force reliance only on current data to produce a current fix. In that case, there is no beneficial effect of noise reduction from multiple measurements.

This subsection presents an analysis allowing an approximate assessment of the effect of the uncertainty in the user flight path on navigation accuracy. The NAVSAP program (app. J) considers a user

moving along a nominal great circle flight path, taking an instantaneous fix from all visible satellites every 16 sec.* The program does not provide for the estimation of user velocity, but does permit uncertainties in user velocity and heading to be introduced, using the state noise feature of the Kalman filter. Although this is a simplified model of the actual system operation, the results do point up some important aspects of the sequential estimation problem.

Three runs were made with varying magnitudes of the flight path uncertainties as tabulated below:

Case	Heading Error (rad-1σ)	Velocity Error (ft/sec-1σ)
1	0	0
2	0.01	20
3	0.10	100

The user was assumed to be flying just outside of London on a great circle route to New York at a speed of 2000 ft/sec. and an altitude of 50,000 ft. Satellite estimation errors were 98 ft radial, 720 ft in-track, and 198 ft cross-track (Table K-II - app. K), and the measurement noise was 50 ft (1σ). The exact values used are relatively unimportant; the purpose is to illustrate the effect. The satellites considered are the five shown in Figure 19.

The results of the three cases are presented in Table XXVII and plotted as the top two curves in Figure 20. The results for cases 2 and 3 are nearly identical, despite the wide variation in flight-path errors. These errors are only 12 to 15 ft greater than in the case of zero errors, which demonstrates the relatively minor influence of the velocity and heading errors. The curves show an initial rapid drop while the user oscillator is being calibrated.** Thereafter, the curves exhibit a slower decrease toward an asymptotic value determined by the satellite errors. The lower curves illustrate these effects, in both cases, with no heading or velocity errors. The bottom curve shows the results for no satellite

*This is, of course, an approximation, as the data for the fix are taken throughout the 16-sec frame, not instantaneously.

**Uncertainties in velocity and heading do not degrade the estimate of oscillator bias.

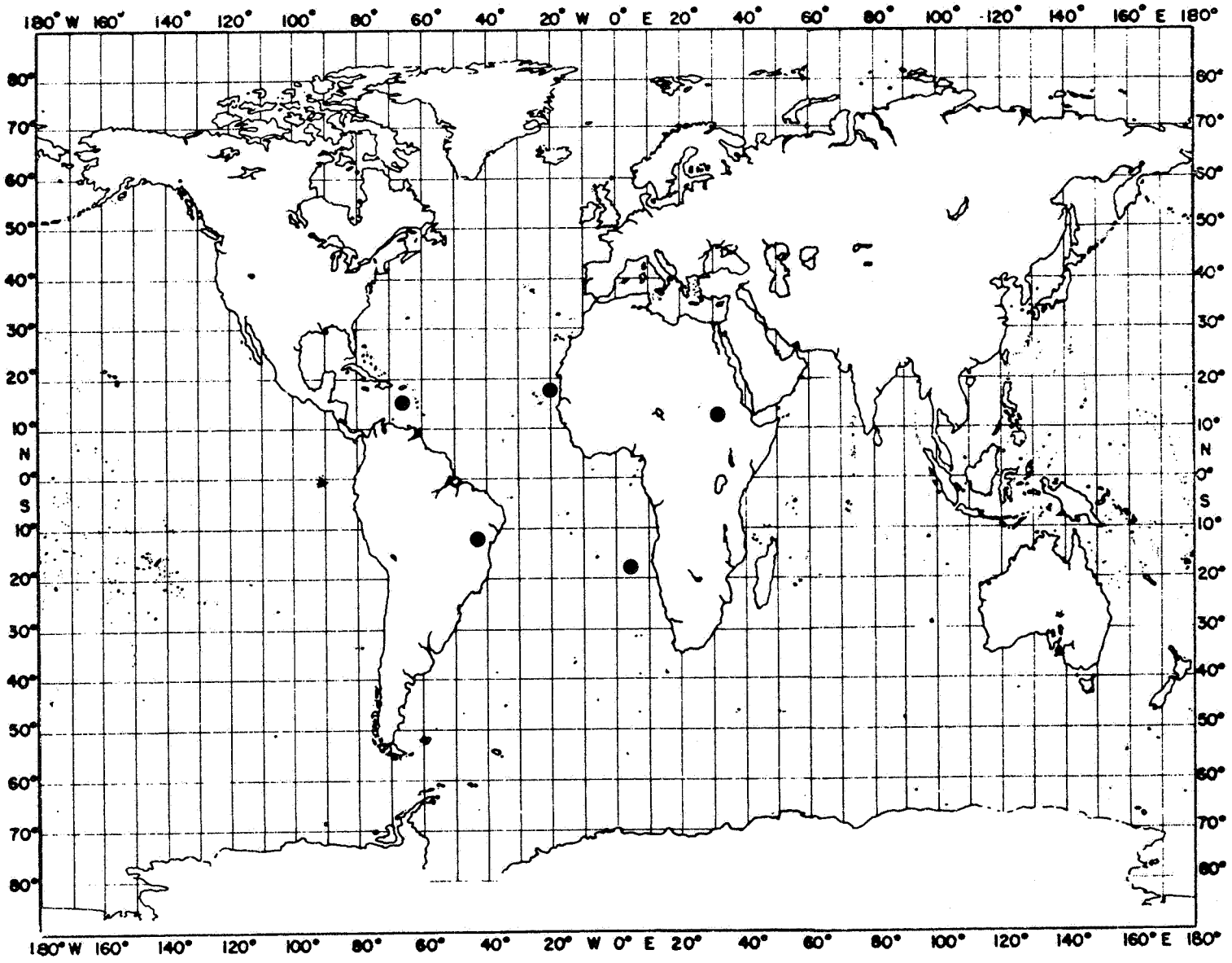

Figure 19. Satellite Positions for User Motion Study

TABLE XXVII

C95 VERSUS TIME FOR A MOVING USER WITH VARIOUS VELOCITY AND HEADING ERRORS

Time (Sec)	$\sigma_v = 0$ $\sigma_\psi = 0$		$\sigma_v = 20$ fps $\sigma_\psi = 0.01$		$\sigma_v = 100$ fps $\sigma_\psi = 0.01$	
	Before Observation	After Observation	Before Observation	After Observation	Before Observation	After Observation
0		302		302		302
16	302	259	505	264	3369	265
32	259	243	484	250	3365	251
48	243	235	477	243	3363	244
64	235	230	474	239	3362	240
80	230	226	471	236	3360	237
96	226	223	470	234	3359	235
112	224	222	469	233	3358	234
128	222	220	468	231	3357	232
144	220	219	467	231	3356	232
160	219	218	467	230	3355	231
176	218	217	466	229	3354	230
192	217	216	466	229	3353	230
208	216	215	465	229	3352	230
224	215	214	465	229	3351	229
240	214	214	465	228	3350	229
256	214	213	464	228	3349	229
272	213	212	464	228	3348	229
288	212	211	464	228	3347	229
304	211	210	464	228	3346	229
320						

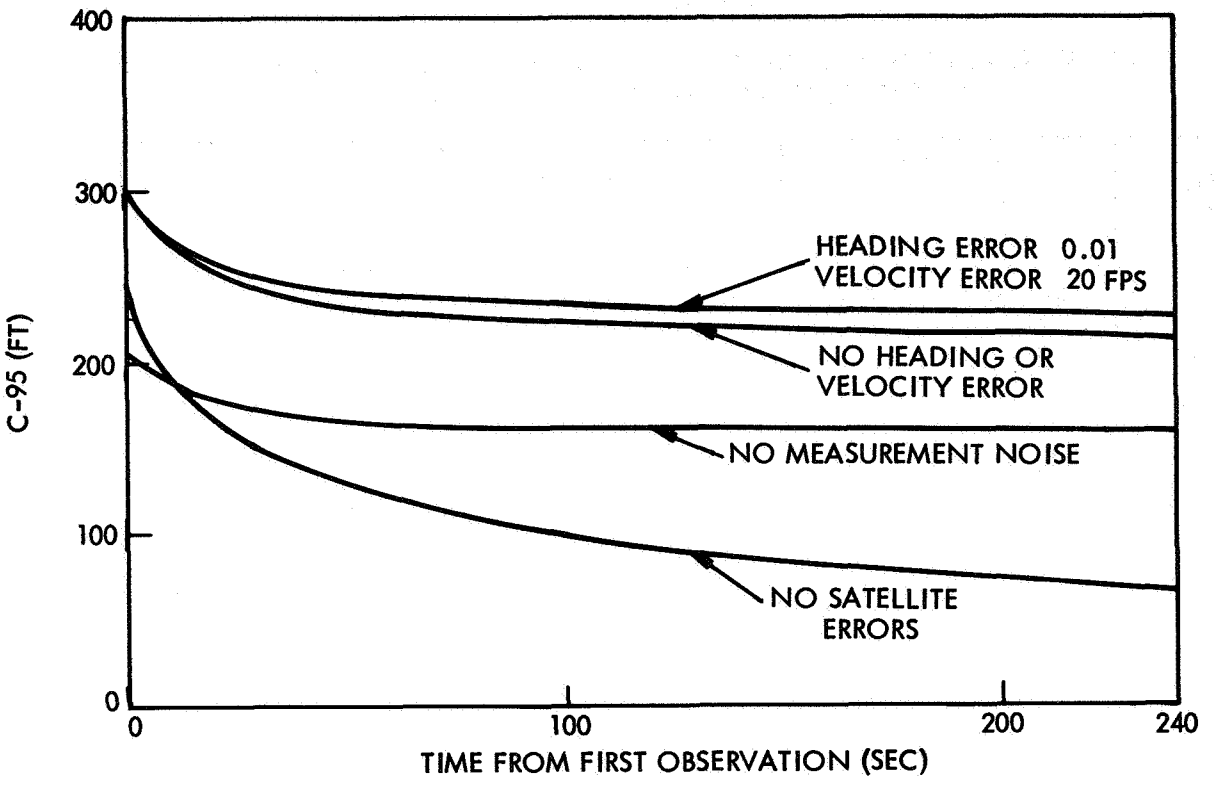

Figure 20. Estimation Error Versus Time

errors, in which case the error continues to decrease as the effect of noise is reduced. In the second curve from the bottom, satellite errors are included, but measurement noise is zero. In that case, the estimation error rapidly approaches the minimum value established by the satellite position errors.

From these results it can be concluded that a sequence of fixes results in an initial increase in accuracy due to improved estimation of the bias (user oscillator calibration). Continual estimation, as provided by the proposed system, will provide accuracies near this reduced value. The minimum attainable is determined by satellite errors, and may approach the case of zero satellite errors due to the correlation effects discussed in par. 2.5.1.

The effect of heading and velocity errors during the interval ($\geq$2 sec) separating observations from different satellites has not yet

been studied. This study would require several modifications to the NAVSAP program as follows:

1) Logic for sequential measurements from one satellite at a time

2) Capability for estimation of user velocity

3) Improved model of aircraft motion.

2.5.3 Effect of Correlations in Range-Difference Measurements

The proposed NAVSTAR measurement system is based on measuring the transmission time of a signal from the satellite to a ground station. If satellite and user clocks are synchronized, the absolute transit time is obtained directly and is proportional to range. However, if a less stable clock is available to the user, the equipment will be more economical. With a less stable clock, the user time reference is accurate for only relatively short time measurements as it is not synchronized with the highly precise satellite clocks. In this case, it is impossible to measure the absolute range from user to satellite directly; however, the arrival times of signals from various satellites can be compared, and will yield, in effect, a range-difference measurement. Thus, a psuedo-range is produced from the difference between the arrival time of the signal and the local clock time. In effect, this measurement is the actual range from satellite to user, plus a large unknown bias caused by lack of synchronization of the satellite and user clocks. Therefore, this same bias appears in simultaneous or near-simultaneous measurements to all visible satellites. These raw measurements, including the common bias, can then be differenced in the computer to produce range-difference measurements, which can then be processed further to produce a position estimate.

An alternate approach is to process the psuedo-range measurements directly, producing a simultaneous estimate of user position plus the unknown bias. It will be shown, subsequently, that the two approaches give the same result under suitable conditions. Since sequential data processing is more straightforward in the second method, it is recommended wherever maximum accuracy is required.

The linearized measurement model relates the psuedo-range measurement vector y to the user position x and bias b by

$$y = Ax + Cb + \epsilon \tag{10}$$

where y, x, and b are small deviations from reference values, A is the sensitivity matrix of the observations with respect to position, ϵ is the measurement error, and C is a column vector with all elements unity.

$$C^T = (1, 1, 1, \ldots, 1) \tag{11}$$

Hence, the bias b is a scalar, and the vector Cb adds the bias to each observation.*

2.5.3.1 Optimum Weighting of Range-Difference Measurements

An m-vector z of range-difference measurements can be interpreted as a linear transformation on y

$$z = Ty \tag{12}$$

where T is an m x n matrix, each row of which contains one +1, one -1, and all other elements zero, i.e.,

$$z_k = T_k y = y_i - y_j \tag{13}$$

The i^{th} element of T_k is +1 and the j^{th} is -1. Multiplying Eq. (10) by T and noting that TC = 0 results in the bias-free observation equation for z

$$z = TAx + T\epsilon \tag{14}$$

*Let y, C, and ϵ be of dimension n, and x be of dimension p.

The range-measurement errors are uncorrelated ($E(\epsilon_i \epsilon_j) = 0$) and are assumed to be of equal variance σ_ϵ^2. Therefore, the range-difference errors are correlated, with covariance matrix

$$\Lambda_\delta = \sigma_\epsilon^2 \, TT^T \tag{15}$$

The minimum variance estimate $\hat{x}$ of x, based on the range-difference measurements z, appropriately weighted by Λ_δ^{-1} is readily found to be

$$\hat{x} = \left[A^T T^T (TT^T)^{-1} TA\right]^{-1} A^T T^T (TT^T)^{-1} z \tag{16}$$

$$= (A^T \overline{W} A)^{-1} A^T \overline{W} y \tag{17}$$

where

$$\overline{W} = \frac{1}{\sigma_\epsilon^2} T^T (TT^T)^{-1} T \tag{18}$$

An interesting result, demonstrated by Soule at the Aerospace Corporation, is that $\overline{W}$ is independent of T, i.e., independent of the choice of range-difference measurements. It is required only that TT^T be nonsingular, which in turn requires that m be n-1. The invariance of $\overline{W}$, along with Eq. (17) shows that the minimum variance estimate is independent of the choice of range differences.

2.5.3.2 Estimation Using Pseudo-Range Measurements

The alternative approach to estimating x is to process the psuedo-range data y directly and attempt to solve for the bias. The resulting estimate, for equally weighted psuedo-range measurements, is

$$\begin{bmatrix} \hat{x} \\ \hat{b} \end{bmatrix} = \begin{bmatrix} A^T A & A^T C \\ C^T A & C^T C \end{bmatrix}^{-1} \begin{bmatrix} A^T \\ C^T \end{bmatrix} y \tag{19}$$

Partitioning the inverse leads to the $\hat{\underset{\sim}{x}}$ component

$$\hat{\underset{\sim}{x}} = (A^T W A)^{-1} A^T W y \tag{20}$$

with

$$W = \frac{1}{\sigma_\epsilon^2}\left(I - \frac{1}{n} CC^T\right) \tag{21}$$

where CC^T is an n x n square matrix with all elements unity.

That $W = \overline{W}$ can be shown by assuming the invariance demonstrated heuristically by Soule and computing $\overline{W}$ for a particular, T, namely,

$$T = \begin{bmatrix} 1 & -1 & 0 & 0 & \dots & 0 \\ 1 & 0 & -1 & 0 & \dots & 0 \\ 1 & 0 & 0 & -1 & \dots & 0 \\ \vdots & & & & & \\ 1 & 0 & 0 & 0 & \dots & -1 \end{bmatrix} = \left[C_m \vdots -I_m \right] \tag{22}$$

Then

$$TT^T = \begin{bmatrix} 2 & 1 & 1 & \dots & 1 \\ 1 & 2 & 1 & \dots & 1 \\ 1 & 1 & 2 & \dots & 1 \\ \vdots & \vdots & \vdots & & \\ 1 & 1 & 1 & \dots & 2 \end{bmatrix}$$

$$= I_m + C_m C_m^T \tag{23}$$

where C_m is an m vector, distinct from $C(= C_n)$, which is an n vector. The inverse of Eq. (23) is

$$\left(TT^T\right)^{-1} = I_m - \frac{1}{1+m} C_m C_m^T \tag{24}$$

Then, by using the partitioned form of T, from Eq. (22), it follows after some computation that

$$T^T(TT^T)T = \begin{bmatrix} 1 & 0 \\ 0 & I_m \end{bmatrix} - \frac{1}{1+m} \begin{bmatrix} 1 & C_m^T \\ C_m & C_m C_m^T \end{bmatrix}$$

$$= I_n - \frac{1}{n} C_n C_n^T \tag{25}$$

where the last step follows from the previously noted equality, $m = n-1$. Hence, $\overline{W} \equiv W$ and the estimates of Eqs. (20) and (16) are identical, with error-covariance matrices

$$\Lambda_{\hat{x}} = \sigma_\epsilon^2 \left[A^T\left(I - \frac{1}{n} CC^T\right)A\right]^{-1}$$

$$= \sigma_\epsilon^2 \left[\sum_{i=1}^{n} A_i^T A_i - \frac{1}{n}\left(\sum_{i=1}^{n} A_i^T\right)\left(\sum_{i=1}^{n} A_i\right)\right]^{-1} \tag{26}$$

where A_i is the i^{th} row of A, corresponding to the i^{th} measurement y_i.

Of further interest is the second term of the estimates Eq. (20) or (17)

$$A^T W y = \frac{1}{\sigma_\epsilon^2} A^T \left(I - \frac{1}{n} C C^T \right) y$$

$$= \frac{1}{\sigma_\epsilon^2} \left[\left(\sum_{i=1}^{n} A_i^T y_i \right) - \frac{1}{n} \left(\sum_{i=1}^{n} A_i^T \right) \left(\sum_{i=1}^{n} y_i \right) \right]$$

$$= \frac{1}{\sigma_\epsilon^2} \sum_{i=1}^{n} A_i^T \left(y_i - \frac{1}{n} \sum_{k=1}^{n} y_k \right) \tag{27}$$

This shows that either scheme uses a kind of weighted difference, where the average of all of the measurements is subtracted from each measurement y_i.

2. 5. 3. 3 Suboptimal Weighting of Range-Difference Measurements

A third possible estimate of x offers advantages from a data-processing point of view, namely,

$$\hat{x}_2 = \left(A^T T^T T A \right)^{-1} A^T T^T z \tag{28}$$

This estimate would be minimum variance if the range-difference errors were uncorrelated. Taking the correlations into account, however, the covariance matrix of this estimate becomes

$$\Lambda_{x_2} = \sigma_\epsilon^2 \left(A^T T^T T A \right)^{-1} A^T T^T T T^T T A \left(A^T T^T T A \right)^{-1} \tag{29}$$

In general, different choices of T can be expected to give different accuracies. The case considered in Eq. (22) can, however, be computed explicitly. In that case

$$A^T T^T = \left(A_1^T - A_2, A_1^T - A_3, \ldots, A_1^T - A_n\right) \tag{30}$$

and

$$A^T T^T C_m = \sum_{1=2}^{n} \left(A_1 - A_i\right)^T \tag{31}$$

So, by using Eq. (23) in the middle of Eq. (29), and applying the partitions of A and T, the covariance matrix Eq. (29) can be brought into the form

$$A_{x_2} = \left(Q^{-1} + Q^{-1} P Q^{-1}\right)\sigma_\epsilon^2 \tag{32}$$

where

$$Q = A^T T^T TA = \sum_{1=2}^{n} \left(A_1 - A_i\right)^T \left(A_1 - A_i\right)$$

$$= n A_1^T A_1 + \sum_{i=1}^{n} A_i^T A_i - A_1^T \sum_{i=1}^{n} A_i - \sum_{i=1}^{n} A_i^T A_1 \tag{33}$$

$$P = A^T T^T TT^T TA = \left[\sum_{i=2}^{n} \left(A_1 - A_i\right)^T\right]\left[\sum_{i=2}^{n} \left(A_1 - A_i\right)\right]$$

$$= n^2 A_1^T A_1 + \left(\sum_{i=1}^{n} A_i^T\right)\left(\sum_{i=1}^{n} A_i\right) - nA_1^T \sum_{i=1}^{n} A_i - n\sum_{i=1}^{n} A_i^T A_1 \tag{34}$$

These formulas can be evaluated and the result compared with Eq. (26) to determine the penalty associated with the suboptimal estimate.

2.5.3.4 Summary

It has been shown that the use of range-difference measurements with optimum weighting to account for correlation is equivalent to the direct application of the heavily biased psuedo-range measurement to solve for the position and the bias. The latter method is recommended, since it is more convenient to implement with the Kalman filter proposed for the user computer. When less accuracy is required, the correlations can be ignored and range differences processed according to Eq. (29). In that case, the accuracy of the estimate can be assessed by means of Eqs. (32) through (34).

2.5.4 Effect of Increasing Minimum Elevation Angle

The navigation accuracies given in pars. 2.1.1 and 2.1.2 are based on a minimum user-to-satellite angle of 5^{o} above the horizon, as noted earlier. Since hardware considerations indicated that a value of 10^{o} or more might be more realistic, the effect of increasing the minimum elevation angle to 10^{o}, 20^{o}, and 30^{o} was investigated.

Results are shown in Figures 21, 22, and 23 for 10^{o}, 20^{o}, and 30^{o}, respectively. A comparison of the 10^{o} case (Figure 21) with the corresponding map of Figure 2 shows that system coverage is degraded. The areas of indeterminacy (0 or 2 satellites visible) extend over some areas of interest, and a single failed satellite would make the system of questionable value above 50^{o} latitude at certain times of the day.

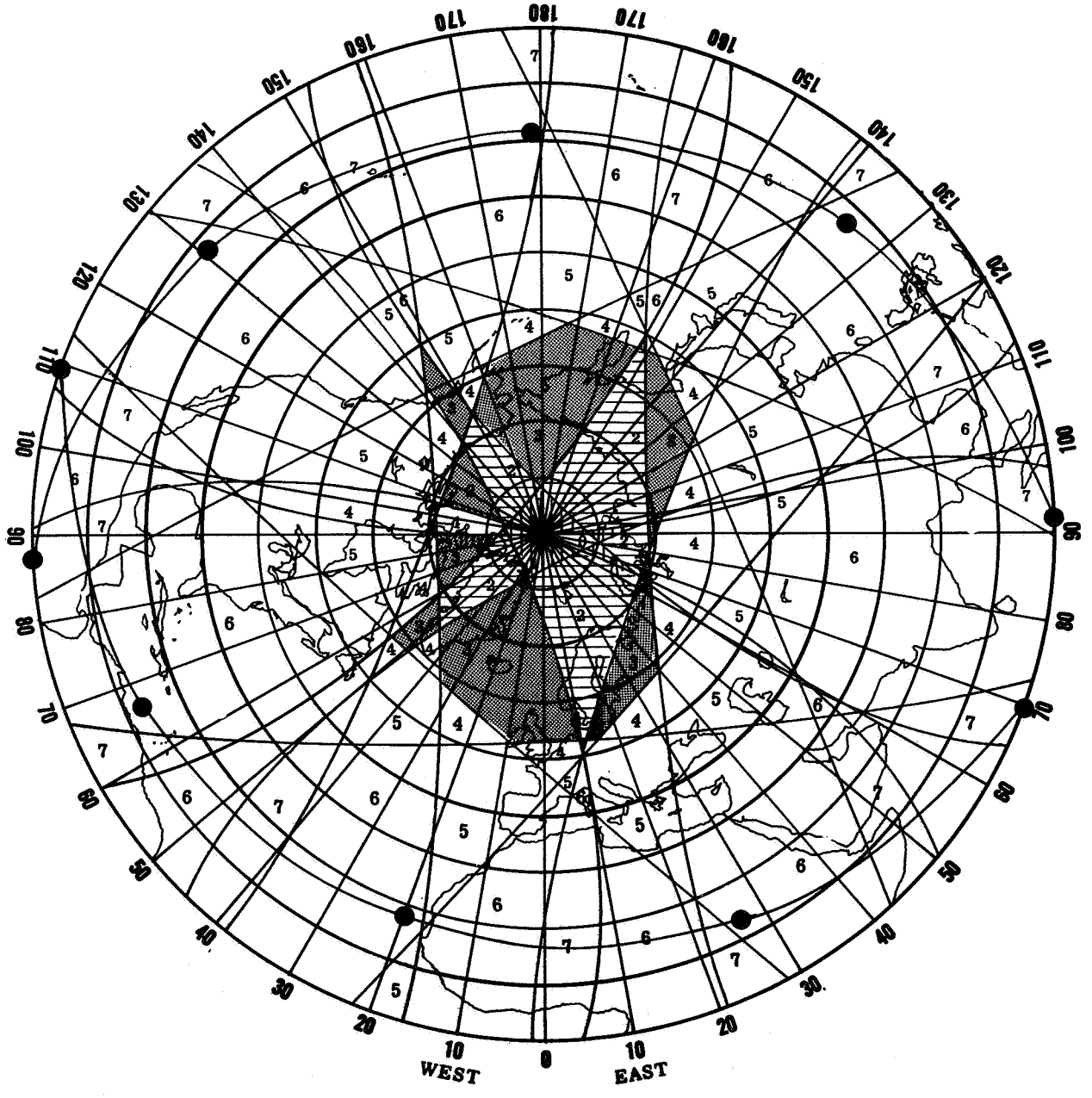

Figure 21. Worldwide System Coverage at T_0 With 10° Minimum Incidence Angle (Numbers Denote Satellites Visible)

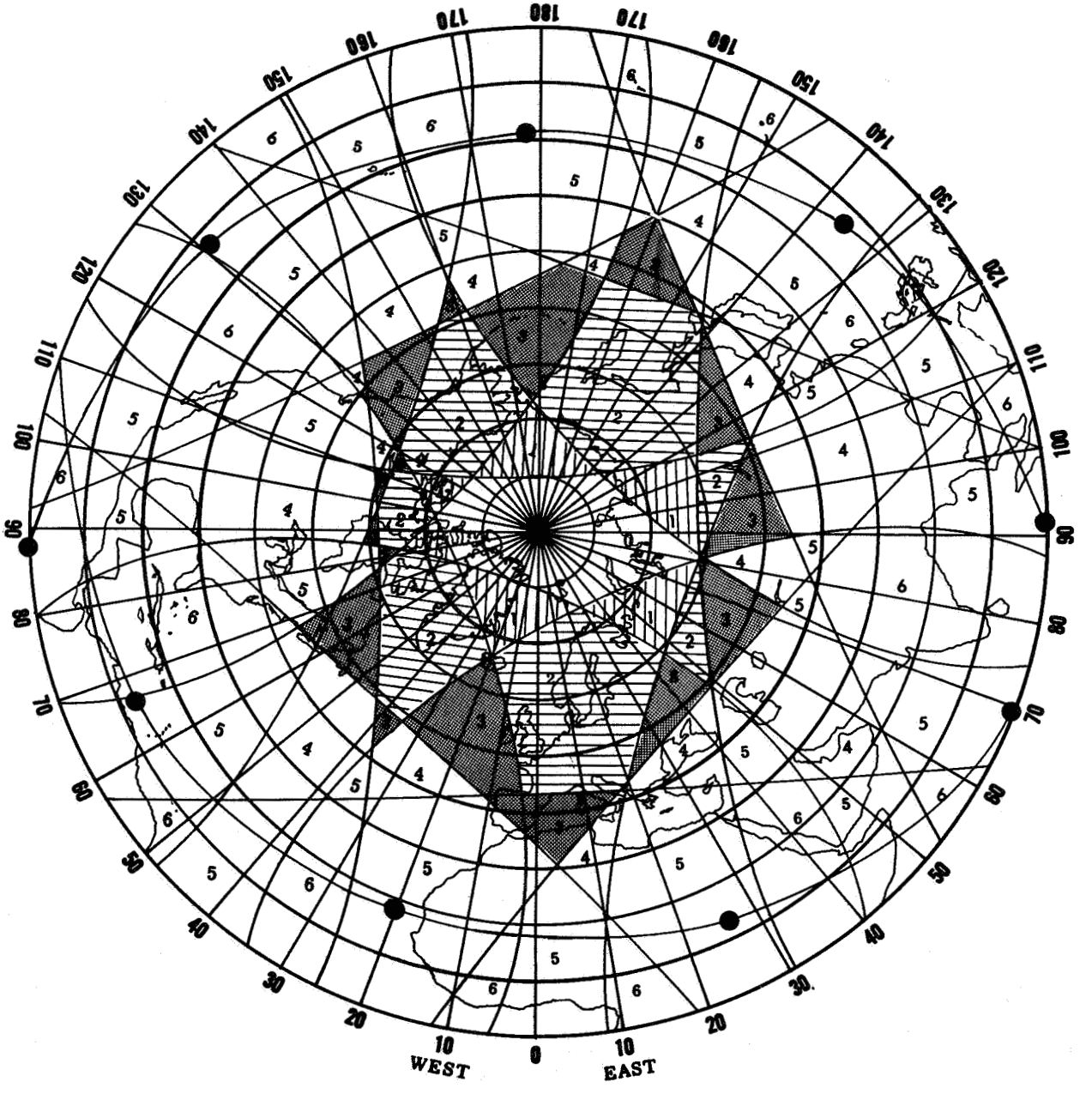

Figure 22. Worldwide System Coverage at T_0 With 20° Minimum Incidence Angle (Numbers Denote Satellites Visible)

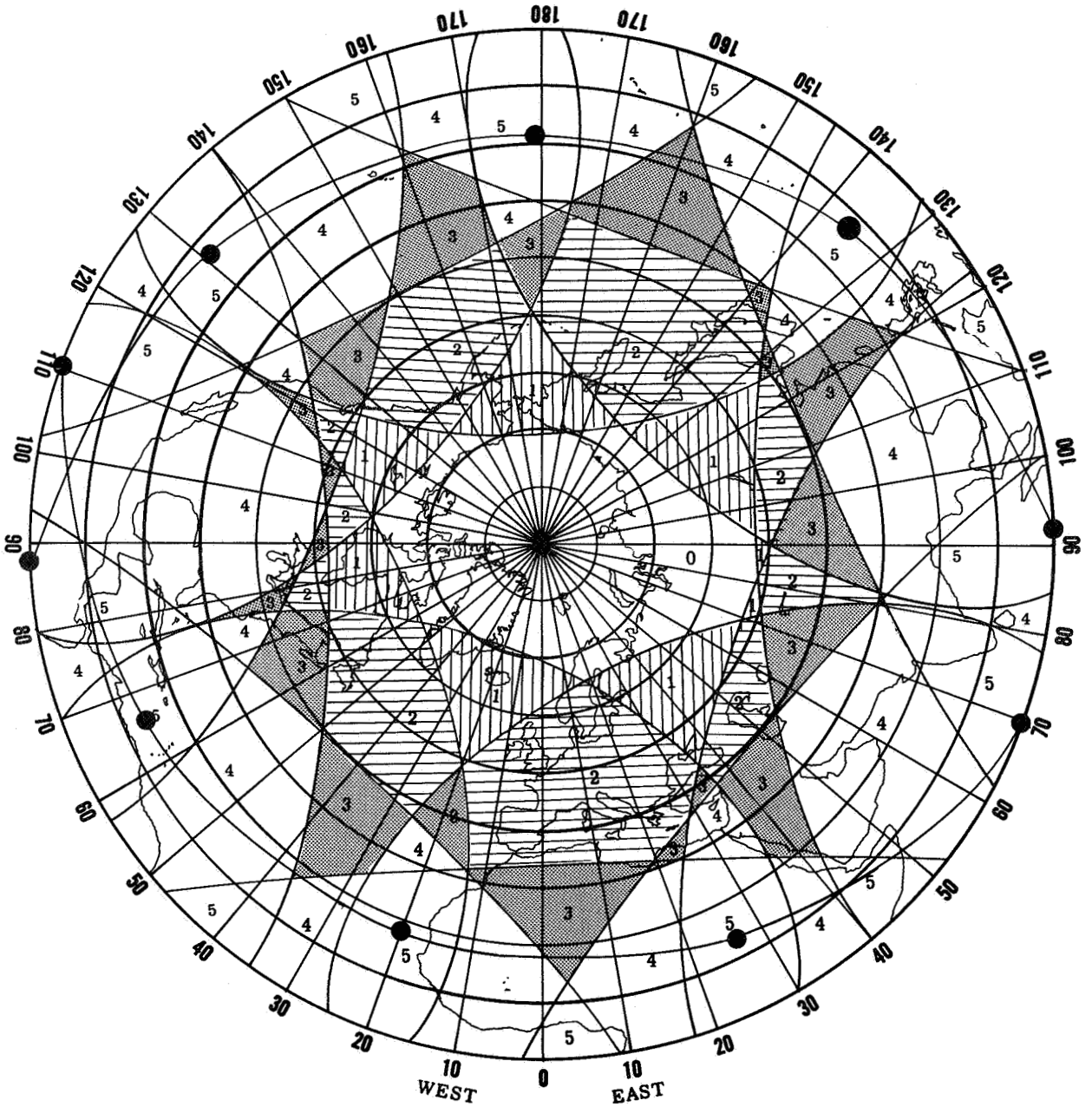

Figure 23. Worldwide System Coverage at T_0 With 30° Minimum Incidence Angle (Numbers Denote Satellites Visible)

3. NAVIGATION EQUATIONS

The computations described in the following sections must be performed for a user to determine his position, and possibly his velocity, from satellite observations. The four classes of user considered (three with standard ephemeris data, one with extra data) are the following: 1) a relatively sophisticated user, such as a supersonic transport, desiring maximum accuracy; 2) a user with somewhat more limited computational facilities than the SST, but who nevertheless requires a reasonably high degree of accuracy; 3) a simplest class of user, who will use charts and make hand calculations to compute his position to within nominal accuracy requirements, and 4) user who is provided additional data to make his computations near-trivial.

Two kinds of constraints must be satisfied by an effective set of user equations: computational requirements must be such that 1) the computations can be performed by a reasonably small computer; 2) the estimates produced by them can achieve the desired degree of accuracy. The equations presented here consequently serve as inputs to two separate studies: 1) determination of the computer size necessary for actual implementation, and 2) analysis of the estimation accuracy of the filter equations.

3.1 THE KALMAN FILTER

The Kalman filter permits sequential computation of a minimum-variance estimate of the state of a linear, discrete-time system excited by a Gaussian white-noise random sequence. This filter has the added advantage that during the process of computing the estimate, it generates the covariance matrix of the estimation error.*

If it is desired to estimate the state of a system described by nonlinear difference equations, the Kalman filter may still be used if sufficiently good linear approximations to the nonlinear equations can be found.

*Several programs used in the error analysis portion of this study use the better known batch processing techniques known as weighted-least-squares. The prime advantage of batch processing is that it permits analysis of the effect of errors in parameters which are not estimated. For example, a user will not estimate the satellite position, but errors in these positions are important. While these effects can also be treated in the Kalman filter program, the method is cumbersome and somewhat inefficient with respect to computer time. The results are, of course, independent of whether a sequential or batch processing algorithim is used.

This is usually done by expanding the system equations at some sampling instant about the state estimate at the previous sampling instant and neglecting second and higher order terms. The Kalman filter equations presented here have been linearized in this manner. Since the derivation of these equations appears in many places in the technical literature, it will not be reproduced here.

The system whose state it is desired to estimate is described by the difference equations:

$$\underline{x}\,(n+1) = \underline{f}\left(\underline{x}(n)\right) + \underline{z}(n)$$

$$\underline{y}\,(n) = \underline{g}\left(\underline{x}(n)\right) + \underline{w}(n)$$

where $\underline{x}(n)$ and $\underline{y}(n)$ are the dynamic state and measurement vectors with n_x and n_y components, respectively, $\underline{f}(\cdot)$ and $\underline{g}(\cdot)$ are n_x and n_y vector functions of $\underline{x}$, and $\underline{z}(n)$ and $\underline{w}(n)$ are zero-mean random vectors with covariance matrices:

$$E\left|\underline{z}(n)\,\underline{z}^T(m)\right| = Z(n)\,\delta_{mn}$$

$$E\left|\underline{w}(n)\,\underline{w}^T(m)\right| = W(n)\,\delta_{mn}$$

where δ_{mn} is the Kronecker delta.

Define the $n_x x n_x$ matrix U by:

$$U = \left[\frac{\partial f_i}{\partial x_j}\right]$$

and the $n_y x n_x$ matrix M by:

$$M = \left[\frac{\partial g_i}{\partial x_j}\right]$$

where f_i, x_i and g_i are the i^{th} components of $\underline{f}$, $\underline{x}$ and $\underline{g}$, respectively.

We denote the estimate of the state at the n^{th} sampling instant before the measurement is processed by $\underline{\hat{x}}(n)$, and its error-covariance matrix by $J(n)$. The estimate after the n^{th} measurement is processed is denoted by $\underline{\hat{x}}(n^+)$, and the corresponding error-covariance matrix by $J(n^+)$.

The estimate error-covariance matrix is first propagated from the n^{th} to the $(n+1)^{th}$ sampling instant by:

$$J(n+1) = U\left(\underline{\hat{x}}(n^+)\right) J(n^+) U^T \left(\underline{\hat{x}}(n^+)\right) + Z(n)$$

The estimate is propagated by:

$$\underline{\hat{x}}(n+1) = \underline{f}\left(\underline{\hat{x}}(n^+)\right)$$

The predicted observation is:

$$\underline{\hat{y}}(n+1) = \underline{g}\left(\underline{\hat{x}}(n+1)\right)$$

The residual between actual and predicted observations is:

$$\Delta(n+1) = \underline{y}(n+1) - \underline{\hat{y}}(n+1)$$

The filter gain (weighting matrix of the residual) is:

$$K(n+1) = J(n+1)\, M^T \left(\underline{\hat{x}}(n+1)\right) \left[M\left(\underline{\hat{x}}(n+1)\right) J(n+1) M^T \left(\underline{\hat{x}}(n+1)\right) + W(n+1) \right]^{-1}$$

The estimate is then updated by the $(n+1)^{th}$ measurement as:

$$\underline{\hat{x}}(n+1^+) = \underline{\hat{x}}(n+1) + K(n+1)\, \Delta(n+1)$$

Finally, the error-covariance matrix of the new estimate is obtained as:

$$J(n+1^+) = \left[I - K(n+1)\, M \left(\underline{\hat{x}}(n+1)\right) \right] J(n+1)$$

Estimates are computed sequentially in this manner; the filter is initialized with an a priori guess and an a priori error-covariance matrix.

We will now proceed to a description of the application of the equations written above to the determination of a NAVSTAR user's position and velocity.

3.2 EQUATIONS FOR HIGH ACCURACY

3.2.1 Data Received

The user receives three types of data:

1) At each 2-sec interval, a number R_i^* from which the range to the i^{th} satellite is to be determined, and a measurement $\dot{R}_i^*$ of the range rate between the user and the i^{th} satellite.

2) At intervals greater than 2 sec, numbers b_{io} and b_{i1}, which are to be used to correct the range measurement for oscillator drift in the i^{th} satellite.

3) At intervals greater than those for which oscillator drift corrections are sent, numbers $\Delta\rho_i$, $\Delta\lambda_i$ and Δi_i which are to be used to correct the ephemeris of the i^{th} satellite for drift from a circular orbit.

3.2.2 Sequence of Calculations

The measurements are to be processed in a simplified Kalman filter with peripheral logic. In general terms, the sequence of calculations shown in the flow chart of Figure 24 is the following:

1) Calculate the coordinates of the satellites in an earth-fixed rectangular system and the time derivatives of these coordinates from stored ephemeris data; the stored-ephemeris data are to be periodically corrected by the transmitted perturbations mentioned in (3) above.

2) Correct the measurement R_i^* for satellite-oscillator drift, and convert this corrected measurement into a range measurement.

3) Process the range measurement and the range-rate measurement in a Kalman filter, and obtain an estimate of the user position and velocity in an earth-fixed rectangular system.

4) Convert the estimate of (3) into an estimate of user latitude, longitude, altitude, position, and heading.

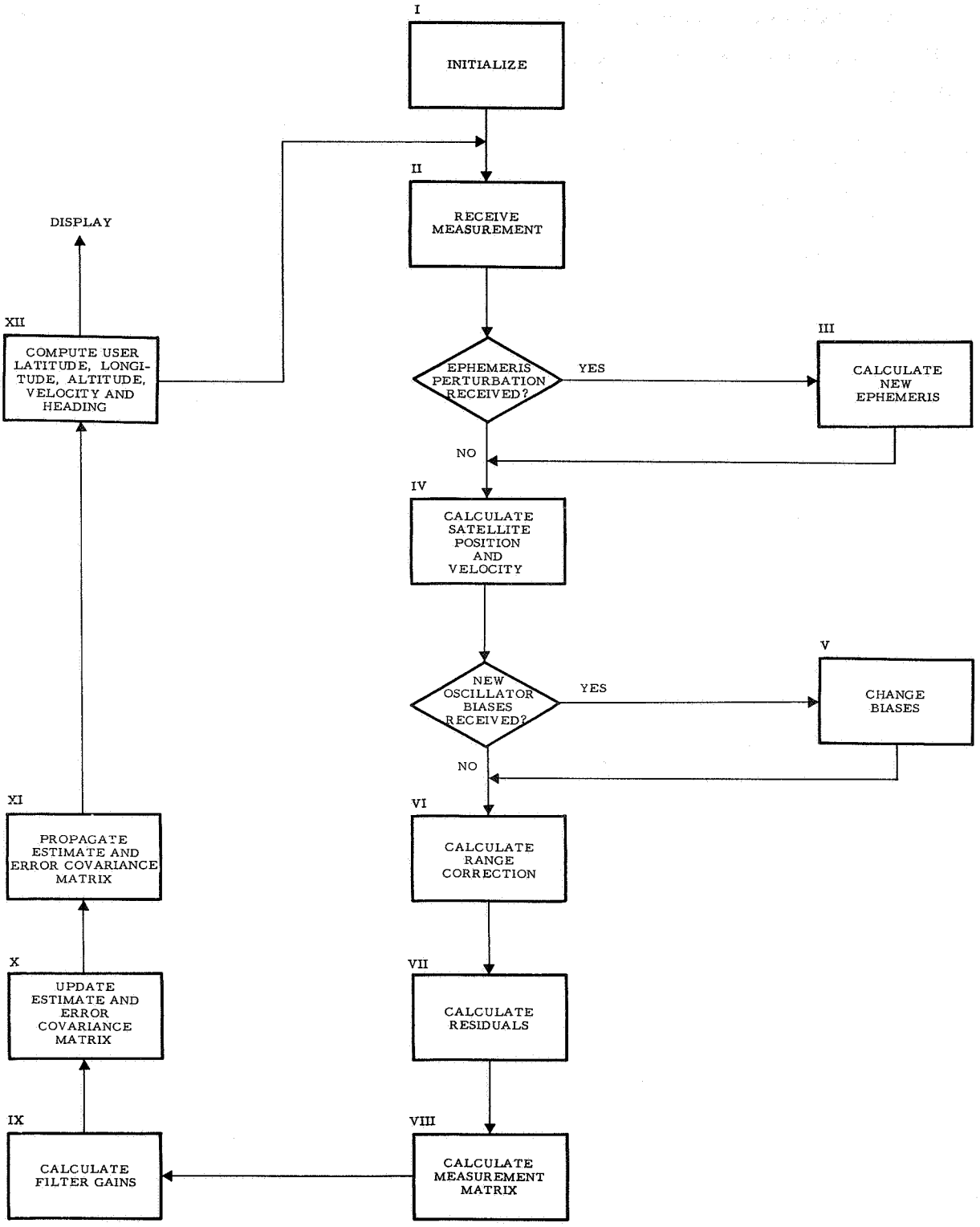

Figure 24. Filter Flow Chart for High Accuracy Navigation Equations

It should be emphasized at this point that we are processing a range measurement rather than a range-difference measurement. This introduces the necessity of solving for the bias B_o (caused by the difference in turn-on time between the satellite and user oscillators) but eliminates the following problems which are present when range differences are used.

1) The noise on the range-difference measurements is correlated between measurements; optimally processing noise of this nature makes the filter equations very cumbersome.

2) The bias B_o is actually not constant between measurements, but will change due to user oscillator drift; this introduces an error in the range differences. The nonconstancy of B_o can easily be handled when processing range measurements by the addition of state noise. (See par. 3.2.3).

3) Processing ranges eliminates the necessity of having to decide which satellite ranges should be differenced to produce the range differences.

As indicated above, the range (suitably modified) and range-rate measurements are to be processed in a filter of the type described in subsec. 3.2 in which the (nonlinear) system equations have been linearized. Of course, the equations are linearized first about the a priori estimate and for succeeding calculations about the current state estimate. The possibility thus arises that if the a priori state estimate is not sufficiently close to the actual state the linearization of the equations will not be valid and the equations should be relinearized two or more times. Alternatively, the estimate could simply be propagated to the next measurement interval and a new measurement processed; after one or two measurements, the estimate should be sufficiently close to the actual value so that the linearization will be valid. This is the procedure used to avoid the necessity of several filter iterations with the first measurement.

We will now proceed to an expanded description of the filter calculations, and a detailed explanation of each. The computations performed in each block are stated and explained in the order in which the blocks are numbered in the flow chart, Figure 24.

Symbols used in the equations are as follows:

$\hat{x}$, $\hat{y}$, $\hat{z}$	estimate of user's coordinates in earth-fixed Cartesian system (computed)
$\hat{\dot{x}}$, $\hat{\dot{y}}$, $\hat{\dot{z}}$	estimate of Cartesian components of user's velocity (computed)
X_i, Y_i, Z_i	Cartesian coordinates of i^{th} satellite (computed)
$\dot{X}_i$, $\dot{Y}_i$, $\dot{Z}_i$	velocity components of i^{th} satellite (computed)
λ	user's longitude (input or computed)
ϕ	user's latitude (input or computed)
v	user's velocity (input or computed)
h	user's altitude above sea level (input or computed)
ψ	user's heading east of north (input or computed)
J_u	user's a priori error-covariance matrix (input), or error-covariance matrix of current estimate (computed)

J_u is partitioned as:

$$J_u = \begin{bmatrix} J_p & J_{pv} \\ J_{pv}^T & J_v \end{bmatrix} ; \; J_p \text{ is } 4 \times 4, \; J_v \text{ is } 3 \times 3$$

R_e	radius of earth (input)
R_i^*	range measurement from user to i^{th} satellite (transmitted)
$\dot{R}_i^*$	range-rate measurement between user and i^{th} satellite (transmitted)
b_{i0}	bias on i^{th} satellite clock (transmitted)
b_{i1}	drift rate on i^{th} satellite clock (transmitted)
ρ_{oi}, λ_{oi}, i_{oi}, t_i	nominal ephemeris of i^{th} satellite (input)
$\Delta\rho_{oi}$, $\Delta\lambda_{oi}$, Δi_{oi}	perturbations to nominal ephemeris (transmitted)
t	current time (transmitted)
$R_i^{*'}$	range measurement corrected for satellite clock drift (computed)
$\hat{R}_i$	range computed from estimate of user position
B_o	bias in range measurement due to difference in initial phase between satellite and user clock (not known)
$\hat{B}_o$	estimate of B_o from user filter (computed)
$\hat{B}'_o$	estimate of B_o used to correct range measurement for 2,000-mile ambiguity (computed)
$R_i^{*''}$	range measurement corrected for satellite clock drift and 2,000-mile ambiguity (computed)
Δ_R	range measurement residual (computed)
$\hat{\dot{R}}_i$	range rate computed from estimate of satellite position and velocity

Δ_D range rate residual (computed)

M measurement matrix (computed)

M is partitioned as:

$$M = \begin{bmatrix} M_1 & 0 \\ 0 & M_2 \end{bmatrix}; \; M_1 \text{ is } 1 \times 4, \; M_2 \text{ is } 1 \times 3$$

W covariance matrix of observation noise (input)
W is 2 x 2, and written:

$$W = \begin{bmatrix} w_{11} & w_{12} \\ w_{12} & w_{22} \end{bmatrix}$$

K_{p1} weight of range residual in position estimate (4 x 1 matrix) (computed)

K_{p2} weight of range-rate residual in position estimate (3 x 1 matrix) (computed)

K_{v1} weight of range residual in velocity estimate (4 x 1 matrix) (computed)

K_{v2} weight of range-rate residual in velocity estimate (3 x 1 matrix) (computed)

$\underline{\hat{x}}$ or $\underline{\hat{x}}^+$ the 4 x 1 array:

$$\begin{bmatrix} \hat{x} \\ \hat{y} \\ \hat{z} \\ \hat{B}_o \end{bmatrix} \quad \text{or} \quad \begin{bmatrix} \hat{x}^+ \\ \hat{y}^+ \\ \hat{z}^+ \\ \hat{B}_o{}^+ \end{bmatrix} \quad \text{(computed)}$$

$\hat{\underline{x}}$ or $\hat{\underline{x}}^+$ the 3 x 1 array:

$$\begin{bmatrix} \hat{x} \\ \hat{y} \\ \hat{z} \end{bmatrix} \quad \text{or} \quad \begin{bmatrix} \hat{x}^+ \\ \hat{y}^+ \\ \hat{z}^+ \end{bmatrix} \quad \text{(computed)}$$

e quantity related to earth flattening (input)

a major axis of earth ellipsoid (input)

ω earth rotation rate (input)

$\hat{\underline{x}}$ estimate of $\underline{x}$ before a measurement is processed

$\hat{\underline{x}}^+$ estimate of $\underline{x}$ after a measurement is processed

I. INITIALIZE

INITIALIZE

Input: $\lambda, \phi, v, h, \psi$

Input: $$J_u = \begin{bmatrix} J_p & J_{pv} \\ J_{pv}^T & J_v \end{bmatrix}$$

Calculate A Priori Estimates:

$$\hat{x} = (R_e+h)\cos\phi\cos\lambda$$

$$\hat{y} = (R_e+h)\cos\phi\sin\lambda$$

$$\hat{z} = (R_e+h)\sin\phi$$

$$\hat{\dot{x}} = -v(\sin\phi\cos\lambda\cos\psi + \sin\lambda\sin\psi)$$

$$\hat{\dot{y}} = -v(\sin\phi\sin\lambda\cos\psi - \cos\lambda\sin\psi)$$

$$\hat{\dot{z}} = v(\cos\phi\cos\psi)$$

$$\hat{B}_o = 0 \text{ nmi}$$

In this box, the user calculates a priori estimates of his position and velocity in an earth-fixed rectangular system from an estimate of his latitude, longitude, altitude, mean-earth radius, velocity, and heading east of north. The quantities $\hat{x}$, $\hat{y}$, and $\hat{z}$ will be used in Block VI to aid in the resolution of range ambiguity.

The user also inputs an initial error-covariance matrix J_u.

$$\text{Letting } \underline{\hat{x}} = \begin{bmatrix} \hat{x} \\ \hat{y} \\ \hat{z} \\ \hat{B}_o \end{bmatrix} \qquad \text{and} \qquad \underline{\hat{\dot{x}}} = \begin{bmatrix} \hat{\dot{x}} \\ \hat{\dot{y}} \\ \hat{\dot{z}} \end{bmatrix}$$

then

$$J_p = E\left|\underline{\hat{x}}\,\underline{\hat{x}}^T\right|$$

$$J_{pv} = E\left|\underline{\hat{x}}\,\underline{\hat{\dot{x}}}^T\right|$$

$$J_v = E\left|\underline{\hat{\dot{x}}}\,\underline{\hat{\dot{x}}}^T\right|$$

This matrix can be stored permanently in the user's computer and need not be input each time the filter is initialized.

II. RECEIVE MEASUREMENT

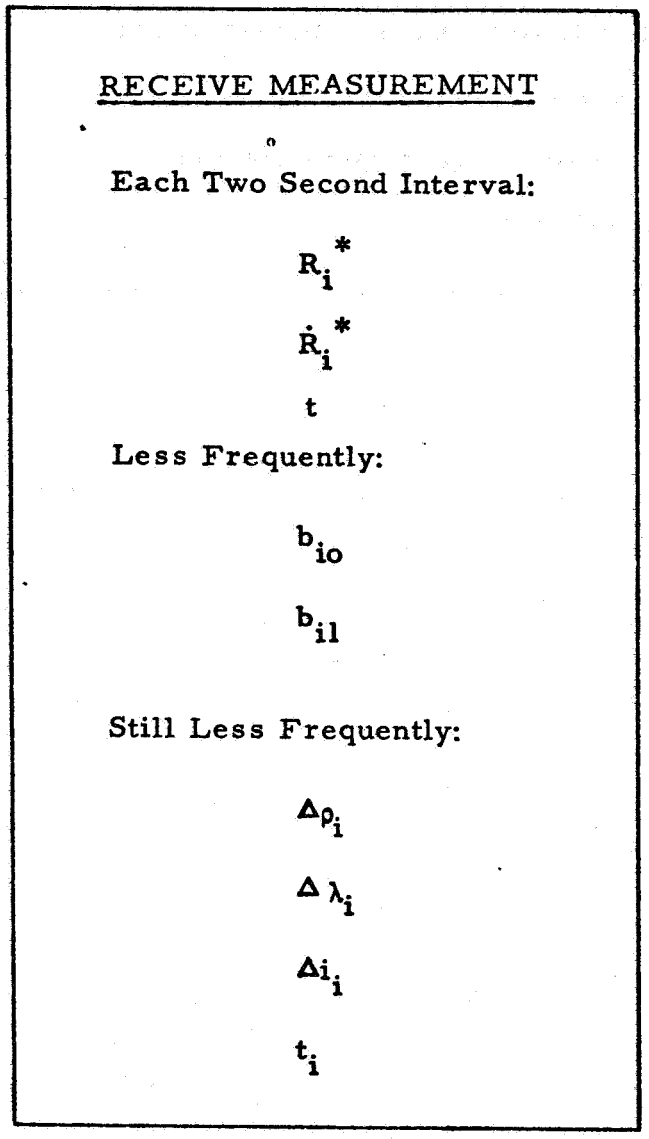

Every 2 sec the user receives a range measurement R_i^*. (The subscript denotes the range and range rate to the i^{th} satellite).

The measurement R_i^* is related to the range R_i as follows:

$$0 \leq R_i^* \leq 2,000$$

$$R_i^* = R_i + B_o + \Delta_i + w_i - 2K_i \times 1,000.$$

Here,

R_i = actual range from user to i^{th} satellite

B_o = bias due to difference in turn-on time

Δ_i = error due to satellite oscillator drift

w_i = white noise on range measurement

K_i = a positive integer

The modified measurement we wish to process in the filter is:

$$R_i^{*''} = R_i + B_o + w_i$$

To obtain $R_i^{*''}$, we must correct R_i^* for the error due to satellite drift (Block VIII), and determine the integer K_i (Block IX).

At intervals greater than 2 sec, numbers b_{io} and b_{il} are received which represent a bias and drift rate on the i^{th} satellite oscillator respectively and are to be used to correct for the error Δ_i.

At still greater intervals, numbers $\Delta\rho_i$, $\Delta\lambda_i$, Δi_i are received which are perturbations to be applied to the nominal ephemeris data of the i^{th} satellite.

III and IV. CORRECT EPHEMERIS AND CALCULATE SATELLITE POSITION

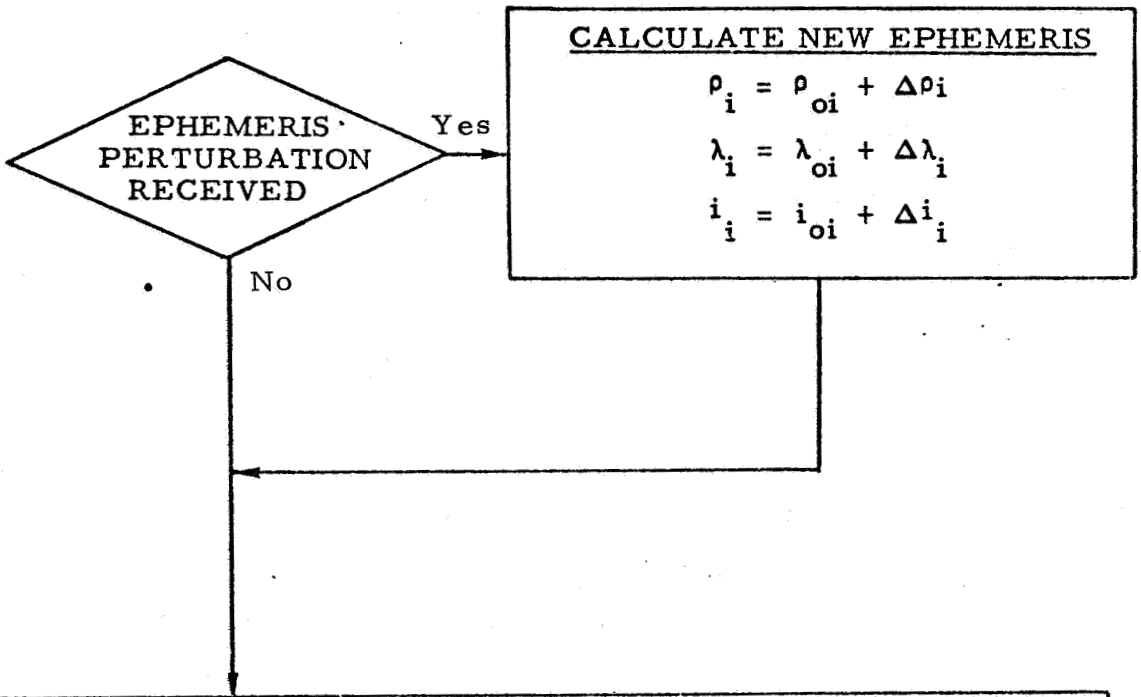

CALCULATE SATELLITE POSITION AND VELOCITY

$$X_i = \frac{1}{2}\rho_i\left[(1 + \cos i_i)\cos\lambda_i + (1 - \cos i_i)\cos(2\omega\tau_i - \lambda_i)\right]$$

$$Y_i = \frac{1}{2}\rho_i\left[(1 + \cos i_i)\sin\lambda_i + (1 - \cos i_i)\sin(2\omega\tau_i - \lambda_i)\right]$$

$$Z_i = \rho_i \sin i_i \sin\omega\tau_i$$

$$\dot{X}_i = -\omega\rho_i(1 - \cos i_i)\sin(2\omega\tau_i - \lambda_i)$$

$$\dot{Y}_i = \omega\rho_i(1 - \cos i_i)\cos(2\omega\tau_i - \lambda_i)$$

$$\dot{Z}_i = \omega\rho_i \sin i_i \cos\omega\tau_i$$

$$(\tau_i = t - t_i)$$

The perturbations received and their use to correct the ephemeris data are shown in the "Calculate New Ephemeris" block.

The satellite position and velocity are then calculated in an earth-fixed coordinate system (with X, Y axes in the equatorial plane with X axis at zero longitude and positive Z axis pointing north). The present time t is transmitted with the range and range-rate measurements.

These calculations assume a nominal circular orbit. The effects of this approximation on accuracy have not yet been assessed. However, the necessary analysis has been developed and is presented in app. L. Numerical results should be obtained in a future study.

V and VI. CHANGE BIASES AND CALCULATE RANGE CORRECTION

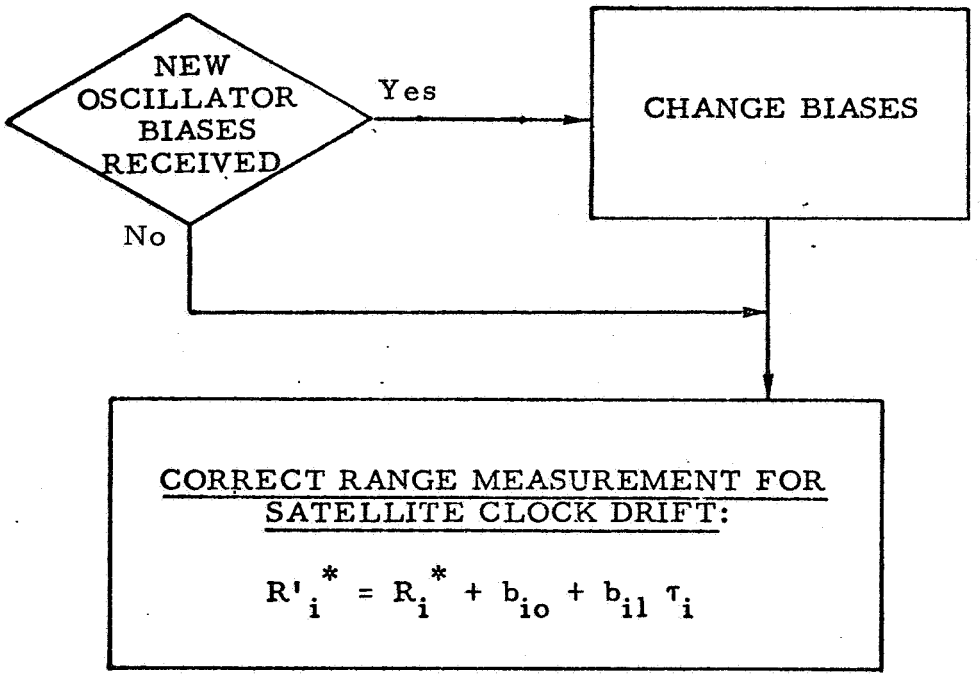

The measurement is next corrected for the error caused by drift in the i^{th} satellite oscillator. The most recently transmitted drift bias b_{io} and drift rate b_{il} are used for this purpose.

VII. CALCULATE RESIDUALS

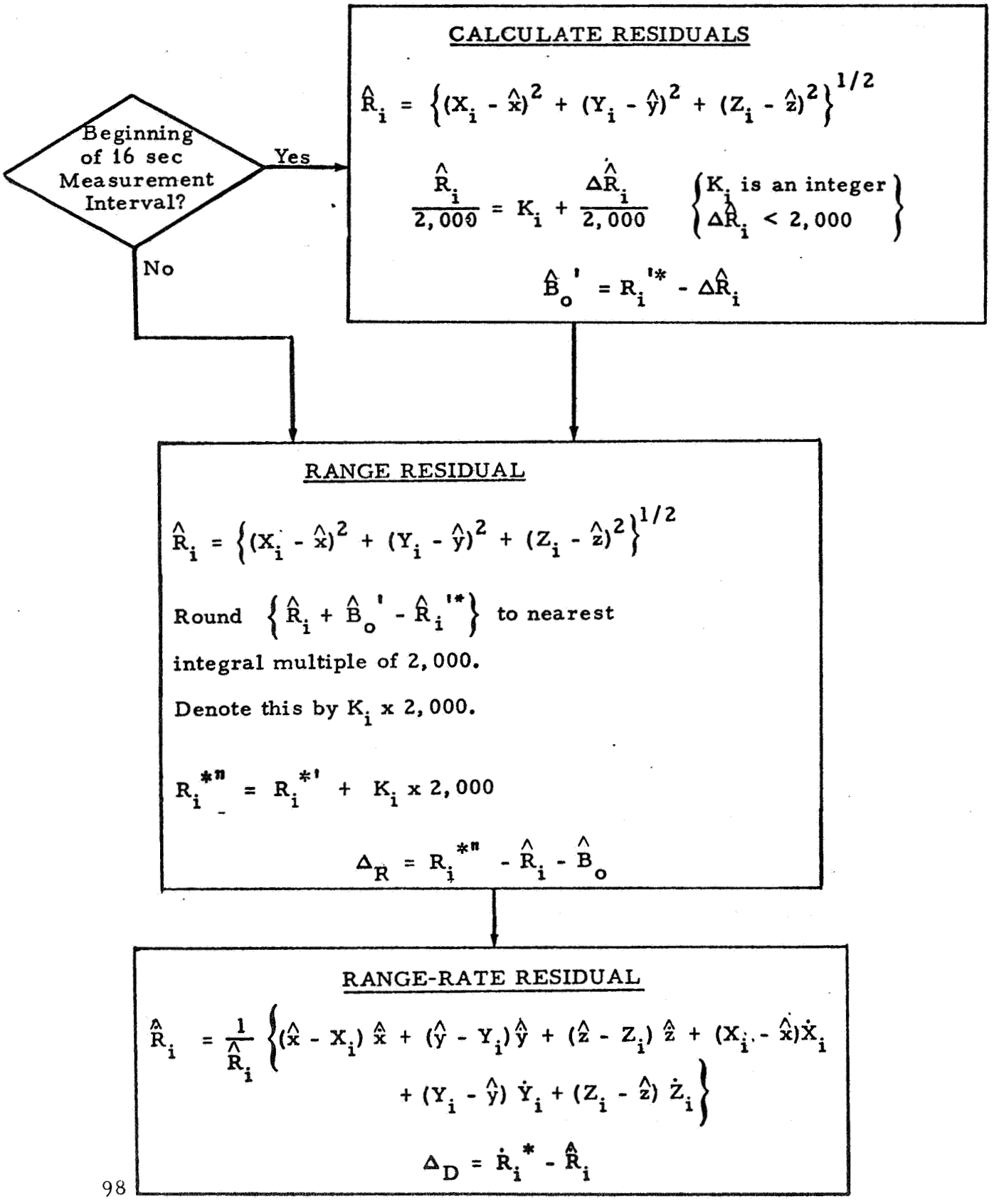

VIII and IX. MEASUREMENT MATRIX AND FILTER GAINS

CALCULATION OF MEASUREMENT MATRIX

Let: $$M_1 = \left[\frac{\hat{x} - X_I}{R_i} , \frac{\hat{y} - Y_I}{R_i} , \frac{\hat{z} - Z_I}{R_i} , 1 \right]$$

Let: $$M_2 = \left[\frac{\hat{x} - X_I}{\hat{R}_i} , \frac{\hat{y} - Y_I}{\hat{R}_i} , \frac{\hat{z} - Z_I}{\hat{R}_i} \right]$$

CALCULATION OF FILTER GAINS

Let: $$b_{11} = M_1 J_p M_1^T + w_{11}$$

Let: $$b_{12} = M_2 J_{pv}^T M_1^T + w_{12}$$

Let: $$b_{22} = M_2 J_v M_2^T + w_{22}$$

Let B = $$\begin{bmatrix} b_{11} & b_{12} \\ b_{12} & b_{22} \end{bmatrix}$$

Invert B: Let B^{-1} = $$\begin{bmatrix} B_{11} & B_{12} \\ B_{12} & B_{22} \end{bmatrix}$$

Let: $$K_{p1} = J_p M_1^T B_{11} + J_{pv} M_2^T B_{12}$$

Let: $$K_{p2} = J_p M_1^T B_{12} + J_{pv} M_2^T B_{22}$$

Let: $$K_{v1} = J_{pv}^T M_1^T B_{11} + J_v M_2^T B_{12}$$

Let: $$K_{v2} = J_{pv}^T M_1^T B_{12} + J_v M_2^T B_{22}$$

The calculations for the filter equations are performed in blocks VII through XI, beginning with the calculation of the range and range-rate residual. The first operation, shown in the "Calculate Residuals" box, is to correct the measurement $R_i^{*'}$ for range ambiguity (justification for this correction is given in app. M). It is assumed that the bias B_o will be approximately constant over the 16-sec measuring interval. At the beginning of the interval, an estimate $\hat{B}_o'$ is calculated from the first-range measurement (say, from the i^{th} satellite) by the three steps shown. The estimate is used throughout the 16-sec interval to correct the range measurements for the 2000-mi ambiguity. The range and range-rate residuals are then calculated as shown.

The range and Doppler measurements are processed simultaneously, since the observation noise on each (from a given satellite) will usually be correlated. The measurement matrix M has the form:

$$M = \begin{bmatrix} \frac{\partial R_i^{*''}}{\partial x} & \frac{\partial R_i^{*''}}{\partial y} & \frac{\partial R_i^{*''}}{\partial z} & \frac{\partial R_i^{*''}}{\partial B_o} & \frac{\partial R_i^{*''}}{\partial \dot{x}} & \frac{\partial R_i^{*''}}{\partial \dot{y}} & \frac{\partial R_i^{*''}}{\partial \dot{z}} \\ \frac{\partial \dot{R}_i^{*}}{\partial x} & \frac{\partial \dot{R}_i^{*}}{\partial y} & \frac{\partial \dot{R}_i^{*}}{\partial z} & \frac{\partial \dot{R}_i^{*}}{\partial B_o} & \frac{\partial \dot{R}_i^{*}}{\partial \dot{x}} & \frac{\partial \dot{R}_i^{*}}{\partial \dot{y}} & \frac{\partial \dot{R}_i^{*}}{\partial \dot{z}} \end{bmatrix}$$

If we assume

$$\frac{\partial \dot{R}^*}{\partial x} = \frac{\partial \dot{R}^*}{\partial y} = \frac{\partial \dot{R}^*}{\partial z} = 0,$$ then M has the block diagonal form

$$M = \begin{bmatrix} M_1 & 0 \\ 0 & M_2 \end{bmatrix}$$

with M_1 and M_2 as shown in the upper box.

X and XI. UPDATE ESTIMATE AND ERROR-COVARIANCE MATRIX, PROPAGATE ESTIMATE AND MATRIX

ESTIMATE AND ERROR COVARIANCE MATRIX UPDATE

Estimate Update:

$$\hat{x}^{+} = \hat{x} + K_{p1}\,\Delta_R + K_{p2}\,\Delta_D$$

$$\hat{\dot{x}}^{+} = \hat{\dot{x}} + K_{v1}\,\Delta_R + K_{v2}\,\Delta_D$$

Error-Covariance Matrix Update:

$$J_p^{+} = [I - K_{p1}\,M_1]\,J_p - K_{p2}\,M_2\,J_{pv}^{T}$$

$$J_{pv}^{+} = [I - K_{p1}\,M_1]\,J_{pv} - K_{p2}\,M_2\,J_v$$

$$J_v^{+} = [I - K_{v2}\,M_2]\,J_v - K_{v1}\,M_1\,J_{pv}$$

ESTIMATE AND ERROR COVARIANCE MATRIX PROPAGATION

Estimate Propagation:

$$\hat{x} = \hat{x}^{+} + \hat{\dot{x}}\,\Delta t$$

$$\hat{y} = \hat{y}^{+} + \hat{\dot{y}}\,\Delta t$$

$$\hat{z} = \hat{z}^{+} + \hat{\dot{z}}\,\Delta t$$

(Δt = interval between measurements)

Error-Covariance Matrix Propagation:

$$\text{Let } K = \begin{bmatrix} 1 & 0 & 0 \\ 0 & 1 & 0 \\ 0 & 0 & 1 \\ 0 & 0 & 0 \end{bmatrix}.$$

$$J_p = J_p^{+} + (K J_{pv}^{+T} + J_{pv}^{+} K^{T})\,\Delta t + K J_v K^{T} \Delta t^2$$

$$J_{pv} = J_{pv}^{+} + K\,J_v^{+}\,\Delta t$$

$$J_v = J_v^{+}$$

The block diagonal form of M makes partitioned computations of the filter gain particularly easy. Recall that the optimal filter gain (weight to be applied to the residuals) is:

$$K = J_u M^T \left[M J_u M^T + W \right]^{-1}$$

If we let

$$B = \begin{bmatrix} b_{11} & b_{12} \\ b_{12} & b_{22} \end{bmatrix} = M J_u M^T + W,$$

then in terms of partitions of M and J_u, we have the results shown in the lower box.

The position and velocity estimates, before the current measurement is processed are combined with the range and range-rate residuals to produce the estimate update.

The error-covariance matrix of this updated estimate is

$$J_u^+ = \left[I - KM \right] J_u = \begin{bmatrix} J_p^+ & J_{pv}^+ \\ J_{pv}^{+T} & J_v \end{bmatrix}$$

In terms of the partitions of J_u, K and M, this has the form shown for the error-covariance matrix update.

Recalling that

$$\underline{x} = \begin{bmatrix} x \\ y \\ z \\ B_o \end{bmatrix}, \qquad \underline{\dot{x}} = \begin{bmatrix} \dot{x} \\ \dot{y} \\ \dot{z} \end{bmatrix}$$

and that the user is assumed to move in a straight line with constant velocity, the manner in which the position estimate propagates over the time interval between measurements is determined as follows:

Let

$$H = \begin{bmatrix} 1 & 0 & 0 \\ 0 & 1 & 0 \\ 0 & 0 & 1 \\ 0 & 0 & 0 \end{bmatrix}$$

Then

$$\underline{\hat{\hat{x}}} = \underline{\hat{\hat{x}}}^{+} + H^{T}\,\underline{\hat{\dot{x}}}^{+}\,\Delta t$$

where Δt = time interval between measurements

Of course,

$$\underline{\hat{\dot{x}}} = \underline{\hat{\dot{x}}}^{+}.$$

The error-covariance matrix propagates as:

$$J_u = \begin{bmatrix} J_p & J_{pv} \\ J_{pv}^{T} & J_v \end{bmatrix} = \begin{bmatrix} I & H\Delta t \\ O & I \end{bmatrix} J_u^{+} \begin{bmatrix} I & O \\ H^{T}\Delta t & I \end{bmatrix}$$

Formulas for the partitions are shown in the block.

XII. USER FIX AND HEADING CALCULATION

USER FIX AND HEADING CALCULATION

LONGITUDE:

$$\lambda = \tan^{-1}\left\{\frac{\hat{y}}{\hat{x}}\right\}$$

LATITUDE:

$$\text{Let } \phi_o = \tan^{-1}\left\{\frac{\hat{z}}{\sqrt{\hat{x}^2 + \hat{y}^2}}\right\}$$

$$\text{Let } \nu(\phi_o) = \frac{a}{\left[1 - e^2 \sin^2 \phi_o\right]^{1/2}}$$

$$\text{Let } f(\phi_o) = \frac{\cos \phi_o}{\sqrt{\hat{x}^2 + \hat{y}^2}} - \frac{\sin \phi_o}{\hat{z} + e^2 \nu(\phi_o) \sin \phi_o}$$

$$\text{Let } \phi_1' = \phi_o + \Delta\phi_o$$

COMPUTE $\nu(\phi_1')$, $f(\phi_1')$

$$\phi = \phi_o - \frac{f(\phi_1') - f(\phi_o)}{f(\phi_o)\ \Delta\phi_o}$$

ALTITUDE:

$$h = \frac{\hat{y}}{\cos \phi \sin \lambda} - \nu(\phi)$$

VELOCITY:

$$v = \sqrt{\hat{x}^2 + \hat{y}^2 + \hat{z}^2}$$

HEADING:

$$\psi = \cos^{-1}\left\{\frac{\hat{z}}{v \cos \phi}\right\}$$

When the user calculates his latitude, longitude, and altitude, significant errors can result if earth aspheroidicity is neglected.

The equations for the user's coordinates in an earth-fixed rectangular system with x and y axes in the equatorial plane and x axis at zero longitude, and with positive z axis coincident with the polar axis and in the direction of the north pole, are (Ref. 7)

$$x = (\nu(\phi) + h) \cos\phi \cos\lambda \tag{35}$$

$$y = (\nu(\phi) + h) \cos\phi \sin\lambda \tag{36}$$

$$z = \left[(1 - e^2)\,\nu(\phi) + h\right] \sin\phi \tag{37}$$

$$\nu(\phi) = \frac{a}{\left[1 - e^2 \sin^2\phi\right]^{1/2}}$$

Here,

a = major axis of earth ellipsoid

e = eccentricity of earth ellipsoid

h = altitude perpendicular to earth ellipsoid

ϕ = ellipsoidal latitude

λ = ellipsoidal (or geocentric) longitude

Eqs (35) and (36) are straightforwardly solved for λ as shown.

Eliminating λ from Eqs. (35) and (36), we get:

$$\sqrt{x^2 + y^2} = (\nu(\phi) + h) \cos\phi$$

Eliminating h from this and Eq. (37) gives:

$$\frac{\cos\phi}{\sqrt{x^2 + y^2}} - \frac{\sin\phi}{z + e^2\,\nu(\phi) \sin\phi} = 0.$$

This transcendental equation is solved recursively for ϕ. A first approximation is:

$$\phi_o = \tan^{-1}\left\{\frac{z}{\sqrt{x^2 + y^2}}\right\}$$

Letting

$$f(\phi) = \frac{\cos\phi}{\sqrt{x^2 + y^2}} - \frac{\sin\phi}{z + e^2\,\nu(\phi)\sin\phi}$$

and

$$\phi'_1 = \phi_o + \Delta\phi_o \text{ (where } \Delta\phi_o \text{ is an input constant),}$$

a second approximation is:

$$\phi_1 = \phi_o - \frac{f(\phi'_1) - f(\phi_o)}{f(\phi_o)\,\Delta\phi_o}$$

This should be sufficiently close to the true value. The user altitude is then obtained straightforwardly as indicated.

3.2.3 Remarks

The major simplifying assumptions that have been made in the development of these equations are:

1) Satellite coordinates and velocities computed from ephemeris data are correct

2) The state equations assume a particularly simple form: the bias B_o is constant, and the user moves with constant velocity during the 2 sec between measurements.

In addition, the measurement matrix has been simplified by neglecting the partial derivatives of the doppler measurement with respect to the user position coordinates.

Since fairly extensive satellite tracking facilities are available, assumption (1) is reasonably good. This will not necessarily be the case with assumption (2), since the user will invariably perform maneuvers of varying degrees of severity in the course of the flight. Also, the user clock will drift over long periods of time, so the bias B_o will not be constant. Each of these effects can be approximately accounted for by the addition of state noise on the user velocities and on the bias B_o. This prevents the filter from putting too much weight on a priori estimate which is erroneous because of incorrect modeling.

It should be pointed out that the equations presented here are intended for a user with considerable computational facilities and reasonably high accuracy demands. Substantial refinements would be necessary for a very high accuracy user (such as a tactical bomber), and simplifications can be made for a user with less stringent accuracy demands (such as an ocean liner). The following section presents equations for the latter case.

3.3 EQUATIONS FOR INTERMEDIATE ACCURACY

3.3.1 Discussion

The calculations for a set of filter equations which should satisfy the demands of a "simple user" are described here. A simple user is defined to be one who is moving fairly slowly (less than 30 mi/hr), has limited computational facilities, desires fixes relatively infrequently (no more often than every 15 min), requires no velocity estimate, but who, nevertheless, requires a resonably high degree of accuracy. This simple user is divided into two classes:

1) Three measurements are available
2) More than three measurements are available.

User 1) is further divided as:

1-a) The measurements consist of two range differences and altitude above mean sea level

1-b) The measurements consist of three range differences.

User 2) may or may not have altitude information. The simple user processes range differences rather than ranges. The consequences of this were discussed in par. 2.5.3.

The simple user makes the following basic assumptions:

1) The satellite positions, as computed from transmitted ephemeris data, are correct.

2) A suboptimal filter which considers the measurement noise negligible is sufficiently accurate.

In addition, an assumption is made regarding satellite motion over the time interval when the two (or three) range-difference measurements are obtained. Range measurements are received at separate time instants and differenced to determine the range-difference measurement to be processed; consequently, this difference corresponds to the range difference between satellites at two distinct time instants. It will be assumed that the motion of the satellites and user over the measurement interval is small, so that these measurements can be considered to have occurred

simultaneously. The range rate of a satellite, relative to a stationary user, is of the order of 200 ft/sec, hence, the above assumption will be reasonably good if measurements occurring 2 sec apart are differenced.

An additional motivation for keeping the time interval small over which measurements are differenced is the following: the user oscillator will invariably drift, and this drift will be significant over long periods of time. If the time interval over which range measurements are differenced is too long, the user oscillator bias will not be completely cancelled in the differencing process and an erroneous range-difference measurement will result.

The measurements which the respective users thus process are the following:

User 1-a:

$$\Delta_{ij} = \sqrt{(x-X_i)^2 + (y-Y_i)^2 + (z-Z_i)^2} - \sqrt{(x-X_j)^2 + (y-Y_j)^2 + (z-Z_j)^2}$$

$$\Delta_{jk} = \sqrt{(x-X_j)^2 + (y-Y_j)^2 + (z-Z_j)^2} - \sqrt{(x-X_k)^2 + (y-Y_k)^2 + (z-Z_k)^2}$$

$$h = \sqrt{x^2 + y^2 + z^2} - R_e$$

User 1-b:

$$\Delta_{ij} = \sqrt{(x-X_i)^2 + (y-Y_i)^2 + (z-Z_i)^2} - \sqrt{(x-X_j)^2 + (y-Y_j)^2 + (z-Z_j)^2}$$

$$\Delta_{jk} = \sqrt{(x-X_j)^2 + (y-Y_i)^2 + (z-Z_k)^2} - \sqrt{(x-X_k)^2 + (y-Y_k)^2 + (z-Z_k)^2}$$

$$\Delta_{kl} = \sqrt{(x-X_k)^2 + (y-Y_k)^2 + (z-Z_k)^2} - \sqrt{(x-X_l)^2 = (y-Y_l)^2 + (z-Z_l)^2}$$

User 2:

- more than three range-difference measurements (of Type 1-b).

Each user will linearize these equations about some nominal value of x, y, z, and solve. The solution will be performed iteratively using the Kalman filter equations, since this both permits relinearization after each measurement is processed, and affords a very convenient way of processing the redundant data of User 2.

3.3.2 Sequence of Calculations

The sequence of calculations is shown in the flow chart of Figure 25. The following pages show the computations performed in each block, accompanied by discussion where appropriate.

I. INITIALIZE

INITIALIZE

Input λ, ϕ, h

(for User 1, h = 0; for User 2, h = Altimeter Reading)

Calculate A Priori Estimates

$$\hat{x} = (R_e + h) \cos \phi \cos \lambda$$

$$\hat{y} = (R_e + h) \cos \phi \sin \lambda$$

$$\hat{z} = (R_e + h) \sin \phi$$

The user inputs an a priori estimate of his latitude ϕ, longitude λ, and altitude h. User 1-a inputs h = 0, while Users 1-b and 2 input an altimeter reading if one is available. The a priori estimates of user position are then calculated as shown.

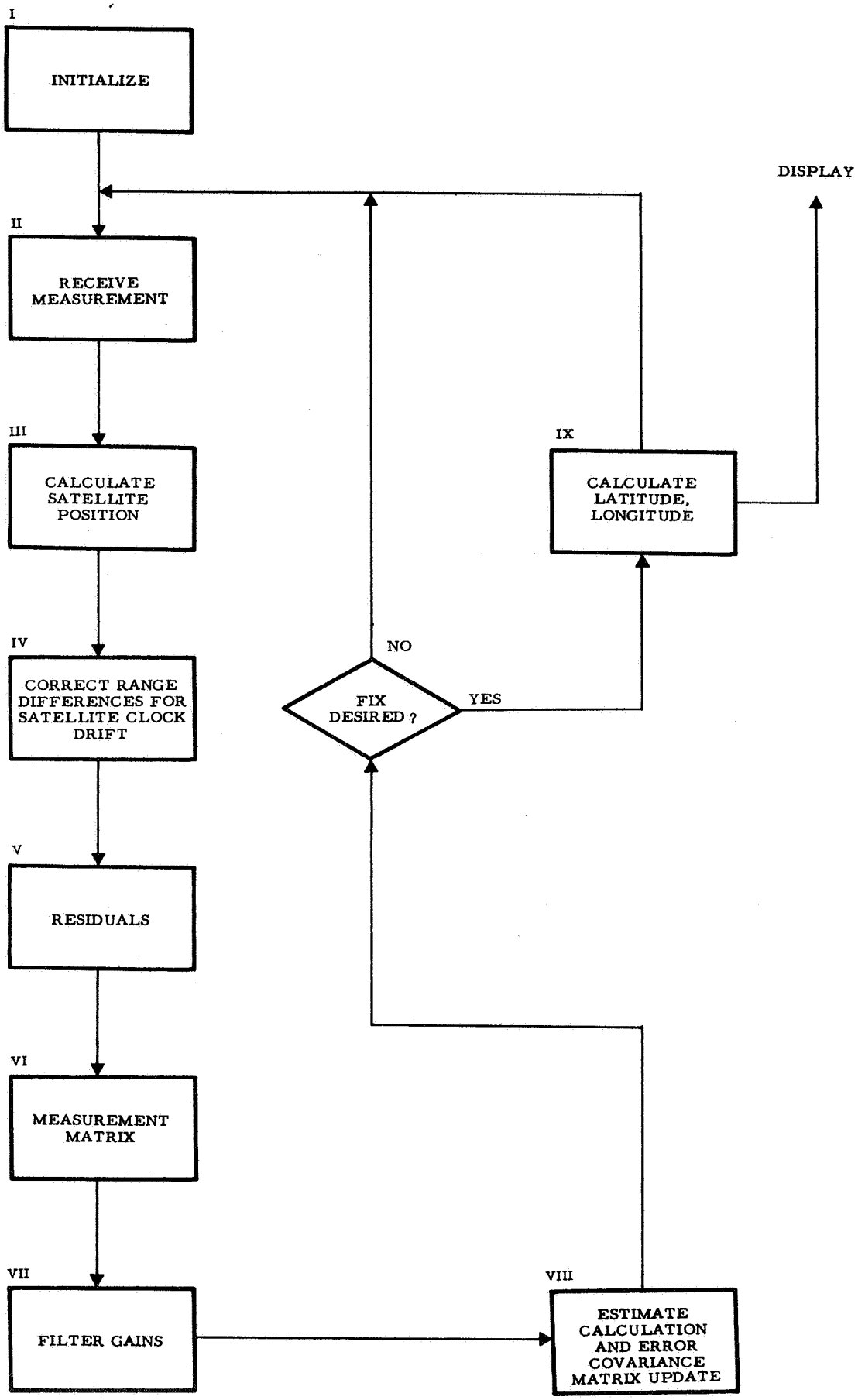

Figure 25. Flowchart for Intermediate Accuracy Navigation Equations

II. RECEIVE MEASUREMENT

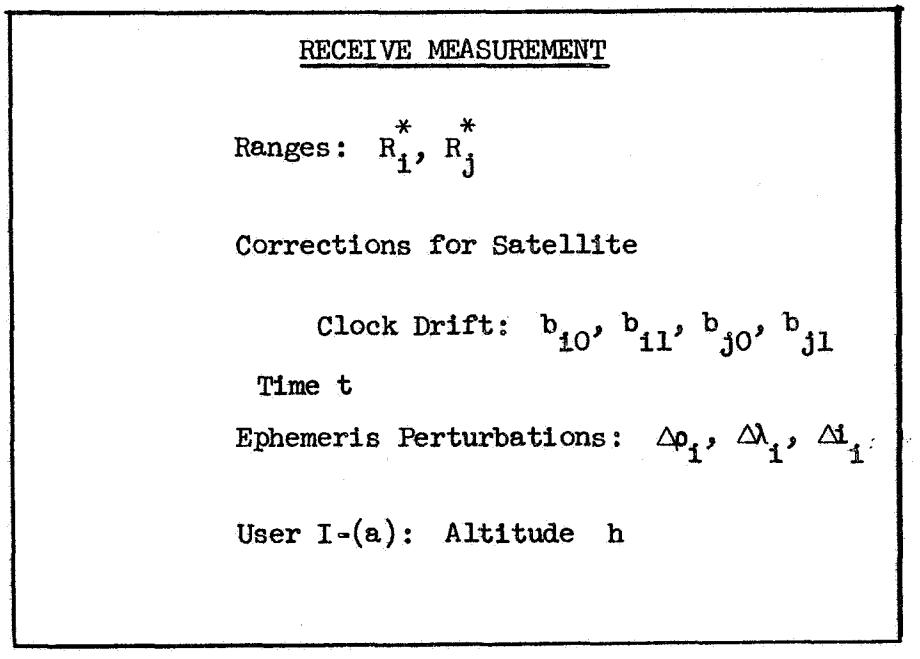

All users will receive range measurements and difference them; measurements received over consecutive time intervals should be differenced. User 1-a considers his altimeter reading as a measurement and processes it accordingly. In addition, users have stored biases and drift rates on all satellite clocks involved in the range-difference measurement. These are periodically retransmitted. At intervals, the user also receives corrections to the nominal stored ephemeris data.

III. CALCULATE SATELLITE POSITION

CALCULATE SATELLITE POSITION

Correct Ephemeris:

$$\rho_i = \rho_{0i} + \Delta\rho_i$$

$$\lambda_i = \lambda_{0i} + \Delta\lambda_i$$

$$i_i = i_{0i} + \Delta i_i$$

Calculate Satellite Position:

$$X_i = \frac{1}{2}\rho_i\left[(1+\cos i_i)\cos\lambda_i + (1-\cos i_i)\cos(2\omega\tau_i - \lambda_i)\right]$$

$$Y_i = \frac{1}{2}\rho_i\left[(1+\cos i_i)\sin\lambda_i + (1-\cos i_i)\sin(2\omega\tau_i - \lambda_i)\right]$$

$$Z_i = \rho_i \sin i_i \sin\omega\tau_i \qquad (\tau_i = t - t_i)$$

The first step in the estimate determination is the calculation of the positions of the satellites involved in the difference measurements, using the most recently corrected ephemeris data. The orbit parameters ρ_i, λ_i, and i_i are corrected if the corresponding perturbations have been received. For a range difference between satellite i and j, for example, the coordinates of the i^{th} satellite are calculated as shown, and those of the j_{th} satellite are determined in the same way.

IV. RANGE-DIFFERENCE COMPUTATION

COMPENSATE RANGE DIFFERENCE FOR SATELLITE OSCILLATOR DRIFT

$$\Delta = R_i^* + b_{i0} + b_{i1}\tau_i - R_j^* - b_{j0} - b_{j1}\tau_j$$

The range-difference measurement shown above is computed and corrected for the oscillator drift of satellites i and j.

V. RANGE-DIFFERENCE AMBIGUITY RESOLUTION AND RESIDUAL CALCULATION

RESIDUAL

$$\hat{R}_i - \hat{R}_j = \sqrt{(X_i - \hat{x})^2 + (Y_i - \hat{y})^2 + (Z_i - \hat{z})^2} - \sqrt{(X_j - \hat{x})^2 + (Y_j - \hat{y})^2 + (Z_j - \hat{z})^2}$$

Round $\hat{R}_i - \hat{R}_j - \Delta$ To Nearest Multiple of 2,000.

Call this K x 2,000:

$$\Delta_R = K \times 2{,}000 + \Delta - (\hat{R}_i - \hat{R}_j)$$

The corrected measurement Δ calculated in the previous box must still be adjusted for the range-difference ambiguity. This is done by first calculating a range difference $\hat{R}_i$ based on the a priori (or current) estimate of the user's position. The difference is then rounded and corrected for the 2000-mi ambiguity and the range-difference residual Δ_R is computed as shown. (See app. M for justification of this procedure.)

VI. MEASUREMENT MATRIX CALCULATION

MEASUREMENT MATRIX

$$M_i = \frac{1}{\hat{R}_i} [\hat{x} - X_i, \hat{y} - Y_i, \hat{z} - Z_i]$$

$$M_j = \frac{1}{\hat{R}_j} [\hat{x} - X_j, \hat{y} - Y_j, \hat{z} - Z_j]$$

$$M_{ij} = M_i - M_j$$

User 1 Processing Altitude

$$M_h = \frac{1}{\sqrt{\hat{x}^2 + \hat{y}^2 + \hat{z}^2}} \quad [\hat{x}, \hat{y}, \hat{z}]$$

For a range-difference measurement between the i^{th} and j^{th} satellites, the measurement matrix has the form $M_{ij} = M_i - M_j$. User 1-a processes his altimeter reading as a measurement, using the measurement matrix M_h shown in the box.

VII. FILTER GAIN CALCULATION

FILTER GAINS

$$K_{ij} = J M_{ij}^T [M_{ij} J M_{ij}^T]^{-1}$$

User 1-a Processing Altitude:

$$K_h = J M_h^T [M_h J M_h^T]^{-1}$$

The filter gains are the same as those which would be used for an optimal filter with no observation noise and have the form shown. When user 1-a precesses his altimeter reading, he uses a gain of K_h of the form shown.

VIII. ESTIMATE AND COVARIANCE MATRIX UPDATE

ESTIMATE AND COVARIANCE MATRIX UPDATE

$$\underline{\hat{x}}^+ = \underline{\hat{x}} + K_{ij} \Delta_R$$

For User 1-a: $\underline{\hat{x}}^+ = \underline{\hat{x}} + K_h \, h$

$$J^+ = [I - K_{ij} M_{ij}]J$$

User 1-a Processing Altitude:

$$J^+ = [I - K_h M_h]J$$

The updated estimates are calculated using the residuals and the gains as $\underline{\hat{x}}^+$ in the box for each range measurement and for user 1-a altitude measurement. The error-covariance matrices are then updated as shown for the range-difference and altitude measurements.

IX. USER FIX CALCULATION

USER FIX CALCULATION

LONGITUDE:

$$\lambda = \tan^{-1} \left\{ \frac{\hat{y}}{\hat{x}} \right\}$$

LATITUDE:

$$\text{Let } \phi_o = \tan^{-1} \frac{\hat{z}}{\sqrt{\hat{x}^2 + \hat{y}^2}}$$

$$\text{Let } \nu(\phi_o) = \frac{a}{[1 - e^2 \sin^2 \phi_o]^{1/2}}$$

$$\text{Let } f(\phi_o) = \frac{\cos \phi_o}{\sqrt{\hat{x}^2 + \hat{y}^2}} - \frac{\sin \phi_o}{\hat{z} + e^2 \nu(\phi_o) \sin \phi_o}$$

$$\text{Let } \phi_1' = \phi_o + \Delta\phi_o$$

$$\text{Compute } \nu(\phi_1'),\ f(\phi_1')$$

$$\phi = \phi_o - \frac{f(\phi_1') - f(\phi_o)}{f(\phi_o)\ \Delta\phi_o}$$

ALTITUDE:

$$h = \frac{\hat{y}}{\cos \phi \sin \lambda} - \nu(\phi)$$

In the calculation of user latitude, longitude, and altitude a correction is made for earth aspheroidicity. The equations which must be inverted are (Ref. 7).

$$\hat{x} = \left(\nu(\phi) + h\right) \cos\phi \cos\lambda$$

$$\hat{y} = \left(\nu(\phi) + h\right) \cos\phi \sin\lambda$$

$$\hat{z} = \left[(1 - e^2)\,\nu(\phi) + h\right] \sin\phi$$

Here

$$\nu(\phi) = \frac{a}{\left[1 - e^2 \sin^2\phi\right]^{1/2}}$$

e is the eccentricity and a the major axis of the earth ellipsoid.

The values of λ and ϕ are then obtained as shown. When a sufficiently good approximation of ϕ has been obtained, the altitude is solved for as indicated.

3.4 PROCEDURE FOR HAND CALCULATION WITH SIMPLIFIED EQUATIONS

This section presents a sequence of hand calculations from which a simple user can obtain latitude and longitude. The computations may be performed with a desk calculator, trigonometric tables, and a chart from which satellite coordinates may be determined. The equations are essentially those of subsec 3.3, with the exception of the charts for determining the satellite coordinates. The time required for the fix calculation should be of the order of 15 minutes.

3.4.1 Equations to be Solved

The user considered here is assumed to have the following equipment:

1) A desk calculator with square root capability

2) A table of sines, cosines, and tangents

3) A table from which satellite rectangular coordinates may be determined from transmitted ephemeris data.

With the use of this equipment, the user is to determine his latitude and longitude from two range differences and an altitude measurement.

To do this, he performs essentially the calculations stated and explained in subec 3. 3. The only difference is the manner in which the satellite's rectangular coordinates are determined. Rather than use the equations of par. 3. 3. 2 to calculate satellite X, Y, Z coordinates from transmitted ephemeris data and current time, a table is used containing the X, Y, Z coordinates tabulated as a function of time from the satellite equatorial crossing. In addition, he will iterate only once.

The equations the user must solve are:

$$\Delta_{ij} = \sqrt{(x-X_i)^2 + (y-Y_i)^2 + (z-Z_i)^2} - \sqrt{(x-X_j)^2 + (y-Y_j)^2 + (z-Z_j)^2}$$

$$\Delta_{jk} = \sqrt{(x-X_j)^2 + (y-Y_j)^2 + (z-Z_j)^2} - \sqrt{(x-X_k)^2 + (y-Y_k)^2 + (z-Z_k)^2}$$

$$h = \sqrt{x^2 + y^2 + z^2} - R_e$$

This is reduced to two equations in x and y by solving for z.

$$z = \pm \sqrt{(h + R_e)^2 - x^2 - y^2}$$

The plus sign is for the northern hemisphere users, the minus sign for southern hemisphere users. This is then substituted in the first two equations. The partial derivatives used to solve the linearized equations are:

$$\frac{\partial \Delta_{ij}}{\partial x} = \frac{1}{R_i}\left\{\frac{Z_i x}{z} - X_i\right\} - \frac{1}{R_j}\left\{\frac{Z_j x}{z} - X_j\right\}$$

$$\frac{\partial \Delta_{ij}}{\partial y} = \frac{1}{R_i}\left\{\frac{Z_i y}{z} - Y_i\right\} - \frac{1}{R_j}\left\{\frac{Z_j y}{z} - Y_j\right\}$$

$$\frac{\partial \Delta_{jk}}{\partial x} = \frac{1}{R_j}\left\{\frac{Z_j x}{z} - X_j\right\} - \frac{1}{R_k}\left\{\frac{Z_k x}{z} - X_k\right\}$$

$$\frac{\partial \Delta_{jk}}{\partial y} = \frac{1}{R_j}\left\{\frac{Z_j y}{z} - Y_j\right\} - \frac{1}{R_k}\left\{\frac{Z_k y}{z} - Y_k\right\}$$

where the a priori estimate of x, y, z is used.

The detailed sequence of computations the user must perform is given in the next paragraph.

3.4.2 Sequence of Calculations

1) Receive range measurements R_i^* , R_j^*.

2) Correct range measurements and calculate range differences:

$$\Delta_{ij} = R_i^* + b_{io} + b_{il}\tau_i - R_j^* - b_{jo} - b_{jl}\ \tau_j$$

$$\Delta_{jk} = R_j^* + b_{jo} + b_{jl}\ \tau_j - R_k^* - b_{ko} - b_{kl}\ \tau_k$$

3) Determine satellite coordinates from table.

4) Determine a priori latitude and longitude from map and calculate coordinate estimates:

$$\hat{x} = (R_e + h)\cos\phi\cos\lambda$$

$$\hat{y} = (R_e + h)\cos\phi\sin\lambda$$

$$\hat{z} = (R_e + h)\sin\phi$$

5) Compute a priori range estimates:

$$\hat{R}_i = \sqrt{(\hat{x} - X_i)^2 + (\hat{y} - Y_i)^2 + (\hat{z} - Z_i)^2}$$

$$\hat{R}_j = \sqrt{(\hat{x} - X_j)^2 + (\hat{y} - Y_j)^2 + (\hat{z} - Z_j)^2}$$

$$\hat{R}_k = \sqrt{(\hat{x} - X_k)^2 + (\hat{y} - Y_k)^2 + (\hat{z} - Z_k)^2}$$

6) Resolve ambiguity (app. M)

Round $\hat{R}_i - \hat{R}_j - \Delta_{ij}$ to nearest multiple of 2, 000 (say k x 2, 000)

Form $\Delta_{ijR} = k \times 2,000 + \Delta_{ij} - (\hat{R}_i - \hat{R}_j)$

Calculate Δ_{jkR} similarly.

7) Compute partials:

$$b_{11} = \frac{1}{\hat{R}_i}\left\{\frac{Z_i\hat{x}}{\hat{z}} - X_i\right\} - \frac{1}{\hat{R}_j}\left\{\frac{Z_j\hat{x}}{\hat{z}} - X_j\right\}$$

$$b_{12} = \frac{1}{\hat{R}_i}\left\{\frac{Z_i\hat{y}}{\hat{z}} - Y_i\right\} - \frac{1}{\hat{R}_j}\left\{\frac{Z_j y}{\hat{z}} - Y_j\right\}$$

$$b_{21} = \frac{1}{\hat{R}_j}\left\{\frac{Z_j\hat{x}}{\hat{z}} - X_j\right\} - \frac{1}{\hat{R}_k}\left\{\frac{Z_k\hat{x}}{\hat{z}} - X_k\right\}$$

$$b_{22} = \frac{1}{\hat{R}_j}\left\{\frac{Z_j\hat{y}}{\hat{z}} - Y_j\right\} - \frac{1}{\hat{R}_k}\left\{\frac{Z_k\hat{y}}{\hat{z}} - Y_k\right\}$$

8) Compute corrections to a priori estimate (δx, δy):

$$\delta x = \frac{1}{b_{11} b_{22} - b_{12} b_{21}} \left\{ b_{22} \Delta_{ijR} - b_{12} \Delta_{jkR} \right\}$$

$$\delta y = \frac{1}{b_{11} b_{22} - b_{12} b_{21}} \left\{ b_{21} \Delta_{ijR} + b_{11} \Delta_{jkR} \right\}$$

$$\hat{z} + \delta z = \pm \sqrt{(R_e + h)^2 - (x + \delta x)^2 - (y + \delta y)^2}$$

9) Calculate latitude and longitude:

$$\lambda = \tan^{-1} \left\{ \frac{\hat{y} + \delta y}{\hat{x} + \delta x} \right\}$$

$$\phi = \sin^{-1} \left\{ \frac{\hat{z} + \delta z}{R_e + h} \right\}$$

This concludes the calculations the user must perform to determine his fix.

3.5 SIMPLEST USER HARDWARE EQUATIONS

The preceding computations are rather involved and the more complex sets require considerable computational equipment by the user. However, it may be observed that for any small region on the earth or in near earth space, very simple functional relationships may be used to derive user position in spherical earth-centered coordinates from the range-difference measurements. Furthermore, these simplified computations for angular position are essentially independent of altitude and, hence, for those cases where conventional methods of measuring altitude are adequate for navigation, only two pairs of satellites (or a minimum of three satellites) are required for a navigation solution. Any additional measurements available from other pairs of satellites can then be used as redundant measurements to increase the accuracy of the computed position fix.

In the simplified satellite hyperbolic navigation scheme described here, the mathematical function that is used to relate the user's measurements to his position is a power series expansion in the range-difference measurements about a reference point of known location. The degree of the polynomial used in this expansion depends on the accuracy required for the navigation fix and the user's distance from the reference point. Navigational accuracy by this scheme is also influenced by the number of sets of range differences used in the solution, i. e., the number of satellites visible, and their geometry.

In the simplest situation, the following equations suffice:

$$\Delta \text{ NS} = \left\{ \begin{array}{l} \text{User position in nautical miles north or south of nearest reference point, measured along a great circle on earth's surface, (map coordinates).} \end{array} \right\} = k_1 + k_2\Delta R_1 + k_3\Delta R_2 + \Delta R_3$$

$$\Delta \text{ EW} = \left\{ \begin{array}{l} \text{User position in nautical miles east or west of nearest reference point, measured along a great circle on earth's surface, (map coordinates).} \end{array} \right\} = k_5 + k_6\Delta R_1 + k_7\Delta R_2 + k_8\Delta R_3$$

where kl, k_2, k_3, ... etc. are constants applicable to a particular grid transmitted by a satellite prior to the user's position computation. (These constants are used in lieu of satellite ephemeris and satellite oscillator drift correction data which must be transmitted for the complete hyperbolic solution.) ΔR_1, ΔR_2, and ΔR_3 are the measured range differences between three pairs of the four visible satellites. If Δ NS, Δ EW, and ΔR's are given in units of nautical miles, typical values for k_1 and k_5 are in the range of 0 to 2000 nmi, and typical values for the other k's are between 0. 5 and 3. The latter terms are sometimes referred to as the geometric dilution of precision (GDOP) factors since they transform the hyperbolic measurements into map coordinates. This technique can provide 1-nmi accuracy over a 12,000,000 sq mi region of the earth. The data rate required to transmit these constants, assuming users desire a fix every 5 min is only 60 b/sec. This technique provides significant computation reduction and thus has a large cost advantage over the more conventional techniques previously discussed.

4. RELATED STUDIES

4.1 EFFECTS OF GRAVITATIONAL PERTURBATIONS ON STATION-KEEPING AND COVERAGE

A repeating ground-track satellite is subject to orbital disturbances caused by repeated passage over the same features on a planet. The motion caused by these disturbances is libration, a free oscillation of the ascending node about a stable point on the equator, with an amplitude equal to its initial displacement from the stable point (Ref. 8). By means of the RESORB program (app. N), the effect of libration on eight satellites spaced at 45° intervals along a 24-hr circular orbit was determined. The resulting characteristic velocity requirement to maintain position within 5° and 3° deadband limits* was computed. The maximum velocity required is about 30 ft/sec, essentially independent of the deadband. Individual corrections are of the order of 1 to 3 ft/sec every 6 to 7 months.

A second cause of orbit perturbation is the out-of-plane gravitational force due to the sun and moon. This can cause a small shift in the orbital inclination, a maximum of about 4° during the 5-yr satellite lifetime. This is acceptable for purposes of the proposed system, and can be held to a lower value by appropriate launch timing.

4.1.1 In-Plane Effects

RESORB runs were made to investigate effects on eight satellites initially distributed uniformly in a 24-hr, 18.5° inclined circular orbit. Figure 26 shows the time history of libration of these satellites. Due to the J_{22}, J_{31}, J_{33}, J_{42}, J_{44} tesseral harmonics, the longitude of the ascending node does not stay constant, but exhibits a libration with amplitude equal to the initial separation from the stable nodes which are at about 77 and 257°. This motion of the longitude of the ascending node can best be understood by imagining a roller-spring-hoop system as

*This refers to total travel, not plus or minus; i.e., 5° deadband limits means nominal longitude $\pm 2.5^{\circ}$.

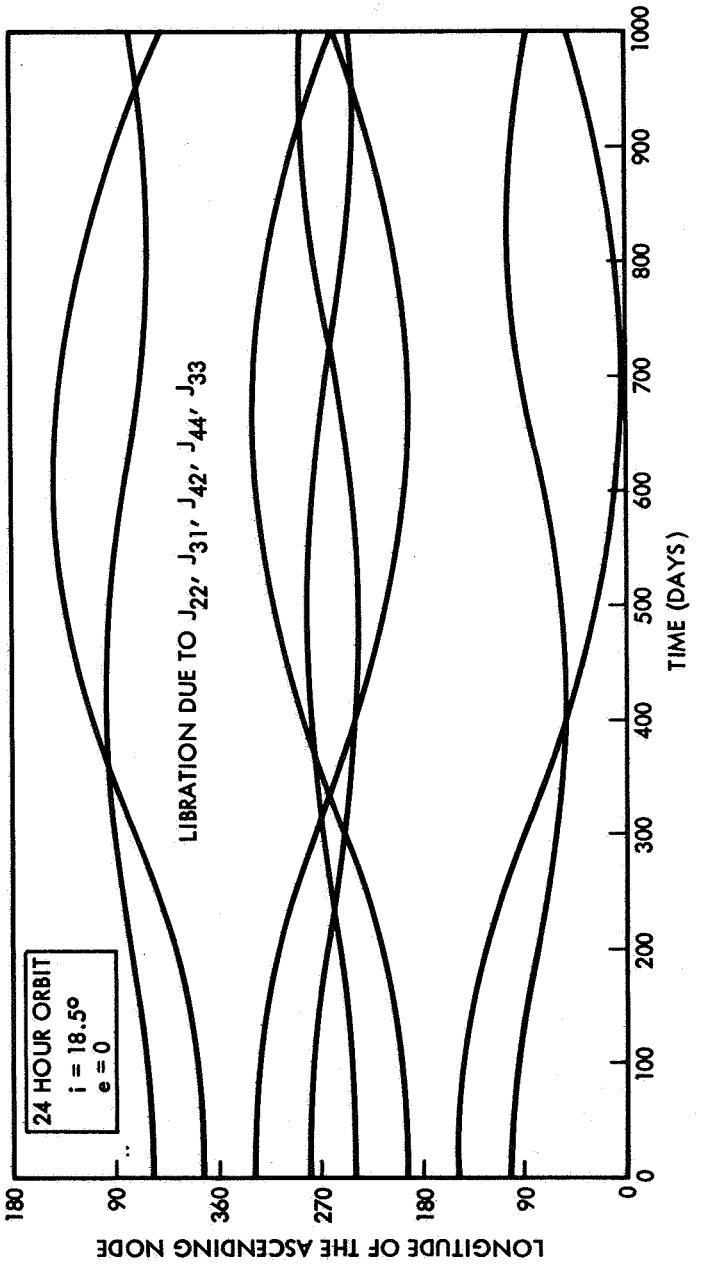

Figure 26. Libration Due to J_{22}, J_{31}, J_{42}, J_{44}, J_{33}

shown in Figure 27. The lows of the hoop correspond to the stable nodes and represent potential wells in the gravitational field. The number of lows and highs is defined by m in $J_{\ell m}$, but their orientation (with respect to Greenwich) depends on both ℓ and m. For circular 24-hr orbits, J_{22} dominates, resulting in the rather regular motion shown in Figure 26. This is not at all the case with eccentric orbits. The period of small amplitude libration is shown in Figure 28. For large amplitudes, these periods must be multiplied by a complete elliptical integral of the first kind (modulus = amplitude) to obtain the periods shown in the previous figure.

Figures 29a and b present libration histories up to a maximum of 5° displacement for eight satellites, with ascending nodes as indicated on the figure and spaced at 45° intervals. It can be seen that the time to drift 3° is from 60 to 93 days and to drift 5° is from 50 to 118 days. The velocity, ΔV, required to reverse this motion, is shown for both 3 and 5° drifts and is repeated in Figures 30 and 31 to indicate the effect of initial longitude on stationkeeping requirements. The total ΔV requirement over the 5-year satellite lifetime as a function of longitude of the ascending node is shown in Figure 32. The result is a maximum requirement of 30 ft/sec, with reduced velocities in the vicinities of the stable and unstable nodes.

Figure 33 shows the effect of libration on the relative position of four satellites over a period of 120 orbits. In the absence of resonance, all four satellites would stay at their initial longitude and latitude. In this case, only the fourth satellite stayed close to its initial position, which was very close to an unstable node (347°). The acceleration at this point is very small; thus, it takes a long time to leave the vicinity of the unstable node. (Given enough time, however, the amplitude of this satellite would be the largest.) The positions when the satellites reach 5° deviation from their original location are also marked. After 85 days one of the satellites will have shifted 5° and the others lesser amounts depending on their initial longitudes.

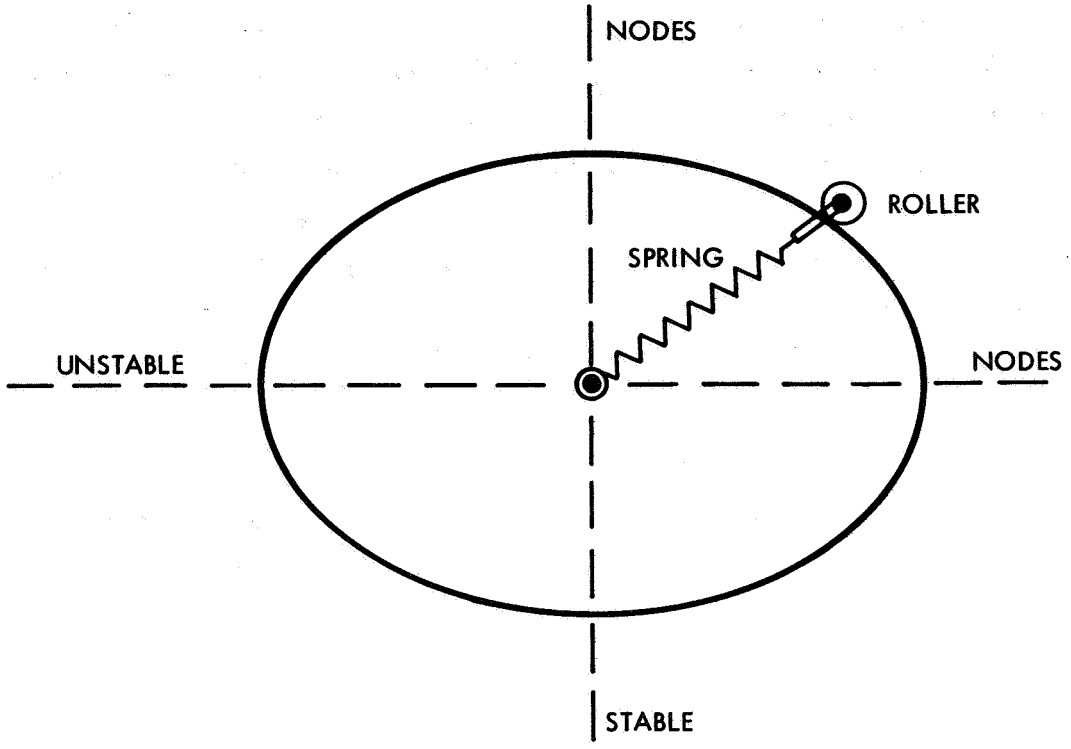

Figure 27. Simulation of the Gross Characteristics of Libration

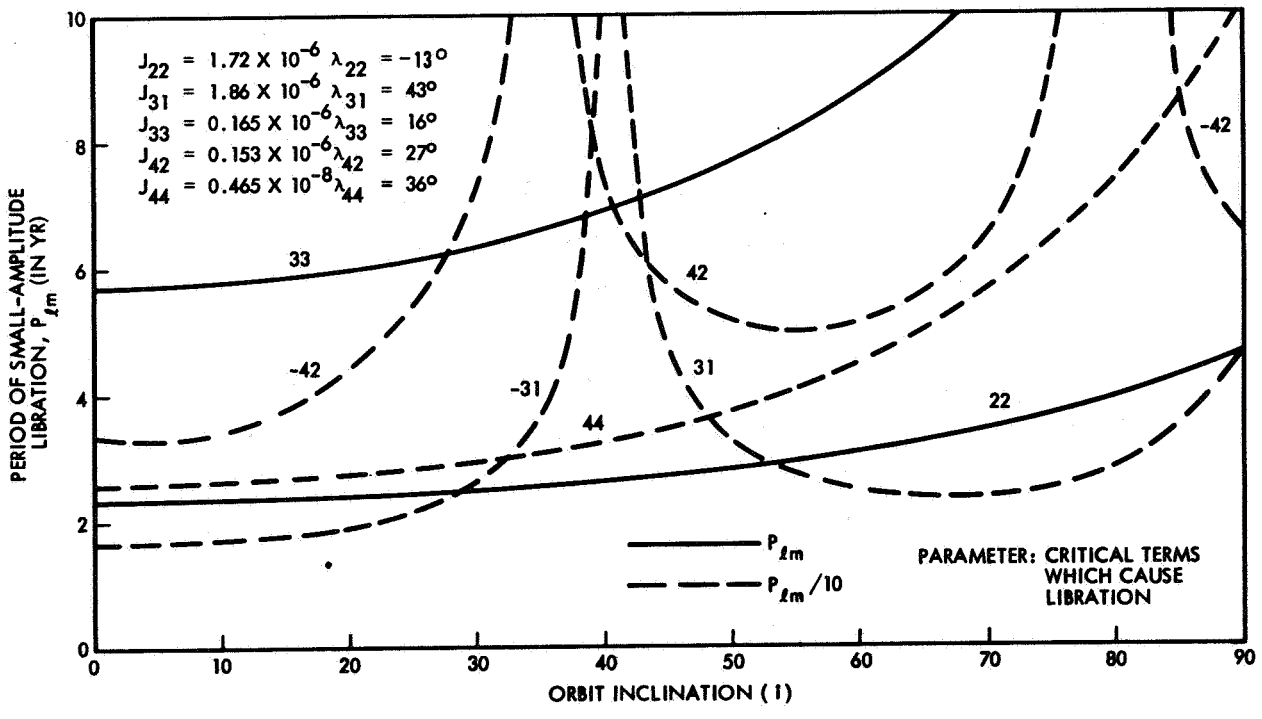

Figure 28. Libration Periods of 24-Hr Circular Orbits

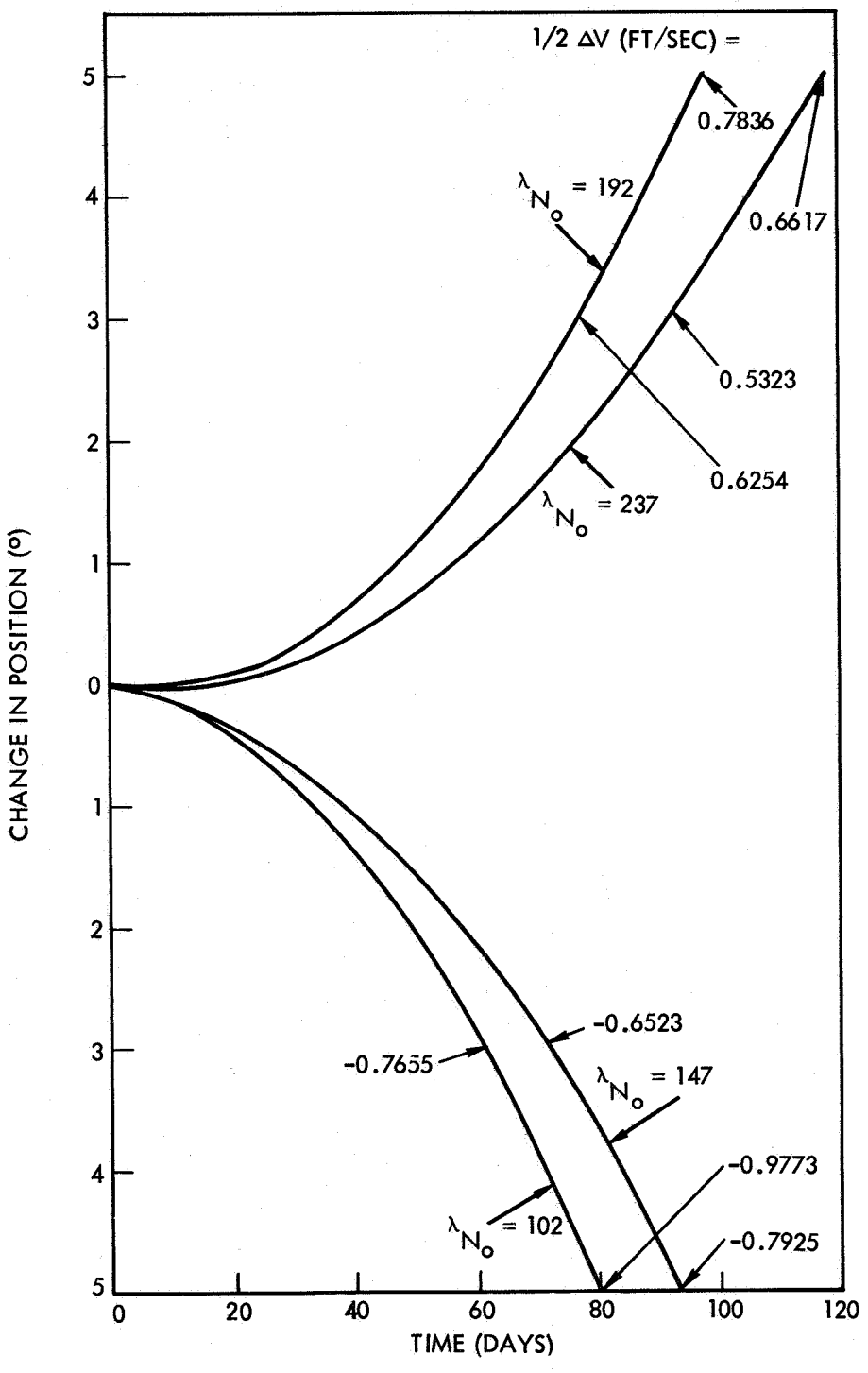

Figure 29a. Libration Histories for 24-Hr 18.5° Inclined Circular Orbits with Various Ascending Nodes

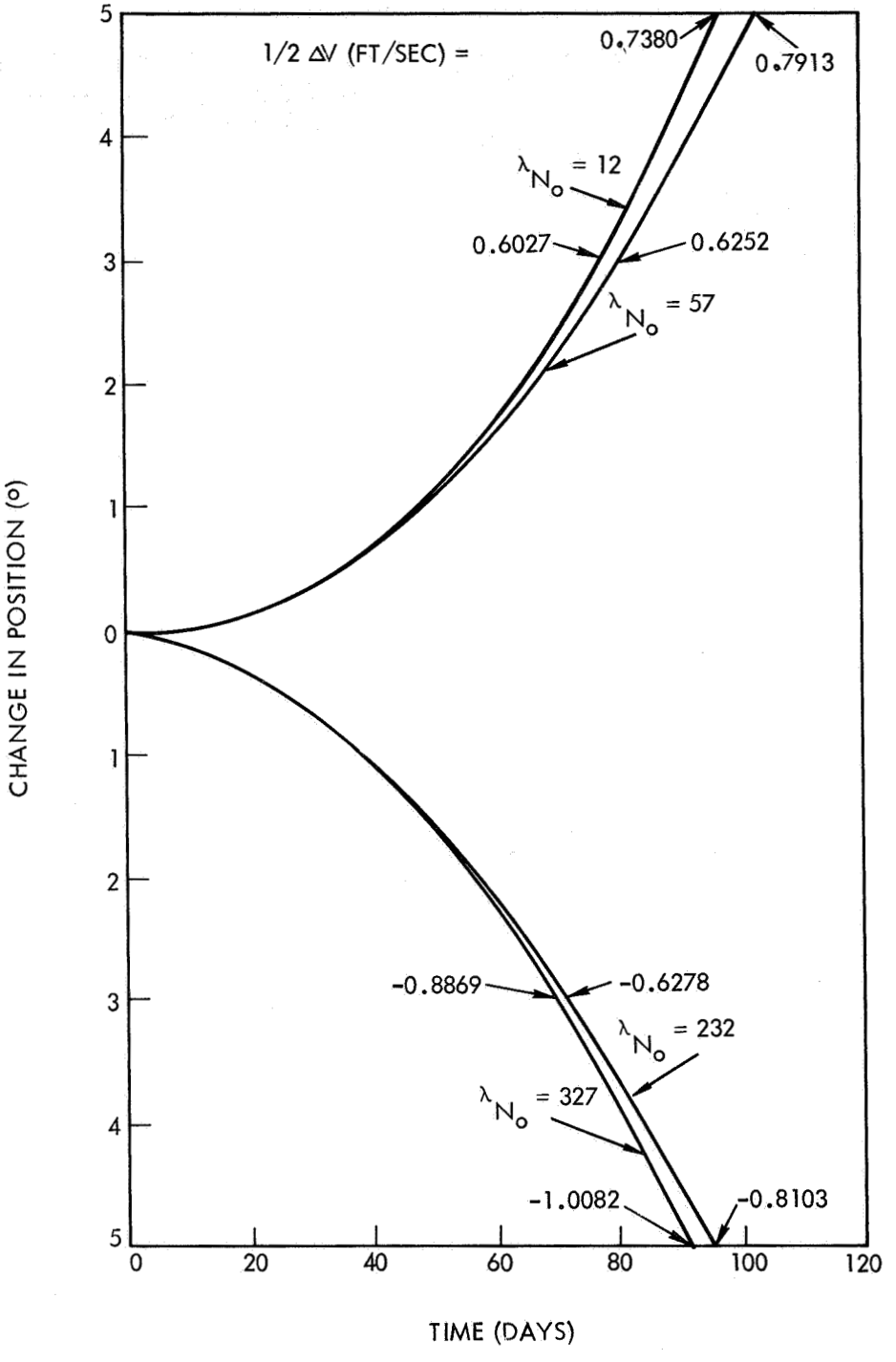

Figure 29b. Libration Histories for 24-Hr 18.5° Inclined Circular Orbits with Various Ascending Nodes

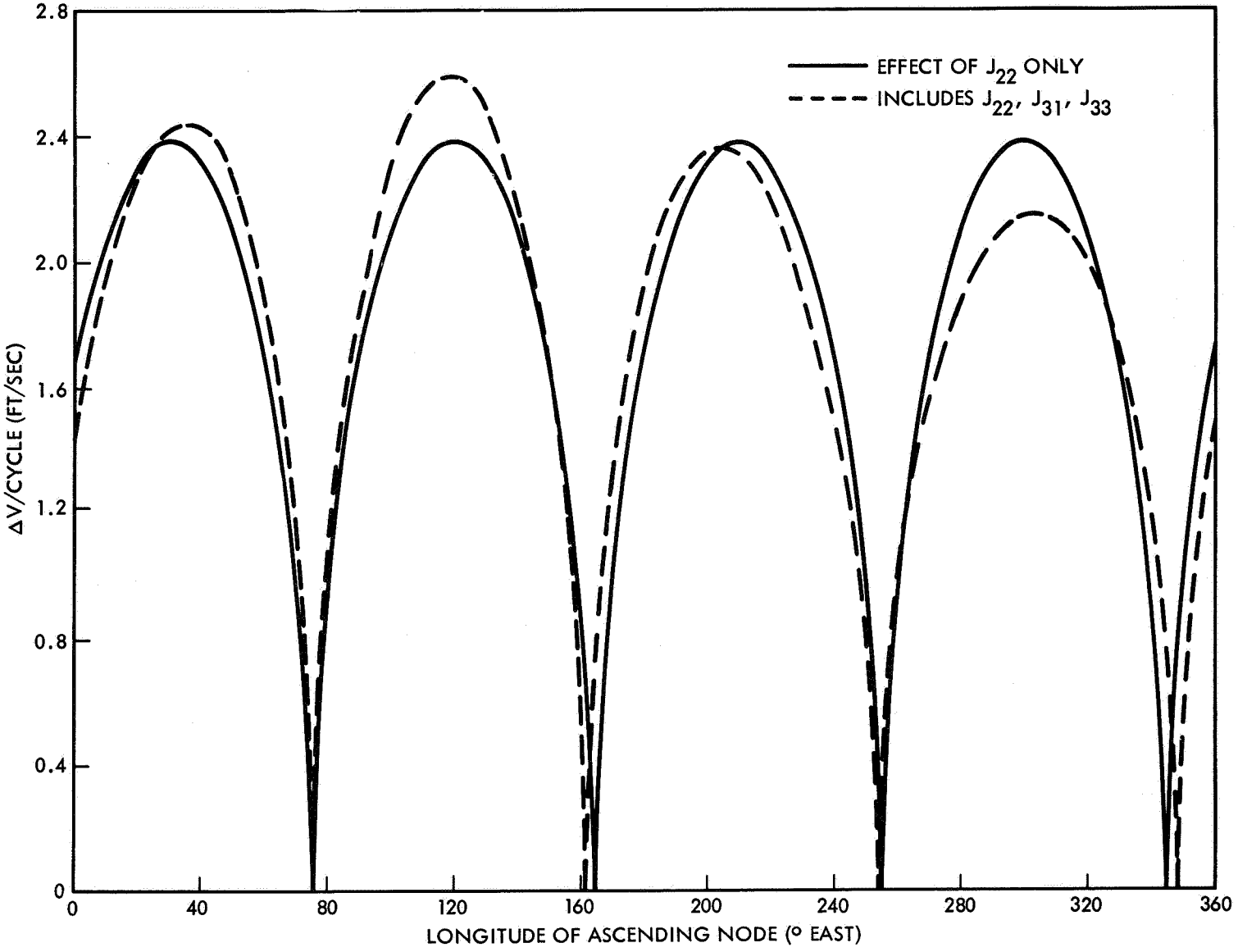

Figure 30. ΔV Required for 5° Limit Cycle

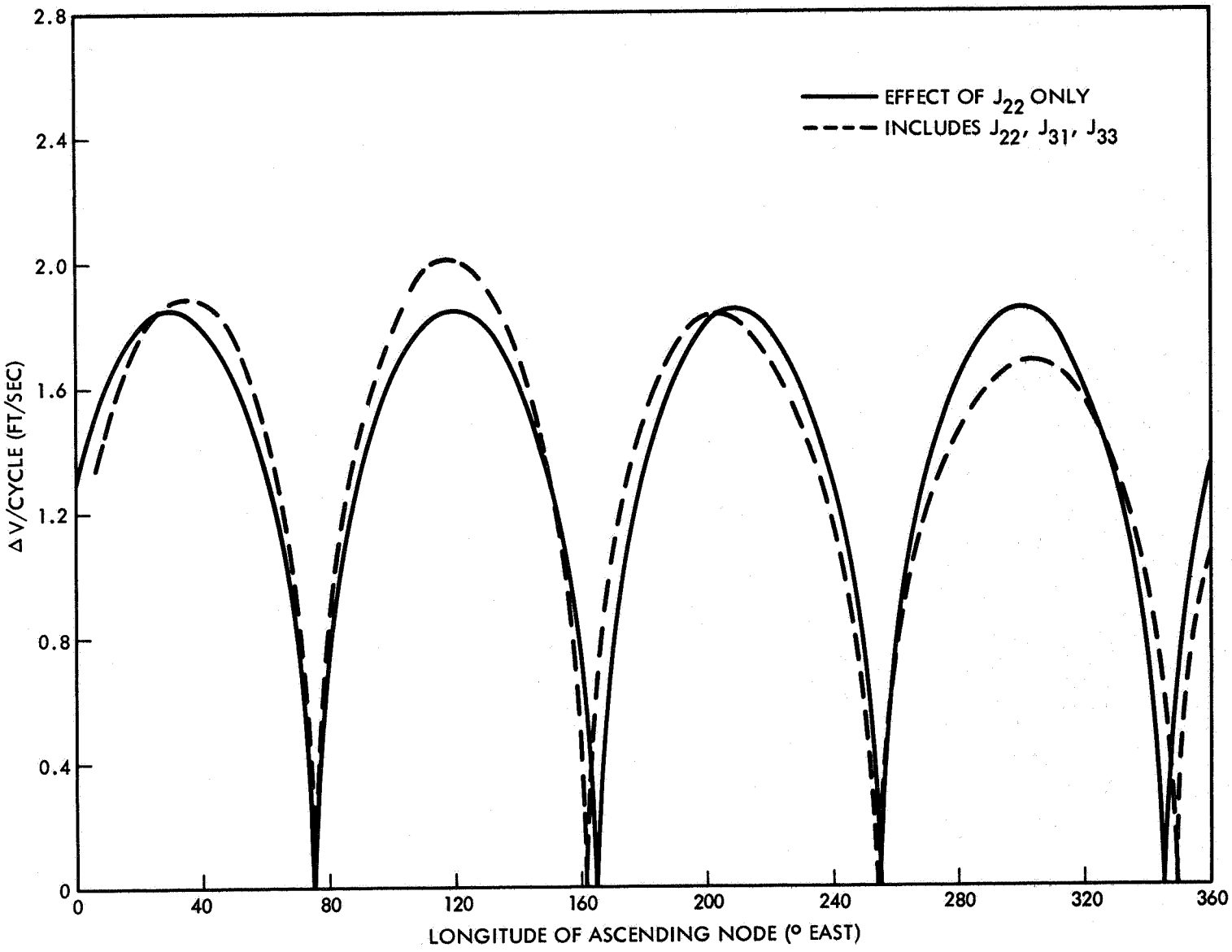

Figure 31. ΔV Required for 3^{o} Limit Cycle

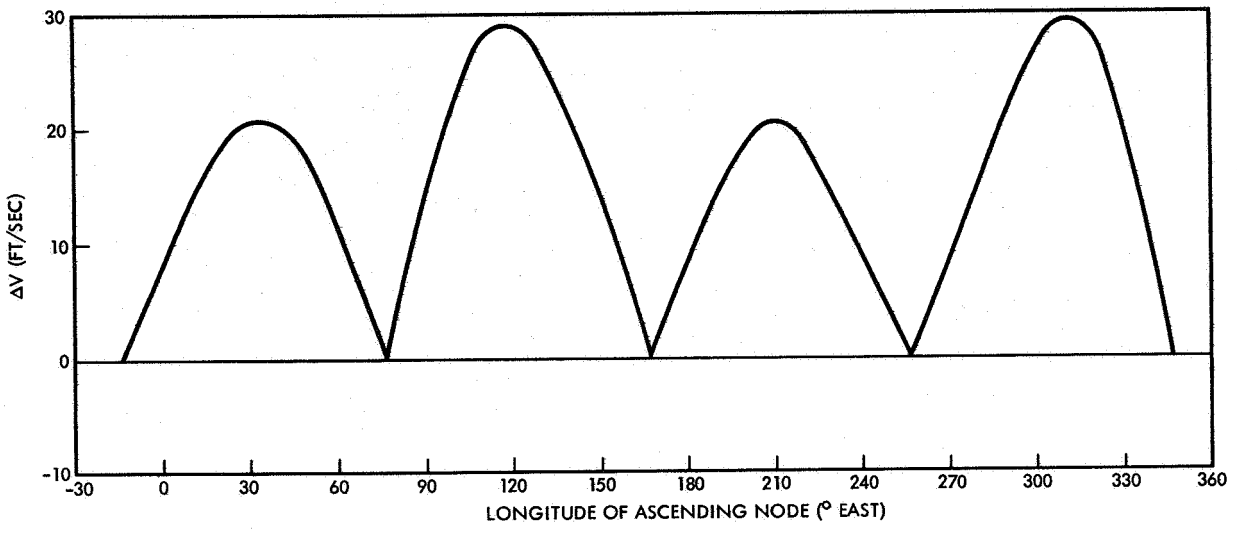

Figure 32. Total Characteristic Velocity Requirement for 5-Yr In-Plane Stationkeeping

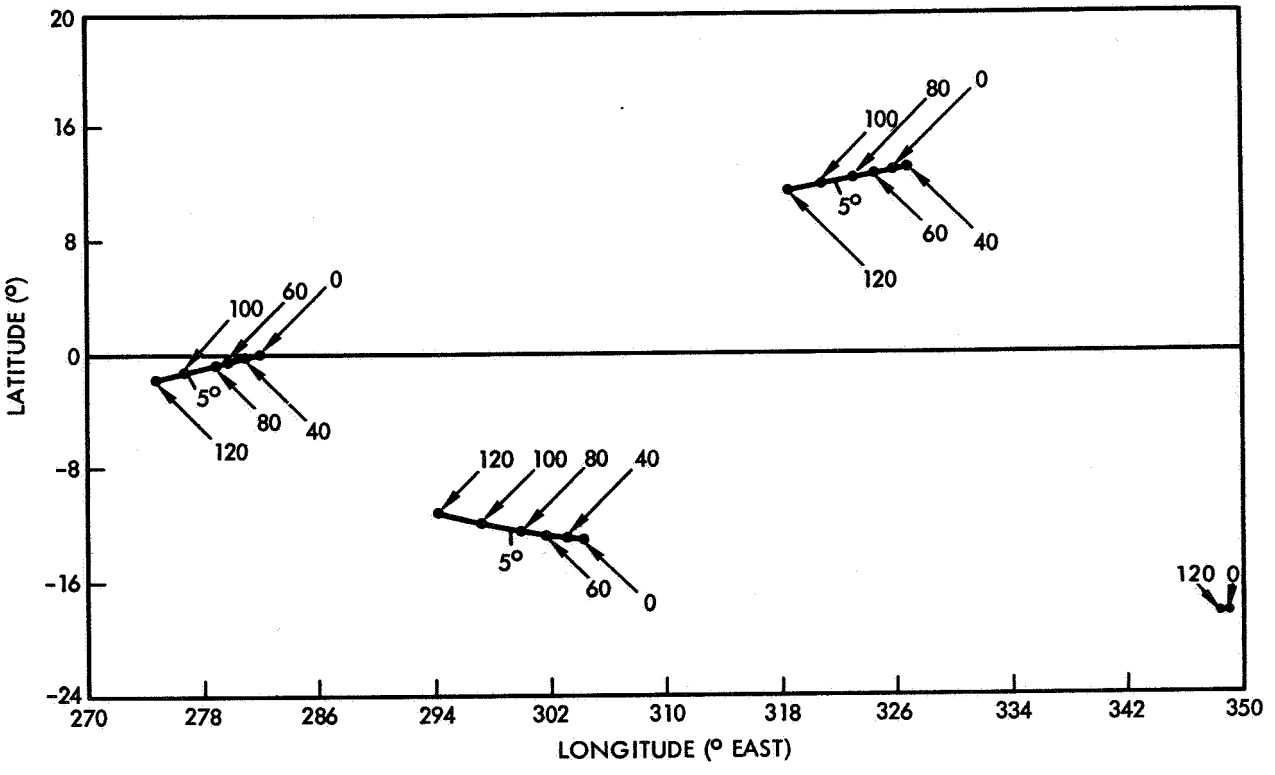

Figure 33. Positions of Four Synchronous Satellites After the Same Number of Orbits

The effect on coverage is shown in Figure 34 for time T_0. The change in coverage, seen by comparing this figure with Figure 35* (the clear overlay), is small and is primarily in longitude. Similar maps for times T_{45}, T_{90}, T_{135}, and T_{180} were plotted, indicating that the effect of in-plane drift is of the same order of magnitude for these times. The regions where only two satellites are visible expand to a maximum of 5° in longitude, with negligible latitude change.

In order to preserve the desired satellite constellation, it is necessary to provide in-plane stationkeeping within some deadband region. With some stationkeeping methods, it is possible for two or more satellites to approach deadband limits simultaneously, which may have an adverse effect on coverage. For example, it was found that if two satellites reached a 5° deadband limit simultaneously, the coverage at T_{45} would have regions of indeterminacy (only two satellites visible) extending below 58° latitude. Therefore, it may prove desirable to set deadband limits somewhat lower than 5° or, alternatively, to use station-keeping logic that prevents two or more satellites from approaching the limits simultaneously.

4.1.2 Out-of-Plane Effects

Earth oblateness, the sun, and the moon exert a torque on the orbital momentum of the satellite. The result is a regression of the line of the nodes and a periodic change of the orbit plane. Figure 36 demonstrates the combined effect of these perturbations on orbits with varying initial inclination. Inclination is plotted along the radius and Ω, the right ascension of the node, in the circumferential direction. All curves start at $\Omega = 180^{\circ}$, with tick marks at 2-yr intervals. The 10-yr points are connected by dashed lines. Initially, the heliocentric longitude of the ascending node of the moon was $\Omega_M = 0$, which corresponds to Julian date 2440310 (30 March 1969).

*This transparency can be found in the pocket on the inside of the back cover.

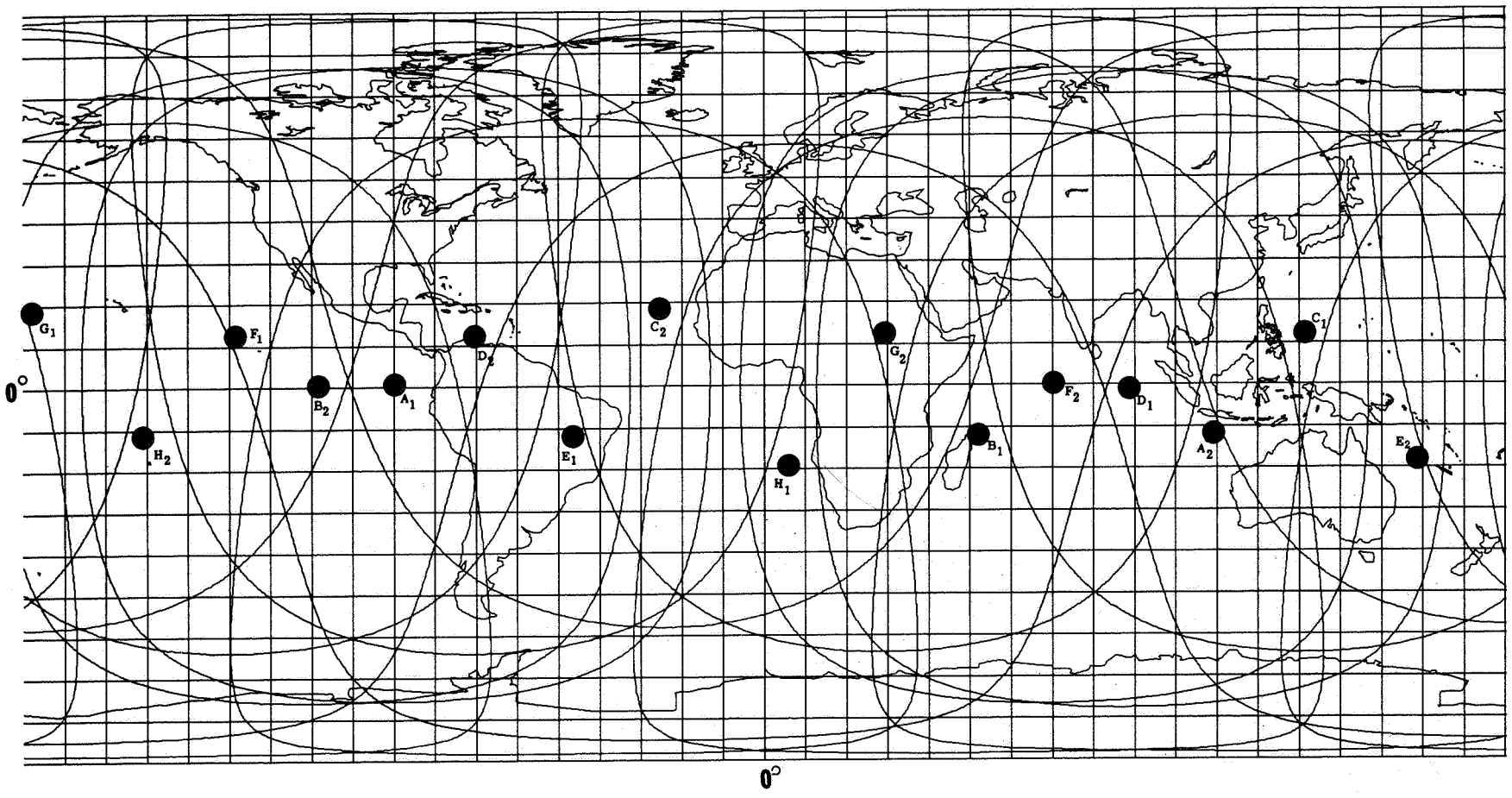

Figure 34. In-Plane Resonance Effects On Coverage at T_0

Figure 37 was obtained from Figure 36 by starting at an inclination of 18.5° at $\Omega = 0, 90^{\circ}, 180^{\circ}, 270^{\circ}$ and following the trend for 5 yr. It can be seen that for $\Omega = 0$ and 270°, the inclination increases 4° and 1°, respectively.

Figure 36 was generated with the moon's initial longitude at zero. Similar curves were generated at TRW with $\Omega_M = 90^{\circ}$, 180°, and 270°. The greatest difference is for $\Omega_M = 180^{\circ}$ and, on Figure 37, the dashed lines represent regression based on $\Omega_M = 180^{\circ}$. The variation is rather small. Although the influence of the date can be evaluated with the complete set of charts, it is easier to make a RESORB run for any chosen date and obtain the variations with eight figure accuracy. Figures 36 and 37, however, demonstrate the results of these perturbations rather clearly.

The effect of inclination change on coverage was determined for a slightly pessimistic value of 4.3°. It was assumed that the orbit planes were positioned initially at 2.15° below the 18.5° nominal value (i.e., at 16.34°) and that, after 5 yr, they had drifted apart to final inclinations of 20.65°. Figure 38 indicates the coverage to be expected under these conditions at time T_0. Comparison with Figure 34 shows the small effect on coverage. Furthermore, it is possible to attain substantially lower values by selecting appropriate launch times. It is therefore concluded that out-of-plane stationkeeping is not required.

Figure 39 shows how resonance affects satellites whose orbital periods differ slightly from 24 hr. The lower curve corresponds to a repeating ground-track orbit (in the absence of tesseral harmonics); it librates with a period of about 1000 days and an amplitude of about 47°. The next curve corresponds to an orbit whose longitude of the ascending node drifts at a rate of 0.75° per day. It can be seen that the motion (called circulation) is related to that of an overturning pendulum with an amplitude of irregularity of about 2° and a period of about 240 days. The third curve corresponds to an orbit with 1° per day nodal drift rate. The period of circulation is 180 days and the amplitude is about 1°.

Slowly drifting orbits provide the benefit of greatly reduced effects of libration and, hence, require no stationkeeping. A disadvantage of this scheme, however, is the increased difficulty of keeping track of the

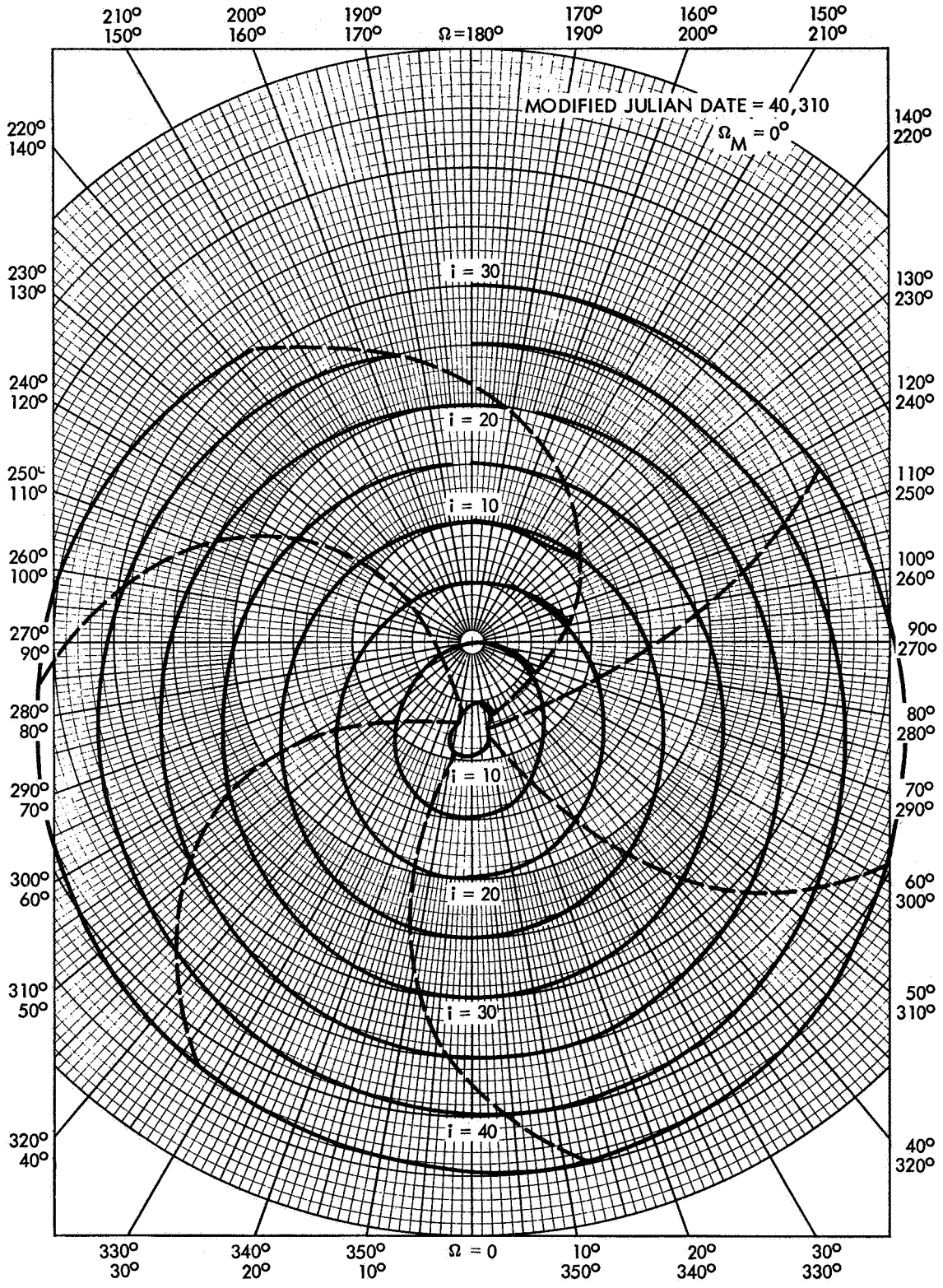

Figure 36. Out-of-Plane Perturbation Effects

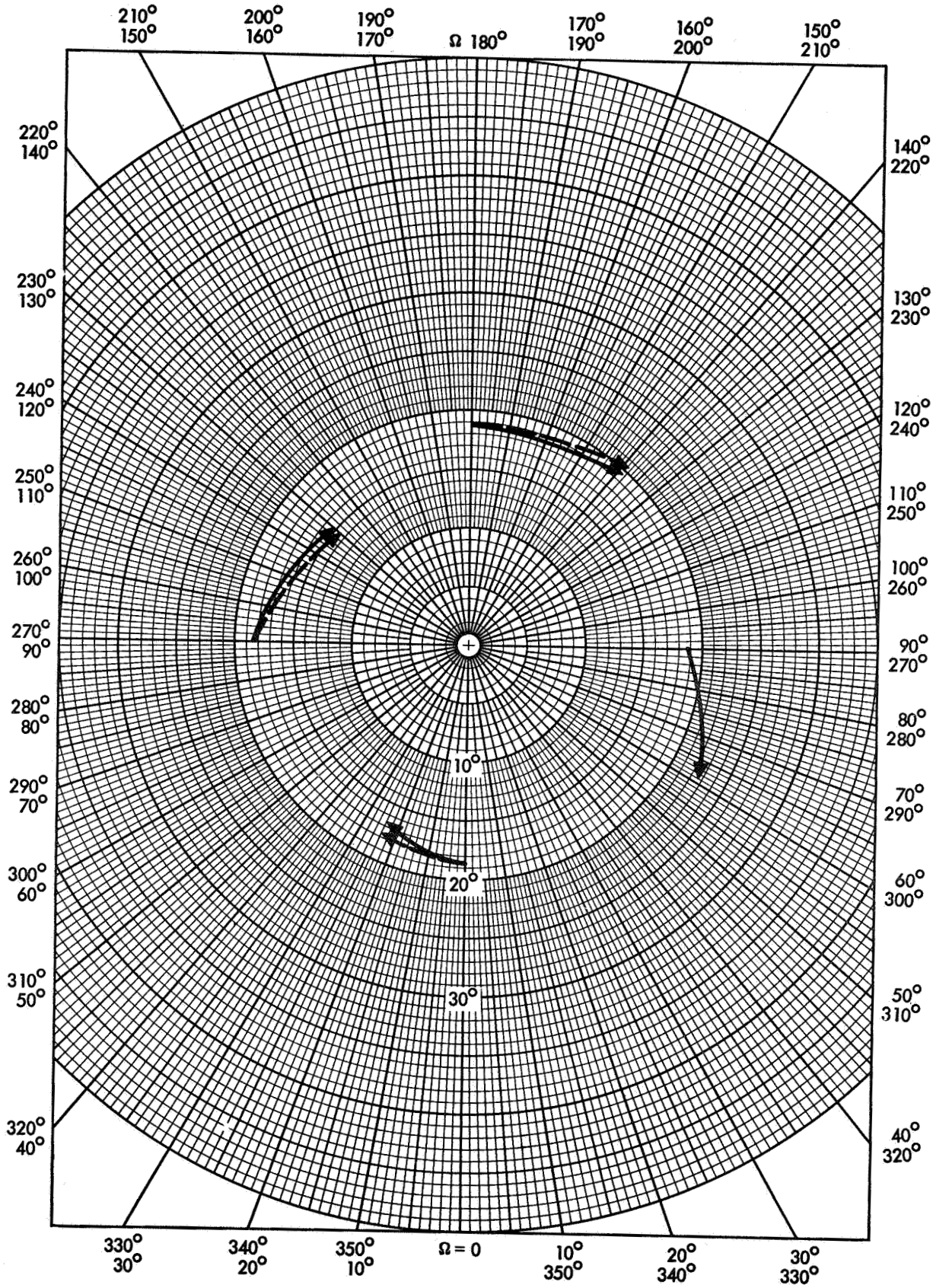

Figure 37. Luni-Solar Effects on Orbital Inclination Over 5-Yr Satellite Lifetime

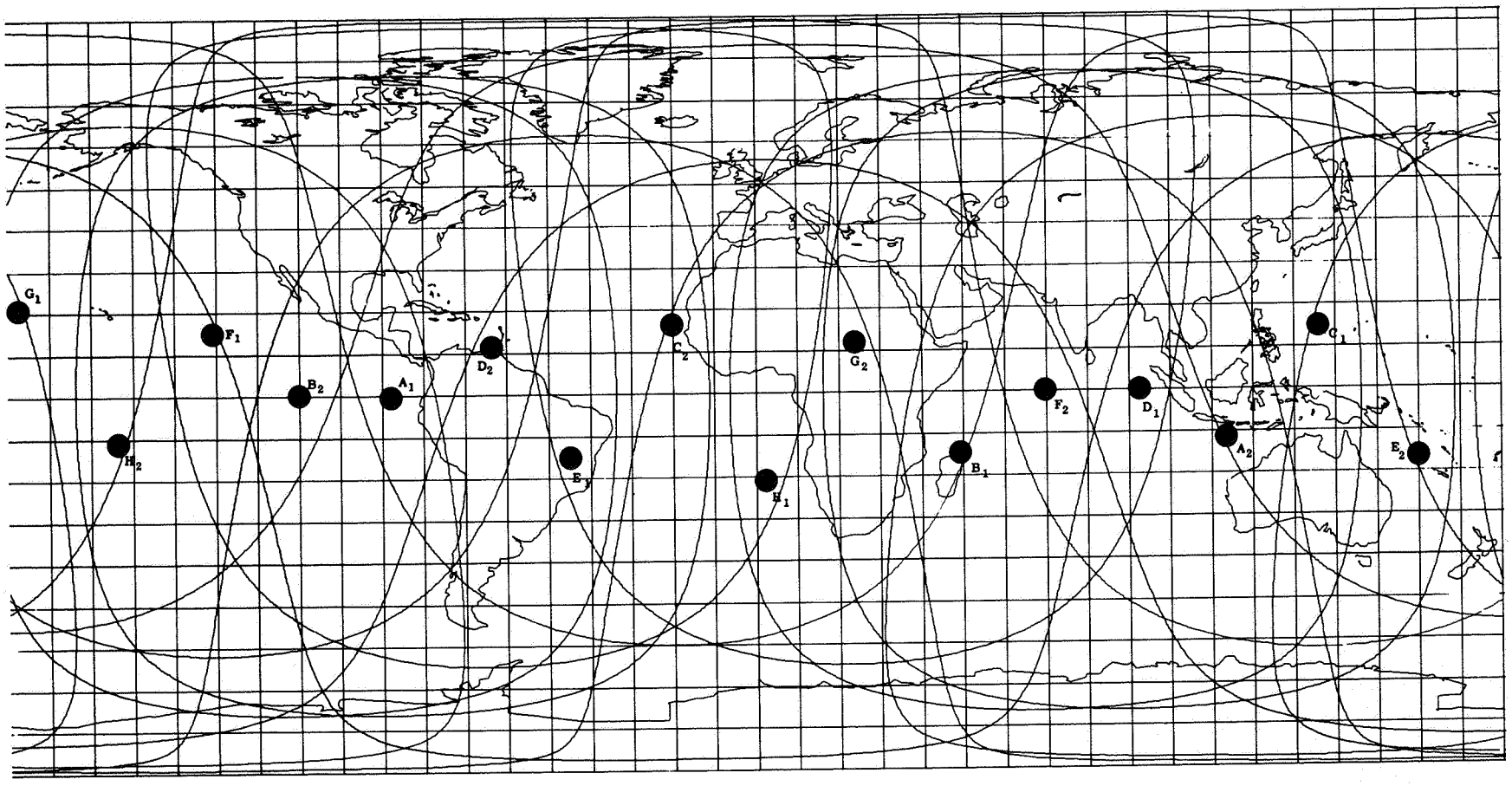

Figure 38. Inclination Change Effects Upon Coverage for T_0

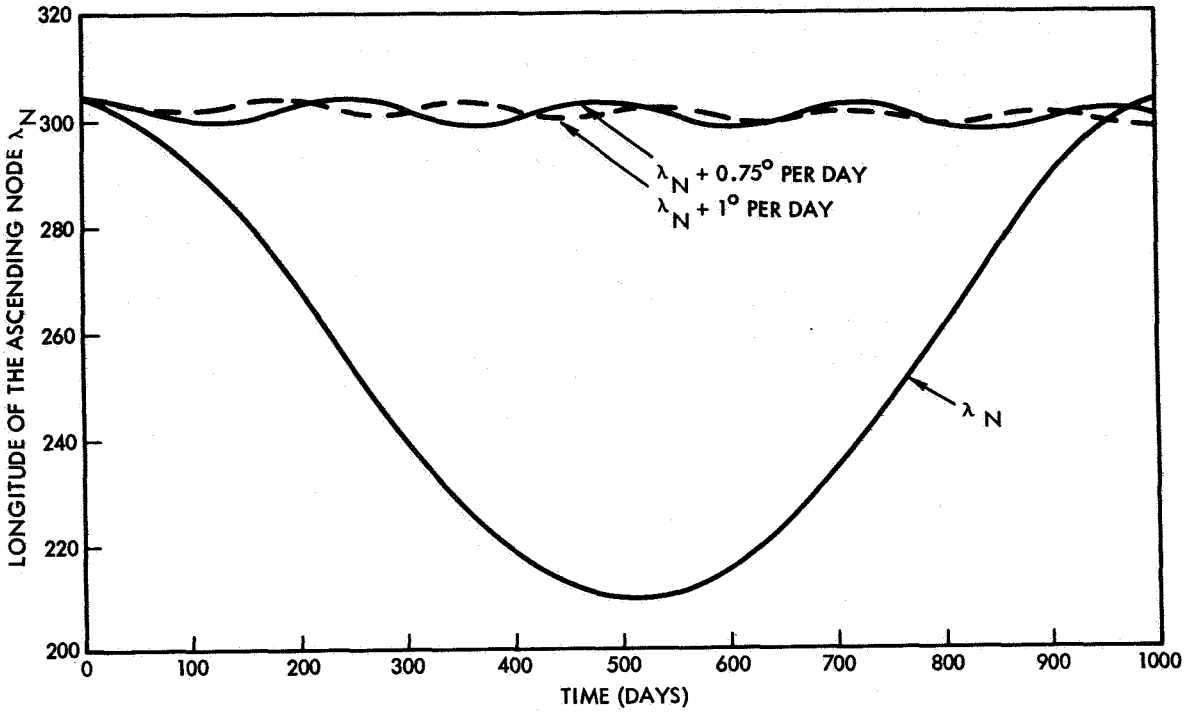

Figure 39. Comparison of Resonance Effects on Synchronous and Nearly Synchronous Satellites in Circular 18.5° Inclined Orbits

system and arranging for hand-over between tracking stations. Also, stationkeeping requirements are not particularly severe for a 24-hr system, so the drifting system has not been considered further.

4.2 SATELLITE ECLIPSE PERIODS

Satellite eclipse duration is important from a satellite design standpoint in that it affects the power supply design and the radiant heat lost through the spacecraft skin. An eclipse of the satellite is defined as the passage of spacecraft through the umbra and/or penumbra created on the dark side of the earth. The eclipse season is defined to be the number of consecutive days that the spacecraft experiences an eclipse during each successive revolution. For a satellite in a circular orbit, there will be no eclipse seasons or there will be two eclipse seasons during the year.

The condition of no eclipses requires specific combinations of spacecraft altitude, orbit-plane inclination, and injection node which do not occur in the TRW navigation satellite system.

An eclipse on every revolution occurs when the inclination of the spacecraft orbit plane to the ecliptic plane is less than the angular radius of the earth shadow at the orbit altitude; as with the completely sunlit orbit, this case requires specific ranges of inclination, altitude, and injection node. For the proposed navigation satellite system, there is a range of injection nodes approximately 41° wide that will produce the continual eclipse cycle. The positions of these bands are dependent upon whether the orbital inclination is positive or negative.

A computer program was used to obtain the eclipse seasons and durations. A spherical earth and unperturbed orbits were used to minimize the cost of obtaining these data. The equations are presented in app. O.

The maximum eclipse duration is the same for all the spacecraft in the system, since for this system it is a function of orbit altitude only. Twice each year each spacecraft experiences a maximum of 70.5 min of eclipse duration per revolution. Since the maximum eclipse durations are all the same, it is necessary only to define the eclipse seasons to see the variation of eclipse duration for each satellite throughout the season. The eclipse seasons and, hence, the duration of eclipses during eclipse season are a function only of the injection node (measured from vernal equinox). This, in turn, makes both the season and eclipse duration functions of time-of-day at injection for any specific date.

The eclipse seasons are presented in Figures 40 and 41 as a function of injection node for $+18.5^{\circ}$ and -18.5° inclination. There are two eclipse seasons during the year. When one season is less than one-half year (182.7 days), the spacecraft also experiences two seasons of no eclipse during the year. Conversely, for the narrow injection node bands producing half-year eclipse seasons, the spacecraft enters one eclipse season directly from another, with no periods of complete orbital sunlight.

The eclipse durations for eclipse seasons less than 182.7 days are presented in Figure 42 as a function of the fraction of season length into the season. In this manner, Figures 40 through 42 may be combined to produce the eclipse durations as a function of eclipse season time, simply

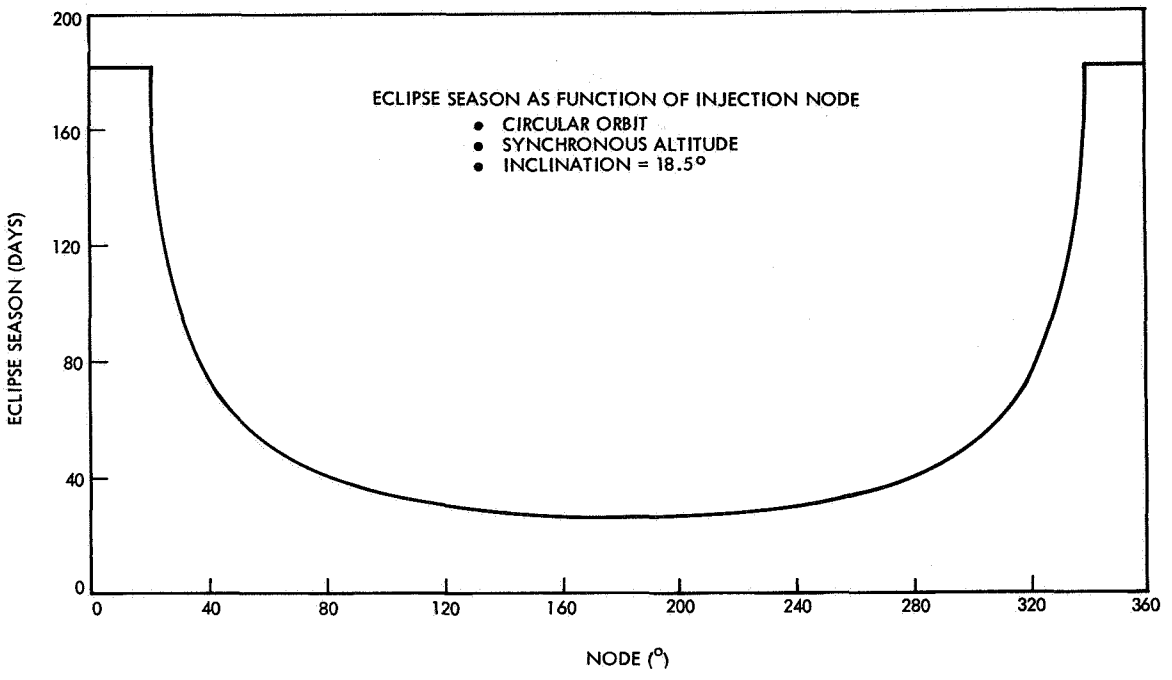

Figure 40. Eclipse Season as Function of Injection Node for +18.5° Inclined 24-Hr Circular Orbit

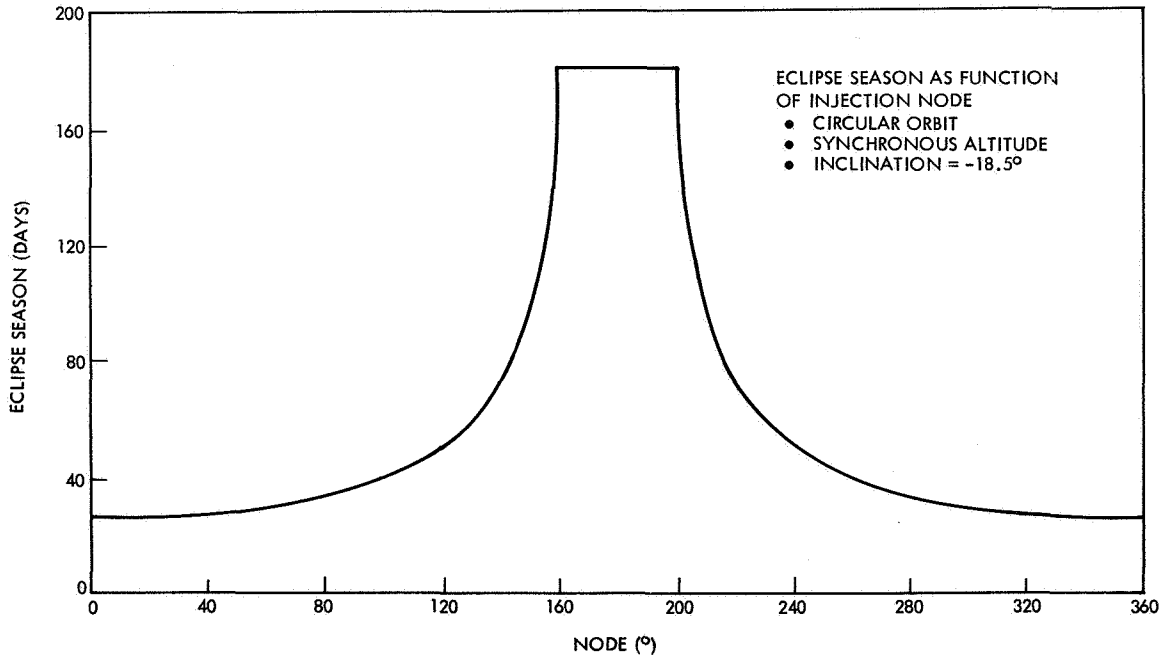

Figure 41. Eclipse Season as Function of Injection Node for -18.5° Inclined 24-Hr Circular Orbit

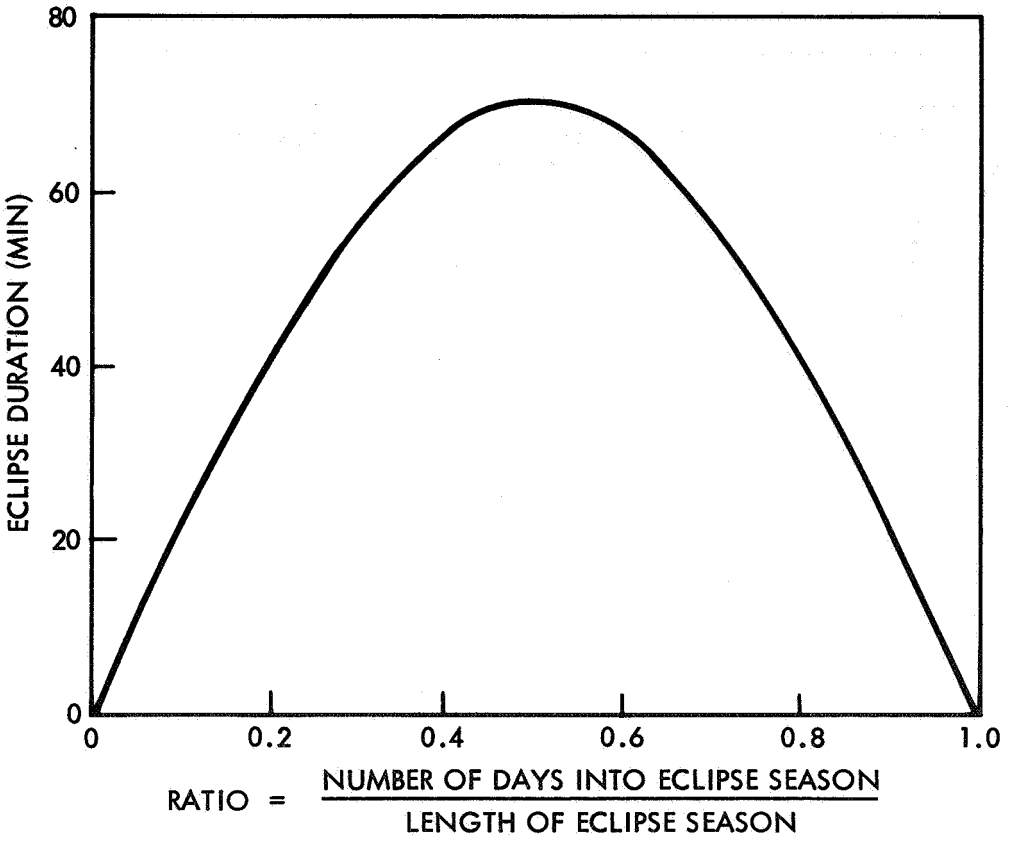

Figure 42. Eclipse Duration During Season

by multiplying the fractional part of the season (Figure 42) by the total season length from Figures 40 and 41. This method of presenting the data eliminates the necessity of presenting data for all possible injection conditions.

Eclipse seasons lasting a full half year require a different method of presentation; the season length is the same for all seasons in this category, whereas the minimum duration of eclipse varies as a function of the injection node. In Figures 43a and b, the minimum eclipse durations are presented as functions of injection node for $+18.5^{\circ}$ and -18.5° inclination. Figure 44 presents an eclipse duration ratio as a

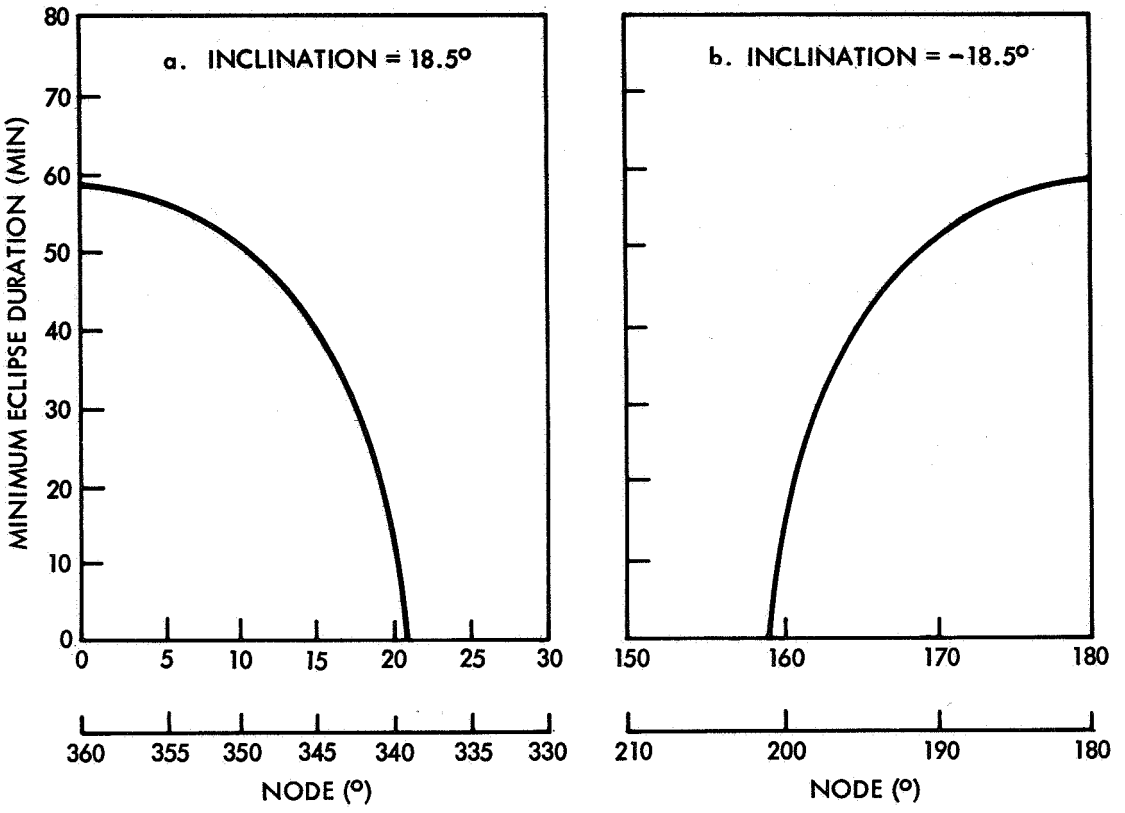

Figure 43. Minimum Eclipse Duration for Continual Seasons

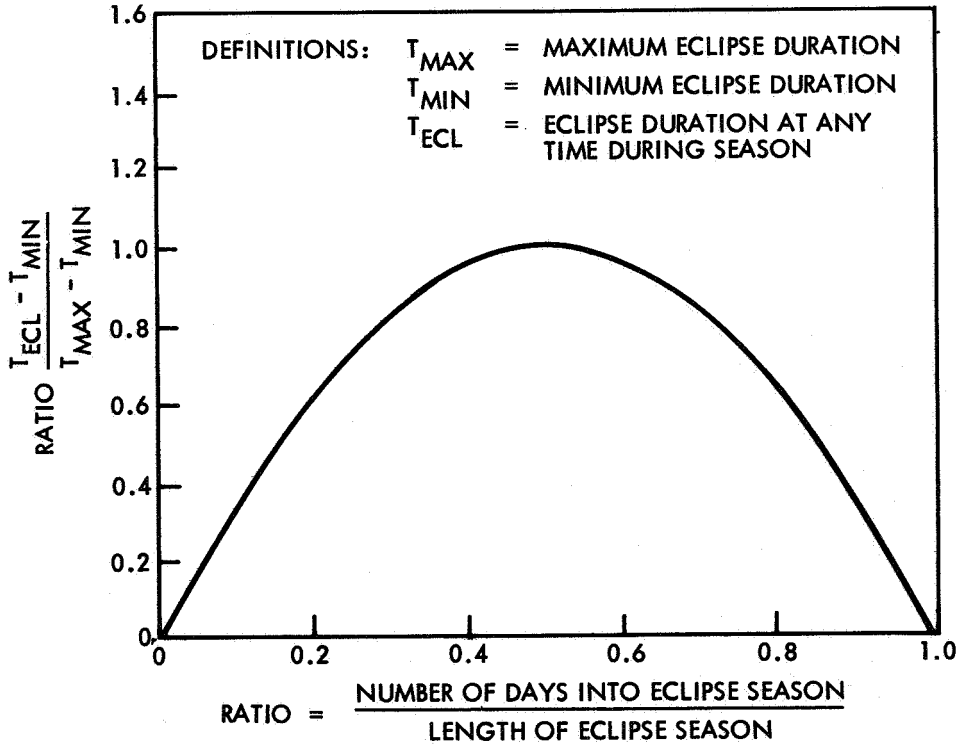

Figure 44. Eclipse Duration Ratio for Continual Eclipse Season

function of time into the eclipse season. To understand the use of the eclipse duration ratio, the following definitions are made:

T_{MAX} = maximum eclipse duration (70.5 min for the system as proposed)

T_{MIN} = minimum eclipse duration, which is a function of the injection node and is obtained from Figure 43.

T_{ECL} = eclipse duration at any time during the season.

$$\text{Eclipse duration ratio} = \left[\frac{T_{ECL} - T_{MIN}}{T_{MAX} - T_{MIN}}\right] = \left[\frac{T_{ECL} - T_{MIN}}{70.5 - T_{MIN}}\right]$$

With these definitions, Figures 43 and 44 may be combined to produce the eclipse durations at any time during the eclipse season for those injection nodes producing continuous seasons by first finding the value of T_{MIN} from Figure 43 for any injection node under consideration. The eclipse duration at any time in the season, then, is found by obtaining the eclipse duration ratio from Figure 44 and

$$T_{ECL} = (\text{eclipse duration ratio})(T_{MAX} - T_{MIN}) + T_{MIN}$$

Although this presentation at first appears more awkward to utilize than the method used for the two distinct seasons, it regains some simplicity when it is realized that the ordinate of Figure 44 becomes the fractional part of maximum minus minimum eclipse duration.

To complete the analysis, solar time of injection as functions of time of year and injection node are presented in Figure 45. With this figure, it is possible to specify the time of injection (and, hence, launch time) to meet any eclipse season and/or eclipse duration specified.

The accuracy of this analysis is limited solely by the use of unperturbed orbits and a spherical earth. The effects of an aspherical earth are such that the maximum eclipse duration becomes a function of the time of day of injection, but the variation is less than 5 percent. The effects of the orbit perturbations consist primarily of a slight distor-

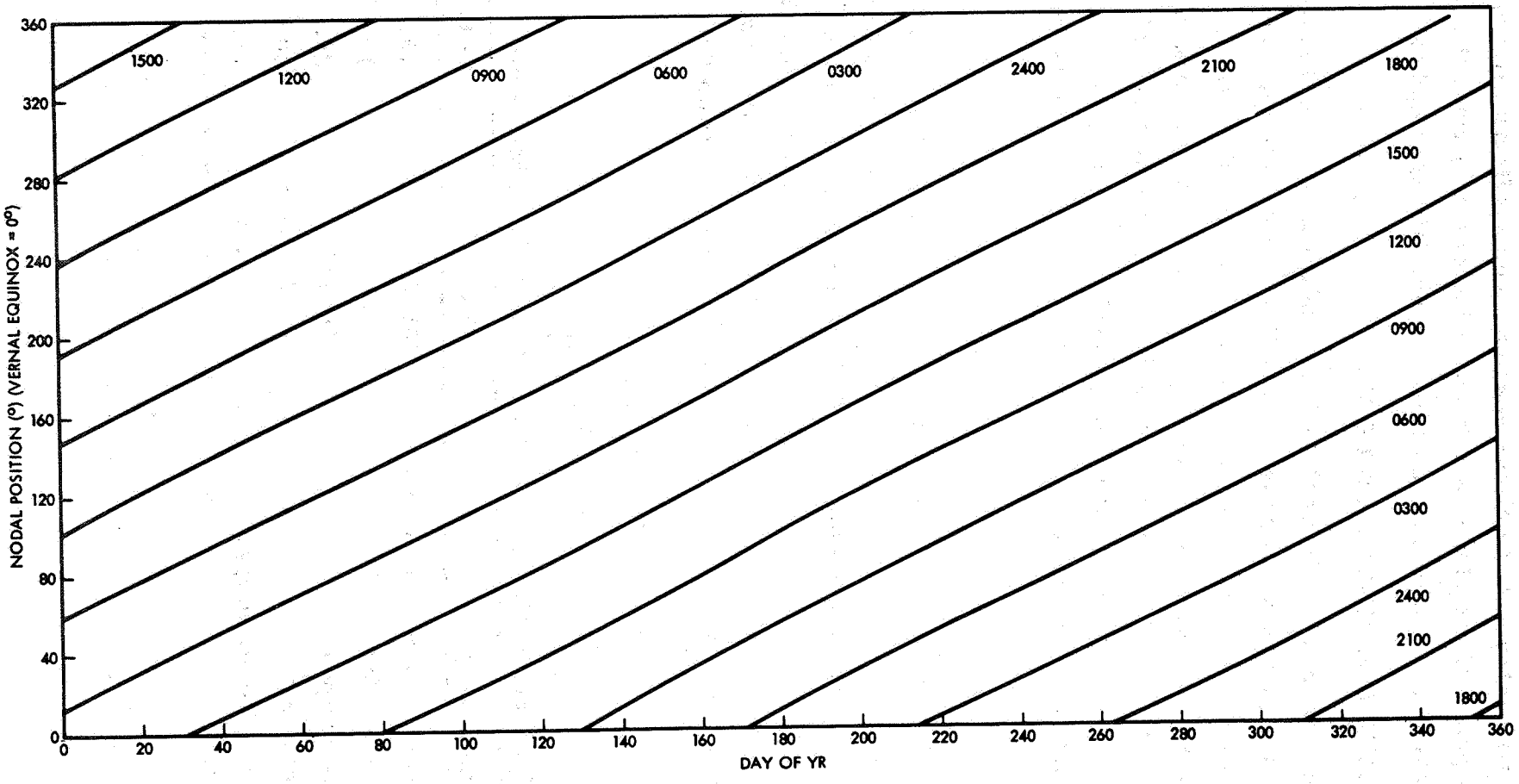

Figure 45. Local Solar Time as Function of Day of Year and Nodal Position

tion of the symmetry of the eclipse season. These effects are negligible during this phase of the study, and become factors only when the system requirements become well defined and a launch date approaches.

4.3 SELECTION OF INJECTION NODES

From a spacecraft thermal design standpoint, it is desirable for the eclipse seasons to be as short as possible and for all spacecraft in the system to experience the same eclipse durations and seasons. For the electrical power system, it is desirable to have the orbit planes as close to the plane of the ecliptic as possible to obtain an angle of incidence of the sun's rays as nearly normal as possible. Power system design is also simplified if all spacecraft in the system receive solar radiation at the same angle of incidence.

These factors are affected by the injection nodes chosen; an analysis was made to determine the most favorable injection nodes with respect to the above requirements. With the given constraints of 18.5° orbit-plane inclination and 157.5° nodal separation, it was found that the injection nodes shown in Table XXVIII yielded the minimum inclination angle to the ecliptic plane, with the associated eclipse parameters as shown.

TABLE XXVIII

INJECTION NODES AND ASSOCIATED PARAMETERS

Parameter	Plane 1	Plane 2
Right ascension of injection node	281.25°	78.75°
Inclination to equator	18.5°	18.5°
Inclination to ecliptic	26.54°	26.54°
Length of eclipse season	40.7 days	40.7 days
Duration of maximum eclipse	70.8 min	70.8 min

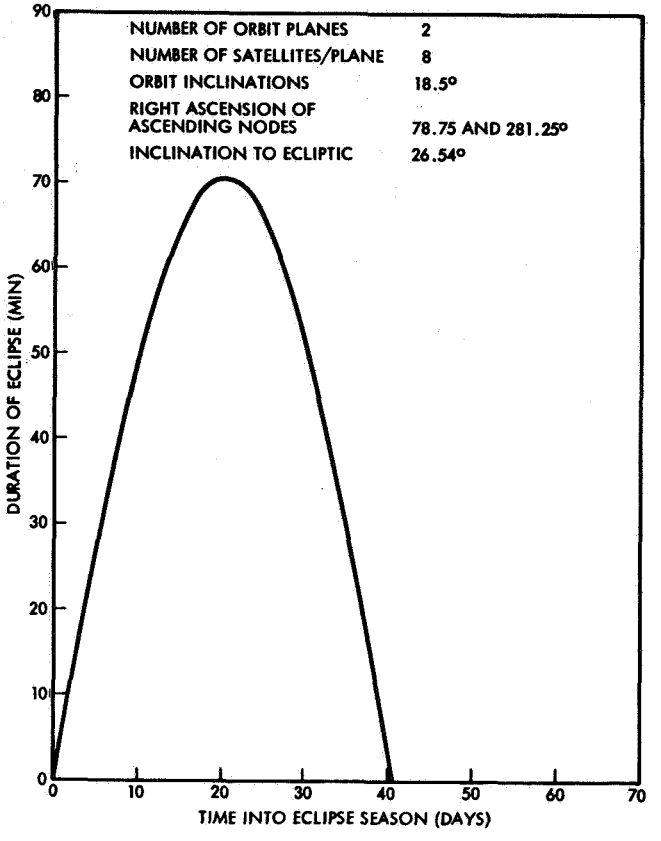

Figure 46. Eclipse Duration for Proposed Navigation Satellite System

Figure 46 shows the eclipse duration for these injection nodes; it is identical for all satellites in the system. Figure 47 shows the injection epochs (as functions of the day of the year) for achieving the indicated nodal positioning.

At the present time, there are insufficient subsystem-requirements data to establish launch-window criteria, and a launch-window analysis has not been performed for the system described in this document. It is possible, however, to indicate the effects of off-nominal launch time on the inclination of the orbit planes to the ecliptic (which, in turn, affects the length of the eclipse season). These variations are shown in Figure 48 as a function of deviation of launch time from the nominal.

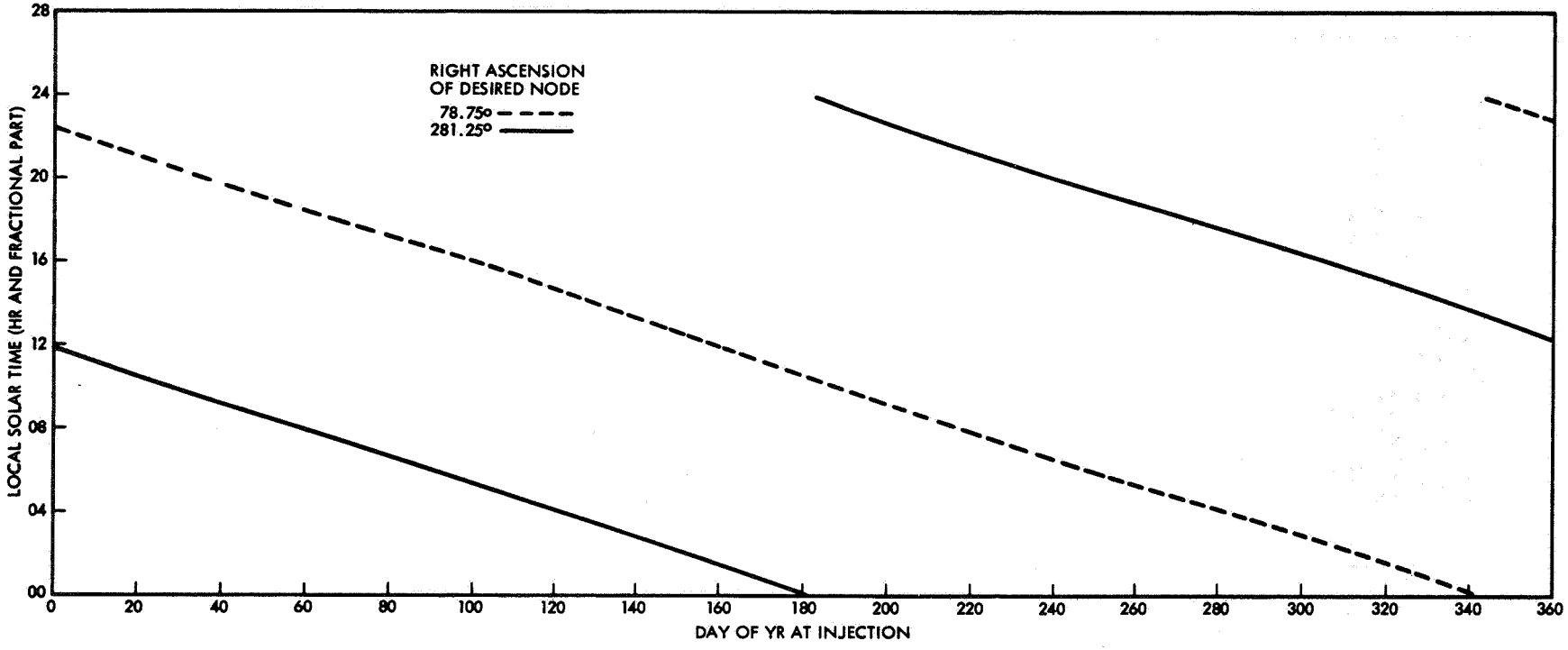

Figure 47. Injection Epochs for Achieving Desired Nodal Positioning

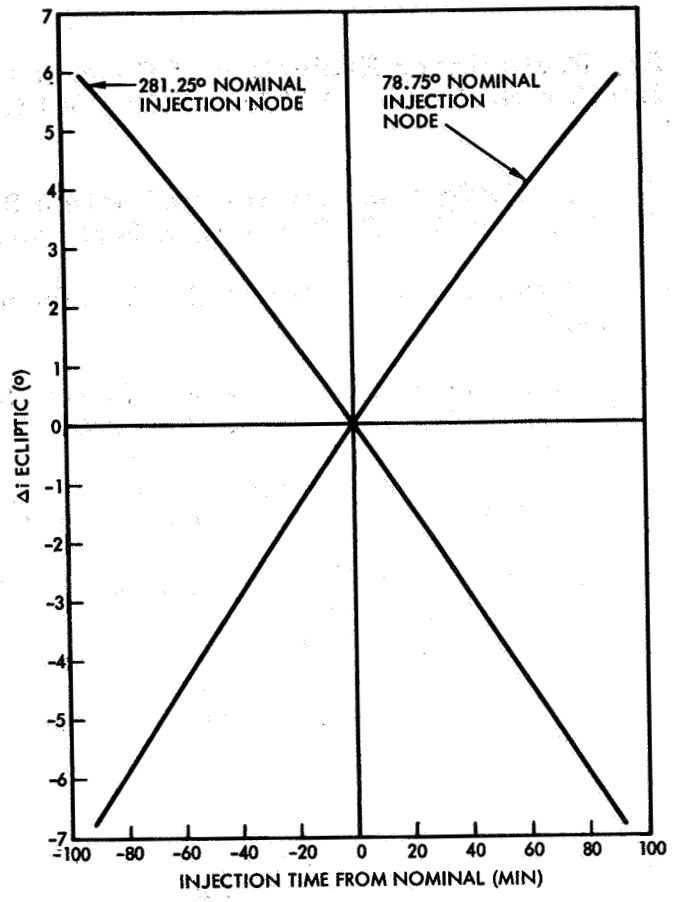

Figure 48. Variation of Orbit Inclination to Ecliptic from Nominal Inclination as Function of Injection Time off Nominal

REFERENCES

1. Mielak, E. B., Preliminary Evaluation of Coverage for Several Navigation Satellite Systems, TRW Memo No. 3414.1-56, 9 June 1967

2. Wilkerson, J. L., "Navigation Satellite Refraction Range Errors (Revised)," TRW Memo No. 7323.3-115, 8 September 1966

3. Millman, G. H., "Radar Propagation," G. E. Report No. R60 EMH 36, June 1960

4. Holmes, F. M., "Navigation Satellite Constellation Study," TRW Report No. 09424-6001-T000, 14 November 1967

5. Mallinckrodt, A. J., "Oscillator Error Statistics for NAVSAT," TRW Report No. 08710-6005-T000, 22 August 1967

6. Wong, G. G., "NAVSAT Hardware Error Sources," TRW Memo No. 67-7321.3-71, 26 June 1967

7. Wyndham, J. D., Geodesy and the Determination of Station Coordinates, TRW Report 3412.9-102, 14 April 1967

8. Francis, M. P., Gedeon, G. S., and Douglas, B. C., "Perturbations of Repeating Groundtrack Satellites by Tesseral Harmonics in the Gravitational Potential," AIAA Journal, Vol. 4, No. 7, July 1966, pp 1281-1286

9. Mallinckrodt, A. J., "Frequency Synchronization for Doppler Tracking Systems," Part II, Propagation Modes, Communication Research Labs, CRL 509, 20 June 1966

10. Thompson, Janes, and Kirkpatrick, "An Analysis of Time Variations in Tropospheric Refractive Index and Apparent Path Length," Journal Geophysics Research V 65, p 201, 1960

11. James, Kirkpatrick, Waters and Smith, "Phase and Amplitude Diversity in Over-Water Transmissions at Two Microwave Frequencies," NBS Report 7656, February 1963

APPENDIX A

NEW TECHNOLOGY

New technology and innovations developed under this contract are discussed in the appendix to vol. I.

APPENDIX B

WORLDWIDE ACCURACY PROGRAM (MSAT)

1. INTRODUCTION

This appendix contains both a development of the theory for determining navigation accuracies using range-type measurements from satellites and a description of the computer program developed from this theory. The MSAT program provides the capability for a quick analysis of postulated navigation satellite systems, while the NAVSAP program (app. J) provides a more general capability for analysis. In addition, since NAVSAP performs a more complicated operation, the cost is higher for preliminary analysis, and furthermore, NAVSAP is limited to seven satellites.

The MSAT program is applicable to systems employing range-type measurements only. That is, the user obtains estimates of the ranges from his location to the visible satellites or range differences from his location to two satellites.

The problem may be stated as follows. Given the location and inertial azimuth of the satellites in the system, the location of the user, the orbit-plane position uncertainties of the satellites, the measurement noise sigma, the satellite contributed measurement bias sigma, the user contributed bias sigma, and the user visibility constraints, to what accuracy can the position of the user be determined with range measurements to the visible satellites? It is assumed in the development that the user solves for his position and measurement bias; that satellite position errors and bias are "considered"* parameters; and that satellite position errors are independent of other satellite position errors and satellite measurement bias.

The essentials of the theory are covered in sec. 2, and a flow diagram for MSAT is presented as Figure B-1 at the end of this appendix.

*Considered parameters are parameters which are not estimated but whose affects are considered in the error analysis. In this case, user observations not used to solve for satellite positions, but the effects of errors in satellite position on user position are considered.

2. THEORY

Consider a user with ECI coordinates, x_u, y_u, and z_u. The ECI coordinate system is defined as the x axis passing through the Greenwich meridian in the plane of the equator and the z axis through the North Pole. The user receives a range measurement, r_i, from the i^{th} satellite which has coordinates x_i, y_i, and z_i. This range measurement is equal to the linear sum of the following: the true range from the user to the satellite, $\tilde{r}_i$; the user bias, b_u; measurement noise, η_i; and minus the satellite bias, b_i. That is,

$$r_i = \tilde{r}_i + b_u - b_i + \eta_i \tag{B-1}$$

The signs on the biases are chosen for convenience only. From geometry,

$$\tilde{r}_i^{\,2} = (x_u - x_i)^2 + (y_u - y_i)^2 + (z_u - z_i)^2 \tag{B-2}$$

From variations in Eq. (B-2), perturbations in the true range can be expressed as a function of perturbations in the user and satellite coordinates as,

$$\begin{aligned} \delta\tilde{r}_i = {} & \cos\alpha_i\,(\delta x_u - \delta x_i) \\ & + \cos\beta_i\,(\delta y_u - \delta y_i) \\ & + \cos\gamma_i\,(\delta z_u - \delta z_i) \end{aligned} \tag{B-3}$$

where $\cos\alpha_i = \dfrac{x_u - x_i}{\tilde{r}_i}$, etc.

Define the solve-for vector and consider vector

$$\begin{aligned} x &= (x_u \;\; y_u \;\; z_u \;\; b_u)^T \\ z_i &= (x_i \;\; y_i \;\; z_i \;\; b_i)^T \end{aligned} \tag{B-4}$$

From all of the visible satellites, the above equations can be combined to yield

$$\begin{bmatrix} \delta r_1 \\ \delta r_2 \\ \delta r_n \end{bmatrix} = \begin{bmatrix} A_1 \\ A_2 \\ A_n \end{bmatrix} \delta x - \begin{bmatrix} A_1 & & 0 \\ & A_2 & \\ 0 & & A_n \end{bmatrix} \begin{bmatrix} \delta z_1 \\ \delta z_2 \\ \delta z_n \end{bmatrix} + \begin{bmatrix} \eta_1 \\ \eta_2 \\ \eta_n \end{bmatrix} \qquad \text{(B-5)}$$

where

$$A_i = \left[\cos \alpha_i \cos \beta_i \cos \gamma_i \; 1\right]$$

which is in the desired linear form

$$\bar{Y} = A\,\bar{X} + B\,\bar{Z} + \bar{n} \qquad \text{(B-6)}$$

where $\bar{Y}$ is the observation vector, $\bar{X}$ is the vector of parameters to be estimated, $\bar{Z}$ is the vector of parameters to be considered, and $\bar{n}$ is the noise vector. The well known covariance matrix of the estimate is

$$P(\hat{x}) = (A^T P_n^{-1} A + P_o^{-1})^{-1} + (A^T P_n^{-1} A + P_o^{-1})^{-1} \cdot A^T P_n^{-1} B P_z B^T P_n^{-1} A (A^T P_n^{-1} A + P_o^{-1})^{-1} \qquad \text{(B-7)}$$

where $P(\hat{x})$ = covariance matrix of estimate
P_o = a priori covariance matrix of $\bar{X}$
P_z = a priori covariance matrix of $\bar{Z}$
P_n = noise covariance matrix.

With the assumption of independent noise,

$$P_n = \sigma_n^2 I \qquad \text{(B-8)}$$

where I is the identity matrix, and the independent satellite errors are

$$P_z = \begin{bmatrix} Q_1 & & & 0 \\ & Q_2 & & \\ & & \ddots & \\ 0 & & & Q_n \end{bmatrix} \qquad \text{(B-9)}$$

where Q_1 is the 4x4 covariance matrix of ECI satellite position errors and bias variance

$$Q_i = \begin{bmatrix} P_{s_i}{}^{(3x3)} & & 0 \\ & & \\ 0 & & q_{b_i}^2 \end{bmatrix} \qquad \text{(B-10)}$$

The covariance matrix of the user's estimate in ECI coordinates is

$$P^*(\hat{x}) = \left(\frac{1}{\sigma_n^2} \sum_1^n A_i{}^T A_i + P_o^{-1} \right)^{-1} \quad \text{(no satellite errors)} \qquad \text{(B-11)}$$

$$P(\hat{x}) = P^*(\hat{x}) + \left(\frac{1}{\sigma_n} \right)^4 P^*(\hat{x}) \left(\sum_1^n A_i{}^T A_i Q_i A_i{}^T A_i \right) P^*(\hat{x})$$

(with satellite errors)

(B-12)

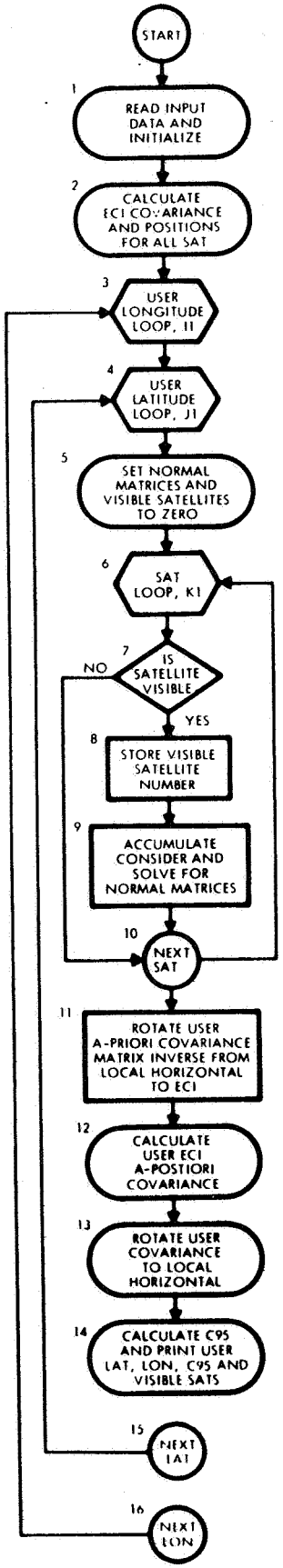

Figure B-1. MSAT Flow Diagram

APPENDIX C

PHASED SATELLITE COVERAGE PROGRAM (AT-034)

An analytical computer program is available to analyze the ground coverage of a system of satellites phased in orbit with respect to each other. Circular or elliptical orbits may be considered. Given the initial condition of each satellite, the program determines rise and set times with respect to each ground station. As many as four orbit planes consisting of ten satellites in each plane can be examined with respect to one or two ground stations.

The output quantities include the percentage of time that at least $n(0 \leq n \leq 10)$ satellites are visible, the probability distribution of satellite "outrate" (not visible) time, and the probability distribution of satellite visibility time.

The running time depends upon the number of satellites in the system and the number of orbits necessary to establish valid statistical data. The typical time is one minute for a case providing statistical data at one pair of ground stations.

APPENDIX D

WORLD MAP GENERATING PROGRAM (AT-86)

AT-86 is a general-purpose program designed to draw maps on the 10 or 30 in. CALCOMP plotter. The program will optionally draw the following:

a) A map of the world

b) Lines of constant latitude and longitude

c) A satellite earth trace

d) Visibility circles for a circular satellite

e) City designations, represented by various symbols on the map.

These options may be utilized one per map or all may be included on one map.

The projections optionally available are:

a) A plate carrée projection (latitude and longitude equally spaced)

b) A satellite map projection on which a satellite in a circular or eccentric orbit traces a straight line

c) A polar projection with an arbitrary point on the earth as the center of the projection.

When a polar projection is selected, an additional option of lines of constant latitude and longitude symmetric about a set of poles of variable position is available.

APPENDIX E

APPLICATION OF NAVSAP TO ESTIMATION OF VELOCITY FROM DOPPLER DATA

The NAVSAP program does not contain the user's velocity components in the state vector. Therefore, several modifications to the normal mode of operation must be made in order to apply the program to velocity estimation. These modifications are based on the fact that the measurement matrix for range measurements used to estimate user position is identical to range-rate measurements used to estimate velocity. That is,

$$\frac{\partial R}{\partial \underline{X}_{sat}} = \frac{\partial \dot{R}}{\partial \underline{X}_{sat}} = -\frac{\partial R}{\partial \underline{X}_{user}} = -\frac{\partial \dot{R}}{\partial \underline{X}_{user}} = \left[\frac{x}{R} \; \frac{y}{R} \; \frac{z}{R}\right]$$

where x, y, and z are cartesian coordinates of the relative position $\underline{R}$ between the satellites and ground user. Hence, range measurements were simulated, but velocity a priori covariance matrices were inserted in place of position a priori covariance matrices, and the measurement error used was the velocity error of 0.707 ft/sec.

This usage of the program neglects error contributions from user position error uncertainties. These negligible effects are justified below, based on the consideration that user position components are only weakly observable in doppler data. Let

$\delta\dot{y}$ = variation in range-rate measurement vector $\dot{y}$

$\delta\dot{x}$ = variation in user's velocity vector $\dot{x}$

δx = variation in user's position vector x

η = range-rate measurement error vector

$Q_{\dot{x}}$ = user's a priori velocity error covariance matrix

Q_x = user's a priori position error covariance matrix

$Q\eta$ = measurement noise error covariance matrix

$W = Q_\eta^{-1}$

The linear observation model is

$$\delta\dot{y} = A\,\delta\dot{x} = B\,\delta x + \eta$$

where A and B are the appropriate partial derivative matrices. If the program had used the measurements to solve for $\dot{x}$, but considered the errors in x, the a posteriori errors in $\dot{x}$ would have been

$$\Sigma_{\dot{x}} = (A^T W A + Q_{\dot{x}}^{-1})^{-1} + (A^T W A + Q_{\dot{x}}^{-1})^{-1}$$

$$A^T W B\, Q_x\, B^T W A (A^T W A + Q_{\dot{x}}^{-1})^{-1}$$

The program calculated only the first term of the above. This is equivalent to assuming that BQ_xB^T is small compared to Q_η, which follows from an alternate form of the above equation:

$$\Sigma_{\dot{x}} = (A^T W A + Q_{\dot{x}}^{-1})^{-1} \left[A^T W (Q_\eta + BQ_xB^T) W A + Q_{\dot{x}}^{-1} \right]$$

$$(A^T W A + Q_{\dot{x}}^{-1})^{-1}$$

that $BQ_xB^T << Q_\eta$ can be seen from a simple hand check using typical standard deviations for x and η. Since

$$\dot{R} = \frac{x\dot{x} + y\dot{y} + z\dot{z}}{R}$$

where $\dot{x}$, $\dot{y}$ and $\dot{z}$ are the components of the relative velocity between the satellite and ground user, it follows that a typical term of B is

$$b \sim \frac{\partial R}{\partial X_u} : = -\frac{R\dot{x} - x\dot{R}}{R^2} \leq \frac{\dot{x} + \dot{R}}{R} < \frac{3 \times 10^3}{1.2 \times 10^8} = 2.5 \times 10^{-5}$$

Hence, a typical diagonal term of BQ_xB^T is

$$(\sigma_x^2 B^2)_{diag} \sim \sigma_x^2 (3b)^2 \sim (400)^2 [3(2.5 \times 10^{-5})]^2 = 9 \times 10^{-4}$$

Comparing this to a diagonal term of Q_η ($\sigma_\eta^2 \sim 0.5$), it is apparent that the approximation is justified.

It is proposed to increase the dimension of the user's state vector in NAVSAP from three to six in order to estimate user position and velocity simultaneously. This modification will permit a more complete treatment of the velocity estimation errors, with or without doppler measurements.

APPENDIX F

RELATIVE NAVIGATION ACCURACY ANALYSIS USING THE NAVSAP PROGRAM

As indicated in subsec. 2.3.4 in the main body of this report, the error covariance matrix of relative error of user 2 with respect to user 1 is given by

$$\Sigma_R = \Sigma_{11} + \Sigma_{22} - \Sigma_{12} - \Sigma_{21} \tag{F-1}$$

where

$$\begin{aligned} \Sigma_{11} &= \Sigma_{1n} + \Sigma_{1s} \\ \Sigma_{22} &= \Sigma_{2n} + \Sigma_{2s} \end{aligned} \tag{F-2}$$

The question treated in this appendix is how to compute these component error-covariance matrices using the NAVSAP error analysis program described in (app. J).

The satellite states x_1 and x_2 are estimated based on the usual linearized tracking model*.

$$\begin{aligned} y_1 &= A_1 x_1 + B_1 z + \epsilon_1 \\ y_2 &= A_2 x_2 + B_2 z + \epsilon_2 \end{aligned} \tag{F-3}$$

where y_1, y_2 are the observations by users 1 and 2, and z is the vector of the common error sources of satellite position and clock errors. x, y, and z are to be interpreted as deviations from reference values, a and ϵ_1, ϵ_2 are the measurement errors. The users will estimate their positions from

$$\begin{aligned} \hat{x}_1 &= (A_1^T W_1 A_1)^{-1} A_1^T W_1 y_1 \\ \hat{x}_2 &= (A_2^T W_2 A_2)^{-1} A_2^T W_2 y_2 \end{aligned} \tag{F-4}$$

*See par. 2.3.4 for notation and definition of terms.

where

$$W_1 = \left[E(\epsilon_1 \epsilon_1^T)\right]^{-1}$$
$$W_2 = \left[E(\epsilon_2 \epsilon_2^T)\right]^{-1} \qquad \text{(F-5)}$$

These estimates are minimum variance only in the absence of the satellite errors z. The estimation error covariance matrices which account for the effect of z are

$$\Sigma_{11} = E(\delta x_1 \delta x_1^T) = (A_1^T W_1 A_1)^{-1} + (A_1^T W_1 A_1)^{-1} A_1^T W_1 B_1 Q B_1^T W_1 A_1 (A_1^T W_1 A_1)^{-1} \qquad \text{(F-6)}$$
$$\Sigma_{22} = E(\delta x_2 \delta x_2^T) = (A_2^T W_2 A_2)^{-1} + (A_2^T W_2 A_2)^{-1} A_2^T W_2 B_2 Q B_2^T W_2 A_2 (A_2^T W_2 A_2)^{-1}$$

where $Q = E(zz^T)$ is the satellite error covariance matrix and the terms on the right side of Eq. (F-6) are Σ_{1n}, Σ_{1s}, Σ_{2n}, Σ_{2s} as given in Eq. (F-2). The remaining term required for the evaluation of the relative error accoring to Eq. (F-1) is Σ_{12}. This follows from Eqs. (F-4) and (F-3) in the same way that Eq. (F-6) is obtained. The result is

$$\Sigma_{12} = E(\delta x_1 \delta x_2^T) = (A_1^T W_1 A_1)^{-1} A_1^T W_1 B_1 Q B_2^T W_2 A_2 (A_2^T W_2 A_2)^{-1} \qquad \text{(F-7)}$$

Denoting the correlations between user and satellite errors as Σ_{1z} and Σ_{2z} and noting from Eqs. (F-2) and (F-3) that

$$\Sigma_{1z} = E(\delta x_1 z^T) = (A_1^T W_1 A_1)^{-1} A_1^T W_1 B_1 Q$$
$$\Sigma_{2z} = E(\delta x_2 z^T) = (A_2^T W_2 A_2)^{-1} A_2^T W_2 B_2 Q \qquad \text{(F-8)}$$

it follows that Eq. (F-7) can be written

$$\Sigma_{12} = \Sigma_{1z} Q^{-1} \Sigma_{2z}^T \qquad \text{(F-9)}$$

Consequently Eq. (F-1) becomes

$$\Sigma_R = \Sigma_{11} + \Sigma_{22} - \Sigma_{1z} Q^{-1} \Sigma_{2z}^T - \Sigma_{2z} Q^{-1} \Sigma_{1z}^T \qquad \text{(F-10)}$$

An alternate form of Eq. (F-10) is obtained from Eqs. (F-6) and (F-8)

$$\Sigma_R = \Sigma_{1n} + \Sigma_{2n} + \Sigma_{1z} Q^{-1} \Sigma_{1z}^T + \Sigma_{2z} Q^{-1} \Sigma_{2z}^T$$

$$- \Sigma_{1z} Q^{-1} \Sigma_{2z}^T - \Sigma_{2z} Q^{-1} \Sigma_{1z}^T \qquad \text{(F-11)}$$

The first terms are the estimation errors without satellite errors. The remaining terms tend to cancel as Σ_{2z} approaches Σ_{1z}.

A single run on NAVSAP corresponding to user 1 produces the matrices Σ_{11} and Σ_{1s}. A second run results in Σ_{22} and Σ_{2s}, and Q is input. Furthermore, by setting satellite errors to zero, the individual terms Σ_{1n} and Σ_{2n} can be computed. In this way the individual columns of the table in subsec. 2.3.4 were computed and assembled into the final relative navigation error covariance matrix of Eqs. (F-10) or (F-11).

APPENDIX G

ESPOD – PRECISION ORBIT DETERMINATION PROGRAM

1. PROGRAM DESCRIPTION

The AT4 System was designed to support the Able and early Ranger launches. Subsequent development led to a family of orbit-determination programs covering a range of applications from real-time operations to a solution for gravitational harmonics using the simultaneous observations of several satellites. The current ESPOD Orbit Determination Program is the result of 7 years of development effort. This program is the basis for several other closely related special-purpose programs, and has basic characteristics common to the entire family of programs.

The ESPOD program is a precision-trajectory propagation and statistical orbit determination program written in FORTRAN IV language. Versions of the program operate on the IBM 7094, IBM 7030, IBM 360, GE 635, and SDS 9300 computers.

The force model includes a recursive computation of the central body gravitational accelerations, allowing inclusion of harmonics of any desired degree and order. Aerodynamic drag may be computed by using the COESA static, Paetzold, or Lockheed Jacchia (1964) dynamic atmospheres. Gravitational attractions due to other bodies in the solar system are computed by using planetary ephemerides stored on tape. Provision has been made to account for vehicle thrusting, low thrusts due to random venting, and radiation pressure.

The trajectory is computed by numerical integration of the equations of motion using a 10th-order Cowell formulation, with an automatically computed, variable step size.

Integration takes place in the mean of 1950.0 coordinate frame centered at an arbitrary body. All rotations required for proper evaulation of the gravitational potential and representation of observations are performed.

Observation types that are accepted by the program and used to differentially correct the components of the solution vector include the following:

1) Range, azimuth, and elevation

2) Topocentric right ascension and declination

3) Geocentric right ascension and declination

4) Range rate

5) Range acceleration

6) One-, two-, and three-way doppler data

7) Range differences and range-rate differences (interferometer measurements)

8) Rectangular components of estimated position

9) Accelerations as measured by onboard accelerometers

Sensors taking observation types 1 through 8 may be located on the central body, on any other body for which coordinates are available, or onboard the vehicle.

Corrections to the components of the solution vector are computed by using an iterative weighted-least-squares process. Provision for bounding the size of the corrections or any given iteration and automatic convergence logic has been included. The program will compute corrections to the following quantities:

- Initial position and velocity in terms of Cartesian or polar-spherical coordinates, Keplerian elements, or a special set of α-variables designed to improve the numerical conditioning of the differential correction process
- Ballistic coefficient
- Burn parameters, including thrust-to-weight ratio, flow rate, body-orientation angles, and body-axis rates
- Potential constants of the central body (any degree and order)

- Observational and timing biases
- Observation of station locations
- Any linear combinations of the above

All program constants, error bounds (e.g., on step-size control), and contributors to the force model may be easily modified on input.

A completely flexible phase logic allows use of several central bodies in succession, interspersed free-flight and powered-flight arcs, and accurate prediction of reentry trajectories. The phase logic, plus several special coordinate transformations, are combined in a version of ESPOD which is designed to track lunar satellites.

The trajectory and the covariance matrices describing uncertainties in the components of the solution vector may be output in any of ten coordinate systems. Provision has been made for updating covariance matrices to any desired epoch. Prior estimates of the solution vector components, along with uncertainties in these estimates, may be input to the program to be combined statistically with the estimate derived from the current observation data. In addition, the effects of uncertainties in parameters not included in the solution vector (e.g., certain gravitational harmonics) may be accounted for in the computation to the covariance matrix for those parameters that have been included.

The ESPOD program has been employed in real data analyses for flight reconstruction of Vela, Minuteman, Gemini, and Apollo. The Gemini and Apollo experiences indicate that a complete revolution of tracking data (approximately 1000 points) can be processed and used to compute a differential correction to the orbital elements in less than 1 min on the IBM 7094-Mod II.

Recent modifications have given the program complete capability for analysis of errors in the estimation process. In particular, the effect of errors in parameters not estimated can be treated in a straightforward manner. Also of interest for navigation satellite error analysis is a modification, currently in progress, that will enable the simultaneous tracking of multiple vehicles.

2. ESPOD GENERAL PRINCIPLES

2.1 Estimation Theory

To introduce and to define the terminology, consider the trajectory estimation problem in the presence of random errors only. Let x be the actual vehicle state vector of position and velocity at some epoch and let n be the vector of unbiased Gaussian random noise on the vector of measurements y. Then, if the equation relating the measurements to the state vector, $y = f(x)$, is expanded in a first-order Taylor's series about a reference trajectory, we have

$$\delta y = A\,\delta x + n$$

where $A = \partial f/\partial x$. δy is the difference between the observed and computed measurements, and δx is a small deviation from the reference state vector. Then, the weighted-least-squares estimate of δx is

$$\hat{\delta x} = \left(A^T W A\right)^{-1} A^T W\,\delta y$$

and the covariance of the estimate is

$$\Sigma_x = \left(A^T W A\right)^{-1}$$

where W^{-1} is the covariance of the noise, n. The matrix $A^T W A$ is often referred to as the tracking normal matrix.

As the amount of data increases, the covariance of the estimate $(A^T W A)^{-1}$ approaches zero. In reality no such simple state of affairs exists. First and most important, the errors or noise on the measurements do not have a zero mean, i.e., the measurement biases, station location errors, etc. (called systematic errors) are not zero. Secondly and less important, since random errors are normally a relatively small magnitude, it is unlikely that the noise is strictly Gaussian distributed. Finally, errors in the modeling of the physical situation will also contribute to uncertainty in the state vector. Thus, one expects that uncertainty will first decrease, but then may level off or increase due to the systematic effects.

It is possible to reduce this uncertainty by solving for systematic errors in the estimation process. Let z be the vector of systematic errors to be included in the solution vector and let B be a matrix relating small changes in z to small changes in the measurements y. Then

$$\delta y = A\,\delta x + B\,\delta z + n$$

or

$$\delta y = \left(A \mid B\right)\left[\begin{array}{c}\delta x \\ \hline \delta z\end{array}\right] + n$$

The corresponding least-squares estimates of x and z are found to be

$$\left[\begin{array}{c}\delta x \\ \delta z\end{array}\right] = \left(\left[A \mid B\right]^T W \left[A \mid B\right]\right)^{-1} \left[A \mid B\right]^T W\,\delta y$$

or

$$\left[\begin{array}{c}\delta x \\ \hline \delta z\end{array}\right] = \left[\begin{array}{c|c}A^T W A & A^T W B \\ \hline B^T W A & B^T W B\end{array}\right]^{-1} \left[\begin{array}{c}A^T W \\ \hline B^T W\end{array}\right] \delta y,$$

and the covariance of the solution parameters is

$$\Sigma = \left[\begin{array}{c|c}A^T W A & A^T W B \\ \hline B^T W A & B^T W B\end{array}\right]^{-1}$$

That is, the solution now converges to an estimate that yields an essentially unbiased noise and residual vector. However, one cannot solve for every one of the large number of parameters that might conceivably affect the solution. Indeed, it is desirable to solve for as few as possible, while including the error resulting from the unsolved parameters. Then, if any of these unsolved parameters cause an intolerable error, one can consider solving for it. The technique for evaluating the uncertainty caused by the unestimated parameters is derived below.

Let x be the vector of all solved-for parameters, z be the vector of all unsolved-for parameters (whether their effect be a bias or a time-varying influence), and let n be the Gaussian random noise on the measurements. As before

$$\delta y = A\,\delta x + B\,\delta z + n$$

The weighted least-squares estimate of δx is

$$\hat{\delta x} = \left(A^T W A\right)^{-1} A^T W\,\delta y\,, \qquad \text{(G-1)}$$

and the error in the estimate is

$$\hat{\delta x} - \delta x = \left(A^T W A\right)^{-1} A^T W\,(B\,\delta z + n) \qquad \text{(G-2)}$$

If W^{-1} is set equal to the covariance of the noise, and the noise is assumed to be independent of the unsolved-for parameters, the following is obtained for the total covariance on the estimate, δx:

$$\text{cov}\,(\hat{\delta x}) = \Sigma_x = \left(A^T W A\right)^{-1} + \left(A^T W A\right)^{-1} A^T W B\,\Sigma_z\,B^T W A \left(A^T W A\right)^{-1} \qquad \text{(G-3)}$$

The first term is a contribution from only the random noise, and the second term contains the contribution from the unsolved-for parameters. Σ_z is the covariance of these unsolved-for parameters. Both of the terms are functions of the amount of tracking data. A characteristic of the $(A^T W A)^{-1}$ matrix is that it decreases roughly as the square root of the amount of data, while the characteristic behavior of the second matrix is that it increases with time or the amount of tracking data.

2.2 Combining Two Least-Squares Estimates

It is often required to combine two least-squares estimates when it is desired to combine current tracking data with some a priori estimate. Then the new estimate δx, resulting from combining the two estimates δx_1 and δx_2, with covariance matrices Σ_1 and Σ_2, respectively, is

$$\delta x = \left(\Sigma_1^{-1} + \Sigma_2^{-1}\right)^{-1} \left(\Sigma_1^{-1}\, \delta x_1 + \Sigma_2^{-1}\, \delta x_2\right)$$

and the new covariance matrix is

$$\Sigma = \left(\Sigma_1^{-1} + \Sigma_2^{-1}\right)^{-1}$$

2.3 Propagation Matrices

It is often desirable to propagate a least-squares estimate from time t_1 to time t_2. The linearized equations for the propagation are

$$\delta x_2 = \frac{\partial x_2}{\partial x_1}\, \delta x_1 + \frac{\partial x_2}{\partial z_1}\, \delta z_1 \qquad \text{(G-4)}$$

and

$$\delta z_2 = \frac{\partial z_2}{\partial x_1}\, \delta x_1 + \frac{\partial z_2}{\partial z_1}\, \delta z_1 \qquad \text{(G-5)}$$

where it is assumed that x_i is the vector of vehicle parameters at time i, and z_i is the vector of systematic errors at time i for i = 1, 2. Since the systematic errors are not affected by the orbit parameters,

$$\frac{\partial z_2}{\partial x_1} = 0$$

and if it is assumed that the systematic errors are constant, regardless of epoch time, then

$$\frac{\partial z_2}{\partial z_1} = I$$

where I is the identity matrix. Thus, Eqs. (G-4) and (G-5) become

$$\begin{bmatrix} \delta x_2 \\ \\ \delta z_2 \end{bmatrix} = \begin{bmatrix} \dfrac{\partial x_2}{\partial x_1} & \dfrac{\partial x_2}{\partial z_1} \\ \\ O & I \end{bmatrix} \begin{bmatrix} \delta x_1 \\ \\ \delta z_1 \end{bmatrix}$$

when written in matrix form.

The propagated covariance matrix is given by

$$\Sigma_2 = \begin{bmatrix} \dfrac{\partial x_2}{\partial x_1} & \dfrac{\partial x_2}{\partial z_1} \\ \\ 0 & I \end{bmatrix} \Sigma_1 \begin{bmatrix} \dfrac{\partial x_2}{\partial x_1} & \dfrac{\partial x_2}{\partial z_1} \\ \\ 0 & I \end{bmatrix}^T$$

where

$$\Sigma_1 = E\left[\begin{pmatrix} \delta x_1 \\ \delta z_1 \end{pmatrix} \begin{pmatrix} \delta x_1 \\ \delta z_1 \end{pmatrix}^T\right]$$

$$\Sigma_2 = E\left[\begin{pmatrix} \delta x_2 \\ \delta z_2 \end{pmatrix} \begin{pmatrix} \delta x_2 \\ \delta z_2 \end{pmatrix}^T\right]$$

and E is the expectation operator.

2.4 Sensitivity of Solved-For Parameters to Unsolved Parameters

In accuracy analysis studies, it is often desirable to determine the degradation of the estimation accuracy due to unestimated systematic errors. These aspects have been discussed elsewhere and the results are as follows.

We can rewrite Eq. (G-2) as

$$\hat{\delta x} = \delta x + \left(A^T W A\right)^{-1} A^T W (B\delta z + n)$$

where again δx is the vector of solved-for parameters, and δz is the vector of unsolved systematic errors. Then the partial derivative of the estimate of the solved-for quantities with respect to the unestimated variables can be written as

$$\frac{\partial(\hat{\delta x})}{\partial(\delta z)} = \left(A^T W A\right)^{-1} A^T W B$$

APPENDIX H

APPLICATION OF THE SPIT PROGRAM

1. INTRODUCTION

This appendix contains a description of results of computations made with a special Single Point in Time (SPIT) computer program which considers simultaneous measurements from ground stations and user to a system of satellites. These results have provided valuable information on the influence of correlations in navigation satellite error analysis and have been useful in ground station preliminary design.

The computer program performs the function of determining and propagating the ground-station determined, full satellite covariance matrix into user accuracy at variable locations, given specifications on measurement mode and accuracy (random and bias), a priori satellite and station location uncertainties, and satellite locations. The program is not intended to simulate the process of long-term tracking and data smoothing involved in accurately determining satellite position, but rather to study the influence of satellite/ground station interactions on user accuracy once such a process has been completed. One user area with a fixed four-satellite array representing $\pm 18\text{-}1/2^{\circ}$ synchronous orbits was considered. Figure H-1 shows this geometry including a set of 5 potential ground station sites.

User and ground station measurements can be represented in the program as either:

a) "absolute" range: that is range with a zero or small finite a priori bias comparable to the random error

b) "relative" range: That is range with a large or essentially infinite a priori bias which, however, is common to all measurements made by that station or user

c) range difference—"uncorrelated": having independent random errors

d) range difference—"correlated": having the intercorrelation structure that obtains by deriving such range differences from basic range measurements by differencing by pairs.

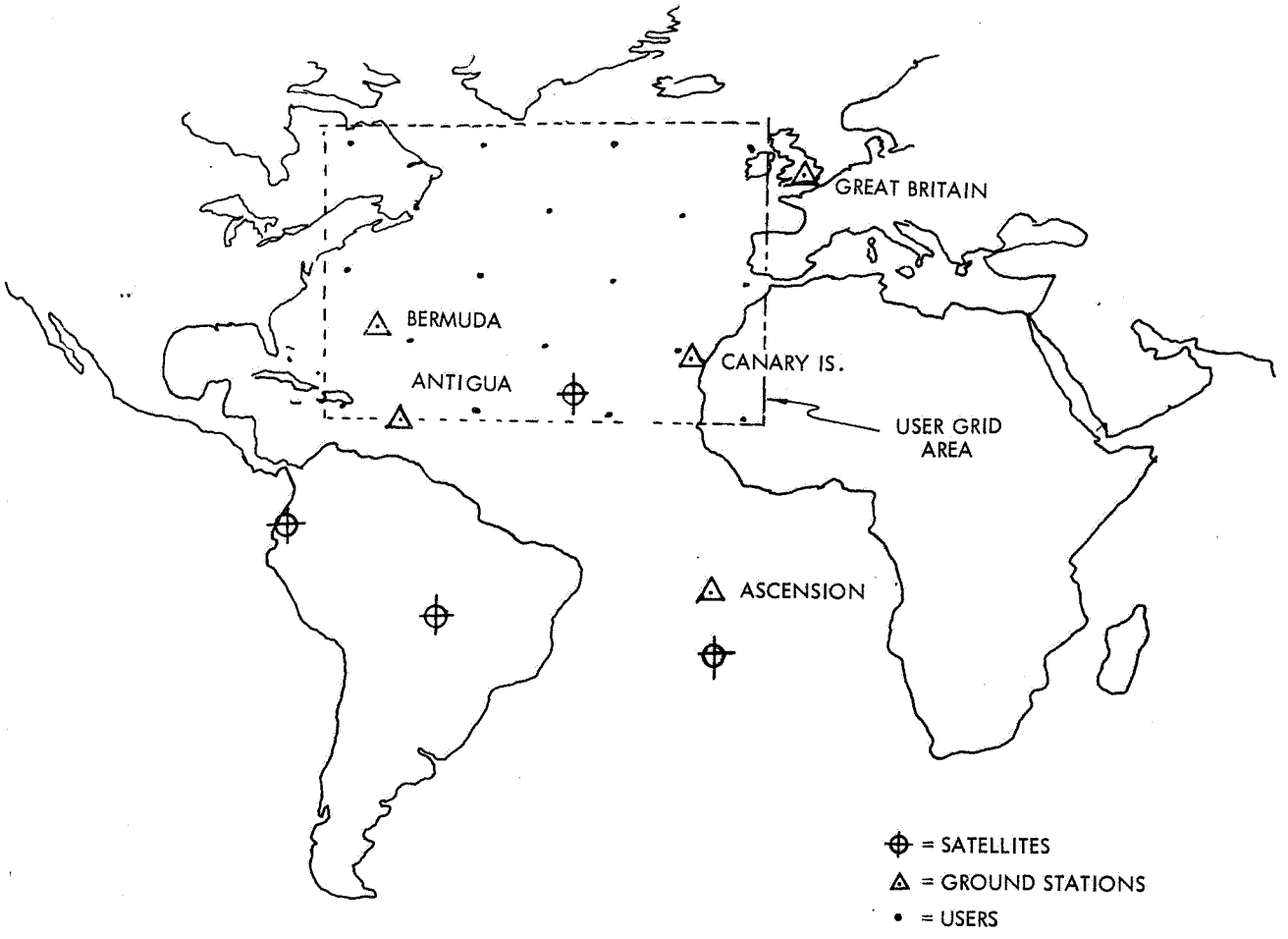

Figure H-1. Error Analysis Geometry

The NAVSTAR system proposed in this report uses type b measurements, which a high-accuracy user will process directly. The intermediate-accuracy user will difference these range measurements to obtain type d measurements, which he will process suboptimally, assuming they are uncorrelated (type c). These distinctions are discussed more fully in sec. 3.

Random measurement errors were taken as 100 ft (1σ) on range for cases a, b, d, and 100 ft on range difference for case c. The results can be scaled within reason to correspond to other basic measurement errors (Ref. 4, Figure 4-23). Details of the SPIT computer program are included in app. I. Results of the computer study complete this section.

The main topics studied in this error analysis are listed below and discussed in the Preliminary Results, sec. 4, of this appendix. These topics cover the effects of:

1) Measurement mode (range or range difference)

2) Ground station and user making similar measurements

3) Geometric correlations (defined as the correlation effects arising because of the geometrical position of the ground stations with respect to the satellite and independent of the measurement process)

4) Varying the number of ground stations

5) Measurement correlations in range difference measurements.

2. PRELIMINARY RESULTS

The results of the accuracy analyses are position uncertainties over the grid of user locations shown in Figure H-1. Figure H-2 shows the geometrical distribution of user uncertainty for four possible combinations of (absolute) range and (correlated) range-difference measurements by the users and five ground stations. The ranges of user accuracies represented on this and other maps have been condensed into bar graphs in Figures H-3 through -6 for easier interpretation. Each set of numbers in Figure H-2 corresponds to one bar either on Figure H-3 or on Figure H-4.

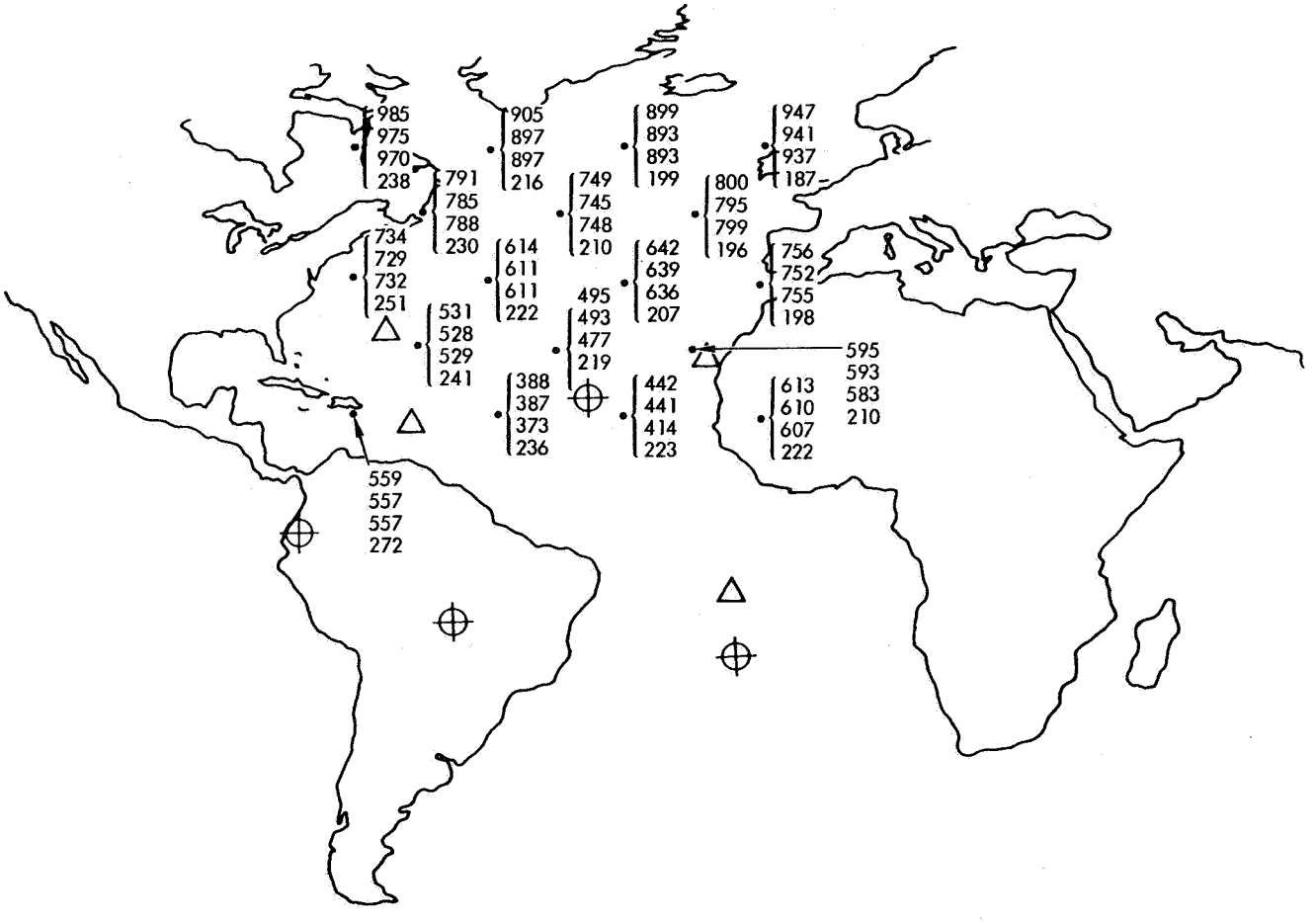

NOTE: INTERPRETATION OF SETS OF NUMBERS IS:

LINE NO.	GROUND STATION MEASUREMENT	USER MEASUREMENT
1	3 RANGE DIFFERENCE	3 RANGE DIFFERENCE
2	3 RANGE DIFFERENCE	4 RANGE
3	4 RANGE	3 RANGE DIFFERENCE
4	4 RANGE	4 RANGE

⊕ = SATELLITES

△ = GROUND STATIONS

• = USERS

RANGE DIFFERENCES ARE "CORRELATED"

RANGES ARE "ABSOLUTE"

Figure H-2. Typical Results for a Grid of User Locations

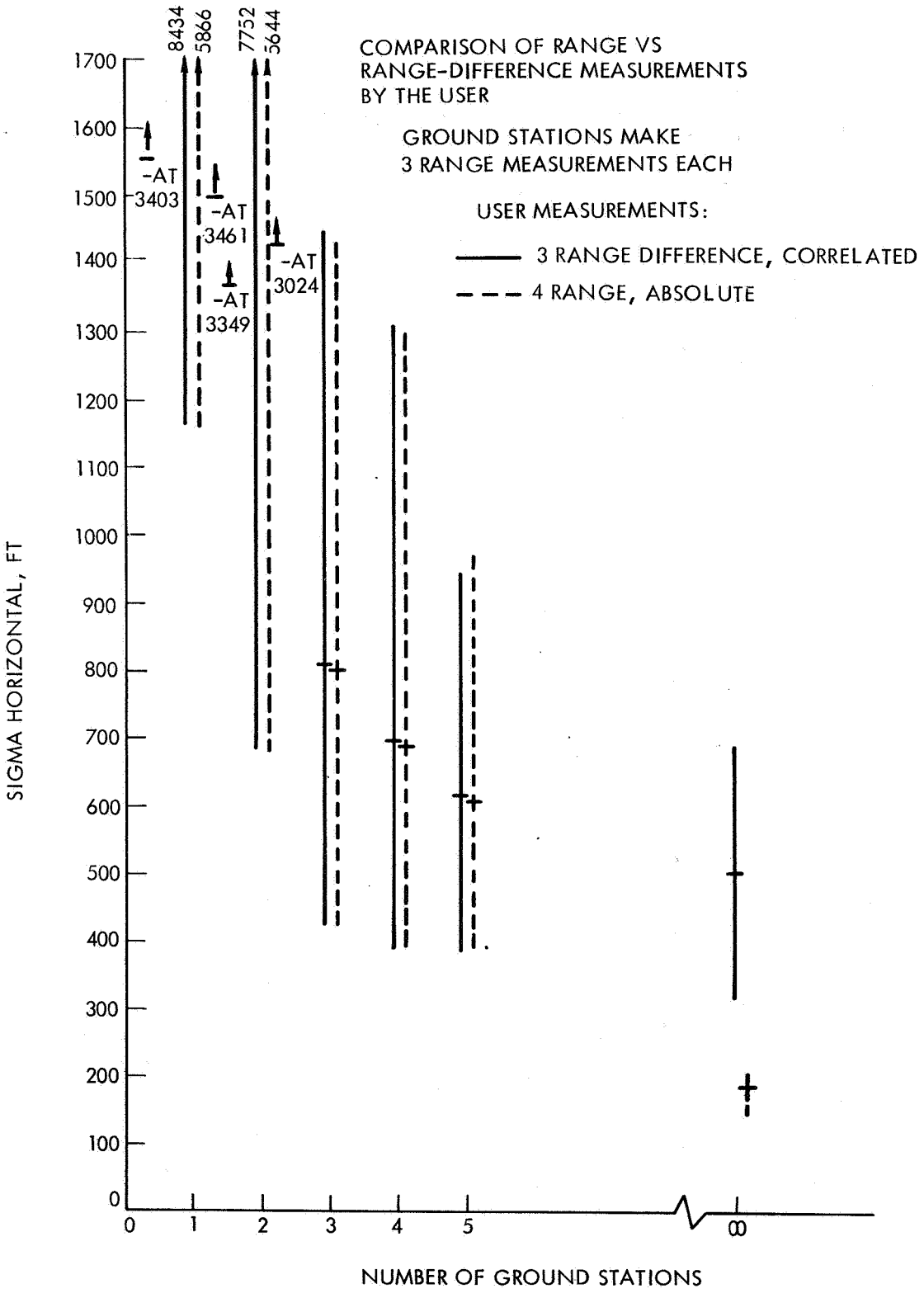

Figure H-3. Comparison of Range Versus Range-Difference Measurements by the User

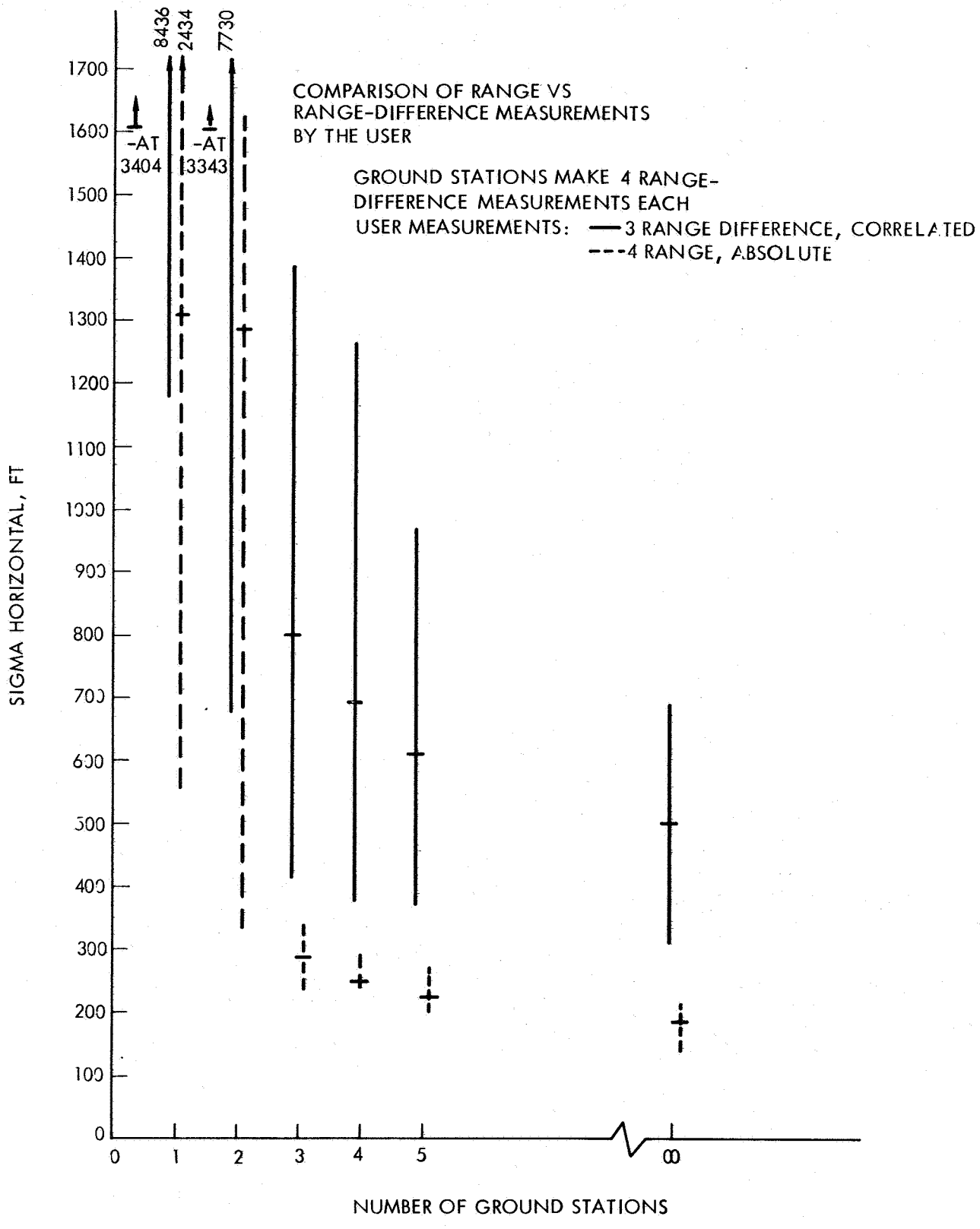

Figure H-4. Comparison of Range Versus Range-Difference Measurements by the User

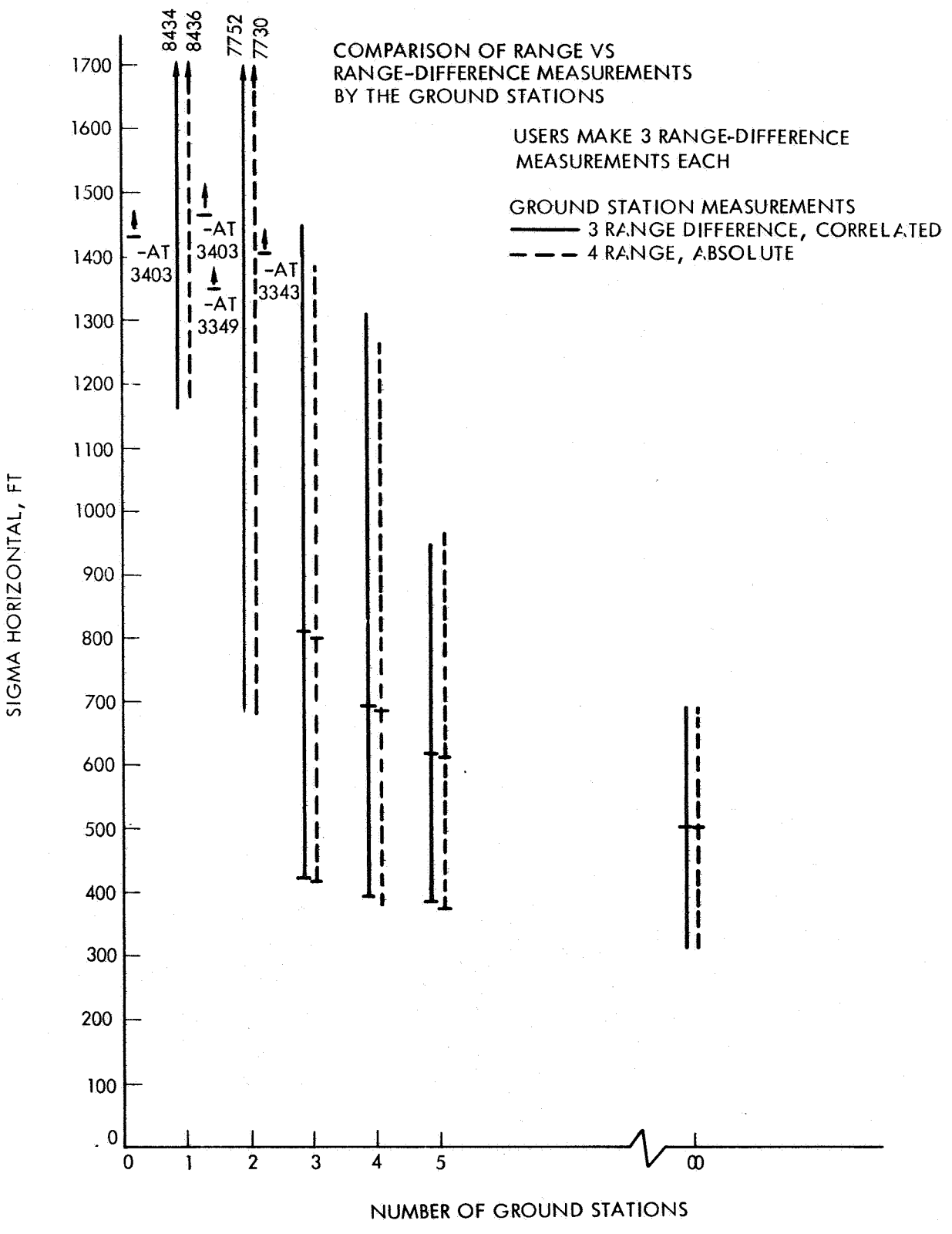

Figure H-5. Comparison of Range Versus Range-Difference Measurements by the User

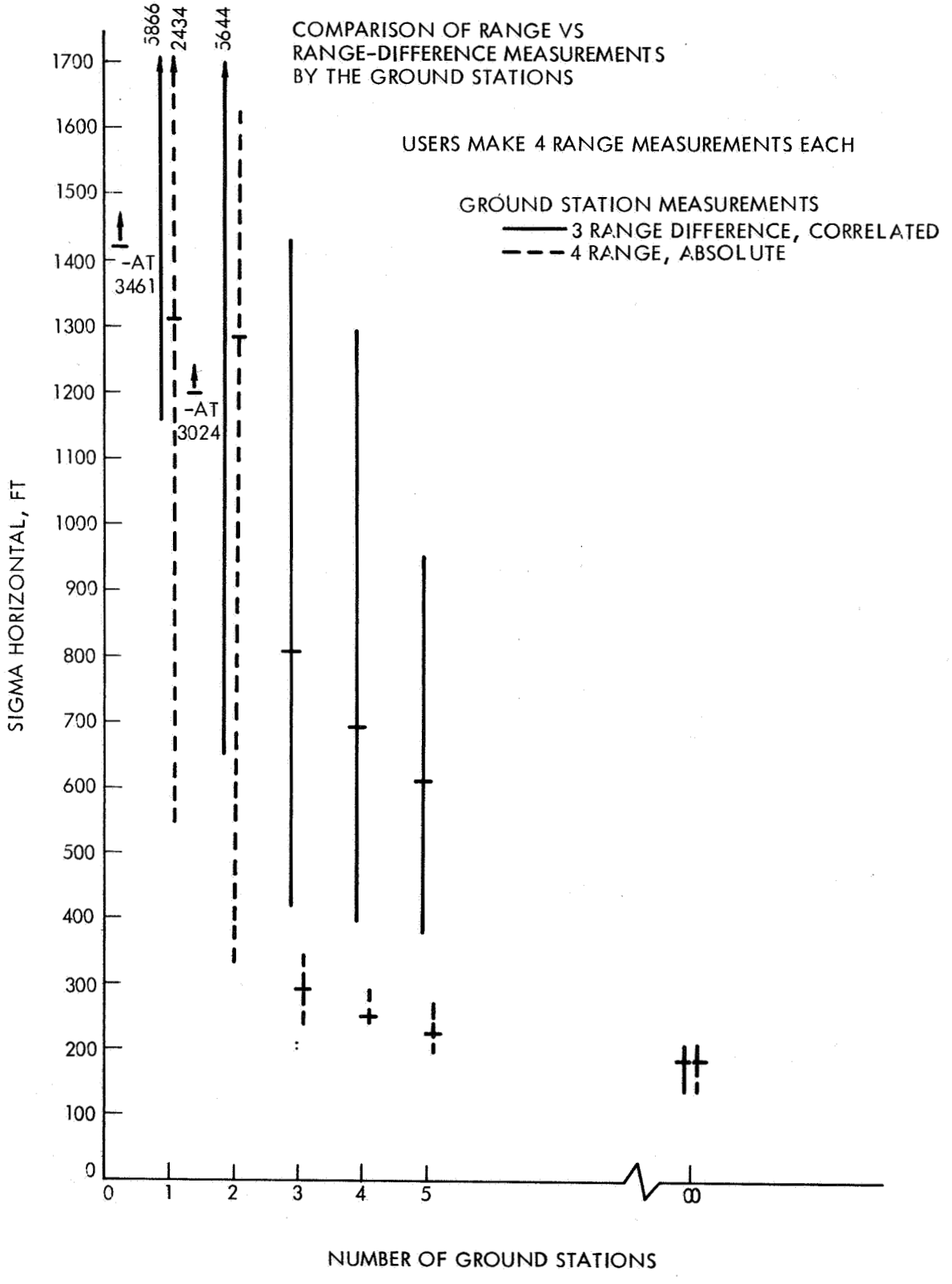

Figure H-6. Comparison of Range Versus Range-Difference Measurements by the User

Tradeoffs between measurement modes are shown in Figures H-3 through -6 as is the range of user accuracies as a function of the number of ground stations. The terms "range of user accuracies" is used to denote the interval bounded by the most accurate and the least accurate user within the grid under consideration and is not a range associated with any one user.

As an aid in visualizing the effect of varying the number of ground stations, a tick mark representing the accuracy of a user at longitude 50°W, latitude 40°N (near the center of the grid) has been placed on each bar of the graph. The best range of accuracies obtainable occurs with an infinite number of ground stations and was obtained by setting the satellite covarance matrix equal to zero.

3. MEASUREMENT MODES AND EFFECT OF SIMILAR MEASUREMENTS

In terms of user accuracy, best results are obtained when both ground stations and users measure absolute range. If either ground stations or users measure range differences, it appears to make no difference what the other measures. However, if either ground stations or users measure range, there is a definite advantage to having the others also measure range. This can be seen from the tabulation given below, which is a condensation of some of the data on Figures H-3 and -4 and other runs. The tabulation corresponds to a network of five ground stations viewing 4 satellites. Accuracies given are those for a user at 50°W, 40°N.

	Accuracies in Feet Ground Stations Measure:		
Users Measure	4 Range (Absolute)	4 Range (Relative)	3 Range Difference (Correlated)
4 Range (Abs.)	222	611	611
4 Range (Rel.)	611+	614	614
3 Range Dif. (Corr.)	611+	614	614

It is clear from an information point of view that 3 Range Differences (Correlated) are equivalent to 4 Range (Relative) from which they are assumed derived. This explains the equalities of the second and third rows and columns in the above table. The apparent equality between the 611 ft terms and the 611+ ft terms appears to be coincidental.

4. EFFECT OF REDUCING NUMBER OF GROUND STATIONS

All the figures examined show the effect of reducing the number of ground stations. Perhaps the most significant fact is that if the best measurement philosophy is used (i.e., both ground stations and users measure range), there is not a great difference in the accuracies obtainable by a relatively modest tracking network and the accuracies obtainable by perfect tracking (or an infinite number of ground stations). This can be seen in Figures H-4 and -6 in which the range of accuracies obtainable by perfect tracking is seen to be from 142 to 210 ft. The range of accuracies obtainable by a system of four ground stations (the existing USBS Network) is from 236 to 285 ft, with no time smoothing. In the present model, which depicts ground stations as making instantaneous single-point-in-time measurements with an a priori constraint, time smoothing may be represented as a smaller a priori satellite covariance matrix, which would lower these figures still further. The effects of time smoothing are investigated in detail in subsec. 2.4.

The bars in Figures H-3 through -6 which denote the accuracies obtainable with one, two, or three ground stations are pessimistic, since no time smoothing was considered. The purpose of the computer runs which generated these data was really to show that underdetermined satellite locations may still lead to quite acceptable user location accuracy. The reasons for this behavior are partly explained in the next section.

5. IMPORTANCE OF CORRELATION IN SATELLITE POSITION (GEOMETRIC CORRELATION)

It is possible to input to the program any desired diagonal satellite covariance matrix. If this matrix corresponds to the diagonal elements of a previously calculated matrix, any change in user accuracy between the two cases may be attributed to the absence of correlation.

This was done, using as the diagonal matrix the diagonal elements of the satellite covariance matrix which yielded the user accuracies shown in Figure H-3 for one ground station. As was expected, the user uncertainty was much larger for the case in which no geometric correlations were considered. Table H-I shows the range of user accuracies with and without geometric correlation for two measurement systems, one in which four ranges were measured and another using three range differences. In each case, the satellite covariance matrix consisted of the diagonal elements of the satellite covariance matrix which resulted from one ground station making three range-difference measurements.

TABLE H-I

RANGE OF USER UNCERTAINTIES

Measurement Mode of User	Correlated (ft)	Uncorrelated (ft)
Three range-difference	1163-8434	33,956 - 74,187
Four range	1159-5866	14,062 - 23,115

The improvement assignable to the off-diagonal (correlation) terms in the satellite covariance matrix is of the order of 10 or 20 to 1, with the greatest improvement associated with those user locations which are closest to the network, or particular stations in the network. This is because, relative to the large volume of space encompassed by the satellite network, the ground station and user positions are very close to one another. Consequently, the partial derivatives of ground station measurements with respect to satellite positions are very nearly equal to the negative of the partials of user measurements with respect to user position. Thus, even in an underdetermined ground measurement setup where the complete satellite position cannot be significantly determined, that component of position corresponding to the projection of satellite position on the partial derivative vector may be very well determined, and to the extent that the partial derivative is the same for the user, that is the only component of satellite position that matters. This emphasizes the importance of a complete error covariance matrix propagation from ground measurements, through satellite, to user position.

Another way of verifying the importance of the correlation terms is to change the covariance matrix artifically so that the diagonal terms are essentially unchanged, but the correlations are lower. This can be accomplished by: 1) making few enough measurements so that the locations are underdetermined; 2) choosing an a priori constraint so that the satellite covariance can be determined, but choosing a standard deviation of ground measurement error such that the matrix will be essentially the same size as the a priori matrix; and 3) repeating the procedure with a much larger value of ground station measurement error. Since the matrix was already essentially the same size as the a priori matrix, specifying a degraded ground measurement accuracy does not appreciably change the size of the diagonal elements of the satellite covariance matrix, but it does significantly lower the correlations between the satellites. This was done, and the user accuracies were significantly worse in the case with lower correlations. This illustrates the effect of low-accuracy tracking, which contributes to user inaccuracies out of proportion to the degradation in satellite ephemeris (as measured by the diagonal terms).

APPENDIX I

SINGLE POINT IN TIME ACCURACY PROGRAM (SPIT)

A. Introduction

The SPIT program is designed to evaluate the satellite covariance matrix which results when a system of ground stations makes range and/or range-difference measurements to a network of satellites, and to then use this satellite covariance matrix to determine the covariance matrix of each user of the system. The analyst may specify any combination of range and/or range-difference measurements for the users as well as for the ground stations.

Three other features may be exercised as options. One allows the analyst to specify that the satellite location is known perfectly except for the satellite drift covariance, which may be any diagonal matrix, including the zero matrix.

Another option allows the analyst to account for correlation between the ground station measurements which arises whenever a ground station measures ranges to the several satellites and uses these to form range differences between one satellite and all other satellites. In this case, correlations exist in the random errors in the range differences. This option is only available if the ground measurement random error is the same for each ground station.

The third option allows one to consider relative navigation between pairs of users. This will be explained in more detail later. A flow diagram of the program is shown as Figure I-1.

B. Limitations

The program is limited to a maximum of nine satellites and nine ground stations. In addition, the total number of measurements made by all ground stations cannot exceed fifty. (Forty-five if the correlated measurement option is used).

Each subcase may consist of a maximum of nine users, making a maximum of nine measurements each. Because each user is processed sequentially and is independent of all other users (except for the relative navigation option), there is no other restriction on the total number of measurements made by all users.

Within each subcase all users must make identical measurements. However, there is no limit to the number of subcases which may be processed in one run.

C. Inputs

Inputs to the program are:

1. Ground station, satellite, and user locations, specified as latitude, longitude and range.

2. Number of ground measurements (NGM). A value of zero is interpreted as meaning that the satellite position is perfectly known except for satellite drift, which may or may not be zero. If this is zero, no GMM matrix need be input.

3. Ground measurement matrix (GMM). This is a three-column matrix which specifies which measurements are being made by the ground station. The first columns are the numbers of satellites A and B. If the third column is zero, the measurement being made is a range measurement to satellite A. If non-zero, the measurement being made is the range difference between satellites A and B. The number of rows of the matrix is equal to the number of ground measurements, NGM.

4. Number of user measurements per user (NUM).

5. User measurement matrix (UMM). This is a control matrix similar to GMM. However, since each user within a subcase makes the same measurements there is no reason to have a first column identifying the user by number, as in GMM.

6. Standard deviation of ground station measurement error. There will be one standard deviation per measurement, or NGM total. If the option to consider the correlation between ground measurements is desired, only one value should be input. This will then be used as the standard deviation for all measurements.

7. Standard deviation of user measurement error. Exactly the same comments made above also apply here.

8. Satellite a priori flag (SAPF). If zero, the effect is the same as if the equations were written with no regard for any a priori values. Note that this is not equivalent to saying the satellite is perfectly known or that its covariance is infinite, since both the covariance matrix and its inverse have zero values. If the flag is non-zero, the standard deviations of longitude, latitude, range, and bias for each satellite must be input.

9. Ground station a priori flag (GAPF). Exactly the same interpretation as for SAPF, but for the ground stations.

10. User a priori flag (UAPF). Exactly the same as above, but the only variables are longitude, latitude and range. Only one set of these numbers is input, and they are used for every user within the subcase.

11. Satellite drift covariance flag (SDCF). Interpretation is the same as for SAPF and GAPF.

12. Relative navigation flag (RNF). If zero, the program operates in the 'normal' mode discussed previously. If non-zero, the covariance matrix associated with the difference vector between the reference user and all other users is computed and printed. The reference user is always the first user.

Nomenclature

Symbol	Meaning
GAP	Ground Station A Priori Position Matrix
GAPEL	Square Roots of Elements of GAP Matrix
GAPE	Ground A Priori Flag
GLOC	Location Vector of Ground Stations (θ, Φ, ρ)
GMC	Ground Measurement Covariance Matrix
GMCA	Ground Measurement Covariance Matrix, Augmented
GMCEL	Elements of GMC Matrix
GMM	Ground Measurement Matrix (A Control Matrix)
NGM	Number of Ground Measurements (Number of Rows of GMM)
NGS	Number of Ground Stations
NS	Number of Satellites
NU	Number of Users
NUM	Number of User Measurements per User (Number of Rows of UMM)
PGMG	Partial Derivatives of Ground Measurements with Respect to the Ground Station
PGMS	Partial Derivatives of Ground Measurements with Respect to the Satellites
SAP	Satellite A Priori Position Matrix
SAPEL	Square Roots of Elements of SAP Matrix
SAPF	Satellite A Priori Flag
SC	Satellite Covariance Matrix
SCA	Satellite Covariance Augmented (Includes Effects of SAP, SDC)
SDC	Satellite Drift Covariance Matrix
SDCEL	Square Roots of Elements of SDC
SDCF	Satellite Drift Covariance Flag
SLOC	Satellite Location (θ, Φ, ρ)
UAP	User A Priori Matrix
UAPEL	Square Roots of UAP
UAPF	User A Priori Flag
UC	User Covariance Matrix
ULOC	User Location (θ, Φ, ρ)
UMC	User Measurement Covariance Matrix
UMCEL	Square Roots of Elements of UMC
UMM	User Measurement Matrix (A Control Matrix)

Greek Symbols

Symbol	Meaning
θ	Longitude, Degrees
Φ	Latitude, Degrees
ρ	Geocentric Range, Nautical Miles

Subscripts

Symbol	Meaning
GS	Ground Station
S	Satellite
U	User

Note: Primed quantities are only the results of intermediate calculations and have no real meaning.

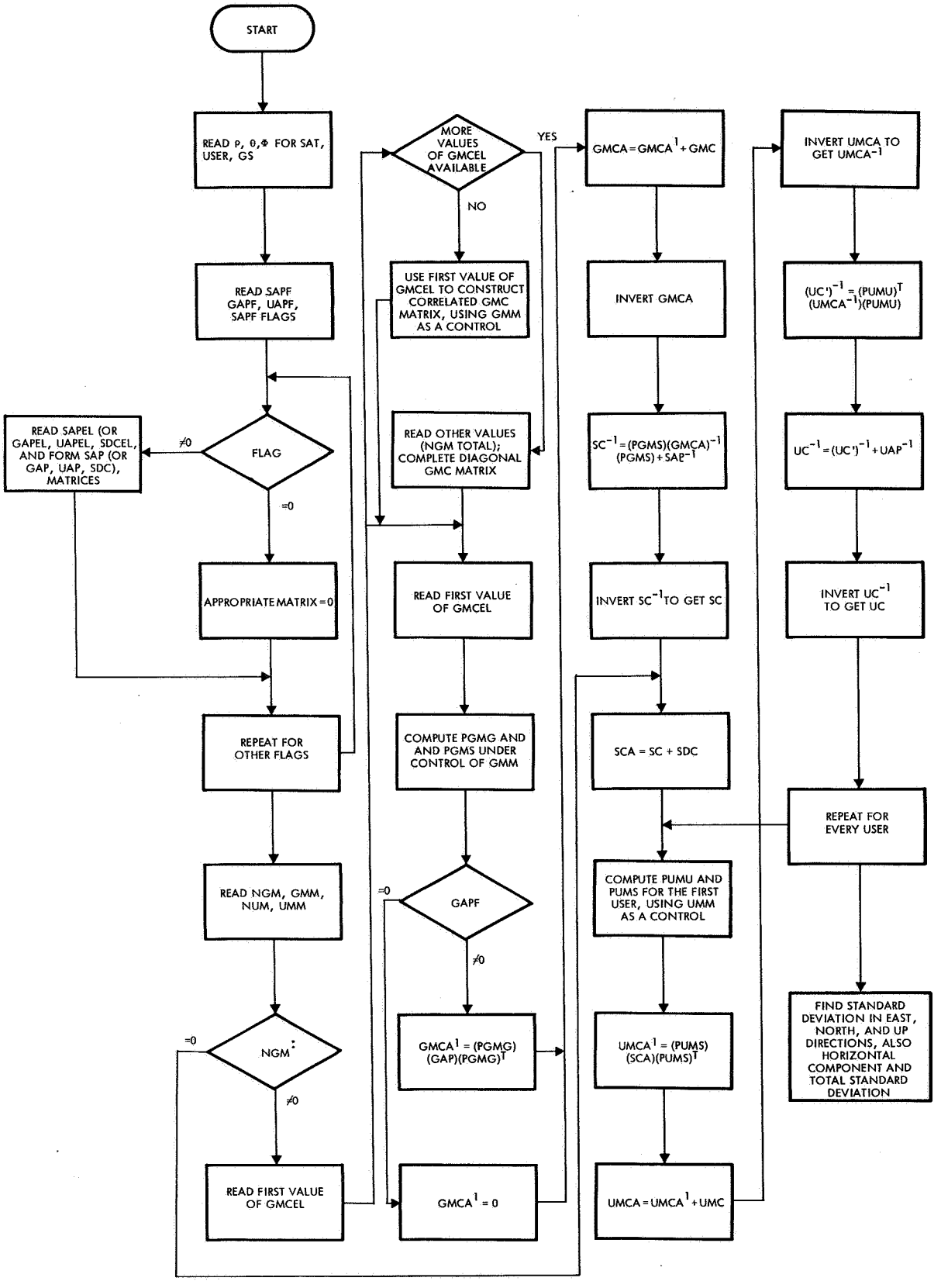

Figure A-1. SPIT Flow Diagram

APPENDIX J

NAVIGATION SATELLITE ACCURACY PROGRAM (NAVSAP)

1. INTRODUCTION

The logical structure of the TRW SVEAD program, delivered to ERC under a separate contract, has been utilized in the development of the Navigation Satellite Accuracy Program. This program (NAVSAP) performs an error analysis for a given satellite configuration and user positions. The analysis is based on minimum variance estimation of the state vector consisting of user position and other parameters of interest, such as measurement bias and satellite positions and velocities. The results are presented in terms of the "C 95", the radius of a circle containing the user with probability 0.95. Range, range difference, or range sum measurements can be considered.

Inputs to the program are the following:

a. The first partition of the state vector comprised of the positions and velocities for as many as 7 satellites

b. The second partition of the state vector comprised of the user latitude, longitude, and altitude (actually a grid of user positions is prescribed in terms of the boundary values of latitude and longitude and the latitude-longitude spacing between users)

c. The error covariance matrix of the uncertainty in the satellites' positions and velocities

d. The error covariance matrix of the uncertainty in the a priori estimate of the user positions

e. The variance of the measurement noise.

For the first user position the program computes the partial derivatives of the observations with respect to the elements of the state vector. The filter equations are then used to adjust the covariance matrix of the state vector to account for the first observation. The C95 is then computed and printed out. This process is repeated until all measurements have been processed, and the final C95 for that position is printed out. This process is repeated until all measurement have

been processed, and the final C95 for that position is printed out. The program then proceeds to the next user position, incrementing first latitude and then logitude, until a C95 is computed for each point in the grid.

The program can also consider a user moving at constant altitude along a great circle path. Measurements are taken at prescribed intervals, and the estimate is continually updated as a result of the new measurements. In this mode it is possible to consider the effect of random perturbations in the user flight path by inserting noise (state noise) on the velocity vector.

The program employs a Runge-Kutta integration package to intergrate the satellites' trajectories, based on input initial positions and velocities. As many as seven satellites may be integrated simultaneously and the state vectors stored at specific measurement times for use in the subsequent error analysis.

This appendix contains a complete engineering description of the program. An accompanying document contains the detailed program implementation and subroutine descriptions. An overall flow diagram appears in Figure 1.

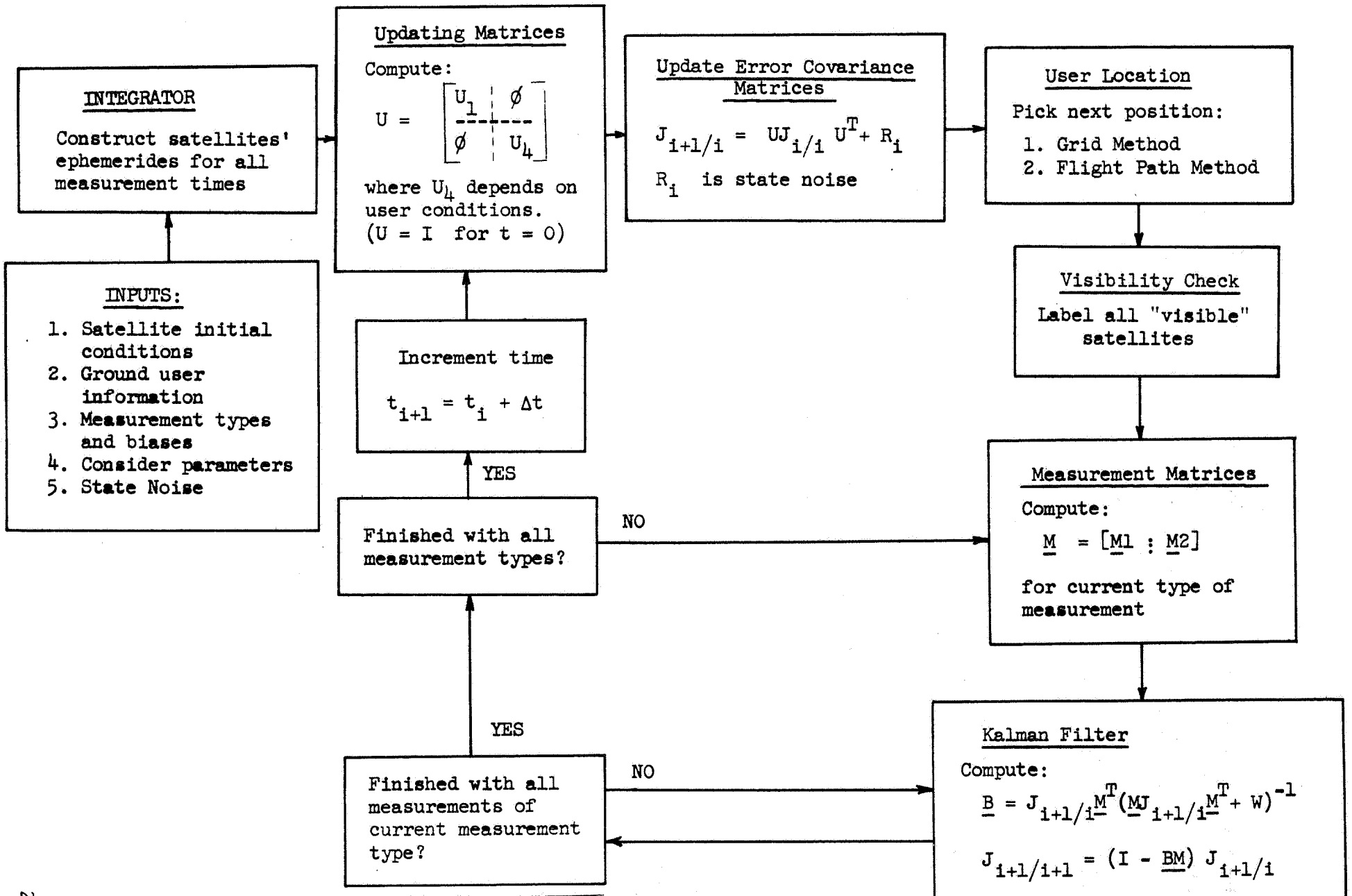

Figure 1-1. NAVSAP – General Flow Diagram

2. STATE VECTOR

The state vector is partitioned into two sections. The first section $\underline{X}_1$ contains the satellite states while the second $\underline{X}_2$ contains the user position and measurement biases. These vectors are constructed as:

$$\underline{X}_1^T = \left[x_1\ y_1\ z_1\ \dot{x}_1\ \dot{y}_1\ \dot{z}_1\ x_2 \cdots z_N\right]_{1 \times 6N} \tag{1}$$

$$\underline{X}_2^T = \left[x_u\ y_u\ z_u\ b_1 \cdots b_M\right]_{1 \times (3+M)} \tag{2}$$

where N is the number of satellites (input) and M is the number of measurement biases. The superscript T denotes transpose; the numerical subscript refers to the satellite and u refers to the user.

The error covariance matrix is correspondingly partitioned

$$J = E\left[\delta\underline{X}\ \delta\underline{X}^T\right]$$

$$= E\begin{bmatrix} \delta\underline{X}_1\ \delta\underline{X}_1^T & \delta\underline{X}_1\ \delta\underline{X}_2^T \\ \delta\underline{X}_2\ \delta\underline{X}_1^T & \delta\underline{X}_2\ \delta\underline{X}_2^T \end{bmatrix} = \begin{bmatrix} J_1 & J_3^T \\ J_3 & J_4 \end{bmatrix} \tag{3}$$

Since J is symmetric, it is only necessary to compute and store the partitions, J_1, J_3, and J_4.

3. COORDINATE SYSTEMS

All quantities in the program are referenced to one of the following four coordinate systems (Figure 3-1):

$\underline{X}_o = (\underline{x}_o, \underline{y}_o, \underline{z}_o)$	Earth-centered inertial (ECI) Cartesian system
$\underline{X} = (\underline{x}, \underline{y}, \underline{z})$	Earth-centered fixed (ECF) Cartesian system
$\underline{\theta} = (\theta, \lambda, r)$	ECF spherical system
$\underline{U} = (\underline{u}, \underline{v}, \underline{w})$	Satellite-centered inertial (SCI) Cartesian system (radial, in-track, cross-track)

The time origin is selected at the first measurement time. At that instant $\underline{X}_o$ and $\underline{X}$ are colinear, $\underline{z}$ passes through the North Pole and $\underline{y}$ is in the equatorial plane, passing through the prime meridian (Greenwich). In the $\underline{\theta}$ system, latitude θ is measured positive north from the equator and longitude λ is measured positive west from Greenwich. In the $\underline{U}$ system, $\underline{u}$ is directed along the radius vector to the satellite, $\underline{w}$ is in the direction of the satellite angular momentum vector, and $\underline{v}$ completes the orthogonal set.

Using the notation that $\partial\underline{A}/\partial\underline{B}$ is the matrix that maps coordinate system $\underline{B}$ into $\underline{A}$, the following transformation matrices are defined:

$$\frac{\partial \underline{X}_o}{\partial \underline{X}} = \left(\frac{\partial \underline{X}}{\partial \underline{X}_o}\right)^{-1} = \left(\frac{\partial \underline{X}}{\partial \underline{X}_o}\right)^{T} = \begin{bmatrix} \cos\omega t & -\sin\omega t & 0 \\ \sin\omega t & \cos\omega t & 0 \\ 0 & 0 & 1 \end{bmatrix} \tag{4}$$

$$\frac{\partial \underline{X}}{\partial \underline{\theta}} = \begin{bmatrix} -\frac{zx}{\gamma} & y & \frac{x}{r} \\ -\frac{zy}{\gamma} & -x & \frac{y}{r} \\ \gamma & 0 & \frac{z}{r} \end{bmatrix} \tag{5}$$

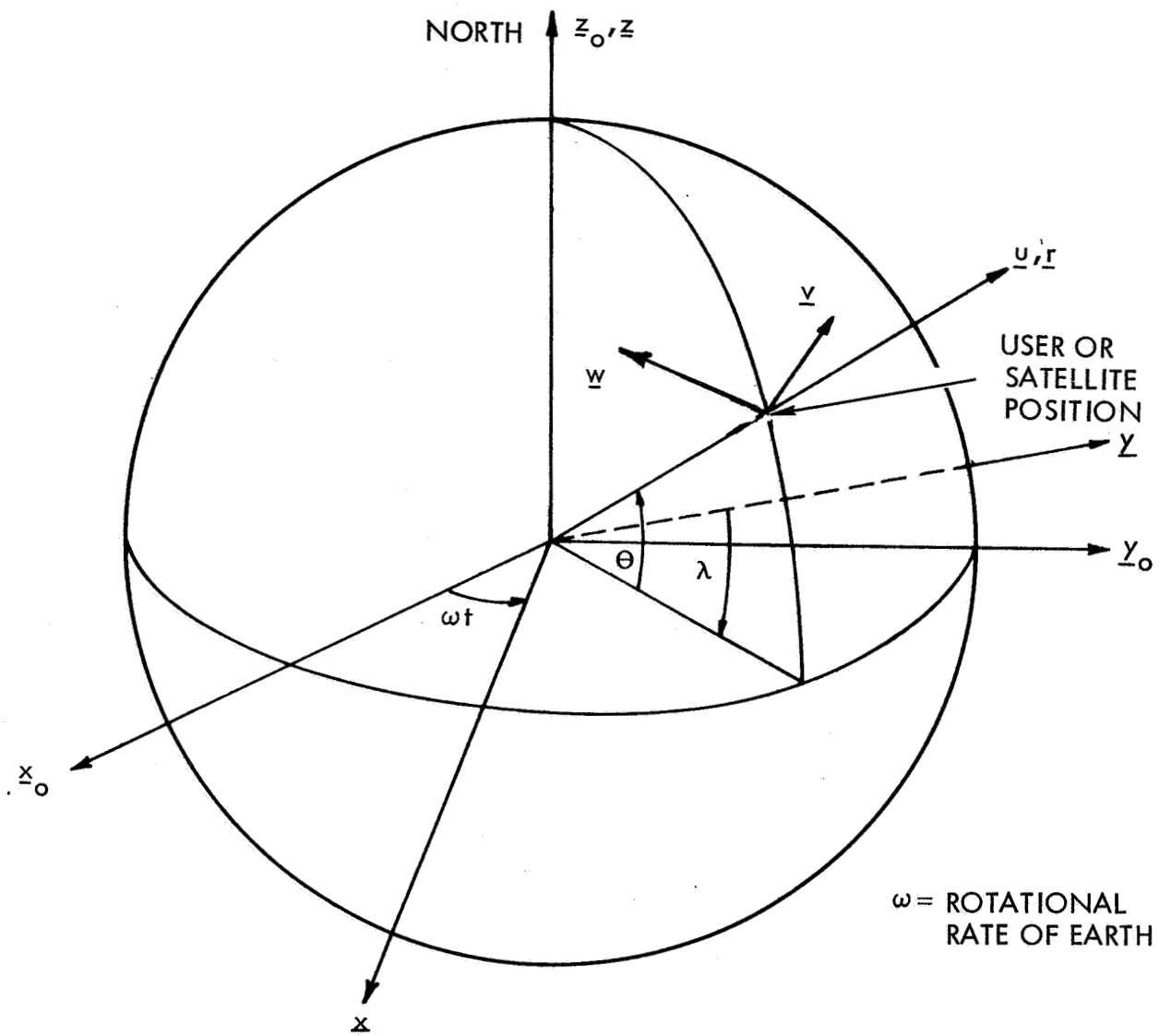

Figure 3-1. Coordinate Systems

$$\frac{\partial \underline{\theta}}{\partial \underline{X}} = \begin{bmatrix} \frac{xz}{\gamma r^2} & -\frac{yz}{\gamma r^2} & \frac{\gamma}{r^2} \\ \frac{y}{\gamma^2} & -\frac{x}{\gamma^2} & 0 \\ \frac{x}{r} & \frac{y}{r} & \frac{z}{r} \end{bmatrix} \tag{6}$$

where

$$\gamma = \sqrt{x^2 + y^2}$$
$$r = \sqrt{\gamma^2 + z^2} \tag{7}$$

$$\frac{\partial \underline{X}_o}{\partial \underline{U}} = \left(\frac{\partial \underline{U}}{\partial \underline{X}_o}\right)^{-1} = \left(\frac{\partial \underline{U}}{\partial \underline{X}_o}\right)^{T} = \begin{bmatrix} u_x & v_x & w_x \\ u_y & v_y & w_y \\ u_z & v_z & w_z \end{bmatrix} \tag{8}$$

using the following equations which define $\underline{U}$

$$\underline{u} = \underline{r}/|\underline{r}|$$
$$\underline{w} = (\underline{r} \times \underline{V}) \left[(rv)^2 - (\underline{r} \cdot \underline{V})^2\right]^{-1/2} \tag{9}$$
$$\underline{v} = \underline{w} \times \underline{u}$$

where $\underline{V}$ is the satellite velocity vector, we find

$$u_x = \frac{x}{r}, \qquad u_y = \frac{y}{r}, \qquad u_z = \frac{z}{r}$$

$$w_x = \frac{1}{D}(y\dot{z} - \dot{y}z) \tag{10}$$

$$w_y = -\frac{1}{D}(x\dot{z} - \dot{x}z)$$

$$w_z = \frac{1}{D}(x\dot{y} - \dot{x}y)$$

$$v_x = w_y u_z - w_z u_y$$

$$v_y = w_z u_x - w_x u_z \qquad \text{(10) con't.}$$

$$v_z = w_x u_y - w_y u_x$$

where

$$D = \sqrt{r^2 V^2 - (x\dot{x} + y\dot{y} + z\dot{z})^2} \qquad (11)$$

and x, y, z denote ECI coordinates.

4. INTEGRATOR

If measurements are taken at times other than t = 0, the program integrates the satellite trajectories to the specified measurement times and constructs an ephemeris. Measurement times are every Δt_m seconds until time is greater than final time t_f. Δt_m is specified as an integral multiple of the integration step size.

The program uses a fourth order, self-starting, Runge-Kutta procedure with a point-mass, two-body force model. The constraint equations for the i^{th} satellite are:

$$\dot{X}_i = \begin{bmatrix} \dot{x}_i \\ \dot{y}_i \\ \dot{z}_i \\ \ddot{x}_i \\ \ddot{y}_i \\ \ddot{z}_i \end{bmatrix} = \begin{bmatrix} \dot{x}_i \\ \dot{y}_i \\ \dot{z}_i \\ -\mu x_i / r_i^3 \\ -\mu y_i / r_i^3 \\ -\mu z_i / r_i^3 \end{bmatrix}_{ECI} \tag{12}$$

where μ is the earth's gravitational constant.

5. ERROR ANALYSIS

5.1 FILTER EQUATIONS

At time t_i after i-1 measurements, let the i^{th} observation ξ_i be linearly related to the column state vector of unknowns $\underline{x}_i$ by the relation

$$\xi_i = \underline{M}_i \underline{X}_i + w_i$$

where $\underline{M}_i$, the measurement vector, is a row vector of the partial derivatives of ξ_i with respect to the components of $\underline{X}_i$, and w_i is zero mean, uncorrelated, random noise. That is,

$$\begin{aligned} E(w_i) &= 0 \\ E(w_i\, w_j) &= 0 \qquad i \neq j \\ E(w_i^2) &= W \end{aligned} \tag{13}$$

where E is the expectation operator.

Let $J_{i/j}$ be the error covariance matrix of $\underline{X}_i$ based on j measurements ($j \leq i$); define the measurement weighting matrix.

$$\underline{B}_i = J_{i/i-1}\, \underline{M}_i^T (\underline{M}_i\, J_{i/i-1}\, \underline{M}_i^T + W)^{-1} \tag{14}$$

and let

$$C_i = I - \underline{B}_i\, \underline{M}_i \tag{15}$$

The general formula for the current error covariance matrix is then

$$J_{i/i} = C_i\, J_{i/i-1}\, C_i^T + \underline{B}_i\, W\, \underline{B}_i^T \tag{16}$$

which, when B is given by Equation (14), assumes it minimum value

$$J_{i/i} = C_i J_{i/i-1} \tag{17}$$

Let $U_{i/j}$ be the state transition matrix for $\underline{X}_j$ from time t_j to t_i. Then $J_{i/i}$ is propagated to the next measurement time t_{i+1} according to the relation

$$J_{i+1/i} = U_{i+1/i} J_{i/i} U_{i+1/i}^T + R_i$$

where R_i is a random disturbance covariance matrix (state noise). These equations are programmed in NAVSAP in partitioned form corresponding to the partitioning of the overall program state vector.

5.2 CONSIDER OPTION (SUBOPTIMAL FILTERING)

The program can compute the estimation errors caused by errors in parameters which are not estimated. These parameters may include the state vector of any satellite and any of the measurement biases. This option requires that two stacked cases be run on NAVSAP. In the first case, all portions of the measurement vector $\underline{M}$ pertaining to the considered parameters are zeroed out. The measurement weighting vector $\underline{B}$ computed using this $\underline{M}$ is then stored on tape. In this phase, the program uses the optimal error covariance matrix computation given by Equation (17). In the second case, the full $\underline{M}$ along with the corresponding $\underline{B}$ computed in the first case is used in the suboptimal error covariance matrix computation according to Equation (16).

5.3 MEASUREMENT TYPES

The program can process several types of measurements, taken in any desired order. It is assumed that all measurements of all specified types are taken simultaneously at each measurement time.

5.3.1 Range and Range Rate Measurements

The range R from the s^{th} satellite to the user is defined to be the magnitude of the separation vector R (see Figure 5-1).

$$R = |\underline{R}| = |\underline{R}_s - \underline{R}_u| \tag{18}$$

The components of $\underline{R}$ are

$$x = x_s - x_u,\ y = y_s - y_u,\ z = z_s - z_u \tag{19}$$

The range is then

$$R = \sqrt{x^2 + y^2 + z^2} \tag{20}$$

from which the range rate is

$$\dot{R} = \frac{\underline{R} \cdot \dot{\underline{R}}}{R} = \frac{x\dot{x} + y\dot{y} + z\dot{z}}{R} \tag{21}$$

From these equations it follows that the partials of R and $\dot{R}$ with respect to the components of $\underline{R}_s$ are

$$\frac{\partial R}{\partial(x_s,\ y_s,\ z_s)} = \underline{m}_s = \frac{1}{R}\left[x,\ y,\ z\right]_{1x3} \tag{22}$$

$$\frac{\partial \dot{R}}{\partial(x_s,\ y_s,\ z_s)} = \dot{\underline{m}}_s = \frac{1}{R^2}\left[(R\dot{x} - x\dot{R}),\ (R\dot{y} - y\dot{R}),\ (R\dot{z} - z\dot{R})\right] \tag{23}$$

$$\frac{\partial R}{\partial(\dot{x}_s,\ \dot{y}_s,\ \dot{z}_s)} = \left[0,\ 0,\ 0\right]_{1x3} \tag{24}$$

$$\frac{\partial \dot{R}}{\partial(\dot{x}_s,\ \dot{y}_s,\ \dot{z}_s)} = \underline{m}_s \tag{25}$$

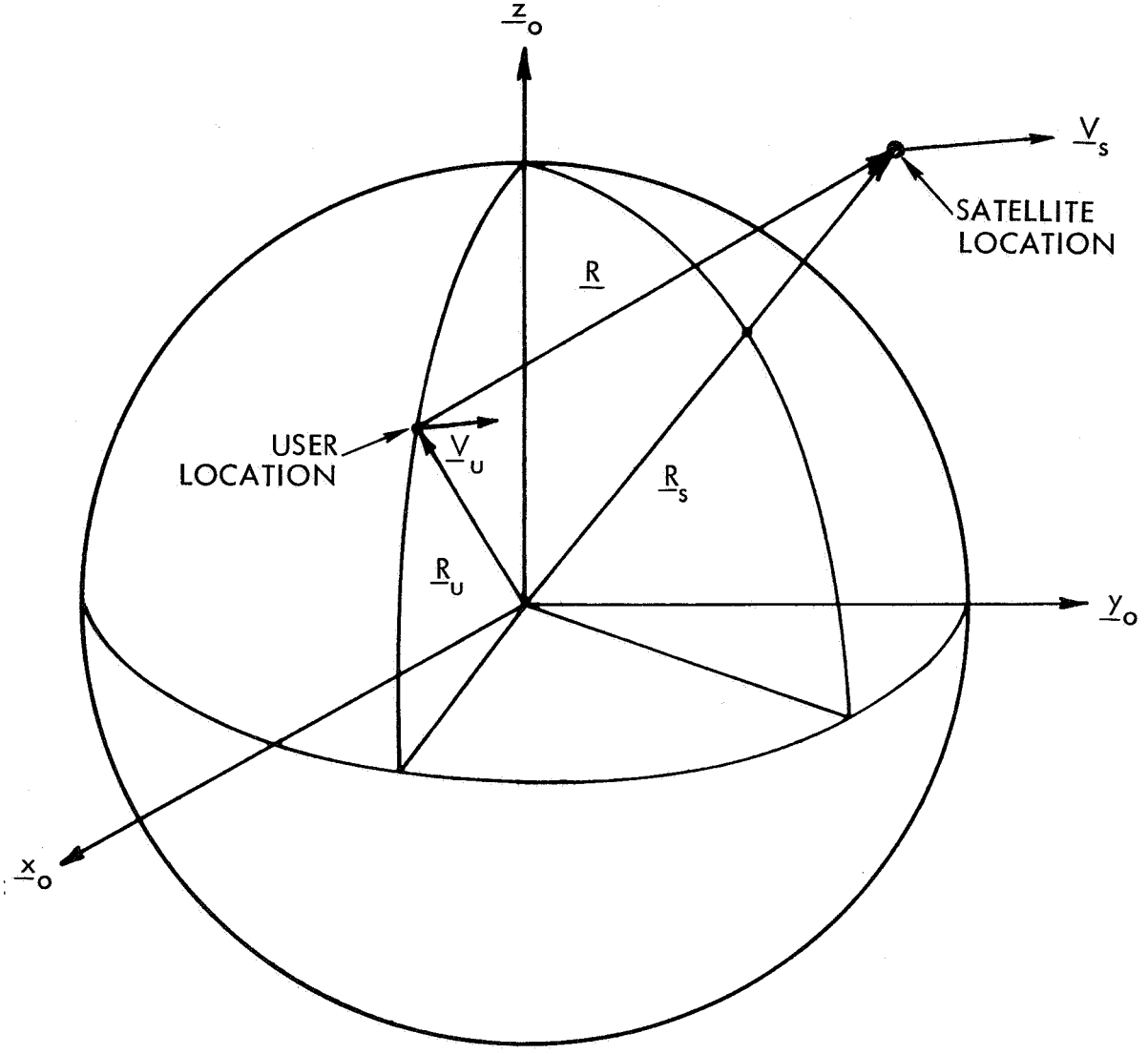

Figure 5-1. Satellite-User Geometry

Hence, the measurement vector corresponding to $\underline{X}_1$ has the form

$$\underline{M}_1 \begin{cases} \left[\phi \ \underline{m}_s \ \phi\right]_{1 \times 6N} & \text{(range)} \\ \left[\phi \ \dot{\underline{m}}_s \ \underline{m}_s \ \phi\right]_{1 \times 6N} & \text{(range-rate)} \end{cases} \tag{26}$$

where the first possible nonzero element of $\underline{M}_1$ is the $(6S - 5)^{th}$ term and ϕ denotes the appropriate null array. The measurement vector corresponding to $\underline{X}_2$ has the form

$$\underline{M}_2 = \begin{cases} \left[-\underline{m}_s \quad \underline{m}_b\right]_{1 \times (3+M)} & \text{(range)} \\ \left[-\dot{\underline{m}}_s \quad \underline{m}_b\right]_{1 \times (3+M)} & \text{(range-rate)} \end{cases} \tag{27}$$

where $\underline{m}_b$ is the vector of appropriate measurement bias partials (see Section 5.4).

5.3.2 Sums and Differences of Range or Range-Rate Measurements

A range (range rate) sum measurement to satellites I and J is defined to be the sum of the individual ranges (range rates) to these satellites. Similarly, a range (range rate) difference measurement to these satellites is defined to be the difference between the ranges (range rates). Using the notation Σ for sums and Δ for differences, the measurements are:

$$\begin{aligned} \Sigma R_{ij} &= R_i + R_j \\ \Sigma \dot{R}_{ij} &= \dot{R}_i + \dot{R}_j \\ \Delta R_{ij} &= R_i - R_j \\ \Delta \dot{R}_{ij} &= \dot{R}_i - \dot{R}_j \end{aligned} \tag{28}$$

Hence, the measurement vector corresponding to $\underline{X}_1$ has the form

$$M_1 = \begin{cases} \left[\phi \quad \underline{m}_i \quad \phi \quad \pm\underline{m}_j \quad \phi \right] & \text{(range)} \quad (29) \\ \left[\phi \quad \dot{\underline{m}}_i \quad \underline{m}_i \quad \phi \quad \pm\dot{\underline{m}}_j \quad \pm\underline{m}_j \quad \phi \right]_{1 \times 6N} & \text{(range rate)} \quad (30) \end{cases}$$

where $\underline{m}_i$ in Equation (29) and $\dot{\underline{m}}_i$ in Equation (30) start at the $(6i-5)^{th}$ term and $\underline{m}_j$ in Equation (29) and $\dot{\underline{m}}_j$ in Equation (30) start at the $(6j-5)^{th}$ term. The plus signs correspond to sum measurements, and the minus to differences. The measurement vector corresponding to $\underline{X}_2$ has the form

$$\underline{M}_2 = \begin{cases} \left[-(\underline{m}_i \pm \underline{m}_j) \,\middle|\, \underline{m}_b \right] & \text{(range)} \\ \left[-(\dot{\underline{m}}_i \pm \dot{\underline{m}}_j) \,\middle|\, \underline{m}_b \right] & \text{(range rate)} \end{cases} \quad (31)$$

5.4 MEASUREMENT BIASES

These biases reflect constant measurement errors originating in the user equipment. The number and order in which they are to be included at the end of $\underline{X}_2$ are specified by input quantities. As mentioned in Section 5.2, they can be individually solved for or considered in the error analysis.

The partials of an observation with respect to these biases depend only on the type of measurement being taken. The quantities input to $\underline{m}_b$ are

$$\frac{\partial(\text{observation})}{\partial(\text{bias})} = \begin{cases} 1 & \text{for} \quad R, \dot{R} \\ 0 & \text{for} \quad \Delta R, \Delta\dot{R} \\ 2 & \text{for} \quad \Sigma R, \Sigma\dot{R} \end{cases} \quad (32)$$

6. USER POSITION SELECTION

The program has two methods of sequentially selecting user positions. In either case, this is done after all combinations of all desired measurement types have been processed for the current user position as indicated in Figure 1-1.

6.1 GRID METHOD

In this method, the area over which user positions are to be selected is defined by boundary values of latitude and longitude and the actual positions by the latitude-longitude spacing between users. This information is input in the following form (see Figure 6-1).

θ_i = initial latitude

θ_f = final latitude

$\Delta\theta$ = incremental change in latitude

λ_i = initial longitude

λ_f = final longitude

$\Delta\lambda$ = incremental change in longitude

6.2 FLIGHT PATH METHOD

This method sequentially selects user positions along a great circle arc at every measurement time. The user is assumed to be moving at a constant speed and altitude. The positions are determined from the initial position, velocity, and heading by use of the following identities from spherical trigonometry (Figure 6-2).

$$\sin\theta = \cos\omega \sin\theta_i + \cos\alpha_i \cos\theta_i \sin\omega \tag{33}$$

$$\cos\alpha = \cos\alpha_i \cos\beta - \sin\beta \sin\alpha_i \sin\theta_i \tag{34}$$

$$\frac{\sin\omega}{\sin\beta} = \frac{\cos\theta_i}{\sin\alpha} = \frac{\cos\theta}{\sin\alpha_i} \tag{35}$$

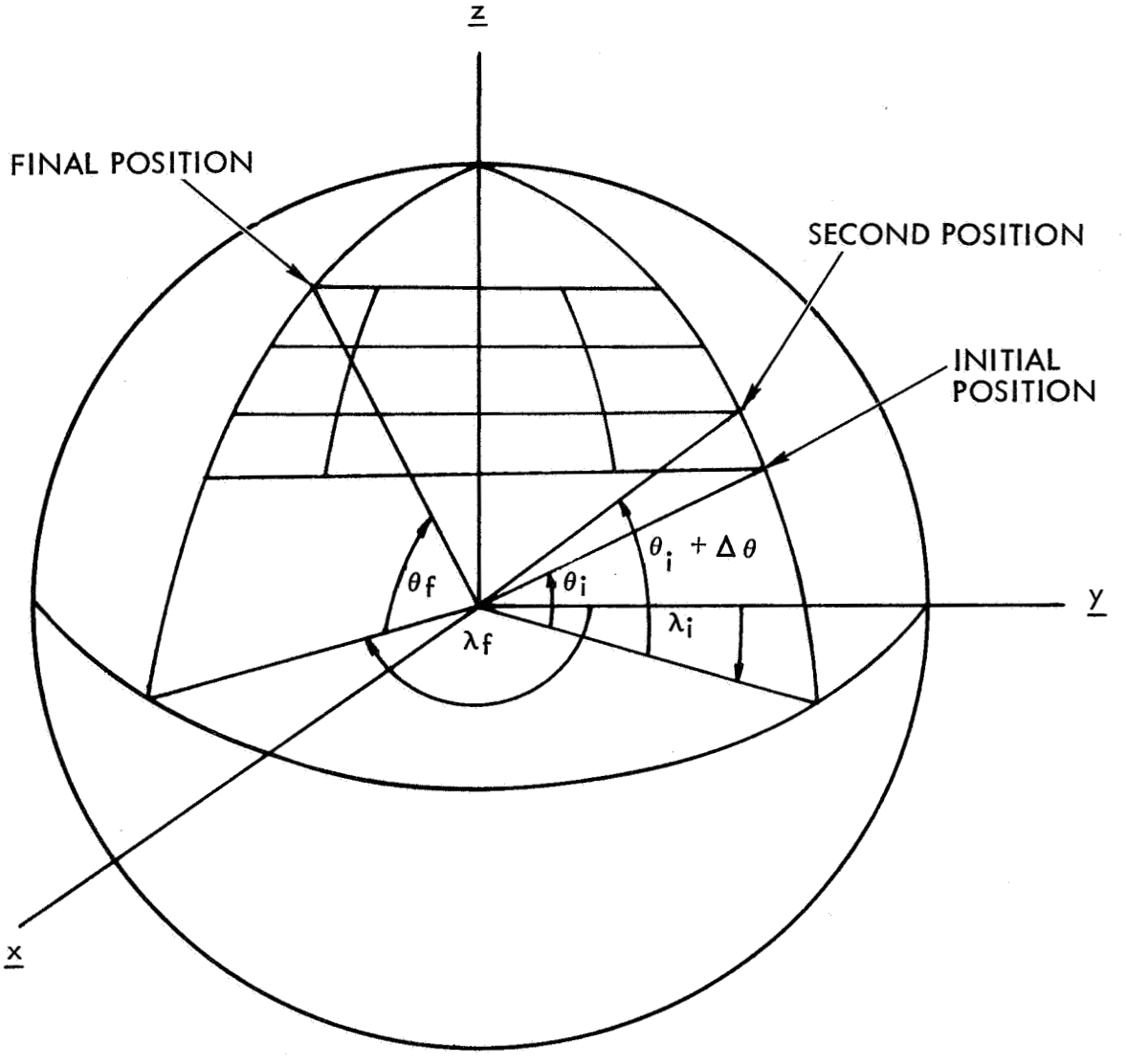

Figure 6-1. Grid Method

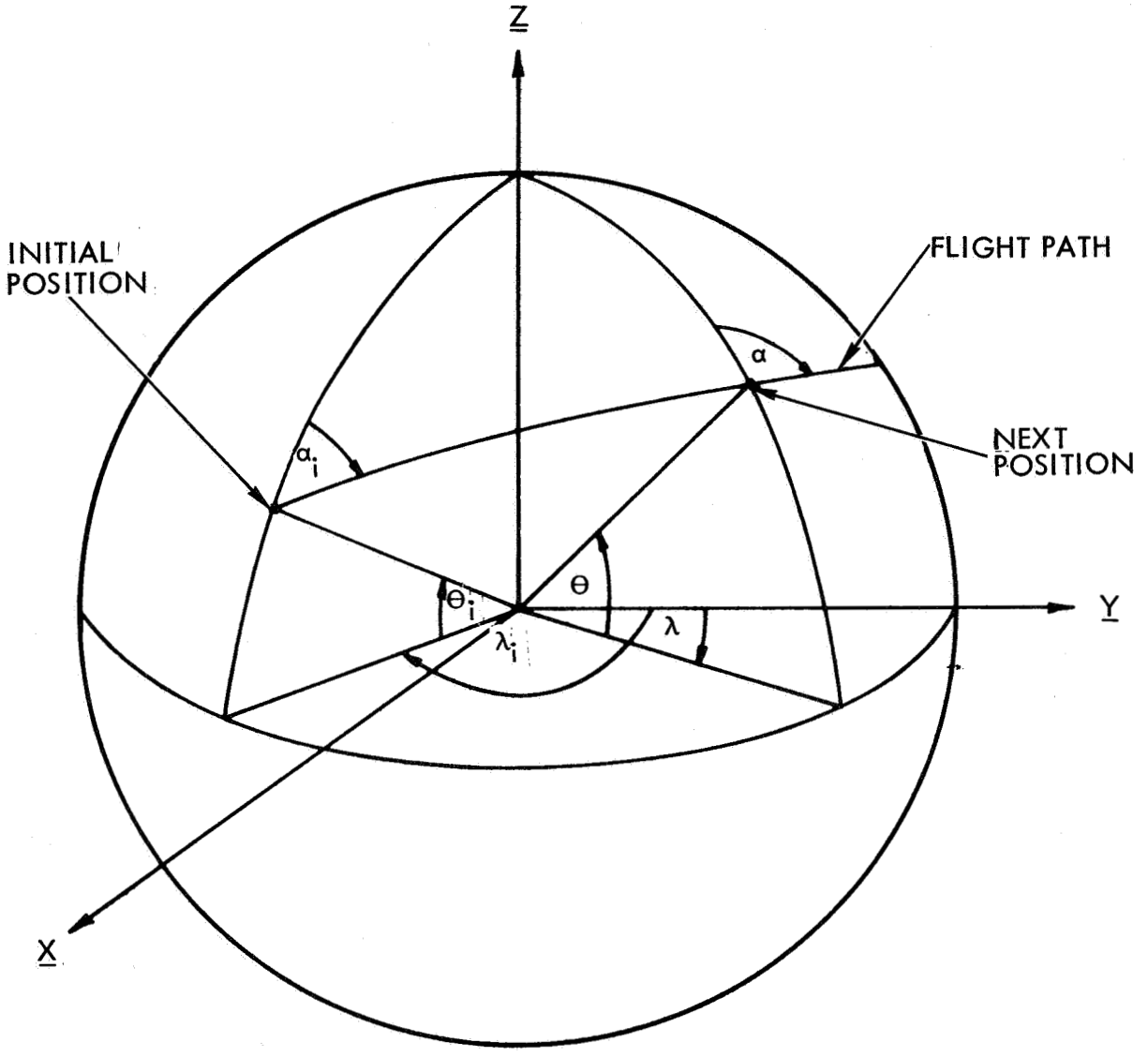

Figure 6-2. Flight Path Method

where θ, θ_i are the final and initial latitudes, α, α_i are the final and initial headings (positive east of north), β is minus the change in west longitude and ω is the angle traversed along the great circle. If V is the user's velocity, and Δt_m is the time between measurements, then ω is given by

$$\omega = \frac{V\Delta t_m}{R} \tag{36}$$

where R is the distance from the user to the center of the earth. In Equations (33) and (34) the angles are restricted to the following ranges:

$$-\frac{\pi}{2} \leq \theta \leq +\frac{\pi}{2}$$

$$\omega \geq 0$$

$$-\pi \leq \alpha \leq +\pi$$

Since the initial conditions are known and ω is readily computed from Equation (36), the latitude θ can be computed from Equation (33) and β follows from Equation (35) which in turn leads to the longitude

$$\lambda = \lambda_i - \beta \tag{37}$$

α also follows from Equations (34) and (35) for use at the next measurement point where θ, α, λ become θ_i, α_i, λ_i.

6.3 VISIBILITY CHECK

At each measurement time, the program checks to see which satellites are visible. The criterion is that each satellite's elevation above the user's local horizon be greater than or equal to an input minimum elevation angle ϵ_m. This check is performed in the following manner (see Figure 6-3).

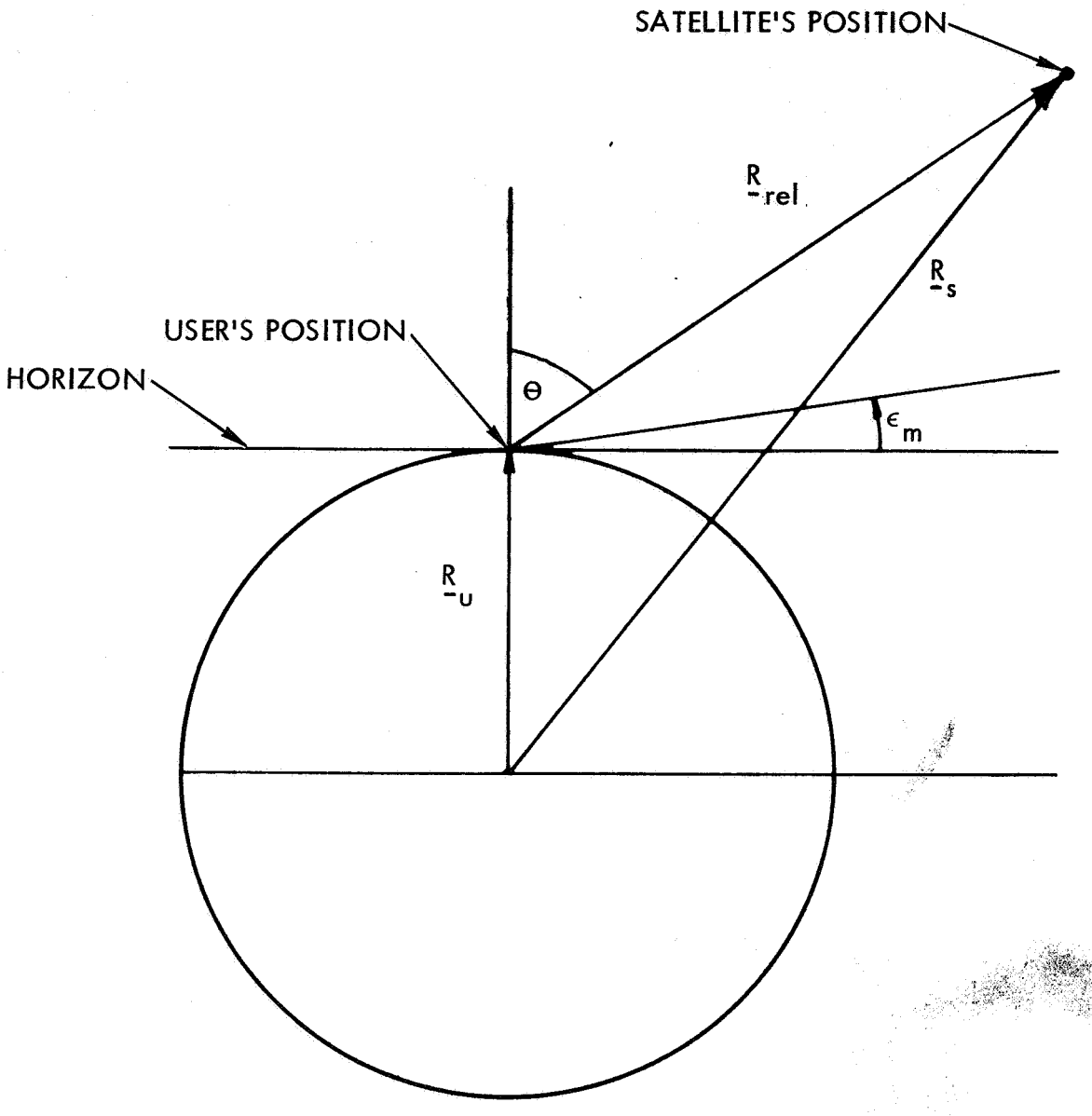

Figure 6-3. Visibility Geometry

Let $\underline{R}_u$ be the user position vector and $\underline{R}_s$ be the satellite position vector. Then the relative range vector $\underline{R}$ is

$$\underline{R} = \underline{R}_s - \underline{R}_u \tag{38}$$

Hence,

$$\cos \theta = \frac{R \cdot R_u}{|\underline{R}||\underline{R}_u|} \tag{39}$$

The visibility criterion requires that

$$\frac{\pi}{2} - \theta \geq \epsilon_m \tag{40}$$

or equivalently

$$\cos \theta \geq \sin \epsilon_m \tag{41}$$

Hence, the program tests on the following relation

$$\frac{\underline{R} \cdot \underline{R}_u}{|\underline{R}||\underline{R}_u|} \geq \sin \epsilon_m \tag{42}$$

7. UPDATE SECTION

To propagate the error covariance matrices between measurement times t_i and t_{i+1}, an updating routine is required. Two updating (state transition) matrices are calculated, one for each partition of the state vector.

7.1 SATELLITE UPDATE

The updating matrix U_1 for $\underline{X}_1$ is calculated from an analytic solution to the variational equations for the satellites.

Let

$$R_j = \sqrt{x_j^2 + y_j^2 + z_j^2} \tag{43}$$

be the magnitude of the relative range of the j^{th} satellite from the user. Define k_j to be

$$k_j = \frac{\mu}{R_j^5} \begin{bmatrix} 3x_j^2 - R_j^2 & 3x_j y_j & 3x_j z_j \\ & 3y_j^2 - R_j^2 & 3y_j z_j \\ \text{symmetric} & & 3z_j^2 - R_j^2 \end{bmatrix}_{3 \times 3} \tag{44}$$

Let

$$\bar{k}_j = \frac{1}{2}\left[k_j(t_{i+1}) + k_j(t_i)\right] \tag{45}$$

be an approximation to the time averaged value of k_j over the updating interval. Using I to denote the identity matrix and Δt to denote the updating interval $(= t_{i+1} - t_i)$ define

$$K_j = \left[\begin{array}{c|c} I + \frac{\Delta t^2}{2}\bar{k}_j & (\Delta t)I + \frac{\Delta t^3}{6}\bar{k}_j \\ \hline (\Delta t)\bar{k}_j + \frac{\Delta t^3}{6}\bar{k}_j\bar{k}_j^T & I + \frac{\Delta t^2}{2}\bar{k}_j \end{array}\right]_{6x6} \tag{46}$$

Using the above, U_1 can be written as a block diagonal matrix of the form

$$U_{1_{i+1/i}} = \begin{bmatrix} K_1 & & & \phi \\ & K_2 & & \\ & & \bullet & \\ & & & \bullet \\ & & & \bullet \\ \phi & & & K_N \end{bmatrix}_{6Nx6N} \tag{47}$$

where ϕ denotes the appropriate array of zeros.

7.2 USER UPDATE

The updating matrix U_4 for the second partition $\underline{X}_2$ is computed in one of two ways corresponding to the mode of selecting user positions (see Section 6). In either case, U_4 is a block diagonal matrix of the form

$$U_4 = \left[\begin{array}{c|c} U_{4user} & \phi \\ \hline \phi & I_{MxM} \end{array}\right]_{(3+M)\ x\ (3+M)} \tag{48}$$

where U_{4user} is the state transition matrix for the user position coordinates.

7.2.1 Grid Method

In the grid method, the user is stationary in an ECF system. Hence, his associated position error covariance matrix remains constant that system. Since this matrix is computed in an ECI system, the

corresponding updating matrix is the product of two coordinate transformations as follows: (see Sections 3 and 5.1 for notation)

$$U_{4user,\ i+1/i} = \frac{\partial \underline{X}_{o_{i+1}}}{\partial \underline{X}_{o_i}} = \frac{\partial \underline{X}_{o_{i+1}}}{\partial \underline{X}_{i+1}} \frac{\partial \underline{X}_{i+1}}{\partial \underline{X}_i} \frac{\partial \underline{X}_i}{\partial \underline{X}_{o_i}} = \frac{\partial \underline{X}_{o_{i+1}}}{\partial \underline{X}_{i+1}} \frac{\partial \underline{X}_i}{\partial \underline{X}_{o_i}} \quad (49)$$

7.2.2 Flight Path Method

In the flight path method of selecting user positions, the user motion is specified in the ECF system. The program calculates U_{4user} from

$$U_{4user,\ i+1/i} = \frac{\partial \underline{X}_{o_{i+1}}}{\partial \underline{X}_{i+1}} \frac{\partial \underline{X}_{i+1}}{\partial \underline{\theta}_{i+1}} \frac{\partial \underline{\theta}_{i+1}}{\partial \underline{\theta}_i} \frac{\partial \underline{\theta}_i}{\partial \underline{X}_i} \frac{\partial \underline{X}_i}{\partial \underline{X}_{o_i}} \quad (50)$$

where

$$\frac{\partial \underline{\theta}_{i+1}}{\partial \underline{\theta}_i} = \begin{bmatrix} \frac{\partial \theta_{i+1}}{\partial \theta_i} & \frac{\partial \theta_{i+1}}{\partial \lambda_i} & \frac{\partial \theta_{i+1}}{\partial r_i} \\ \frac{\partial \lambda_{i+1}}{\partial \theta_i} & \frac{\partial \lambda_{i+1}}{\partial \lambda_i} & \frac{\partial \lambda_{i+1}}{\partial r_i} \\ \frac{\partial r_{i+1}}{\partial \theta_i} & \frac{\partial r_{i+1}}{\partial \lambda_i} & \frac{\partial r_{i+1}}{\partial r_i} \end{bmatrix}$$

From the equations in Section 6.2, it follows that

$$\frac{\partial \underline{\theta}_{i+1}}{\partial \underline{\theta}_i} = \begin{bmatrix} \frac{\partial \theta_{i+1}}{\partial \theta_i} & 0 & 0 \\ \frac{\partial \lambda_{i+1}}{\partial \theta_i} & 1 & 0 \\ 0 & 0 & 1 \end{bmatrix} \quad (51)$$

where

$$\frac{\partial\theta_{i+1}}{\partial\theta_i} = \frac{1}{\cos\theta_{i+1}}\left(\cos\theta_i \cos\omega - \sin\theta_i \sin\omega \cos\alpha_i\right)$$

$$\frac{\partial\lambda_{i+1}}{\partial\theta_i} = \frac{-\sin\omega \sin\alpha_i \sin\theta_{i+1}\left[\frac{\partial\theta_{i+1}}{\partial\theta_i}\right]}{\cos(\lambda_i - \lambda_{i+1})\cos^2\theta_{i+1}} \qquad (52)$$

Using Equations (47) through (52) to define U_1 and U_4, the updating section calculates the following:

$$\begin{aligned} J_{1,\,i+1/i} &= U_{1,\,i+1/i}\, J_{1,\,i/i} U^T_{1,\,i+1/i} \\ J_{3,\,i+1/i} &= U_{4,\,i+1/i}\, J_{3,\,i/i} U^T_{1,\,i+1/i} \\ J_{4,\,i+1/i} &= U_{4,\,i+1/i}\, J_{4,\,i/i} U^T_{4,\,i+1/i} + R_i \end{aligned} \qquad (53)$$

The random disturbance covariance matrix R_i adds the effect of state noise to the updated user position error covariance matrix $J_{4,\,i+1/i}$. State noise results from random disturbances in the user's speed and heading. R_i is computed as follows:

$$R_i = \begin{bmatrix} J_{R(3\times3)} & \phi \\ \phi & \phi \end{bmatrix}_{(3+M)\times(3+M)} \qquad (54)$$

where

$$J_R = \left(\frac{\partial \underline{X}_o}{\partial \underline{\Psi}}\right) J_\psi \left(\frac{\partial \underline{X}_o}{\partial \underline{\Psi}}\right)^T \tag{55}$$

J_ψ is a 2 x 2 input error covariance matrix of speed and heading and $\partial \underline{X}_o / \partial \underline{\Psi}$ is the 3 x 2 transformation matrix that maps these errors into the user's position coordinates.

That is

$$\frac{\partial \underline{X}_o}{\partial \Psi} = \frac{\partial \underline{X}_o}{\partial \underline{X}} \frac{\partial \underline{X}}{\partial \underline{\theta}} \frac{\partial \underline{\theta}}{\partial \underline{\Psi}} \tag{56}$$

$$\frac{\partial \underline{\theta}}{\partial \underline{\Psi}} = \begin{bmatrix} \frac{\partial \theta}{\partial V} & \frac{\partial \theta}{\partial \alpha_i} \\ \frac{\partial \lambda}{\partial V} & \frac{\partial \lambda}{\partial \alpha_i} \\ \frac{\partial r}{\partial V} & \frac{\partial r}{\partial \alpha_i} \end{bmatrix} \tag{57}$$

From the equations in Section 6.2, it follows that

$$\frac{\partial \theta}{\partial V} = \frac{\Delta t}{R \cos \theta} (\cos \theta_i \cos \omega \cos \alpha_i - \sin \theta_i \sin \omega)$$

$$\frac{\partial \theta}{\partial \alpha_i} = - \sin \omega \sin \alpha$$

$$\frac{\partial \lambda}{\partial V} = - \frac{1}{\cos (\lambda_i - \lambda)} \left[\frac{\Delta t}{R} \frac{\cos \omega \sin \alpha_i}{\cos \theta} + \frac{\sin \omega \sin \alpha_i \sin \theta}{\cos^2 \theta} \frac{\partial \theta}{\partial V} \right] \qquad (58)$$

$$\frac{\partial \lambda}{\partial \alpha_i} = - \frac{1}{\cos (\lambda_i - \lambda)} \left[\frac{\sin \omega \cos \alpha_i}{\cos \theta} + \frac{\sin \omega \sin \alpha_i \sin \theta}{\cos^2 \theta} \frac{\partial \theta}{\partial \alpha_i} \right]$$

$$\frac{\partial r}{\partial V} = 0 \qquad \frac{\partial r}{\partial \alpha_i} = 0$$

8. EFFECT OF SATELLITE ESTIMATION ERRORS

The user of a navigation satellite system does not estimate the satellite positions. The satellite orbits are determined by prior tracking from ground stations, and are transmitted to the user after being computed at a central site. Errors in the satellite locations are determined by orbit determination studies. In a least squares analysis this is done by appending to the inverse normal matrix an additional term accounting for the satellite errors. In the filter analysis of NAVSAP, it is necessary to do the computation twice as described in Sec. 5.2. In the first pass, the gain is computed assuming the satellite errors are zero; in the second, the gain is used in a fictitious attempt to solve for the satellite locations. The resulting error covariance matrix of user position contains the desired effect of satellite errors.

This multiple pass through the filter is undesirable for parametric studies and it turns out to be unnecessary. Since the satellite locations are essentially not observable in the user data (tracking with a single station of unknown location), it can be postulated that, even when the satellite position is included in the regression vector, the satellite errors are only slightly reduced, and the effect on user position errors is essentially the same as when the satellite positions are not solved for. Hence, error analysis runs can be made, assuming that satellite positions are estimated, with the results showing only the effect of the initial satellite position uncertainties.

In more concrete terms, consider the linear observation model

$$y = Ax + Bz + \epsilon \tag{59}$$

where y is the observation vector, x is the user position vector, z is the satellite position vector, and ϵ is an error vector with uncorrelated components. A and B are matrices of partial derivatives relating the deviations x and z to the observation deviations z. Assuming the satellite positions are known perfectly ($z = 0$), the minimum variance estimate of x is

$$\hat{x} = (A^T W A)^{-1} A^T W y \tag{60}$$

where

$$W = \left[E(\epsilon\epsilon^T)\right]^{-1} \tag{61}$$

The covariance matrix of the error in this estimate, considering the effect of a priori satellite errors z, is

$$\text{Cov}\,(\hat{x}-x) = (A^TWA)^{-1} + (A^TWA)^{-1}A^TWBQB^TWA(A^TWA)^{-1} \tag{62}$$

where Q is the a priori satellite error covariance matrix

$$Q = E(zz^T)$$

On the other hand, if the satellite position is included in the regression vector, the estimate becomes

$$\begin{pmatrix}\hat{x}\\ \hat{y}\end{pmatrix} = \begin{pmatrix}A^TWA & A^TWB\\ B^TWA & B^TWB + Q^{-1}\end{pmatrix}^{-1}\begin{pmatrix}A^T\\ B^T\end{pmatrix}Wy \tag{63}$$

with error covariance matrix

$$E\left[\begin{pmatrix}\hat{x}-x\\ \hat{z}-z\end{pmatrix}\begin{pmatrix}\hat{x}-x\\ \hat{z}-z\end{pmatrix}^T\right] = \begin{pmatrix}A^TWA & A^TWB\\ B^TWA & B^TWB + Q^{-1}\end{pmatrix}^{-1} \tag{64}$$

Partitioning Equation (64) leads to the individual results for x and z

$$\begin{aligned}\text{Cov}\,(\hat{x}-x) &= (A^TWA)^{-1}+(A^TWA)^{-1}A^TWB\left[B^TWB+Q^{-1}-B^TWA(A^TWA)^{-1}A^TWB\right]^{-1}\\ &\quad\cdot B^TWA(A^TWA)^{-1}\\ &= \left[A^TWA - A^TWB(B^TWB + Q^{-1})^{-1}B^TWA\right]^{-1} \qquad (65)\end{aligned}$$

$$\text{Cov}\,(\hat{z}-z) = \left[B^TWB + Q^{-1} - B^TWA(A^TWA)^{-1}A^TWB\right]^{-1} = Q^* \tag{66}$$

Using Equation (66) in (65) leads to the desired expression

$$\text{Cov}\,(\hat{x}-x) = (A^TWA)^{-1} + (A^TWA)^{-1}A^TWB\,Q^*\,B^TWA(A^TWA)^{-1} \tag{67}$$

Assuming the satellite positions are solved for is equivalent to using Equation (67) in place of Equation (63), which is a good approximation if $Q^* \approx Q$. This will be true if the satellite positions are only weakly observalbe in the data.

The correctness of this hypothesis is shown by comparison of the computer results presented in Table 1. The first column shows results for no satellite errors. The second column considers, satellite

position errors, requiring two passes through the filter as described in Section 5.2. The third column results when satellite positions are solved for.

The last two columns are nearly equal, which demonstrates conclusively that solving for satellite positions is essentially equivalent to considering them. Hence, the extra pass through the filter is not required.

Table 1. Comparison of Solving for and Considering Satellite Errors.

East Longitude	North Latitude	No Satellite Errors	Consider Satellite Errors	Solve for Satellite Errors
30°	0	347	448	448
	30	468	588	586
60	0	327	442	441
	30	341	455	454
	60	364	474	473

Notes: Measurement noise = 100 ft (1σ)
User altitude error = 150 ft (1σ)
Satellite position errors from Appendix K based on 72 hours tracking from three stations.

APPENDIX K

SUPPORTING ORBIT DETERMINATION ANALYSIS

In order to assess the magnitudes and importance of certain variables in the satellite tracking and orbit determination process, several runs were made with the TRW Systems ESPOD computer program. The purpose of the program was to determine the effects of the following: of using angle measurements and range-rate measurements in addition to range measurement, of using two tracking stations or three, of tracking for 72 hours or 36 hours, and of solving or not solving for the earth's gravitational constant and two or more harmonics.

A single satellite whose ground trace is centered at 75^{o} west longitude and inclined at 18.5^{o} to the equatorial plane was chosen for the first series of tracking analyses. The orbit ground trace and tracking station locations are shown in Figure K-1. Stations 1 and 2 are used in all cases where only two-station tracking is specified. These locations were chosen to provide good tracking geometry while conforming to geographical realities. During the course of the study a recommended tracking network was finalized. A three station, single-satellite tracking arrangement was selected from this network for the final case considered.

Table K-I lists the values and sources of the errors used in the study. The measurement errors are considerably in excess of the expected errors summarized in subsec. 2.4 in the main body of this report, and the data rate was less (1 point/min). The resulting errors turn out, therefore, to be greater than those presented in subsec. 2.4. These preliminary analyses were nevertheless quite adequate to provide the answers to the questions posed.

The study consisted of the following cases:

1) Seventy two-hours tracking with two stations, RAER measurements.
   a) Solve for satellite state. Consider measurement bias errors, survey errors and μ, J_2 uncertainties.
   b) Solve for satellite state and above parameters.

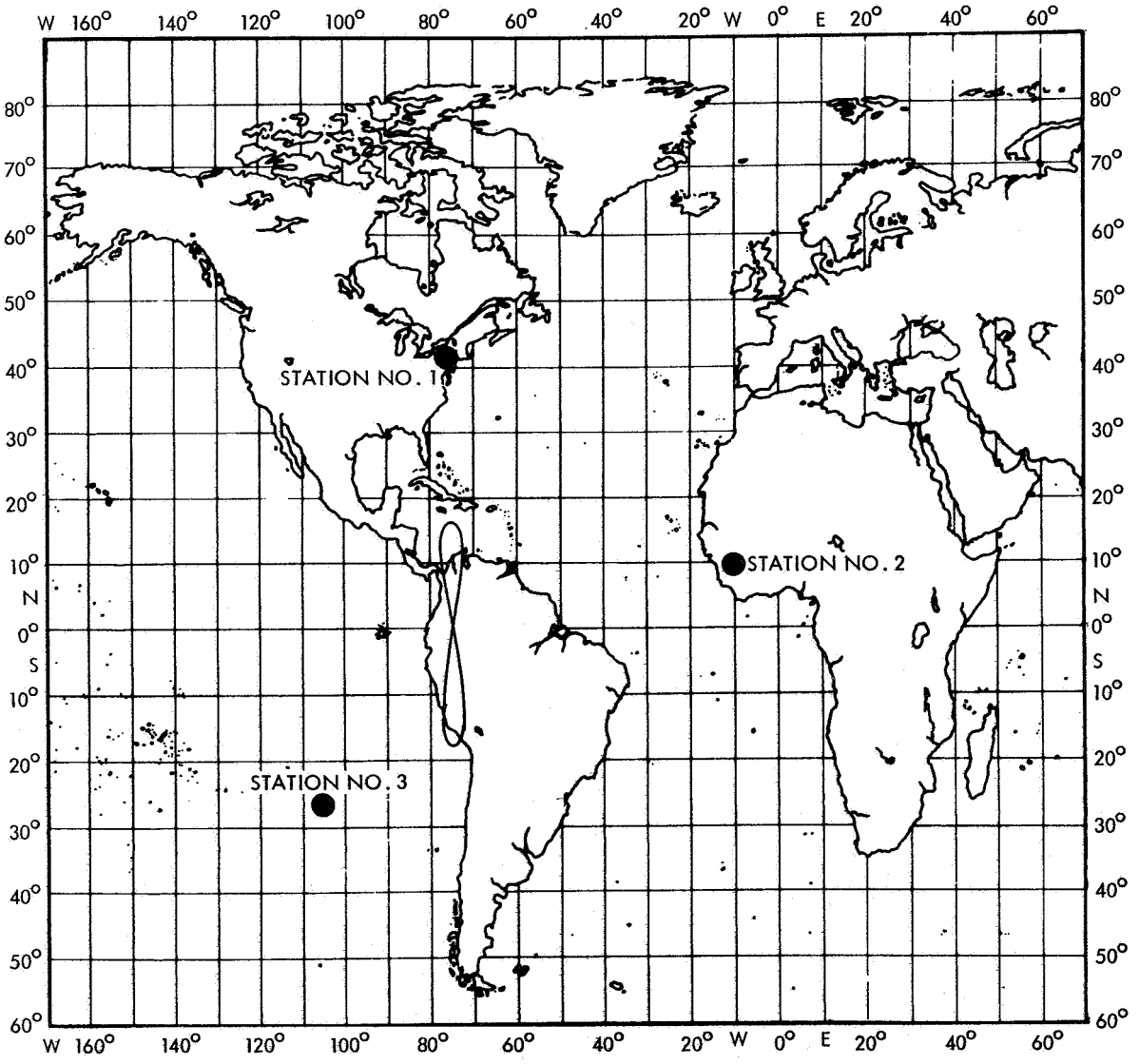

Figure K-1. Tracking Configuration

TABLE K-I

ERROR SOURCES (1-SIGMA)

Measurement Errors

	Noise	Bias
R	60 ft	120 ft
A	1.4 mr	3.2 mr
E	1.4 mr	3.2 mr
$\dot{R}$	0.06 ft/sec	0.06 ft/sec

Station Location Errors

Longitude	100 ft
Latitude	100 ft
Altitude	100 ft

Gravitational Potential Uncertainties

μ	1.06×10^{11} ft^3/sec^2
J_2	2.0×10^{-7}
J_{22}	2.0×10^{-7}
J_{33}	2.6×10^{-7}

c) Range measurements only.

2) Seventy two-hours tracking with three stations, range measurements.

a) Solve for satellite state. Consider parameter errors.

b) Solve for satellite state and parameters.

c) Effect of J_{22} and J_{33}.

3) Thirty six-hours tracking with three stations.

a) Solve for satellite state. Consider parameter errors.

b) Solve for satellite state and parameters.

Results can be scaled to apply to other data rates and noise variances. If n data points are taken in a short time interval Δt, with measurement error variance σ_n^2, then the results will be very nearly the same as for m data points in the same interval with variance

$$\sigma_m^2 = \frac{m}{n} \sigma_n^2$$

Results

The tracking analyses are based on minimum variance estimation. The numerical computations were performed utilizing the TRW System's ESPOD computer program series. A brief description of the methods involved is given in (app. G).

Case 1 - 72-Hr Tracking - Two Stations

Table K-II shows the satellite position and velocity standard deviations in a u, v, w coordinate system, a right-handed set with u in the direction of the geocentric radius vector, w in the direction of the angular momentum vector, and v completing the orthogonal set. The predominant error source is seen to be the uncertainty in the earth gravitational constant μ. This error affects significant period errors, which are manifest in large v (in track) errors.

Solving for the parameters leads to a considerable improvement particularly in the v (downrange) direction. Only the results for range

TABLE K-II

ERRORS FOR CASE 1 - 72-HR TRACKING FROM TWO STATIONS WITH RAE$\dot{R}$ MEASUREMENTS AT 1/MIN

		Solve for Satellite State Only		Solve for State and Parameters
		Total Error	Contribution of μ Uncertainty	Total Error
Position (ft)	σ_u	189	168	98
	σ_v	3250	3060	720
	σ_w	816	742	198
Velocity (ft/sec)	$\sigma_{\dot{u}}$	0.247	0.233	0.0516
	$\sigma_{\dot{v}}$	0.0342	0.0340	0.00687
	$\sigma_{\dot{w}}$	0.151	0.135	0.00705

measurements are not tabulated since there is no significant change from the previous results. Hence, there is no benefit in taking angle measurements.

Case 2 - 72-Hr Tracking - Three Stations

The results are shown in Table K-III. As in case 1, there is considerable benefit in solving for the parameters. The additional station provides the primary benefit of reducing the in-track error from 720 to 452 ft. For shorter tracking periods, it can be expected that this effect would be more pronounced, with a substantial reduction occurring also in the cross track errors.

The last columns show the effect of the uncertainty in the J_{22} earth potential coefficient. The results show a substantial increase in the satellite errors, indicating the need to solve for J_{22}. When this was done, the errors were essentially reduced to their previous values. A further run was made to examine the effect of J_{33}; however, in that case there was no appreciable contribution to the total error.

Case 3 - 36-Hr Tracking - Three Stations

The results, given in Table K-IV, again show the need to solve for the parameters. Comparing with Table K-III shows, furthermore, that there is very little to be gained from increasing the tracking period from 36 to 72 hours.

TABLE K-III

ERRORS FOR CASE 2 - 72-HR TRACKING FROM THREE STATIONS WITH RANGE MEASUREMENTS AT 1/MIN

		Solve for Satellite State Only		Solve for State and Parameters	Consider Effect of J_{22}	
		Total Error	Contribution of μ	Total Error	Total Error	Contribution of J_{22}
Position (ft)	σ_u	141	138	79	96	54
	σ_v	3500	3200	452	1620	1590
	σ_w	338	295	150	508	485
Velocity (ft/sec)	$\sigma_{\dot{u}}$	0.152	0.144	0.0330	0.122	0.117
	$\sigma_{\dot{v}}$	0.0354	0.0351	0.00573	0.00616	0.00228
	$\sigma_{\dot{w}}$	0.0254	0.0231	0.00576	0.00581	0.00020

TABLE K-IV
ERRORS FOR CASE 3 - 36-HR TRACKING FROM THREE STATIONS
WITH RANGE MEASUREMENTS AT 1/MIN

		Solve for Satellite State Only		Solve for State and Parameters
		Total Error	Contribution of μ Uncertainty	Total Error
Position (ft)	σ_u	98	61	80
	σ_v	2550	2340	492
	σ_w	316	46	162
Velocity (ft)	$\sigma_{\dot{u}}$	0.184	0.169	0.0358
	$\sigma_{\dot{v}}$	0.0365	0.00003	0.0060
	$\sigma_{\dot{w}}$	0.0442	0.00002	0.0062

APPENDIX L

EFFECT OF APPROXIMATING ELLIPTICAL ORBITS WITH CIRCLES

This section gives analytic expressions for the in-track and radial errors caused by neglecting the ellipticity of the orbit, as is done in the user computations described in sec. 3 in the main body of this report. These expressions can be used to provide updated satellite errors for use in the NAVSAP error analysis program.

It is assumed that at some instant t_o, radar tracking has determined the position of the satellite in question and the parameters of its (elliptical) orbit.

The plane of the elliptical orbit is defined by:

1) the angle λ of the orbit ascending node with the positive x-axis of some earth-centered inertial system

2) the inclination i of the orbit plane with the equatorial plane.

The approximate satellite position computed by the user is then given by the following equations:

$$X = \frac{1}{2}\rho\left[(1 + \cos i)\cos\lambda + (1 - \cos i)\cos(2\omega\tau - \lambda)\right] \quad \text{(L-1)}$$

$$Y = \frac{1}{2}\rho\left[(1 + \cos i)\sin\lambda - (1 - \cos i)\sin(2\omega\tau - \lambda)\right] \quad \text{(L-2)}$$

$$Z = \rho \sin i \sin\omega\tau \quad \text{(L-3)}$$

where $\omega = \frac{2\pi}{24}$ rad/hr, $\tau = t - t_i$ and t_i will be defined below. This definition of the approximate orbit causes its plane to coincide with the plane of the actual orbit.

The orbit parameters λ and i may be expressed as perturbations about nominal parameters λ_o and i_o as:

$$i_o + \Delta i = i$$

$$\lambda_o + \Delta\lambda = \lambda$$

The radius of the approximate orbit is chosen so that at time t_o, the position of the satellite computed from the equations of the approximate orbit coincides with the position of the satellite in the actual orbit as determined by the orbit determination program. The time t_i of nodal crossing of the approximate orbit is chosen to facilitate this; i.e.,

$$t_i = t_o - \frac{\theta_o}{\omega}$$

θ_o is the angle between the radius vector r_o of the actual orbit at time t_o and the line of nodes.

The radius of the approximate orbit is thus:

$$\rho = \rho_o + \Delta\rho = r_o$$

(Observe that this approximate orbit is not actually a physical orbit, since circular orbits of radius ρ will not in general have 24-hr periods).

The procedure is consequently the following: the ground system tracks for some time interval, and determines the satellite orbit parameters and position and velocity at the end of this interval. From these it determines $\Delta\rho$, $\Delta\lambda$, Δi, and t_i as described above and transmits them to the users via the satellite. The user then uses these values in Eqs. (L-1) through (L-3) to determine the satellite position at this measurement time t. Of interest is the error in this estimate of position at t as compared with the elliptical orbit.

It is most convenient to derive the desired expressions in terms of perturbations from circular orbits[1]. The situation is most easily explained with the aid of Figure L-1 below.

The quantities on Figure L-1 are defined as follows:

Arc DAB - circular approximation to true satellite orbit
Arc DC - true (elliptical) orbit

[1] "Guidance Error Analysis of Satellite Trajectories" by L. J. Skidmore and H. S. Braham, J. Aerospace Sciences, September 1962, pp 1091-1101.

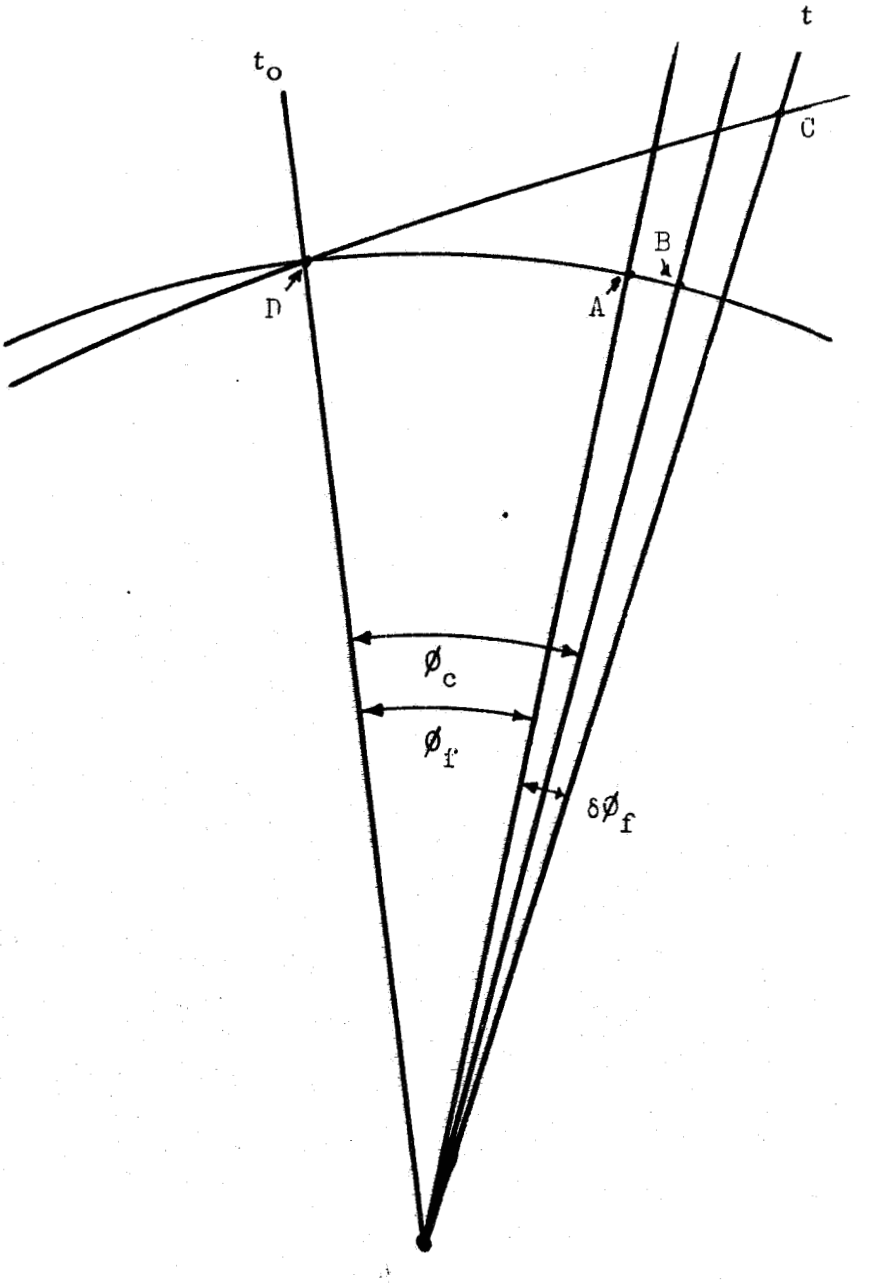

Figure L-1. Geometry of Orbital Perturbations

D - position of satellite at time t_o

C - position of satellite at time $t = t_o + \Delta t$

A - position of satellite in circular orbit of radius ρ at time $t + \Delta t$, starting at D at time t_o

B - position of satellite at time $t_o + \Delta t$ as calculated from Eqs. (L-1) through (L-3).

Then the in-track error ϕ is given by

$$\phi = \phi_f + \delta\phi_f - \phi_c$$

ϕ_f = angle traversed by a satellite in a circular orbit of radius ρ in time Δt.

$$= \sqrt{\frac{\mu}{\rho^3}}\ \Delta t \quad (\mu \text{ is proportional to the gravitational constant}).$$

ϕ_c = angle traversed by satellite in the approximate circular orbit in time Δt.

$$= \frac{2\pi}{24}\ \Delta t \text{ radians.} \quad (\Delta t \text{ in hours}).$$

$\delta\phi_f$ = difference in angular displacement between circular orbit and perturbed circular orbit[2].

$$= (-3\phi_f + 4 \sin \phi_f)\ \frac{\delta v_o}{v_o} + 2\ (1 - \cos \phi_f)\ \delta\beta_o$$

where δv_o is the magnitude of the change in tangential velocity at D which produces the elliptical orbit DC, and $\delta\beta_o$ is the change in the angle of the tangential velocity at D. The angular in-track error is thus:

$$\phi = \left\{\sqrt{\frac{\mu}{\rho^3}} - \frac{2\pi}{24}\right\} \Delta t + (-3\phi_f + 4 \sin \phi_f)\frac{\delta v_o}{v_o}$$

$$+ 2\ (1 - \cos \phi_f)\ \delta\beta_o$$

[2] Skidmore and Braham, op. cit.

ϕ_f will usually be small (for a one hour prediction, $\phi_f = 15$ deg), so that this expression becomes:

$$\phi = \left\{ \sqrt{\frac{\mu}{\rho^3}} - \frac{2\pi}{24} \right\} \Delta t + \phi_f \frac{\delta v_o}{v_o}$$

$$= \left\{ \sqrt{\frac{\mu}{\rho^3}} \left(1 + \frac{\delta v_o}{v_o}\right) - \frac{2\pi}{24} \right\} \Delta t$$

$$\simeq \left\{ \sqrt{\frac{\mu}{\rho^3}} - \frac{2\pi}{24} \right\} \Delta t$$

The radial error is obtained directly from reference as:

$$\frac{\delta r}{r_o} = 2(1 - \cos \phi_f) \frac{\delta v_o}{v_o} - \sin \phi_f \, \delta\beta_o$$

For ϕ_f small, this reduces to:

$$\frac{\delta r}{r_o} \simeq - \phi_f \, \delta\beta_o$$

$$= -\sqrt{\frac{\mu}{\rho^3}} \, \Delta t \, \delta\beta_o$$

(Clockwise angles are positive in the above expressions.)

In-track and radial error can thus be calculated from the tracking interval Δt if the parameters of the (true) elliptical orbit are known.

APPENDIX M

RESOLUTION OF RANGE AND RANGE-DIFFERENCE MEASUREMENT AMBIGUITIES

1. RANGE AMBIGUITY

Let $R_i^{*'}$ be the range measurement from the i^{th} satellite, corrected for satellite oscillator drift. Then $R_i^{*'}$ has the form:

$$R_i^{*'} = R_i + B_o + w_i - K_i \times 2,000$$

and B_o is a number which is unique modulo 2,000. The problem is to determine the quantity $R_i + B_o + w_i$ given the measurement $R_i^{*'}$. The problem will be solved if we can determine a procedure for adding some multiple of 2,000 to each measurement $R_i^{*'}$ (say $K_i' \times 2,000$) so that the quantity

$$R_i^{*'} + K_i' \times 2,000 - R_i - w_i$$

is the same for all i. This quantity will then be the bias common to all range measurements. We proceed as follows:

Suppose $R_i^{*'}$ is the first-range measurement received. Let $\hat{R}_i$ be the computed range based on the a priori estimate of the user's position and the computed satellite position. Let ϵ_i be the error in this computed range, i.e.,

$$R_i = \hat{R}_i + \epsilon_i$$

Since

$$R_i^{*'} = R_i + B_o + w_i - K_i \times 2,000$$

(Recall that K_i is arbitrary, but to each different K_i there corresponds a different value of the bias B_o.)

We have

$$R_i^{*'} = \hat{R}_i + \epsilon_i + B_o + w_i - K_i \times 2,000$$

Expand

$$\hat{R}_i \text{ as } \hat{R}_i = \Delta\hat{R}_i + K_i'' \times 2,000,\ K_i'' \text{ an integer,}$$

Then,

$$R_i^{*'} = \Delta R_i + K_i'' \times 2,000 + \epsilon_i + B_o + w_i - K_i \times 2,000$$

Purely for convenience, choose $K_i = K_i''$. This uniquely determines a value of B_o. We must modify a subsequent measurement, say $R_j^{*'}$, so that the quantity

$$R_j^{*'} + K_j' \times 2,000 - R_j - w_j$$

is the same as the quantity

$$R_i^{*'} - \Delta\hat{R}_i - \epsilon_i - w_i$$

We do this as follows:

For the first measurement, with $K_i = K_i''$, the bias is

$$B_o = R_i^{*'} - \Delta\hat{R}_i - \epsilon_i - w_i$$

An estimate of the bias is

$$\hat{B}_o' = R_i^{*'} - \Delta\hat{R}_i$$

(The error in the estimate is

$$B_o - \hat{B}_o' = -\epsilon_i - w_i)$$

We will now use the estimate $\hat{B}_o'$ to correct the measurement $R_j^{*'}$. To do this, we select K_j' so that

$$R_j^{*'} + K_j' \times 2,000 - \hat{R}_j \simeq R_i^{*'} - \Delta\hat{R}_i = \hat{B}_o'$$

Or select K_j' so that

$$K_j' \times 2,000 \simeq \hat{B}_o' + \hat{R}_j - R_j^{*'}$$

To do this, simply compute $\hat{B}_o' + \hat{R}_j - R_j^{*'}$, and round to the nearest 2,000. The probability of selecting the wrong K_j' is found as follows:

The actual bias is

$$B_o = R_i^* - \Delta\hat{R}_i - \epsilon_i - w_i$$

The correct K_j is the one that satisfies

$$\begin{aligned} R_j^* + K_j \times 2,000 &= R_j + B_o + w_j \\ &= R_j + \underbrace{R_i^{*'} - \Delta\hat{R}_i}_{\hat{B}_o'} - \epsilon_i - w_i + w_j \\ &= \hat{R}_j + \hat{B}_o' + \epsilon_j - \epsilon_i - w_i + w_j \end{aligned}$$

$$\therefore K_j \times 2,000 = \hat{R}_j + \hat{B}_o' - R_j^* + \epsilon_j - \epsilon_i - w_i + w_j$$

So, we will select the wrong K_j if

$$\left|\epsilon_j - \epsilon_i - w_i + w_j\right| \geq 1,000$$

The probability of this happening can be directly calculated, knowing the distributions of ϵ_j, ϵ_i, w_i, w_j.

2. RANGE DIFFERENCE AMBIGUITY

The i^{th} and j^{th} range measurements (corrected for satellite clock drift) have the form:

$$R_i^* = R_i + B_o + w_i - K_i \times 2,000$$

$$R_j^* = R_j + B_o + w_j - K_j \times 2,000 \qquad (K_i,\ K_j \text{ are integers})$$

hence

$$\Delta = R_i^* - R_j^* = R_i - R_j + w_i - w_j - (K_i - K_j) \times 2,000$$

Let $\hat{R}_i$, $\hat{R}_j$ be the values of R_i and R_j computed on the basis of an a priori estimate of the user's position. Let ϵ_i and ϵ_j be the errors in these computations, i.e.,

$$R_i = \hat{R}_i + \epsilon_i$$

$$R_j = \hat{R}_j + \epsilon_j$$

Substituting in the above:

$$\Delta = \hat{R}_i - \hat{R}_j + \epsilon_i - \epsilon_j + w_i - w_j - K_{ij} \times 2,000 \quad (K_{ij} = K_i - K_j)$$

i.e.,

$$K_{ij} \times 2,000 = \hat{R}_i - \hat{R}_j - \Delta + \epsilon_i - \epsilon_j + w_i - w_j$$

So, if we round $\hat{R}_i - \hat{R}_j - \Delta$ to the nearest multiple of 2,000, the probability of rounding to an incorrect K_{ij} equals the probability that $|\epsilon_i - \epsilon_j + w_i - w_j| > 1,000$. This probability may be calculated, knowing the distributions of ϵ_i, ϵ_j, w_i, w_j.

APPENDIX N

THE RESORB PROGRAM

RESORB is a special computer program designed for simulation of commensurate and near-commensurate orbits (synchronous and super or subsynchronous orbits) with or without station keeping. These orbits are subject to resonance due to the longitude dependent (tesseral) harmonics of the potential field. The resonance manifests itself in the libration of the groundtrack with periods measured in years. Since a libration cycle contains many hundred orbits, numerical intergration of the accelerations by Cowell's or Encke's method requires hours of machine time.

RESORB integrates Lagrange's planetary equations. The potential field is expressed by the Keplerian elements (Kaula's formulation) and as long as only the long-periodic (critical) terms are introduced, the integration steps can reach many times the oribital period. Thus, several hundred orbits are integrated in a second. (Long-periodic luni-solar effects are also included in the perturbations.)

This program handles orbits with any inclination except that of exactly zero (for example, even 0.1° can be handled) and any eccentricity from zero to about 0.8. Deviation from exact commensurability slows down the program, noticable only when the oribit is so far off resonance (period off more than 0.1 percent) that it does not librate any more, but these cases are out of the range of RESORB application.

The RESORB program contains an optional subroutine which determines from an initial estimate the correct semimajor axis for the nearest commensurate orbit. Stationkeeping is also optional. If deadband width is given, the program prints out the exact date when the satellite reaches the bottom of the limit cycle. It also prints out the ΔV required for stationkeeping and changes the semimajor axis correspondingly.

Output of RESORB consists of the following:

- Mean elements and their time derivatives
- Longitude of the ascending node of the mean satellite and its time derivative
- Groundtrace and coverage of the n^{th} orbit and its integer multiples plus the orbits where stationkeeping was applied
- Look angles for any ground station during the n^{th} orbit and its integer multiples.

APPENDIX O

SATELLITE ECLIPSE PROGRAM

This analytic (as opposed to integrating) program was used to compute the results presented in subsec. 4.2 in the main body of this report. This program applies to circular orbits and neglects all gravitational perturbations.

Figure O-1 presents a satellite passing along its path P1 to P4.

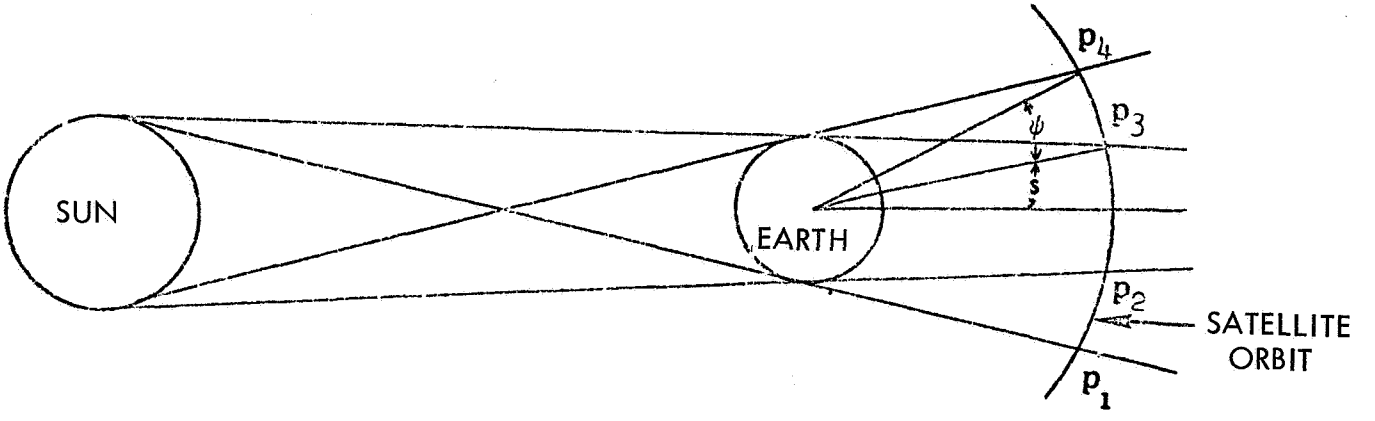

Figure O-1

As the satellite passes the point P1, it enters the penumbra or the zone of partial shadow. While passing point P2 the satellite enters the total shadow or umbra. The umbra shadow angle, s, is given by the relationship:

$$s = 1.02\left[\sin^{-1}\left(\frac{1}{R}\right) - 16'\right]$$

where

s is in degrees

r is the radius (in earth radii) of the satellite orbit.

1.02 is the factor due to the refraction of the atmosphere

The earth-centered angle, ψ, between points (P_1 to P_2 and P_3 to P_4) is the angular width of the penumbra. Regardless of the orbit altitude, this angle is almost constant and is approximately equal to 0.54°.

For a circular orbit, the maximum time per revolution that the satellite is in shadow (umbra and penumbra) is given by

$$T_{MAX} = \frac{2(s+\psi)\ R^{3/2}}{57.3\ \sqrt{\mu}}$$

where

T_{MAX} is in minutes

S and ψ are in degrees

R is in earth radii

$\sqrt{\mu} = 0.0744$ earth radii $^{3/2}$/min

57.3 is the degree to radian conversion.

The eclipse season, N_{MAX}, is defined as the number of consecutive days that the satellite passes through the shadow. Neglecting regression of the line of nodes, N_{MAX} becomes:

$$N_{MAX} = \frac{2}{0.986} \sin^{-1}\left[\frac{\sin(s+\psi)}{\sin i_e}\right]$$

where

i_e is the inclination of the orbit plane to the ecliptic plane

0.986 is the mean motion of the sun in degrees per day

It is noted that there are two such eclipse seasons per year. The variation of the time, T, that the satellite is in the shadow per revolution as a function of the time, N, of the eclipse season is computed as:

$$T = T_{MAX} \sin \left[(180^{\circ}) \left(\frac{N}{N_{MAX}} \right) \right]$$

when the inclination of the orbit plane to the ecliptic plane is greater than the angular size of the shadow, $S + \psi$. When the orbit plane inclination to the ecliptic is less than the angular size of the shadow, the satellite will again experience two eclipse seasons during the year, but each season will be continuous for the full half-year. Therefore, the season will last for a half-year, and will be bounded by minimum eclipse durations rather than periods of no eclipse. For this case, the time, T, the satellite is in shadow per revolution as a function of the time, N, if the eclipse season is computed as:

$$T = T_{MAX} \cos \phi$$

where

$$\phi = \phi_{MAX} \left(\frac{2N}{1 - N_{MAX}} \right)$$

and

$$\phi_{max} = \sin^{-1} \left[\frac{\sin i_e}{\sin(S+\psi)} \right]$$

$$= \tan^{-1} \left[\frac{\sin i_e}{\sqrt{\sin^2 (s+\psi) - \sin^2 i_e}} \right]$$

The inclination of the orbit plane relative to the ecliptic plane, i_e, as used above is directly related to the inclination of the orbit plane relative to the equatorial plane, i_a, through the relationship

$$\cos i_e = \cos 23.45^{\circ} \cos i_a + \sin 23.45^{\circ} \sin i_a \cos \Omega_a$$

where 23.45^{o} is the inclination of the equatorial plane relative to the ecliptic plane

and Ω_a is the longitude of the ascending node measured from the vernal equinox to the orbit crossing of the equatorial plane in degrees.